Geology and Volcanic Petrology of the Lava Mountains, San Bernardino County, California

GEOLOGICAL SURVEY PROFESSIONAL PAPER 457

Prepared partly in cooperation with the State of California, Department of Conservation, Division of Mines and Geology

Geology and Volcanic Petrology of the Lava Mountains, San Bernardino County, California

By GEORGE I. SMITH

GEOLOGICAL SURVEY PROFESSIONAL PAPER 457

Prepared partly in cooperation with the State of California, Department of Conservation, Division of Mines and Geology

A study of late Cenozoic volcanic rocks and a reconstruction of their probable origin in the light of chemical data and the geologic history of the area

UNITED STATES GOVERMENT PRINTING OFFICE, WASHINGTON : 1964

UNITED STATES DEPARTMEN" OF THE INTERIOR

STEWART L. UDALL *Secretary*

GEOLOGICAL SURVEY

Thomas B. Nolan, ***Erector***

The U.S. Geological Survey Library catalog card for this plication appears after index.

For sale by the Superintendent of Documents, U.S. Government Printing Office
Washington, D.C. 20402

CONTENTS

ILLUSTRATIONS

[Plates are in pocket]

TABLES

GEOLOGY AND VOLCANIC PETROLOGY OF THE LAVA MOUNTAINS SAN BERNARDINO COUNTY, CALIFORNIA

By GEORGE I. SMITH

ABSTRACT

The Lava Mountains form a north- to northeast-trending range along the north edge of the Mojave Desert, San Bernardino County, Calif. The 140 square miles of mapped area includes all the Lava Mountains and a range of hills to their southeast. The northeastern third of the area consists of low hills formed mostly of middle Pliocene continental sandstones and conglomerates; the southwestern two-thirds consists of higher hills and low mountains formed by upper Pliocene and lower Pliestocene volcanic rocks that cap the older sandstones. The Garlock fault forms the north edge of the range; the Blackwater fault and Brown's Ranch fault zone converge within it.

The oldest rocks in the area are marble, siliceous marble, slate, phyllite, and hornblende amphibolite that form a few small outcrops. They are intruded by Atolia Quartz Monzonite of probable Cretaceous age, which is exposed throughout several square miles in the northwestern and southeastern sectors of the mapped area; these rocks range in composition from quartz monzonite to granodiorite and have an average mineral and chemical composition about on the boundary between these two types.

Sedimentary and volcanic rocks of middle(?) Tertiary age overlie the metamorphic and plutonic rocks but they are almost entirely covered by younger formations, three of which are named in this report. The most extensive of these younger formations is the Bedrock Spring Formation. It consists of about 5,000 feet of coarse-grained arkosic sandstone and conglomerate plus subordinate amounts of fine-grained sandstone, siltstone, claystone, volcanic breccia, tuff, and lapilli tuff. It is assigned an age of middle Pliocene; vertebrate fossil collections indicate it to be of this age or possibly late early Pliocene.

The Almond Mountain Volcanics, a new formation of late Pliocene age, unconformably overlies the Bedrock Spring Formation. It is commonly from 500 to 900 feet thick, although more than 2 or 3 miles from the volcanic centers it is much thinner. The lower part of the section includes tuff breccia, tuff, lapilli tuff, sandstone, and conglomerate, which grade upward into massive rubble breccia. These stratified rocks grade laterally into their intrusive equivalents, some of which are hydrothermally altered to propylite.

The Lava Mountains Andesite, a new formation of very late Pliocene age, unconformably overlies the Almond Mountain Volcanics. It consists of porphyritic plagioclase andesite, and is found as tabular flows, 200 to 600 feet thick, and as mounds and domes formed above areas of upwelling lava. During the time that the Almond Mountain Volcanics and the Lava Mountains Andesite were being deposited, small volumes of other upper Pliocene(?) volcanic rocks were also deposited; these are mapped separately but are not formally named.

In early Quarternary time, sills, dikes, plugs, and small flows of andesite were deposited in the central part of the range. To their north, gravels were deposited contemporaneously on northeast-sloping pediments cut on the deformed Bedrock Spring Formation. To their east, a newly defined unit, the Christmas Canyon Formation, was deposited on a northwest-sloping pediment as a gravel veneer 75 to 150 feet thick that graded into finer grained lake deposits. This formation is dated as Pleistocene(?). A few dikes of basaltic rocks cut this formation. Since those rocks were deposited, older alluvium, alluvium, and tufa have been formed.

Within the Lava Mountains area, three fault systems converge. The Garlock fault trends N. 75° E. along the north side of the range; it is a left-lateral fault. The Blackwater fault trends N. 45° W. in the southeastern part of the region; it is predominantly a right-lateral fault. The Brown's Ranch fault zone and its associated faults trend about N. 55° E. in the central and western parts of the area; they have sustained both lateral and dip-slip displacements. A small thrust fault is present along the south side of the Garlock fault. The Dome Mountain anticline trends parallel to the Garlock fault and about 3 miles south of it.

The earliest recorded activities on the Garlock fault and the Brown's Ranch fault zone were in middle and late Pliocene times, respectively, although earlier activities are inferred; recorded activity on the Blackwater fault is of early Quaternary age. The order in which the last appreciable displacements took place is: (a) Blackwater fault, (b) Brown's Ranch fault zone, and (c) Garlock fault. The Garlock fault, however, has not moved appreciably in Recent time. This sequence of faulting requires the activity along all three fault systems to have been in part contemporaneous.

The volcanic rocks are virtually all porphyritic plagioclase andesite. Plagioclase megaphenocrysts (3–23 percent), plagioclase microphenocrysts (4–20 percent), biotite (0–2 percent), hornblende or oxyhornblende (0–8 percent), orthopyroxene and clinopyroxene (0–3 percent), quartz (0–3 percent), and opaque minerals (1–11 percent) are found as crystals in a cryptocrystalline to glassy groundmass (60–90 percent). Most rocks contain cristobalite in the submicroscopic fraction of the groundmass, and one contains K-feldspar. Twenty-five major element and 24 minor element analyses are listed. The SiO_2 content ranges from 60 to 72 percent, but most of the rocks fall in the 63- to 66-percent range. In terms of CIPW norms, the rocks are also similar; most are yellowstonose (I.4.3.4.), six are tonalose (II.4.3.4.), and two are lassenose (I.4.2.4.). Even within this small range, however, most major and minor elements show variations that are clearly related; the only exceptions are elements normally included in K-feldspars which, in these rocks, have not crystallized. Some mineral and chemical compositions vary systematically with each other, but neither varies with the age of the rock. An alkali-lime index of 58 indicates that the rocks are calc-alkalic.

The volcanic magma apparently formed by fractional crystallization of a mafic magma prior to its first eruption, probably in middle Pliocene time, and the small amount of compositional variation in all younger volcanic rocks is inherited chiefly from this stage. Between middle and late Pliocene time, a magma of similar composition was added to the partly crystallized magma in the chamber. This caused distinct petrographic changes, but the average chemical composition of this new magma remained the same. Diffusion and mixing in the magma chamber throughout late Pliocene and early Pleistocene times progressively eliminated the inhomogeneities created during early differentiation and subsequent magma mixing.

Three lithologic properties of the volcanic rocks are correlative with their stratigraphic position, and they indicate the process by which the magmas were transported to the surface: (1) all the earlier volcanic rocks were formed by explosive activity, whereas the later products were formed by effusive activity; (2) the frequency of eruption increased with time; and (3) the variety of rock types combined in fragmental volcanic rocks decreased with time. These indicate an eruptive mechanism that combined the effects of increased faulting of the crust, increased temperatures in the conduit walls, and increased vapor pressures in the magma chamber. As the eruptive sequence progressed, these factors allowed eruptions to occur more and more frequently, and the magma to come progressively nearer the surface before solidifying. In the later stages, magma remained fluid until it reached the surface to form effusive flows.

INTRODUCTION

The Lava Mountains consist of a range of hills and low mountains that lie along the north edge of the Mojave Desert, Calif. (fig. 1). They are in the northwestern part of San Bernardino County and lie about 110 miles northeast of Los Angeles and 85 miles east of Bakersfield. The mapped area described in this report covers the Lava Mountains proper and the range of hills to their southeast which includes Almond Mountain. The total area is thus bounded on the north by Searles Valley, on the west by parts of the Rand Mountains and the Summit Range, on the south by Red Mountain and Cuddeback Lake valley, and on the east by Pilot Knob Valley, which contains the U.S. Navy Randsburg Wash Testing Range (fig. 2). The Lava Mountains occupy parts of the Randsburg, Cuddeback Lake, and Searles Lake 15-minute quadrangles.

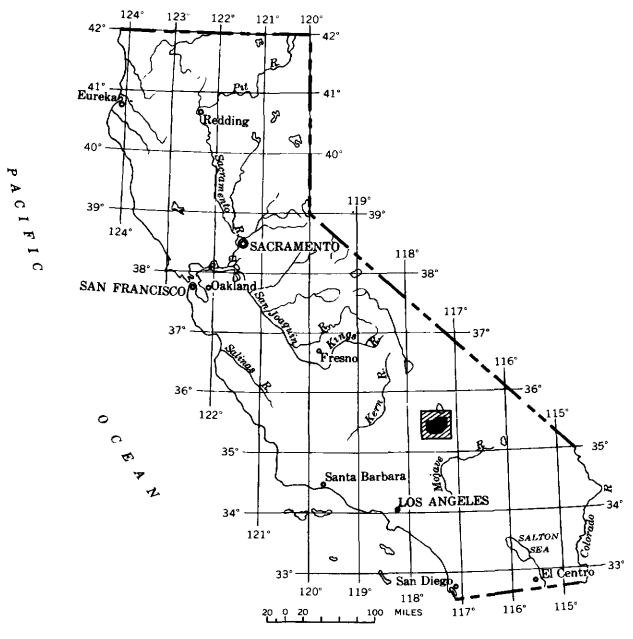

FIGURE 1.—Index map of California showing area of generalized geologic map of figure 2 (heavy outline) and the Lava Mountains area of plate 1 (solid black).

The area is reached by means of a paved road that connects Red Mountain and Trona. A paved U.S. Navy road extends across the northeast corner of the mapped area, but its use is restricted. Supplemental graded roads extend along the north and south edges of the range, and several rough, ungraded roads and trails extend into the mountains from them. A four-wheel drive vehicle can be driven to within 2 miles of any point in the mapped area.

The topographic character of most of the Lava Mountains in that of an irregular older surface that has been dissected (see fig. 3). In the northeastern part of the area, the local relief rarely exceeds 200 feet except where the more resistant volcanic rocks project through the younger gravel-covered surface to form hills. In the remaining areas, as much as 1,000 feet of local relief is provided where lava flows that form the uppermost surface have been breached, exposing to erosion less resistant sandstones that underlie them. Similar relief occurs where intense faulting has reduced the rocks to an easily eroded gouge. Total relief is about 2,800 feet; the lowest area is along the north edge (about 2,200 ft), and the highest point is Dome Mountain (4,985 ft).

The climate of the area is warm and arid. The annual precipitation averages between 4 and 6 inches, most of which falls during the winter months, sometimes as snow. The mean annual temperature is about 63° F. The flora consists predominantly of greasewood and sagebrush, although a few areas that are underlain by arkosic and granitic rocks support some Joshua trees. Coyotes, rabbits, small rodents, lizards, quail, snakes, scorpions, tarantulas, and other small animals inhabit the region.

In the historical record of this part of the Mojave Desert, the Lava Mountains are rarely mentioned except in discussions of the Randsburg mining district, to the southwest, where gold was first discovered in 1895, tungsten in 1904, and silver in 1919. Each of these discoveries set off a new wave of prospecting in the Lava Mountains, and almost every square mile contains mining claims and evidence of prospector's camps. The well-known mule teams from the borate mines in

Death Valley used to pass across Cuddeback Lake a few miles south of this area. The Trona Railway, built into Searles Valley in 1914, lies about 3 miles north of the area. However, lack of water and proven mineral deposits has apparently discouraged any extensive human activity within the Lava Mountains.

PURPOSE AND METHODS OF INVESTIGATION

The initial purpose of this project was to develop a general understanding of the geology in the Lava Mountains. Particular emphasis was placed on the character and extent of the middle Pliocene rocks in order to determine the relative positions in the stratigraphic section of recently discovered vertebrate fossil localities. As mapping progressed, it became evident that much information could also be gathered about the late Cenozoic history of the Garlock and Blackwater faults and their effect on this part of the Mojave Desert. It also became clear that the volanic rocks of this area were exceptionally well exposed and were relatively unaltered. Furthermore, the entire volcanic sequence was preserved and most of the activity could be dated reliably as post-middle Pliocene. This report describes the results of work on the general geology and petrology of the volcanic rocks of this area (pl. 1 and 2).

Mapping was begun in the fall of 1952 by myself accompanied by George N. White. It was resumed and nearly completed in the fall of 1954, though some additional work was done sporadically between 1955 and 1959. About 130 days were spent in the field and an area of about 140 square miles was mapped. The reconnaissance map, figure 2, required about 25 additional days.

The geologic mapping was done on aerial photographs at a scale of about 1:20,000. The geology was then transferred to the topographic base by inspection and proportional dividers. The base map is compiled from parts of three 15-minute topographic quadrangles published at a scale of 1:62,500; the western third is from the Randsburg quadrangle map made in 1900 by planetable methods, whereas the eastern two-thirds is from the newer Searles Lake and Cuddeback Lake quadrangle maps made by photogrammetric methods. So that the topography of the two sets of maps would blend, the contours along the east edge of the older quadrangle have been altered. The large discrepancies between the topography as shown on the Randsburg quadrangle map and on the photographs on which the geology was plotted have made it necessary to distort the actual geologic configuration of many areas to "fit" the topography, although the high-angle faults and contacts have been kept nearly straight to preserve the proportions and the general geometric relations as accurately as possible.

Most of the petrographic study of the volcanic rocks was done on thin sections. A total of about 225 were carefully examined. All textural studies were made in this way, although some mineral identifications required supporting data obtained by oil-immersion and X-ray methods. All thin sections were first studied in a random order.

Modal, spectrochemical, and chemical analyses were made on 25 volcanic rocks and 4 plutonic rocks. The modes were made by the point-counting methods described by Chayes (1949). Between 1,400 and 1,500 points were counted for each slide. To determine the reproducibility of point counts for this type of volcanic rock by the method used, two rocks were analyzed three times, and one was analyzed twice. For each rock analyzed three times, the first two counts were made within a few days of each other, and the third was made about 10 months later. For the rock that was analyzed twice, the counts were made about 10 months apart. All counts were made with the same microscope and using the same conventions. The results, listed in table 17, show that any figure is probably reproducible to within 1.5 percent of the total rock percentage, although the percentage error of any value with respect to the average amount of that component actually present may be much higher. Extreme variability is limited to those components present in small amounts only; they, of course, have not been adequately sampled.

The spectrochemical analyses of all but three elements were made on the facilities of the California Institute of Technology, Division of Geological Sciences. The samples for analysis were collected and prepared in the following manner:

At the localities to be sampled, 2 to 3 pounds of rock, free of weathered surfaces, were collected. These were then reduced to fragments one-half to one inch in diameter. The individual fragments were air-jetted to remove the dust and other impurities. Enough pieces were selected to weigh about 150 grams and these were then crushed in a "diamond" mortar until the entire sample passed through a 40-mesh cloth screen. The minus-40-mesh material was then split by means of a pure aluminum Jones-type splitter until one sample of about 10 grams was obtained. This was used for the spectrochemical analyses and the balance was retained for chemical analyses. The 10-gram sample was then reduced to a flourlike fineness in an agate mortar. The 25-milligram samples actually analyzed were grab samples from this final product.

Contamination of the sample was negligible for most spectrochemically analyzed elements. Some iron and

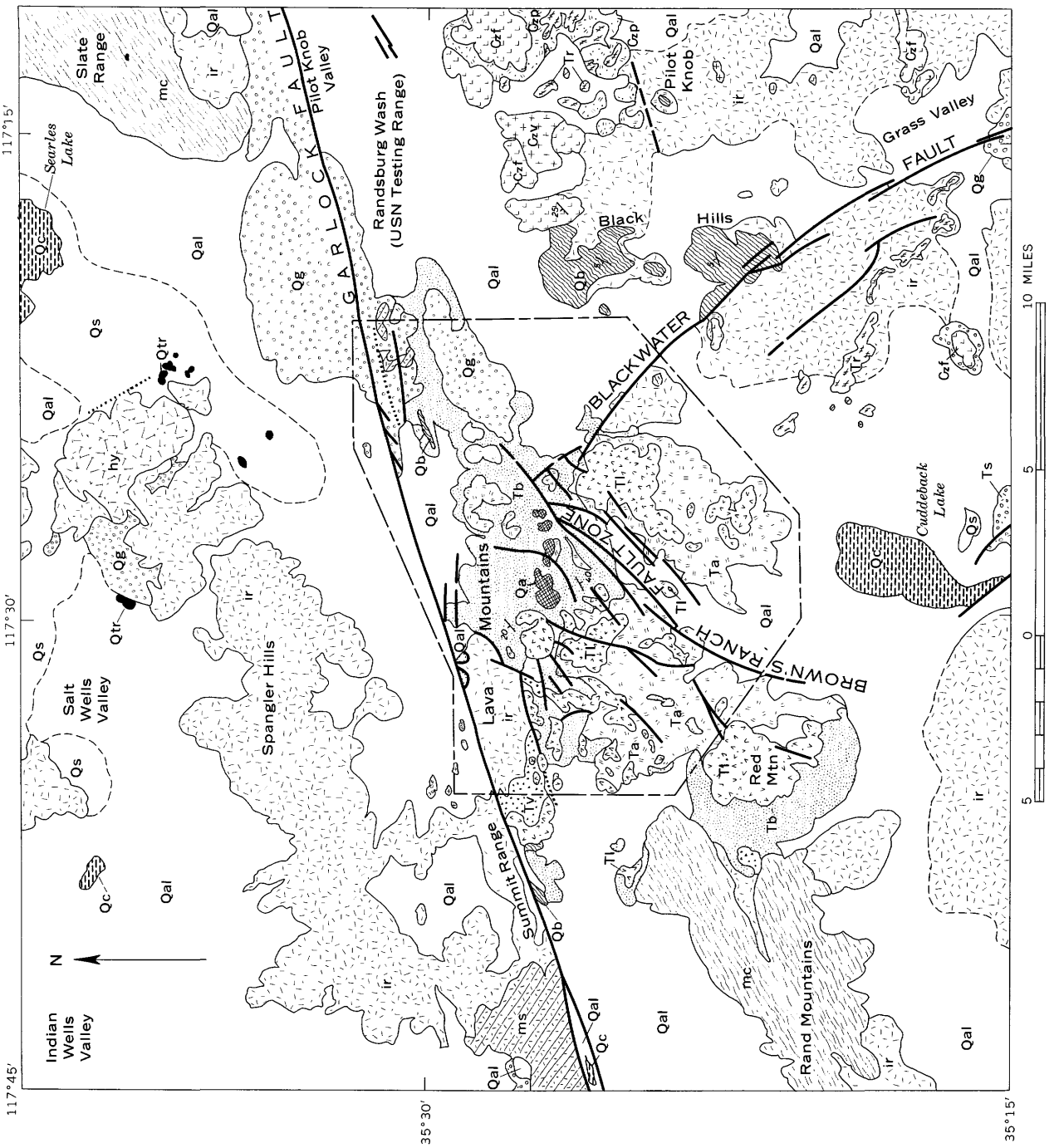
Slate Range
Searles Lake
Salt Wells Valley
Spangler Hills
Indian Wells Valley
Summit Range
Lava Mountains
Randsburg Wash (USN Testing Range)
GARLOCK FAULT
Pilot Knob Valley
BLACKWATER FAULT ZONE
BROWNS RANCH
Red Mtn
Rand Mountains
Black Hills
Pilot Knob
Grass Valley FAULT
Cuddeback Lake
Qal
Qc
Qg
Qs
Qtr
Qa
Qb
Tb
Tl
Ta
Tv
Tr
Ts
Czf
Czp
Czv
mc
ir
hy
ms
N
117°45'
117°30'
117°15'
35°30'
35°15'
10 MILES
5
0
5

EXPLANATION

CENOZOIC

QUATERNARY

Pleistocene and Recent

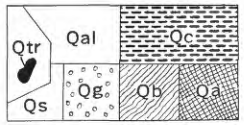

Sedimentary deposits and volcanic rocks

Qal, *alluvium; slightly dissected in some areas*
Qc, *playa-lake deposits with a hard-packed clay surface*
Qtr, *travertine and tufa; as mounds, domes, pinnacles*
Qs, *older sand and silt; now being dissected*
Qg, *older gravels; now being dissected; include the Christmas Canyon Formation of Pleistocene(?) age in the Lava Mountains*
Qb, *basaltic rocks; chiefly tabular flows*
Qa, *andesite sills, dikes, plugs, and flows*

TERTIARY

Middle and upper Pliocene

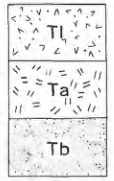

Sedimentary and volcanic rocks

Tl, *Lava Mountains Andesite of late Pliocene age; unit includes some other flows and intrusives*
Ta, *includes the Almond Mountain Volcanics and the other upper Pliocene(?) volcanic rocks of this report*
Tb, *Bedrock Spring Formation; chiefly arkosic sandstone; middle Pliocene or slightly older*

Pre-middle Pliocene

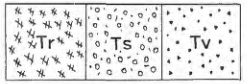

Volcanic and sedimentary rocks

Tr, *rhyolitic intrusives, probably some flows; found as fragments in the Bedrock Spring Formation*
Ts, *sandstones and conglomerates.*
Tv, *assorted volcanic rocks, mostly faulted and brecciated*

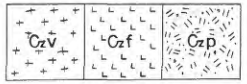

Volcanic rocks

Czv, *volcanic rocks, undifferentiated; complex in most areas; consist of intrusive volcanic rocks with some flows and pyroclastics*
Czf, *volcanic flows of various compositions*
Czp, *pyroclastic rocks*

PRE-TERTIARY

Igneous rocks

ir, *mostly quartz-monzonitic rocks, some dioritic rocks in the southeastern part of the map; local swarms of fine-grained dioritic dikes in Spangler Hills*
hy, *hypabyssal and metasedimentary rocks*

Metamorphic rocks

ms, *metasedimentary rocks*
mc, *complex mixture of metasedimentary, metaigneous, and igneous rocks*

Contact
Dashed where indefinite

Fault
Dashed where indefinite; dotted where concealed

Border of area described in this report

25 Strike and dip of beds

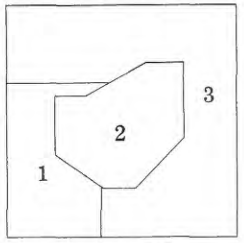

Sources of data
1 Hulin (1925) slightly modified
2 This report
3 G. I. Smith, reconnaissance

FIGURE 2.—Generalized geologic map of the Lava Mountains and vicinity.

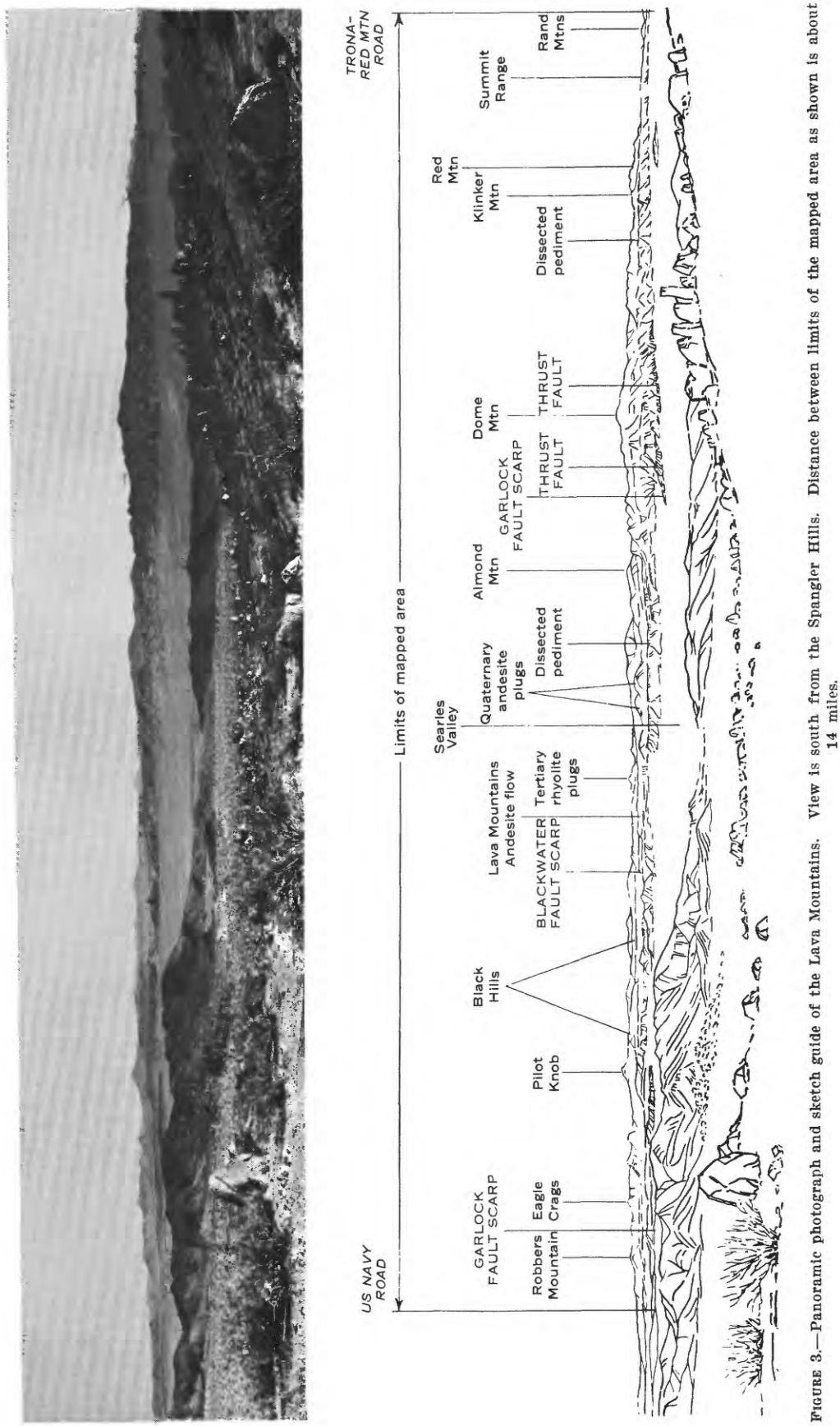

FIGURE 3.—Panoramic photograph and sketch guide of the Lava Mountains. View is south from the Spangler Hills. Distance between limits of the mapped area as shown is about 14 miles.

iron-alloy elements were introduced from the hammer used in the initial breaking. The "diamond" mortar probably added very little. Some Al was probably added by the sample splitting procedure. During the final grinding, only small amounts of SiO_2 were added. Contamination from the graphite electrodes is limited to V (up to about 40 ppm), B (up to about 5 ppm), and insignificant amounts of Si, Ti, and possibly Fe.

The volcanic rocks were analyzed by myself under the supervision of A. A. Chodos; the plutonic rocks were analyzed by Elisabeth Godijn. All the analyses were made by the method described by Rogers (1958, p. 452–453) for the wave length range 2300–4800A, except that the crushed samples were not mixed with "iron quartz." To furnish others with a basis for comparing the spectrochemical values obtained in this work, samples of "G–1" and "W–1", described and discussed by Fairbairn and others (1951, p. 3–4), were analyzed at the beginning and end of each plate of the volcanic rock analyses; the values obtained are listed in table 19.

The elements Rb, Li, and Cs were analyzed spectrochemically by Robert Mays of the U.S. Geological Survey. The samples analyzed were splits of the material used for the other spectrochemical analyses. The analyses follow the procedures used by the Geological Survey. The most sensitive lines of these elements that fall in the visible region (6300–8700A) of the spectrum were used. The results have an overall accuracy of ±15 percent except near the limits of detection where only one digit is reported.

All samples were analyzed at least in duplicate. To determine further the reproducibility of these spectrochemical analyses of elements detected in the 2300A to 4800A range, four of the volcanic rock samples were analyzed four times, and one sample was analyzed six times; the results and the mean deviations are listed in table 18. As a result of the differences in the behavior of various elements during burning, and possibly as a result of incomplete mixing for those elements found in high amounts in sparse minerals (for example, Zr in zircon), there is a great range of reproducibility from one element to the next. The majority, however, are found to have a reproducibility of better than 20 percent.

The volcanic rock samples for chemical analyses were prepared along with those for spectrochemical analyses. The residue from the sample used for spectrochemical analyses was split as many times as necessary to reduce it to about 20 grams. That sample, already screened to 40 mesh, was then sent to the Washington laboratory of the Geological Survey for a rapid rock analysis (Shapiro and Brannock, 1956). The plutonic rocks were similarly prepared and submitted at a later time for similar analysis.

TERMINOLOGY

The terms used to describe fault displacements are in accord with those suggested by Hill (1959). Plutonic and metamorphic rock names follow the recommendations of Travis (1955). The detrital sedimentary rock names used throughout this report are those suggested by Wentworth (1922).

Fragmental volcanic rocks are named according to the system shown in figure 4. These names are applied

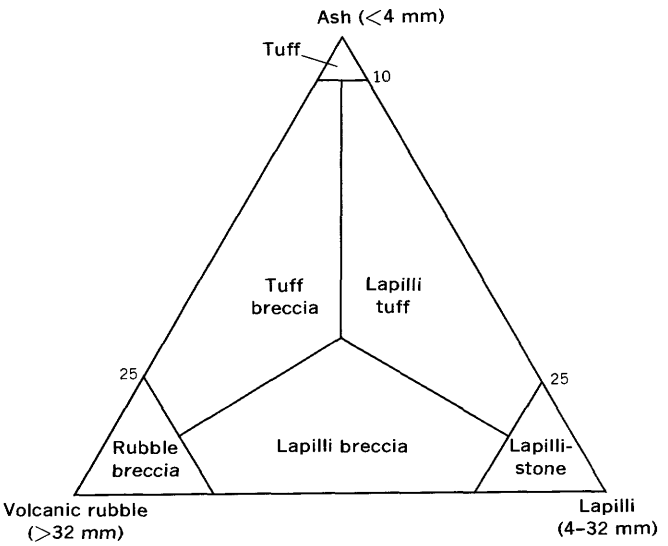

FIGURE 4.—Fragmental volcanic rock terms used in this report. Terms applied on basis of the volume percent of components constituting the rock.

to rocks composed chiefly of volcanic ash, lapilli, or rubble regardless of whether they are intrusive or extrusive, primary or reworked. The basis for distinction is the size of the volcanic fragments composing the rocks. Rocks containing a prominent percentage of angular or rounded fragments of volcanic rock in a lava matrix are called flow breccia or flow conglomerate. Volcanic breccia is used as a general term to include rubble breccia, lapilli breccia, flow breccia, and tuff breccia.

The names of the fine-grained igneous rocks also follow the recommendations of Travis (1955). For rocks

in which the identifications or relative percentages of the visible minerals are doubtful, terms such as dacitic, andesitic, and basaltic are used. The mineral percentages applied to that classification are those of the mode rather than the norm. The volcanic rocks are named on this basis because the majority of published descriptions of volcanic rocks in the Mojave Desert area follow this convention, and because names based on the norm or bulk chemical composition do not indicate the actual mineralogy of the rock. In some of these rocks, the average composition of the plagioclase—the criterion separating andesite from basalt in Travis' classification (1955)—is closed to the dividing line (An_{50}); these rocks are here called andesite because the mafic accessory minerals are chiefly oxyhornblende and biotite rather than olivine and pyroxene.

Fine-grained igneous rocks are commonly named by systems other than this, and some workers may wish to compare the system used in this report with one more familiar to them. The volcanic rocks in the Lava Mountains are so similar that one name describes most of them. By the modal classification used in this report, they are andesite. If they are classified according to their mode by any of the other common classifications listed by Peterson (1961), the same name applies. The modal classification of Rittmann (1952, p. 90–92) applies the name pheno-andesite.

Chemical analyses show that complete crystallization of these magmas under equilibrium conditions would produce rocks that also contain significant amounts of quartz and K-feldspar. If the rocks in the Lava Mountains are named according to any of the systems that anticipate this holocrystalline mineralogy—for example, according to their norms—they would generally be considered dacite or rhyodacite. According to the purely chemical classification of Rittmann (1952, p. 93–94), these rocks are mostly rhyodacite; according to the chemical (CIPW) classification of Washington (1917), they are mostly yellowstonose; and according to the average rock compositions compiled by Nockolds (1954), they most resemble rocks classified by him as dacite.

In the color descriptions of rocks and minerals, the terminology of the Rock-Color Chart (Goddard, 1948) has been used where experience has shown that an accurate color description is important in identification. Color names obtained from this chart are always followed in parentheses by the symbol (such as $5GY$ 8/2).

In the descriptions of rocks in thin section, the terminology, optical properties, and curves given in Winchell and Winchell (1951) have been used with the following four additions or modifications: (a) The borderline between hornblende and oxyhornblende has been drawn at $c \wedge Z = 10°$. (b) Opaque materials have been so called without regard to the properties that might distinguish hematite, magnetite, ilmenite, etc. (c) In describing plagioclase zoning, the term "calcic rim" has been used to denote the outermost zone when it consists of a distinct layer of more calcic plagioclase than the zone on which it rests, and the term "oscillatory-normal zoning" to describe oscillatory zoning that shows an overall normal trend. (d) The terms "megaphenocryst" and "microphenocryst" have been applied to plagioclase phenocrysts to distinguish euhedral crystals more than 0.3 mm long from crystals less than 0.3 mm long.

To aid in describing locations, each of the seven townships in the mapped area has been assigned a capital letter as shown on plate 1. The sections within each township are numbered in the customary order; the sections in township C are projected from adjoining townships. Each section is also subdivided into sixteenths and assigned a small letter as shown on plate 1. For example, "D23-m" refers to the NW¼ of SW¼, sec. 23, T. 29 S., R. 41 E.

ACKNOWLEDGMENTS AND COOPERATION

Many people have assisted in the work represented here. George N. White and Donald H. Kupfer, then of the Geological Survey, provided valuable aid during the first few months of fieldwork. Extensive cooperation and assistance by Mr. and Mrs. A. Hunt of Randsburg and Mr. and Mrs. H. Howard of Johannesburg proved invaluable. The chemical analyses by S. D. Botts, P. L. D. Elmore, M. D. Mack, H. F. Phillips, and K. E. White of the U.S. Geological Survey have been essential in interpreting the results of the fieldwork. Spectrochemical analyses by Elisabeth Godijn and Robert Mays, as well as the supervision by A. A. Chodos of my analytical work are also greatly appreciated. The compiling of this work has benefited especially from discussions with C. R. Allen, W. Barclay Kamb, R. P. Sharp, and L. T. Silver of the California Institute of Technology, with A. M. Bassett of the University of California at San Diego, with Ian Campbell of the California Division of Mines and Geology, and with James F. McAllister, T. W. Dibblee, Jr., G. P. Eaton, W. C. Smith, and P. J. Smith of the U.S. Geological Survey. Final compilation of this work was done in cooperation with the State of California, Department of Conservation, Division of Mines and Geology.

PREVIOUS GEOLOGIC STUDIES

The Randsburg mining district, which lies about 5 miles southwest of the Lava Mountains, has been an area of interest to geologists since its discovery in 1895. Several reports and investigations were made of the

district in the early part of the century. One of the first of these early investigations to include a study of the geology of the surrounding area was that of Hess (1910, p. 24–31), in which he summarized the general geology of the western Lava Mountains as well as the other ranges surrounding the mining district. Among the contributions of that study was the identification and naming of the Garlock fault, which is well exposed near the north edge of the Randsburg quadrangle. No geologic map of the region was published, however, until C. D. Hulin's report on the Randsburg quadrangle in 1925. That report summarized the geology of the entire quadrangle which includes the western third of the Lava Mountains. Later, a very generalized geologic map of a much larger area was published in Thompson's report (1929, pl. 8) on the water resources of the Mojave Desert; the geology around the Randsburg area was based chiefly on a previously unpublished map by Hess. A few years later, Hulin made a geologic reconnaissance of a large area surrounding the Randsburg quadrangle and his map was published at a scale of 1:500,000 as part of a geologic map of California (Jenkins, 1938). Since that time, no map or geologic description of the Lava Mountains has been published.

Hulin's report (1925) of the geology of the area divided the rocks exposed in the western Lava Mountains into three units: the basement of Late Jurassic Atolia Quartz Monzonite, the unconsolidated conglomerates, sandstones, and clays of the middle Miocene "Rosamond Series," and the lavas and agglomerates of the Pliocene "Red Mountain Andesite." His subsequent reconnaissance map (in Jenkins, 1938) carried these units throughout the rest of the Lava Mountains and surrounding areas.

GEOLOGIC SETTING OF THE LAVA MOUNTAINS

The Lava Mountains lie along the north edge of the Mojave Desert physiographic province. To the north lie the Basin Ranges. The Garlock fault approximates the boundary between these provinces, and the different character of the Cenozoic structures to the north and south of this structure cause most of the notable physiographic differences.

The differences between the areas on the north and south sides of the Garlock fault are summarized by Hewett (1954a, 1954b). On the north side, in the Basin Ranges, the Cenozoic faults range in strike between northeast and northwest, have large vertical displacements, and exert a major role in controlling the topography; on the south side, many of the Cenozoic faults also have northwest strikes, but they have small vertical displacements and play a minor role in determining the topography. The ages and lithologies of the rocks on the north and south sides of the Garlock fault are also different. The pre-Cenozoic rocks north of the fault include large areas of pre-Mesozoic sedimentary, metasedimentary, and metaigneous rocks; south of the fault, Mesozoic plutonic rocks form virtually all of the basement. The Cenozoic rocks on the north side of the Garlock fault are of early, middle, and late Cenozoic age, whereas those on the south side are all of middle and late Cenozoic age.

The Blackwater fault, which enters the Lava Mountains range from the southeast (fig. 2), is one of the northwest-trending faults so common south of the Garlock fault. However, it differs from the others in that it forms a boundary between areas that are structurally different. As is evident on geologic and structural maps of the northern Mojave Desert and southwestern Basin Ranges (Jennings and others, 1962; Hewett, 1954b), on the northeast side of the Blackwater fault, the dominant Cenozoic faults trend northeast or east, whereas on the southwest side they trend northwest. The stratigraphic and topographic characteristics of the areas on the two sides of this fault are the same.

The Garlock and Blackwater faults are major Cenozoic structural elements in this part of California. They are predominantly strikeslip, and late Cenozoic vertical displacements along neither have been consistent enough to restrict deposition of sediments to one side. Along segments of the Garlock fault, however, vertical displacements have been consistent enough over appreciable periods of time to form local depositional basins several thousand feet deep.

The middle Pliocene sedimentary rocks that crop out in the Lava Mountains represent deposits formed in one of these basins. In late Pliocene and Pleistocene time, the sense of vertical displacement was reversed, and the area of deposition was uplifted. Volcanic rocks were then deposited on the deformed and eroded basin fill, and the region has been undergoing erosion ever since.

The Blackwater fault had some influence on the sedimentation pattern in the Lava Mountains area, but the areas of middle Pliocene sedimentation and subsequent volcanism were not bounded by it.

STRATIGRAPHY

A summary of the major rock units of the Lava Mountains is shown in table 1. The oldest rocks found in the mapped area (pl. 1) are marble, slate, phyllite, and hornblende amphibolite, which crop out in two small areas. They are intruded by the Cretaceous(?) Atolia Quartz Monzonite, which is exposed over large areas in the northwestern and southeastern parts of the mapped area. Overlying these are pre-middle Pliocene

TABLE 1.—*Major rock units in the Lava Mountains, Calif.*

Formation				Age
Alluvium				Recent and Pleistocene
Older gravels	Quaternary andesite	Quaternary basalt		
		Christmas Canyon Formation		
Lava Mountains Andesite			Other upper Pliocene(?) volcanics	Late Pliocene
Almond Mountain Volcanics				
Bedrock Spring Formation				Middle Pliocene
Volcanic rocks older than the Bedrock Spring Formation				Pre-middle Pliocene
Sedimentary rocks older than the Bedrock Spring Formation				
Atolia Quartz Monzonite				Pre-Tertiary
Metamorphic rocks				

arkosic sandstones, conglomerates, altered volcanics, and unaltered volcanics that crop out in a few small areas. They are nearly concealed by the Bedrock Spring Formation which unconformably overlies them. This newly named formation is the most widespread sedimentary unit in the mapped area. It consists of about 5,000 feet of coarse-grained arkosic sandstone and conglomerate with subordinate amounts of fine-grained sandstone, siltstone, claystone, volcanic breccia, tuff, and lappilli tuff. This formation is assigned an age of middle Pliocene. Overlying the Bedrock Spring Formation with pronounced angular unconformity is the Almond Mountain Volcanics, a new formation of probable late Pliocene age. It consists of interbedded tuff, lapilli tuff, volcanic breccia, flow breccia, sandstone, and conglomerate. Small isolated areas of tuff breccia, volcanic intrusives, felsite, volcanic breccia, and tuff also of probable late Pliocene age, crop out in the mapped area. Unconformably overlying the Almond Mountain Volcanics are flows of the Lava Mountains Andesite, also a new formation of probable very late Pliocene age, whose rocks are mostly dark gray to dark red porphyritic andesites. Small dikes, sills, plugs, and flows of a very dark gray andesite were formed in early Quaternary time.

The relatively unaltered volcanic rocks of the Bedrock Spring Formation, the Almond Mountain Volcanics, the Lava Mountains Andesite, and the Quaternary andesite are all petrographically similar. The pre-middle Pliocene volcanic rocks probably also had these characteristics prior to extensive alteration. Plagioclase, which constitutes 10 to 25 percent of most of these rocks, almost invariably occurs as euhedral magaphenocrysts and microphenocrysts. Megascopic biotite and oxyhornblende, or their opaque pseudomorphs, constitute 2 to 10 percent of the rocks. Megascopic crystals of quartz and microscopic crystals of orthopyroxene and clinopyroxene make up less than 2 percent. The groundmass forms 60 to 90 percent of all the rocks and consists of skeleton crystals, microlites, cristobalite, cryptocrystalline material and glass, and a dust of fine opaque material.

The Pleistocene(?) Christmas Canyon Formation, a new formation, is exposed along the northeast edge of the Lava Mountains. It consists of about 200 feet of fine-grained arkosic sandstone, claystone, and siltstone, which grade southward into boulder conglomerate. A few dikes of basaltic rocks cut the coarser facies of the Christmas Canyon Formation. Pediment gravels were deposited at about the same time in the western part of the area. During late Pleistocene time, alluvium was deposited, shorelines were formed by Cuddeback and Searles Lakes, and local patches of tufa were formed. In Recent time only minor amounts of alluvium have been deposited.

PRE-CENOZOIC ROCKS

METAMORPHIC ROCKS

The oldest rocks in the Lava Mountains are metamorphic rocks which crop out in the northeastern and southeastern parts of the mapped area (pl. 1). Metasedimentary rocks crop out in the northeastern area, and amphibolites crop out in the southeastern area.

The metasedimentary rocks exposed in the northeastern area crop out as low hills projecting slightly above a gravel veneer, and as jagged cliffs bordering the shallow canyons. Most of these exposures consist of gray to yellowish-orange impure marble, and gray or gray-green slate and phyllite. The thickness of this section is estimated to be about 2,000 feet. No fossils were found, and the age of these rocks can be described only as older than the Cretaceous(?) Atolia Quartz Monzonite, which intrudes them.

This series of metamorphic rocks is not clearly correlative with any others exposed in the northern Mojave Desert and southwestern Basin Ranges.

The amphibolites in the southeastern part of the area, near the trace of the Blackwater fault, form a pendant in Atolia Quartz Monzonite. Typically they consist of crystals of hornblende, up to 2 inches long, and minor feldspar, arranged in an unoriented pattern. In some areas, hornblende appears to form the entire rock. Dikes and apophyses of aplite or pegmatite penetrate the mass, especially near the edges, and knotty inclusions of epidote, mostly from ½ inch to 1 inch across, occur near the contacts.

The hornblende amphibolite is probably equivalent to the hornblende gneiss facies of the Johannesburg Gneiss of Hulin (1925, p. 21–23).

ATOLIA QUARTZ MONZONITE

The Atolia Quartz Monzonite, a rock first named and described by Hulin (1925, p. 33–42), is exposed over large areas in the northwestern and southeastern parts of the map. Small outcrops are also exposed in the central part of the area (in sections B26 and B27), and in the northeast corner of the map (in C9).

Hulin designated all coarse-grained intrusive rocks in the Randsburg quadrangle as Atolia Quartz Monzonite. He distinguished several subtypes, which range is composition from quartz monzonite to quartz diorite. Orthoclase, plagioclase, and quartz occur in all these rocks, and biotite and hornblende occur in most. Inclusions are locally common. One type, composed of feldspar and quartz in almost equal proportions, and virtually devoid of dark minerals, was found to be characteristic of the northwestern Lava Mountains.

NORTHWESTERN AREA

Along the north and south edges of the northwestern area of the Atolia Quartz Monzonite, the topography is rugged as a result of late Cenozoic displacements along faults; erosion has created badland topography in areas of extreme brecciation. Between these scarps, however, the rocks form nearly flat areas or low hills. The weathered rocks in this flat area range from grayish pink to grayish orange.

Quartz monzonite and granodiorite underlie about 75 percent of this northwestern area, although, because of their low resistance to weathering, they are mostly concealed by a thin layer of gruss. These rocks are mostly medium grained and equigranular. Orthoclase and microcline are generally anhedral and are slightly altered to clay. Plagioclase crystals are either euhedral or subhedral, are slightly altered to sericite, and are moderately twinned and zoned. Quartz is anhedral and contains small crystals of apatite and magnetite. Biotite, commonly altered in part to chlorite, is the most common dark mineral. Apatite is locally common and magnetite is sparse. Table 2 lists modal, chemical, normative, and spectrochemical analyses of two samples of rock from this area (samples 26–2 and 41–34). Quartz makes up about 29 percent of each sample, and plagioclase makes up about 65 percent of the total feldspar; these two rocks are thus quartz monzonite but their compositions are very close to granodiorite. Relative to Nockolds' (1954) average granodiorite and average adamellite (quartz monzonite), the percentages of Al_2O_3 and Na_2O in Atolia Quartz Monzonite are a little high, and the percentages of CaO and possibly total Fe are a little low. The percentage of MgO is notably low in both samples. The normative compositions of both rocks classify them as toscanose and the normative plagioclase compositions are An_{18} and An_{28}.

TABLE 2.—*Modal, chemical, normative, and spectrochemical analyses of four samples of Atolia Quartz Monzonite*

[Chemical analyses by P. L. D. Elmore, S. D. Botts, and M. D. Mack; spectrochemical analyses for Li and Rb by Robert Mays, remaining spectrochemical analyses by E. Godijn; modal analyses by G. I. Smith]

Modes

[Volume percents]

	26–2	*41–34*	*181–29*
Orthoclase	22.1	21.5	15.7
Plagioclase	42.4	41.6	48.1
Quartz	29.3	29.0	13.2
Biotite	3.9	2.9	2.9
Hornblende	0	0	16.1
Muscovite	.8	1.3	0
Pyroxene	0	Trace	1.5
Opaque minerals	1.1	2.4	1.4
Other minerals	.4	1.4	1.1

Norms

[Weight percents]

	26–2	*41–34*	*41–35*	*181–29*
Q	26.7	22.2	23.5	15.1
C	1.6	1.3	.92	0
or	23.9	22.2	25.0	12.2
ab	34.6	31.4	38.2	25.2
an	7.5	12.2	6.1	25.3
di	0	0	0	6.6
hy	1.2	3.0	1.3	9.6
mt	.9	2.3	.7	4.4
il	.8	1.1	.9	1.4
hm	1.1	0	1.0	0
ap	.3	.3	.3	.3
Symbol (C.I.P.W.)	I.4.2.3	I.4.2.3	I.4.2.3	II.4.4.4

Chemical analyses

[Weight percents]

	26–2	*41–34*	*41–35*	*181–29*
SiO_2	69.9	65.2	69.5	58.2
Al_2O_3	15.5	16.0	15.2	16.4
Fe_2O_3	1.8	1.6	1.5	3.0
FeO	.58	1.9	.58	4.3
MgO	.47	.69	.52	3.3
CaO	2.2	2.5	1.3	6.9
Na_2O	4.1	3.7	4.5	3.0
K_2O	4.0	3.8	4.2	2.1
TiO_2	.40	.55	.45	.74
P_2O_5	.14	.18	.14	.24
MnO	.06	.08	.05	.19
H_2O	.87	1.4	1.5	1.1
CO_2	.38	1.6	.74	.08
Sum	100	99	100	100

Spectrochemical analyses

[Parts per million. Sought but not found: Ag, As, Be, Bi, Cd, Ge, In, La, Pt, Sb, Sn, U, Th, Zn]

	26–2	*41–34*	*41–35*	*181–29*
Cr	28±3	70±10	35±7	35±10
Co	39±2	110±10	44±10	43±14
Mn	335±5	345±15	310±30	510±0
Ni	Trace	5±1	Trace	3±0
Sc	4	4	3	16
Nb	Trace	Trace	Trace	Trace
V	45±20	70±15	60±30	250±30
Mo	----------	2±1	----------	3
Cu	4±1	2±0	2±1	75±1
Ga	10±3	8±2	9±1	9±4
Ti	180±0	180±20	130±10	240±10
B	----------	----------	----------	27±4
Ba	1,300±0	1,200±100	1,700±200	2,200±300
Li	16±3	21±3	19±3	14±2
Pb	24±3	22±1	26±2	----------
Rb	11±2	13±2	12±2	8±1
Sr	610±20	590±20	350±20	500±50
Yb	1	1	1	3
Y	Trace	Trace	12±2	22±0
Zr	175±40	230±20	180±20	140±50

LOCATION OF SAMPLES

26–2. Northwestern outcrop area—sec. A34–b, along road.
41–34. —sec. A35–d, outcrop a few feet north of small prospect along road.
41–35. —sec. A35–r, brecciated outcrop on southeast side of canyon.
181–29. Southeastern outcrop area—sec. F18–a, outcrop along east side of wash.

About 20 percent of this northwestern area is underlain by leucocratic quartz monzonite that is notably seriate and almost devoid of dark minerals. Orthoclase and minor microcline constitute about 25 percent of this rock; they form inequidimensional anhedral crystals that are slightly sericitized and contain inclusions of apatite, quartz, and plagioclase. Plagioclase makes up an estimated 45 percent of the rock and has an apparent composition of sodic oligoclase; it forms both large (1–4 mm) subhedral crystals and small anhedral crystals; both types show strongly developed albite twinning and

faint normal to oscillatory-normal zoning. Quartz constitutes about 25 percent of the rock; the crystals are small, anhedral, and generally embedded in larger anhedral crystals of K-feldspar; they contain small crystals of apatite and magnetite. Biotite, much of which is altered to chlorite, makes up less than 5 percent. Opaque minerals, mostly grouped along boundaries between larger felsic minerals, are present only in minor amounts. Analyses of this rock are listed in table 2 (sample 41–35). The analyzed sample was too badly crushed and altered to allow a reliable modal analysis, but the chemical and normative analyses support the modal estimate given above. Compared to the more common type of quartz monzonite, this leucocratic rock has similar percentages of normative orthoclase and plagioclase, but the plagioclase is distinctly more sodic (An_{14}). The Fe_2O_3 percentage is also similar, and this constituent must be chiefly in the form of hematitic material dispersed throughout the rock.

The remaining 5 percent of the rock found in this area is an aplite. Though less abundant than the other two types, it crops out more commonly because of a greater resistance to weathering. It consists of orthoclase, plagioclase, and quartz with minor microcline, and a trace of chlorite presumably from altered biotite. All minerals are irregular in shape and size. Some crystals are as large as 1.5 mm, but most of them are smaller. The overall texture is seriate, and myrmekitic structures are not uncommon. The feldspars are slightly altered, especially along the cracks, to a claylike material.

SOUTHEASTERN AREA

The second large mass of plutonic rocks, in the southeast corner of the map area, is notable for a paucity of the pink leucocratic and aplitic phases found in the northwestern area. The predominant rock types appear to be biotite monzonite, quartz monzonite, and granodiorite. Dikes and apophyses of aplite and pegmatite, as much as 5 feet wide, are exposed locally, especially around the hornblende amphibolite masses. Colors near gray predominate throughout the area, although iron oxides locally add a tinge of yellow or orange. Most of the southeastern area is deeply weathered and covered by a coarse gruss, so that few outcrops of the bedrock can be found. Where exposed along the Blackwater fault, the rocks are brecciated, altered, and locally silicified.

Modal, normative, spectrochemical, and chemical analyses of one sample of granodiorite are listed in table 2 (sample 181–29). This is the most mafic plutonic rock in this area. The normative composition agrees adequately with the modal composition, and shows the plagioclase to have an average composition of about An_{50}. Its chemical composition bears little resemblance to that of Nockolds' (1954) average granodiorite or any of the other average rocks.

OTHER AREAS

Intrusive rock crops out in two small areas in the northeastern quarter of the Lava Mountains. One exposure is approximately 3,000 feet long in sections B26 and B27, and lies along the axis of the Dome Mountain anticline. Medium- to fine-grained dioritic rocks, which are brecciated, altered, and silicified occupy about 90 percent of this area. Locally, aplitic phases are present. A grayish-red coarse-grained rock, possibly a quartz monzonite which weathers to a very coarse gruss, occupies the remaining 10 percent of the outcrop area. It differs from the pink leucocratic rocks found in the northwestern area in that the average crystal size is larger, and dark minerals make up perhaps 5 to 10 percent of the total.

The second small exposure of plutonic rock is in Christmas Canyon. The rock there is a fine-grained diorite or perhaps tonalite, and consists mostly of plagioclase, hornblende, and biotite, with quartz present as interstitial grains and fillings. The plagioclase forms euhedral to subhedral crystals characterized by having numerous albite twins and only a few Carlsbad twins. Normal zones are found in almost all the plagioclase crystals and alteration of this plagioclase to clay(?) is extensive. Green hornblende occurs as subhedral crystals, which commonly have been altered to chlorite. Biotite, present as flakes and shreds, is partly altered to chlorite. In at least one outcrop, this rock is clearly intruded into metamorphic rock.

ORIGIN OF INTRUSIVE ROCKS

The normative compositions of the analyzed samples of Atolia Quartz Monzonite are plotted in figure 5 on diagrams of the phase system Q-or-ab-an at 5,000 bars water-vapor pressure. The samples that represent the most common type of Atolia Quartz Monzonite (26–2 and 41–34) have compositions that lie approximately on the plagioclase-beta quartz boundary. The leucocratic rock (41–35), which is much less abundant, has its composition on the eutectic side of these points. The granodiorite (181–29) is on the mafic differentiate side.

Apparently this suite of rocks represents solid products of a magma that was partially differentiated during crystallization. The granodiorite represents a small fraction of mafic material that became isolated during crystallization; the leucocratic rock represents the liquid fraction that remained after being depleted in these mafic components. The original composition of the magma probably approximated that of the two representative samples. The positions of the phase

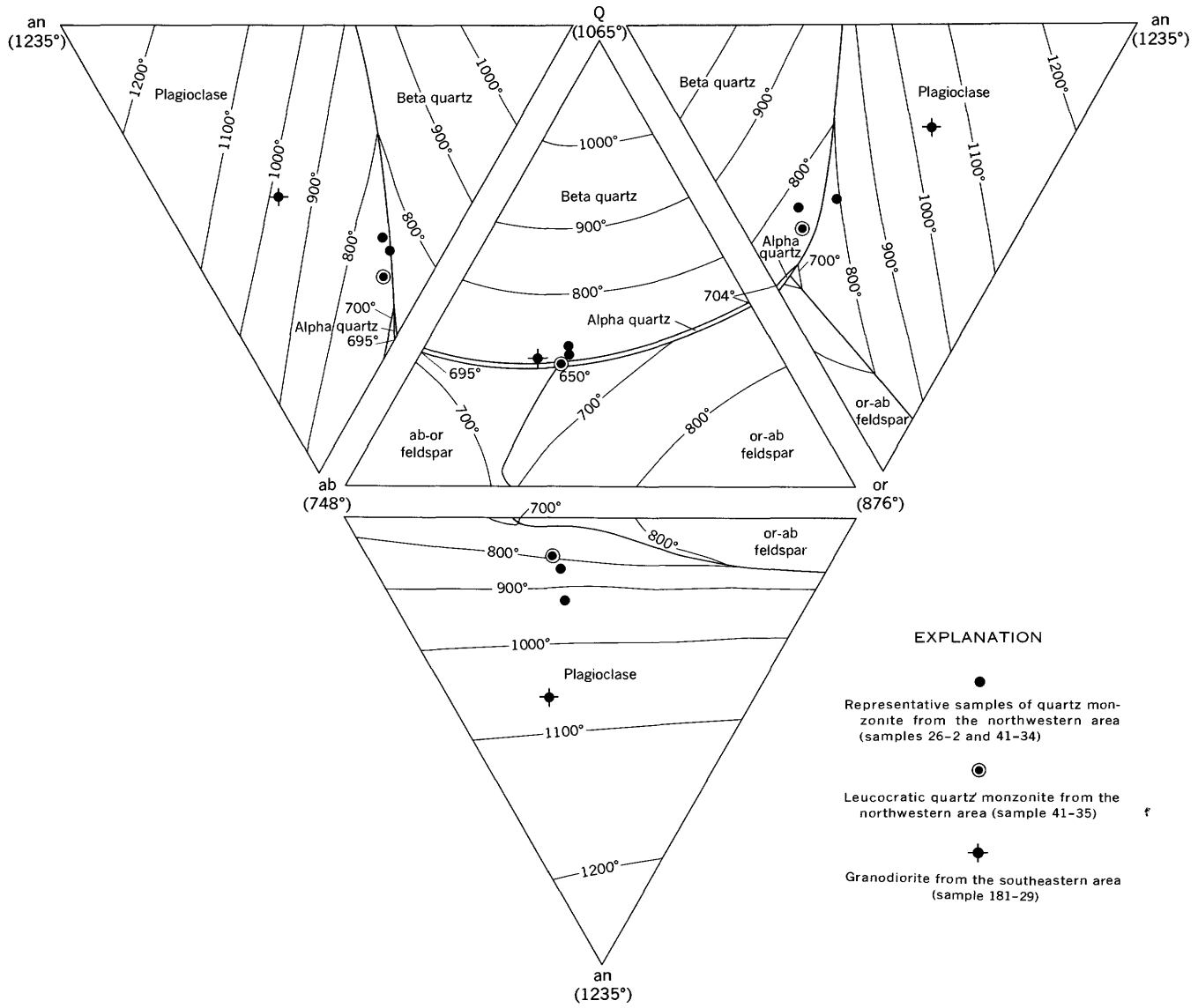

FIGURE 5.—Phase diagram of the system Q-or-ab-an at 5,000 bars water-vapor pressure showing composition of the analyzed samples of Atolia Quartz Monzonite. Phase data and isotherms (in degrees centigrade) from Bateman and others (1963, p. 34). Analyses from table 2.

boundaries in this system shift with changes in vapor pressure, and their positions at about 5,000 bars satisfactorily relate mineralogies and chemical compositions of the coexisting rocks.

AGE OF INTRUSIVE ROCKS

The Atolia Quartz Monzonite in the Lava Mountains is younger than the undated metamorphic section, which it intrudes, and older than the pre-middle Pliocene sedimentary rocks, which contain fragments of it. It was assigned a Jurassic age by Hulin (1925, p. 42) on the basis of indirect evidence. A Cretaceous age is now suggested for the batholithic rocks of the southwestern Basin Ranges and Mojave Desert by more than 20 lead-alpha age determinations on similar rocks (Jaffe and others, 1959, p. 87–90). Ages between 85 and 130 million years are reported (op. cit.), and although radiometric dates by other methods may indicate ages that are slightly different, it is reasonable to conclude that the correct age of the Atolia Quartz Monzonite is in this range. In this paper, this rock unit is assigned an age of Cretaceous(?).

CENOZOIC ROCKS

CONGLOMERATIC AND TUFFACEOUS SANDSTONE OLDER THAN THE BEDROCK SPRING FORMATION

Four small outcrops of conglomeratic and tuffaceous sandstone are grouped along the axis of the Dome Mountain anticline in the central part of the mapped area (secs. B27 and B33). The rocks are well bedded,

weather to a very light gray or yellowish gray, and are slightly more indurated than the overlying Bedrock Spring Formation. They consist chiefly of conglomeratic sandstone and tuffaceous sandstone, but contain a few beds of tuff. The small percentage of cobbles and boulders in the very coarse grained sandstone is the most diagnostic feature of the unit; they are strikingly well rounded, are as much as 1 foot in diameter, and are composed of light-colored plutonic rocks or banded rhyolitic rocks.

The stratigraphic section in B27–n is described below:

Top of section removed by erosion.	*Thickness (feet)*
Tuffaceous sandstone, well-bedded, beds 1–10 in. thick, yellowish-gray (5Y 8/1) to very light gray (*N* 8). Arkosic sand forms 20 to 60 percent of rock	33
Conglomeratic sandstone, well-bedded, light-brown (5*YR* 6–8/4), some very light gray (*N* 8)	7
Conglomeratic and tuffaceous sandstone, interbedded; conglomeratic sandstone, colors similar to those of unit above; tuffaceous white sandstone (*N* 9) with pale brown streaks (5*YR* 6/2). Ratio of epiclastics to pyroclastics about 1 to 1	18
Conglomeratic sandstone, well-bedded, very light gray (*N* 8) to yellowish gray (5Y 8/1). Well-rounded fragments, up to 1 ft across, of quartz monzonitic rocks, some banded rhyolitic rocks; very coarse grained arkosic sandstone forms 95 percent of unit	11
	69

Base of section not exposed.

These rocks are younger than the Atolia Quartz Monzonite and the rhyolite found southeast of the mapped area (see fig. 2), for both rocks are found as boulders in the conglomerate. In section B27–n, the arkosic conglomerate and tuff unit underlies the Bedrock Spring Formation with a well-defined 20-degree angular unconformity. At this contact, the color variations suggest a fossil soil about 1 foot thick.

No fossils were found in this unit; therefore its age remains unproven except within the limits imposed by the Atolia Quartz Monzonite, the rhyolitic rocks, and the middle Pliocene Bedrock Spring Formation. However, it is probably no older than Miocene; in this part of the Mojave Desert, the oldest rocks resting on the plutonic rock basement are Miocene, and the lithology and induration of the rocks described here suggest a similar age.

VOLCANIC ROCKS OLDER THAN THE BEDROCK SPRING FORMATION

Several types of volcanic rocks, known only to be pre-middle Pliocene, occur within the mapped area. All crop out along the axis of the Dome Mountain anticline. The easternmost outcrops are located near the exposures of arkosic conglomerate and tuff in the central part of the mapped area (secs. B33–a and B33–b). About 2½ miles west of that area (between secs. E6–e and E6–k), a single outcrop about 2,000 feet long exposes additional varieties of volcanic rocks. About 1 mile farther northwest (in secs. A33, A34, A35, and D1), still other types of volcanic rock are exposed over a more extensive area. The rocks in each of these three areas have little in common except for their volcanic affinities and the fact that they underlie the Bedrock Spring Formation.

The easternmost outcrop of this group (sec. B33) consists of bedded pyroclastic rocks that dip north. They weather to various shades of gray, yellow, and red. A composite section of these rocks is as follows:

Top of section removed by erosion.	*Thickness (feet)*
Tuff breccia, cliff-forming, massive, very light gray (*N* 8) to light greenish-gray (5*GY* 8/1)	30
Tuffaceous sandstone, tuff, and lapilli tuff, well-bedded, beds 1 in. to 20 in. thick, weathers to light reddish orange (10*R* 6/2)	15
Similar, locally contains small volcanic fragments, weathers to light gray (*N* 7)	25
Massive tuff and lapilli tuff, locally bedded; weathers to yellowish gray (5Y 8/1)	20
	90

Base of section not exposed.

The rocks exposed in the second area of outcrop (sec. E6) are of two types. Those in the western half consist of light-colored arkosic sandstone, tuff, and lapilli tuff that are severely faulted and brecciated. They rest unconformably or in fault contact on a volcanic complex which forms the eastern half of the outcrop. The rocks of this complex are massive andesites(?) that weather to shades of gray, brown, or buff. They are composed chiefly of plagioclase, secondary opaque minerals, calcite, and quartz, all embedded in a groundmass of cyptocrystalline material. The plagioclase crystals are seriate, range in size from microphenocrysts up to 4 mm, and have weak oscillatory or oscillatory-normal zones and well-developed albite twins; the composition ranges from andesine to sodic labradorite. The rock is extensively altered. Opaque minerals, apparently alterations of biotite and hornblende, compose about 10 percent of the rock; initially hornblende was more abundant than biotite. Veinlets and blebs of quartz, composing about 10 percent of the rock, fill vesicles and cracks in the groundmass and plagioclase. Calcite partly replaces a few of the plagioclase crystals. A distinctive feature is that some of the vesicles are filled with green opal(?).

In the third group of outcrops of this unit (sec. A33 and surroundings), two types of volcanic rocks are exposed. Both form areas of complexly brecciated resistant rock. Their contacts with Atolia Quartz

Monzonite commonly dip at high angles, and the entire unit appears to be a shallow intrusive complex. The first of these two types forms about 10 percent of the outcrop and weathers to white or yellowish gray. The rocks in this unit have an estimated original composition of 20 percent plagioclase, 5 percent amphibole, and 75 percent groundmass. Alteration has changed this rock into a propylite or subpropylite (see page 24). The plagioclase is largely altered to calcite, quartz, chalcedony(?), and a trace of opaque minerals; and the amphibole(?) is altered to opaque minerals and zoisite(?). The groundmass now consists of about 98 percent fine-grained quartz(?) with traces of opaque minerals, serpentine, and calcite.

The second type of rock found in this group of outcrops weathers to a grayish green and contains light reddish-brown plagioclase phenocrysts that are a distinctive feature of the rock. Originally this rock probably consisted of plagioclase and amphiboles in a groundmass that made up about 50 percent of the rock. It is also altered to a propylite or subpropylite. The plagioclase has been totally altered to sericite, calcite, and opaque minerals in the approximate ratio of 5:4:1; and the amphiboles(?) have been altered to chlorite, opaque substances, and sericite in the approximate ratio of 4:4:2. Maximum original crystal size of the plagioclase was 4 mm and that of the amphiboles 2 mm. The groundmass is now holocrystalline and consists mostly of patches of fine-grained quartz, but also contains several percent of clay and a few percent of sericite, calcite, and serpentine.

Chemical, spectrochemical, and normative analyses of a sample of this grayish-green rock are given in table 3. The rock is too badly altered for a modal analysis. The large percentages of CO_2 and H_2O indicated by the chemical analysis confirm the extensive alteration. If the analysis is recalculated to 100 percent without CO_2 and H_2O, the SiO_2 percentage increases from 60.2 to 64.1, and all other components increase proportionally. This percentage of SiO_2 is similar to the percentages found in all other volcanic rocks of this area, and the normative composition and name (yellowstonose) confirm this similarity. The subsequent alteration is responsible for all the notable differences.

The CO_2 reported by the analysis is derived from the calcite veins and replacements in the rock, and the CaO that is combined with it to form calcite accounts for most of the CaO in the altered rock. The total amount of CaO in this rock, however, is similar to the amount reported from relatively fresh rocks of this area having the same percentage of SiO_2, and this probably means that the CaO in calcite was present in the original rock, and that only CO_2 was introduced.

TABLE 3.—*Normative, chemical, and spectrochemical analyses for one sample of the volcanic rocks older than the Bedrock Spring Formation*

[Sample 41-39 from top of small ridge in south half of sec. A35-q. A dash means that the element was not present in detectable amounts. Chemical analyses by P. L. D. Elmore, H. F. Phillips, and K. E. White; spectrochemical analyses for Li and Rb by Robert Mays, remaining spectrochemical and modal analyses by G. I. Smith]

Chemical analyses [Weight percents]		Norms [Weight percents]		Spectrochemical analyses [Parts per million]	
SiO_2	60.2	Q	18.0	Cr	20
Al_2O_3	16.4	C	0	Co	20
Fe_2O_3	1.9	or	15.0	Mn	320
FeO	2.9	ab	28.8	Ni	10
MgO	1.4	an	22.0	Sc	10?
CaO	4.6	di	.7	V	50
Na_2O	3.4	hy	5.0	Fe	30,000
K_2O	2.5	mt	2.8	Cu	30
TiO_2	.90	il	2.6	Ga	10
P_2O_5	.22	hm	0	Ti	2,600
MnO	.04	tn	0	B	30
H_2O	3.2	ru	0	Ba	1,100
CO_2	2.9	ap	.3	Be	----
Total	100	Symbol (C.I.P.W.)	I.4.3.4	Li	52
				Pb	10
				Rb	110
				Sr	1,000
				Yb	2
				Y	10?
				Zr	100

AGE AND RELATION TO OTHER FORMATIONS

All these volcanic units are probably younger than the conglomeratic and tuffaceous sandstone described in the previous section. The two units are not in contact, but the volcanic rocks are inferred to be younger because no fragments of similar volcanic rock are found in the sandstone. The contacts of Atolia Quartz Monzonite with these volcanic rocks do not furnish conclusive evidence, but the more probable interpretations suggest that all the volcanics are younger. These volcanics are clearly overlain by the Bedrock Spring Formation, and fragments of them are found throughout most of the Bedrock Spring Formation in the western and northern parts of the mapped area.

BEDROCK SPRING FORMATION

The Bedrock Spring Formation, a new formation named here, is the most widespread sedimentary rock unit in the Lava Mountains region. It is named after Bedrock Spring, 2 miles north of Dome Mountain and about 1 mile west of the type section. The location and lithology of the rocks in the type section are shown in figure 6. It is assigned an age of middle Pliocene; vertebrate fossil collections indicate it to be of this age or possibly late early Pliocene.

The rocks assigned to this formation were included in the Rosamond Formation of Hulin (1925, p. 42–48). That name has not been used in this report because the Rosamond Formation as Hulin mapped it included the Bedrock Spring Formation plus part of the overlying Almond Mountain Volcanics of this report, and because as pointed out by Dibblee (1958, p. 135), the name has been applied so indiscriminately to Tertiary rocks in the Mojave Desert that it has lost its usefulness.

The most extensive exposures of this formation are in the northern half of the mapped area. The formation

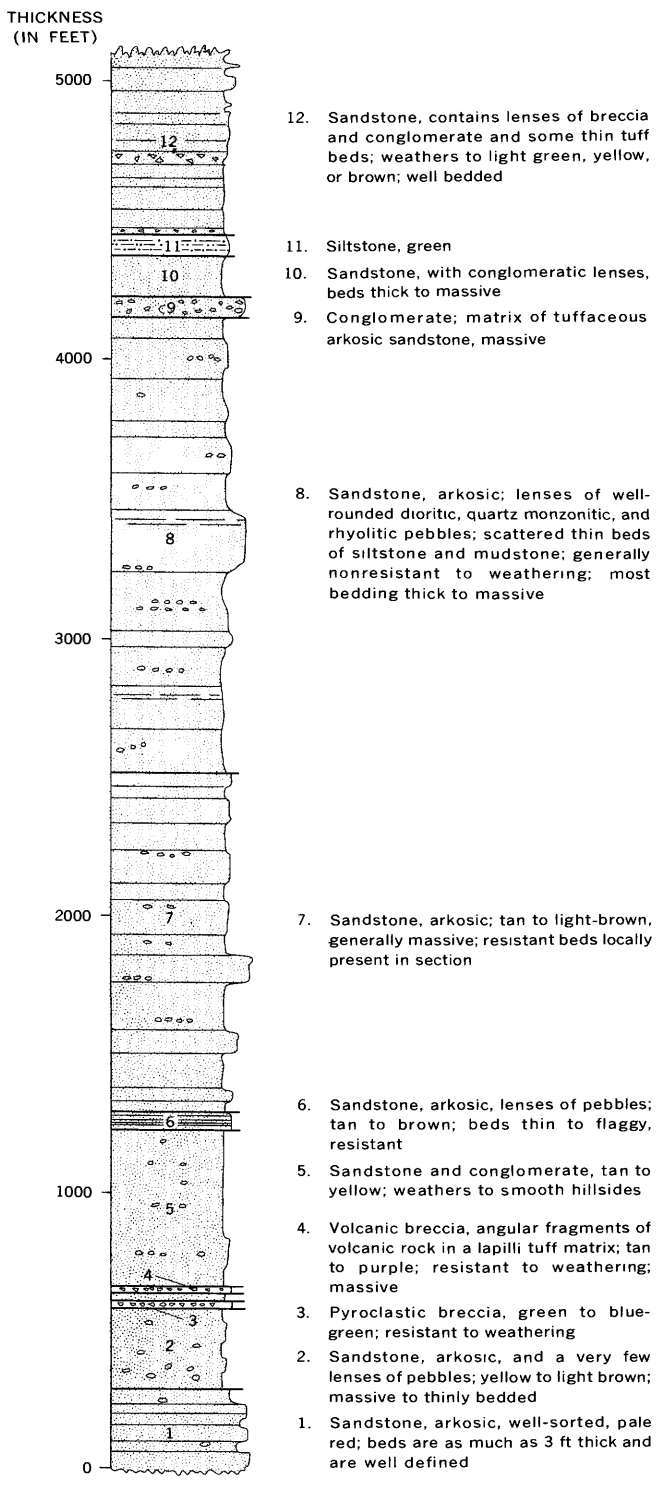

FIGURE 6.—Type section of the Bedrock Spring Formation. The base of the measured column is located in sec. E5–f; from there it extends N. 35° W. for 2,500 feet to the base of unit 4, then is offset northeast to sec. B31–a, and from there extends N. 35° W. for 3,000 feet and then S. 80° W. for 6,500 feet.

thickness is difficult to establish in many areas, though, because of the lack of widespread stratigraphic markers within it. Several thousand feet of section is exposed on the flanks of the Dome Mountain anticline. Sections that exceed 1,000 feet in thickness have been measured elsewhere in the mapped area and to the southwest of it, near Red Mountain. A thickness of more than 5,000 feet is exposed at the type section. This is probably close to the maximum thickness of this formation in the area.

The formation consists chiefly of coarse arkosic conglomerate, sandstone, siltstone, and claystone, with smaller amounts of limestone, evaporites, tuff, tuff breccia, rubble breccia, and lapilli breccia. On the geologic map (pl. 1), the larger lenses of these minor rock types have been differentiated wherever their stratigraphic thickness and extent allowed, but neither a fixed order of succession nor a fixed position within the formation can be assigned. Most of the formation is included within the unit termed "epiclastic rock," which indicates sections composed mostly of conglomerate, sandstone, siltstone, or claystone; the small volumes of limestone and evaporites are also included in this unit because of their intimate association with the finer grained epiclastic rocks. The unit termed "volcanic breccia" indicates those lenses of rock that consist primarily of tuff breccia, rubble breccia, or lapilli breccia. The unit termed "tuff" indicates those lenses of rock that consist primarily of tuff or lapilli tuff.

The contact between Bedrock Spring Formation and older rocks is exposed in many places. These older rocks were almost certainly parts of hills in the depositional basin, though, and still older sediments were deposited in the areas between these hills. Rocks representing these older sediments crop out along the axis of the Dome Mountain anticline in the central part of the range, but the oldest part of the formation is probably not exposed.

The oldest exposed rocks are well-bedded reddish sandstones, which are well sorted and virtually free of conglomerate and volcanic debris (fig. 7); their lithology suggests that they were deposited in a lake (whereas most of the younger sediments of this formation were probably deposited subaerially). Well-bedded reddish sandstones are also exposed about a mile southeast of the fold axis (in sec. E5–r) where an intraformational unconformity separates them from overlying yellowish-tan conglomeratic sandstone, indicating that at least one period of local deformation and erosion occurred very early in Bedrock Spring time.

The top of the Bedrock Spring Formation has probably been everywhere removed by erosion. In most places, the formation was strongly deformed and several thousand feet of material removed by erosion prior to deposition of the overlying Almond Mountain Volcanics. In a few places, the formation is conformably

FIGURE 7.—Lower part of the Bedrock Spring Formation, as exposed in sec. E5–e near the base of the type section. The beds in this area weather to red brown. Pick in the lower left corner gives the scale. Hill in background consists of Quaternary andesite.

overlain by the Almond Mountain Volcanics, but the overlying volcanics were apparently all deposited on a continuation of the same erosional surface, so significant erosion of the underlying formation is likely in these areas as well.

DESCRIPTIONS OF LITHOLOGIC MAP UNITS

EPICLASTIC ROCK

Sandstone and conglomerate.—The best exposed sections of sandstone and conglomerate are at the type section and in sections B32 and D2. Most of the rocks are poorly indurated and weather to form rounded hills in areas of low relief, or to form badland topography. The few beds that are well indurated form conspicuous cliffs, ridges, or ledges on what are otherwise smooth hillsides covered with overburden.

Bedding is obscure except in areas with unusually good exposures, where the beds exhibit all variations ranging from flaggy (as in sec. E1) to massive (as in secs. B20 and B29). Some beds are crossbedded and channeled and commonly contain a few larger boulders or cobbles in the channel bottoms. Few beds can be traced more than 2,000 feet, and most cannot be traced more than 500 feet. A well-exposed section and a detailed view of the most common type of arkosic sandstone are shown in figure 8. The lithologies shown in these photographs are representative of more than three-quarters of the Bedrock Spring Formation.

In most areas these rocks are a light pinkish tan, but in a few areas the rocks are reddish or greenish. Notably red sandstones are found along the axis of the Dome Mountain anticline (in secs. E5–e, E5–f, E4–e, and E4–f), and on the north side of Klinker Mountain (in sec. D2–g); they are most abundant in the lower part of formation. The coloring seems due to iron

FIGURE 8.—Upper photograph shows an example of the dominant lithology of the Bedrock Spring Formation as exposed in sec. B32–c. The beds dip north at about 10° and weather to a uniform light tan. The bushes on the left side are about 1 foot high. Lower photograph is a detail of the lithology shown on the right side of the upper view. Note the crude graded bedding.

oxides, but is not obviously related to grain size, bedding, or any other textural variable. Some beds change color laterally over a distance of a few hundred feet, grading from red into light green, yellow, or the normal color for this formation. As noted by Hulin (1925, p. 43), the red coloring is not a surface effect, and rock samples from mine shafts several hundred feet deep show similar coloration.

The sandstone in this formation is generally composed of angular fragments showing crude sorting. The most common size range is between coarse and very coarse sand but finer material is not uncommon. This rock is only slightly indurated in most areas, and can be gouged out with a pocketknife. The cement is mostly calcareous. Conglomerate clasts, mostly less than 2 inches in diameter, are well rounded to subrounded and

show little sorting (fig. 8). They include the following rocks: pink leucocratic quartz monzonite, pink aplite, gray quartz monzonite, pegmatitic rocks, quartz, metasedimentary rocks, purple porphyritic volcanics, massive rhyolitic rocks with uniform coloring, and rhyolitic rocks showing prominent color banding. Volcanic rocks constitute 10 to 30 percent of the fragments.

Exceptionally well indurated sandstones are found about 2 miles south of Klinker Mountain (in secs. D26 and D27), where they have been silicified as a result of intrusive volcanic activity. They break with a smooth conchoidal fracture and weather to form hills that are smooth and steep. Bedding, where visible, is indicated by linear rows of small rounded fragments. The outcrops are generally light brown, although some are slightly orange. The rock consists of about 60 percent detrital quartz and feldspar, and about 40 percent secondary quartz (and possibly some chalcedony or opal) which now cements the grains together. Minor amounts of sericite(?), serpentine(?), and opaque minerals are also present.

Siltstone and claystone.—Siltstone and claystone crop out in several areas along the flanks of the Dome Mountain anticline. The best examples of these lithologies are found in the central part of the mapped area (in secs. E3–a and E3–g). Although these rocks are composed chiefly of silt- and clay-sized clastic fragments, they consistently contain a small percentage of fine to coarse sand. Both the siltstones and claystones are poorly consolidated and weather to form low smooth hills covered with slumped material. The best fossils found in the Bedrock Spring Formation have come from rocks with these lithologies. The colors of the outcrops range from light green through yellow to gray. Bedding, where visible, is distinct and thin.

Chemical precipitates form a small percentage of the rocks of this type in four areas; their presence is important because it helps confirm that the depositional environment was a closed desert basin. In the siltstones in section E3–h, small amounts of halite are concentrated on the weathered surface as an efflorescence. In sections B26–a, b, and g, thin beds and large crystals of gypsum form several percent of the rock, and beds of greenish or yellowish tuffaceous limestone, 1 to 5 feet thick, occur 200 feet higher in the section. Similar beds of limestone are also found in section B27–h. A distinctive variety of limestone is found about 2 miles east of Dome Mountain (in secs. E9–b, E9–j, and E9–k) where it is shown on the geologic map by marker contacts. It is 2 to 4 feet thick, weathers to a light yellowish gray, and contains abundant ostracods and possibly other fossils. When the rock is dissolved in acid, an oily film rises to the surface.

VOLCANIC BRECCIA

Tuff breccia, rubble breccia, and lapilli breccia form thick and extensive lenses at several horizons within the Bedrock Spring Formation, mostly in the central part of the mapped area. The best examples of these lithologies are found in sections B31, E2, and E4. The rocks generally occur as single thick layers that are more resistant to erosion than the overlying and underlying beds and hence are well exposed. In outcrop, they are hackly and jagged, the fragments being more resistant to weathering than the matrix. Colors vary from brownish gray to gray with an occasional purplish tint. Some layers are as thick as 100 feet, although most have thicknesses between 25 and 50 feet. Many can be traced several thousand feet along the strike and two can be traced nearly a mile.

Most of these rocks consist of randomly oriented angular to slightly rounded fragments in a matrix of tuff or lapilli tuff. These fragments, which form more than 50 percent of the rock in most outcrops, consist of grayish, brownish, or purplish volcanic lavas or tuffs. The lava fragments are virtually all andesite and contain phenocrysts, several millimeters long, of plagioclase, biotite, hornblende or oxyhornblende, and pyroxene.

One bed of tuff breccia contains fragments of only one lava type, and a sample of these fragments was collected and analyzed (table 4). The results are used to represent the petrographic and chemical characteristics of lavas extruded during Bedrock Spring time. The lithology of this bed is not typical of the volcanic rocks in the Bedrock Spring Formation, but the fragments are almost certainly all the product of a contemporaneous volcanic eruption.

This bed of tuff breccia consists of light-gray angular fragments of porphyritic andesite as long as 2 inches, in a tuffaceous matrix of the same color. Color banding in the fragments results from slight variations in the composition of the groundmass. The euhedral plagioclase phenocrysts form crystals as large as 4 mm; microphenocrysts do not form a distinct generation although crystals smaller than 0.3 mm make up about 5 percent of the rock. Zones are oscillatory-normal, normal, or mottled; calcic rims are not present. Albite twinning is well developed in about half the crystals. Biotite is found in some samples as euhedral crystals with no reaction rim. Hornblende, which may be in part oxyhornblende, occurs as euhedral crystals with no reaction rim and very few opaque inclusions. Orthopyroxene, as clear euhedral prisms, commonly has inclusions of magnetite. A few clinopyroxene crystals are present. The groundmass consists of about 68 percent glass, 30 percent cryptocrystalline material, and 2 per-

cent needlelike plagioclase(?) crystals. There is very little opaque material, although color banding is caused by minor variations in this small percentage. Vesicles, mostly microscopic but some as large as 1 mm, are abundant and show a faint alinement. Maximum crystal sizes are: plagioclase, 4 mm; biotite, 3 mm; hornblende, 2.5 mm; and orthopyroxene, 0.3 mm.

Modal, normative, chemical, and spectrochemical analyses of a sample of fragments from this rock are listed in table 4. The modal composition shows that these fragments are andesite. The chemical composition is close to Nockold's "average dacite" (1954b, p. 1015), and it shows such low percentages of CO_2 and excess H_2O that significant alteration is improbable. The normative composition shows that on complete crystallization, K-feldspar would have formed about 16 percent of the total feldspar, and this rock would have become granodiorite with about 18 percent quartz and a plagioclase composition of An_{33}.

TABLE 4.—*Modal, normative, chemical, and spectrochemical analyses for one sample of the volcanic breccias in the Bedrock Spring Formation*

[Sample 128-32 from sec. E2-e, outcrop on south side of wash. A dash means the element was not present in detectable amounts. Chemical analyses by P. L. D. Elmore, H. F. Phillips, and K. E. White; spectrochemical and modal analyses by G. I. Smith]

Modes

[Volume percents]

Plagioclase megaphenocrysts	15.1
Plagioclase microphenocrysts	5.1
Total plagioclase	(20.2)
Biotite	.5
Hornblende	6.3
Oxyhornblende	0
Orthopyroxene	1.2
Clinopyroxene	0
Quartz	0
Opaque minerals	1.5
Other minerals	.1
Groundmass	70.2

Chemical analyses

[Weight percents]

SiO_2	64.8
Al_2O_3	16.6
Fe_2O_3	1.4
FeO	2.2
MgO	2.0
CaO	4.6
Na_2O	4.5
K_2O	2.0
TiO_2	.58
P_2O_5	.20
MnO	.08
H_2O	1.2
CO_2	.27
Total	100

Norms

[Weight percents]

Q	18.2
C	0
or	11.6
ab	38.2
an	19.2
di	2.9
hy	5.1
mt	2.1
il	1.2
hm	0
tn	0
ru	0
ap	.3
Symbol (C.I.P.W.)	I.4.3.4

Spectrochemical analyses

[Parts per million]

Cr	60?
Co	40
Mn	550
Ni	20
Sc	10
V	70
Fe	26,000
Cu	10
Ga	10
Ti	2,400
B	30
Ba	2,400
Be	—
Li	19
Pb	20
Rb	20
Sr	1,600
Yb	1
Y	10
Zr	130

TUFF

Tuff and lapilli tuff occur as thick lenses within the Bedrock Spring Formation, chiefly in the central and northeastern parts of the mapped area. Most of the rocks included in this unit are lapilli tuff. They contain ash-sized fragments of euhedral to subhedral feldspar, quartz, hornblende or biotite, and lapilli-sized fragments of andesite.

In the central part of the area, the best exposures of rocks included in this unit are in sections B31–a and E4–l. They weather light green or light blue green, and form cliffs which have uneven and hackly surfaces. They are most commonly massive. Some beds are as thick as 100 feet, but the average thickness is nearer to 20 or 30 feet. Many can be traced along strike for several thousand feet.

In the northeastern part of the area, these rocks are best exposed in section B24–h, where they weather to smooth slopes colored light shades of pink, yellow, and green. Most of them are very well bedded, although individual beds cannot be traced for more than a few hundred feet.

DISTRIBUTION OF ROCK TYPES AND ENVIRONMENT OF DEPOSITION

The distribution and character of rocks of the Bedrock Spring Formation show that the middle Pliocene sedimentary basin was a closed valley surrounded by alluvial fans that sloped from all directions toward a central lake or playa. The sandstone and conglomerate (see fig. 8) that represent these alluvial fans are strikingly similar to present-day alluvium of areas in the Mojave Desert that have a dominantly quartz-monzonitic provenance. The central lake is represented largely by siltstone and claystone but contains small amounts of gypsum, limestone, and evaporites. The soluble salts entrapped in the sediments, along with a small number of diagnostic diatoms, indicate that the lake much have been saline and without an outlet for much of the time. Snails found in these fine sediments, however, show that the central lake was at times perennially fresh. Most of the lenses of volcanic breccia, tuff, and lapilli tuff also crop out within this central area, but this is probably a result of the position of contemporaneous vents rather than the shape of the sedimentary basin.

The surrounding alluvial fans sloped from all directions toward this central playa as shown by a survey of the rock types found as pebbles in the formation. In the north and northwest exposures of the Bedrock Spring Formation, the fragments are derived from the types of Atolia Quartz Monzonite exposed to the north. In the northeast exposures of the Bedrock Spring Formation, an abundance of fragments derived from the nearby metamorphic rocks shows that these rocks cropped out and persumably formed the northeast edge of the sedimentary basin. In the east and southeast exposures of the Bedrock Spring Formation, the pebbles were derived chiefly from the quartz-monzonitic and rhyolitic rocks exposed 2 or 3 miles southeast of the mapped area (fig. 2); fragments of the hornblende amphibolite exposed near the Blackwater fault are not

found here, however, suggesting that the alluvial sediments extended southeast at least to the area of their present outcrop. To the south and southwest, toward Red Mountain, the full extent of the Bedrock Spring Formation has not been mapped in detail, but reconnaisance suggests that the conglomerates in the southwest extension of the formation on Red Mountain were derived from the plutonic rocks exposed a few miles southwest of that area. Along the west boundary of the map area, fragments in the Bedrock Spring Formation derived from the Rand Schist and Johannesburg Gneiss of Hulin (1925, p. 20–31) indicate a source within a few miles to the west; a few outcrops of the Bedrock Spring(?) Formation on the west end of the Summit Range (fig. 2), however, show that an arm of the middle Pliocene basin probably extended westward to that point.

The approximate outlines of this inferred basin of sedimentation and of the area within it containing finer grained sediments are shown in figure 9. The indicated area of sedimentation is about 200 square miles; the area of playa or lake sedimentation is about 15 square miles. A gravity survey of the area west and south of this region (Mabey, 1960) shows that the bedrock depression containing these rocks is continuous with Cenozoic sedimentary basins south of Cuddeback Lake and northwest of the Rand Mountains. Although the gravity data permit the interpretation that middle Pliocene sediments extended into those basins, the exposed geology of those regions (Dibblee, 1952, p. 38; 1964) indicates that earlier Cenozoic rocks probably occupy them.

Downwarping or faulting between the Garlock fault and Brown's Ranch fault zone is indicated as the cause of a depositional basin in this area. As shown by figure 9, the basin was generally parallel to the Garlock fault, but was slightly elongate to the southwest along a line approximated by the Brown's Ranch fault zone. Although this inferred relation requires both faults to have been active, the proximity of the playa sediments in the Bedrock Spring Formation to the trace of the Garlock fault suggests that during middle Pliocene time that fault was more frequently active than the faults included in the Brown's Ranch fault zone.

The coexistence of evaporites indicative of a saline

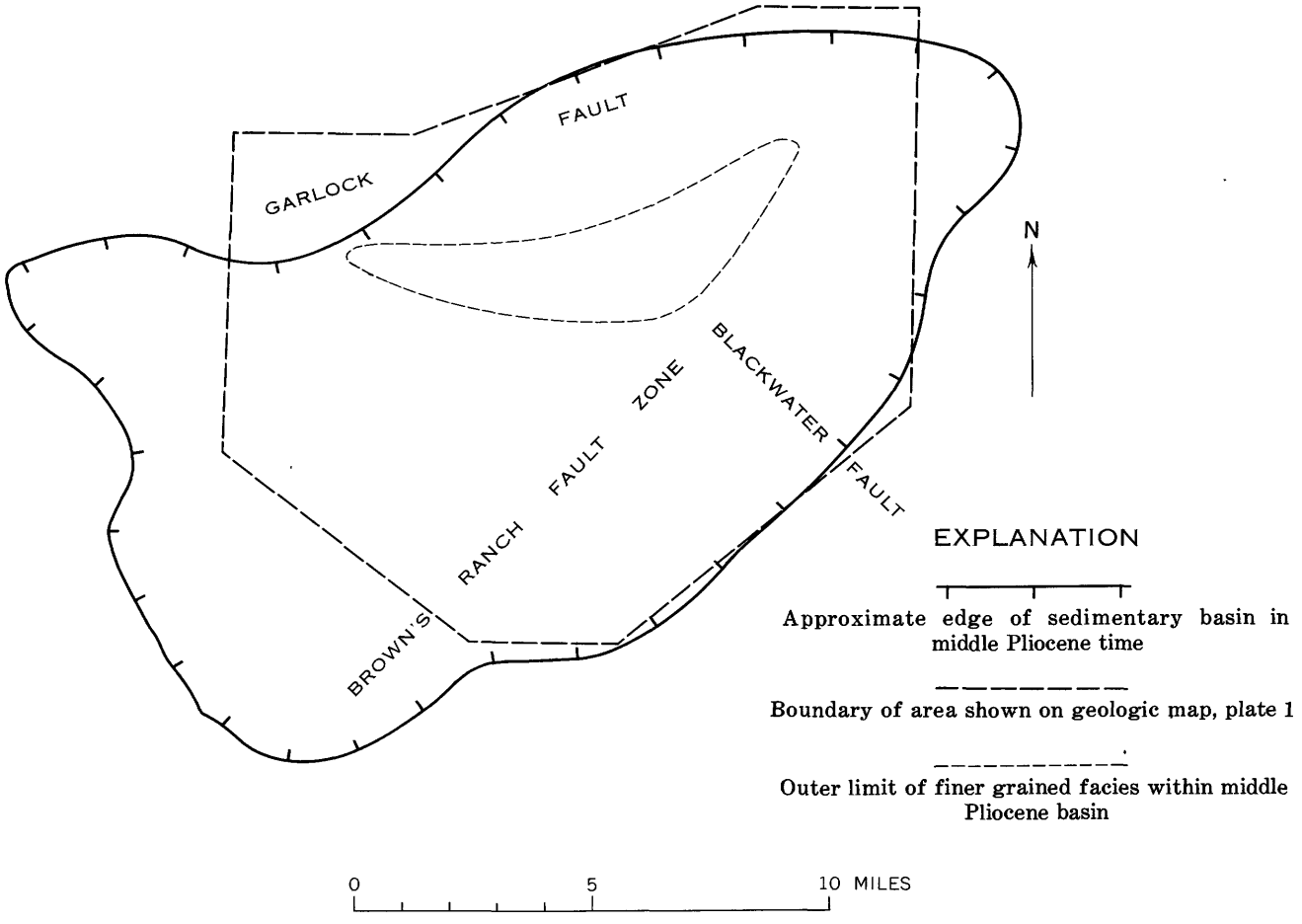

FIGURE 9.—Diagrammatic map showing the inferred limits of the basin of sedimentation in Bedrock Spring (middle Pliocene) time and the approximate limit of the fine-grained facies within the basin.

or dry lake, and snails indicative of a perennial fresh lake, seems contradictory; a probable explanation is that the basin center was occupied by a playa during most of middle Pliocene time, but that occasional wet cycles produced a small lake that could maintain a fresh-water snail population for a few years until evaporation raised the salinity to an unfavorable level; these wet cycles must have also created a connection with a perennial lake in which such snails lived.

The middle Pliocene climate in this area may thus have been similar to that of today's climate in northern Nevada and southeastern Oregon. Many of the closed basins in those areas now contain wet playas or small lakes, and it is evident that small changes in the present climate would convert one type of lake into the other. The precipitation in those areas presently is two to three times that of the Mojave Desert.

AGE AND RELATION TO OTHER FORMATIONS

A large collection of fossils from the Bedrock Spring Formation was made in 1952 by R. H. Tedford and Robert Shultz, Jr. Some additional material was collected by T. W. Dibblee, Jr., G. N. White, and me.

G. E. Lewis writes of the vertebrate fossils as follows (written commun., 1956):

> I have made comparisons with other collections in several museums. My best guess is that the age of most of the fossil vertebrates in your collection from the Lava Mountains area corresponds to that of the middle to upper parts of the Ogallala group of Nebraska. The Lava Mountains fossil vertebrates are comparable to those found in the Ash Hollow formation of the Nebraska Survey, and seem to be intermediate between those of the Chanac and Kern River formations of California. This age may be as young as middle Pliocene (assuming the age of the Villafranchian fauna of Europe, and that of the *Equus* (*Plesippus*) fauna, to be earliest Pleistocene in conformity with interpretations given at the 1948 International Geological Congress), but may be as old as late early Pliocene.
>
> Significant determinations are:
> Order PERISSODACTYLA
> Family Equidae
> *Pliohippus* cf. *P. leardi*, from localities LM–6, LM–13, LM–20, and LM–21.
> *Pliohippus sp.*, from localities LM–10 and LM–15.
> Order ARTIODACTYLA
> Family Camelidae
> *?Pliauchenia* sp., from localities LM–6, LM–8, LM–11, LM–13, LM–15, LM–16, LM–20, and LM–26.
> *?Megatylopus* sp., from localities LM–10, LM–16, and LM–21.
> Order LAGOMORPHA
> Family Leporidae
> cf. *Hypolagus* sp., from localities LM–15 and LM–16.
> Order RODENTIA
> Family Cricetidae
> cf. *Neotomodon* sp., from localities LM–15 and LM–16.
> A complete list of determinations is attached. [See table 20.]

Although these fossil data show that the Bedrock Spring may be as old as late early Pliocene, for simplicity the formation is referred to throughout most of this report as being of middle Pliocene age.

One fossil locality also contained abundant snails of which D. W. Taylor writes the following (written commun., 1960):

> The fossils from locality LM–6 (U.S. Geological Survey Cenozoic locality 22324), represent two kinds of snails. One is a small low-spired or planispiral form not surely identifiable. It may be a land snail, or one of the fresh-water family Planorbidae. The other species is a relatively large fresh-water snail of the genus *Bulimnea*. Perhaps it is *B. megasoma* (Say), recorded from late Miocene deposits in the Barstow syncline to the south (Taylor, 1954), but the material is not well enough preserved for certain identification.
>
> The known range of *Bulimnea* is from the middle to late Miocene Mascall formation, Oregon, to Recent. West of the Rocky Mountains, however, none of the occurrences is younger than middle Pliocene. * * *
>
> The fossils may not belong to the living species *Bulimnea megasoma* (Say). Nevertheless the relatively large size of the Lava Mountains specimens, and their similarity in proportions of shell to the living *Bulimnea*, justify some general inferences about habitat. By analogy with the recent occurrences of *B. megasoma*, the fossils from the Lava Mountains indicate a perennial body of fresh water. This may have been a lake, marshy pond, or swamp, but probably had little current action. No detailed interpretation of local habitat or of climate is warranted, but from the occurrence of a perennial water body in what is now arid desert one may suppose the annual rainfall was formerly somewhat greater.

Only one of 38 samples examined for diatoms by K. E. Lohman contained an identifiable assemblage. Of it, he writes (written commun., 1962):

> The following meager assemblage was obtained from field sample No. LM–119 [same locality as LM–8, shown on plate 1]; USGS diatom locality No. 5451:
>
> *Caloneis* cf. *C. schumanniana* (Grunow) Cleve
> *Caloneis* sp.
> *Navicula* spp.
> *Nitzschia* spp.
> *Rhopalodia gibberula* (Ehrenberg) Muller
> *Surirella* sp.
>
> Of the two diatoms that could be identified specifically, *Caloneis* cf. *C. schumanniana* has a known geologic range of late middle Miocene to Recent, and the identification is a doubtful one as indicated. *Rhopalodia gibberula* was the only diatom found in a state of preservation adequate for definite specific identification. It has a known geologic range of middle Pliocene to Recent and is living today in very saline lakes.
>
> This assemblage was probably deposited in a shallow, very saline lake. The only age assignment that can be made with the meager data at hand is middle Pliocene or younger.

The approximate stratigraphic positions of the fossil localities and the probable correlation between beds in three of the fossil-bearing sections are plotted in figure 10.

No other Pliocene rocks in the northern Mojave Desert or in the southwestern Basin Ranges are known to con-

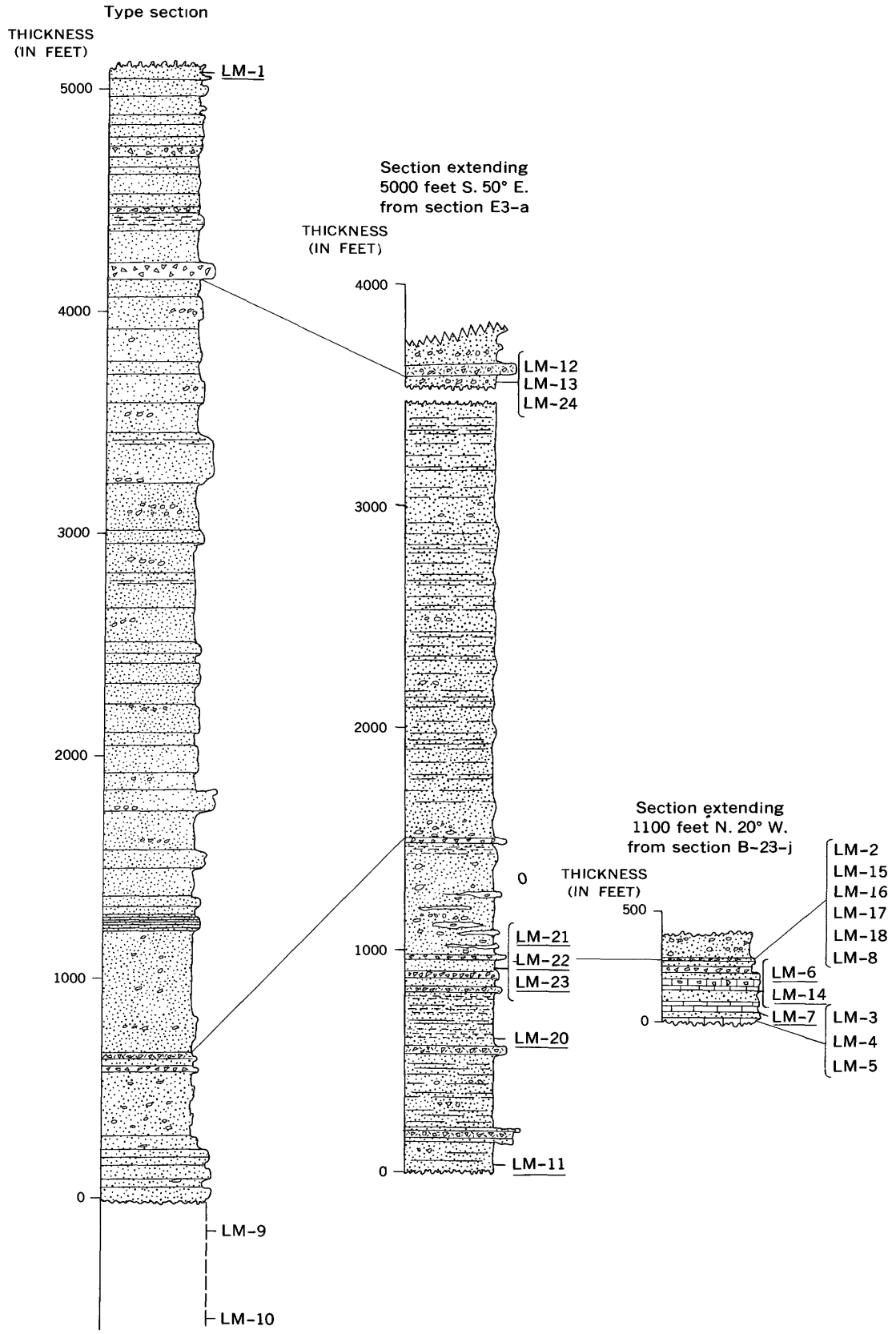

FIGURE 10.—Measured sections of the Bedrock Spring Formation showing the stratigraphic position of fossil localities shown on plate 1. Localities that can be traced directly into the measured sections are underlined and those approximately correlated are not. Localities LM–9 and LM–10 are east of the type section and probably are several hundred feet stratigraphically below its base. Correlated beds are connected by lines. See table 20 for fossil lists.

tain fossils of exactly the same age as those in the Lava Mountains. Within the Mojave Desert, three other Pliocene faunas are known—all only a few miles south of the Garlock fault. In the Avawatz Mountains (Henshaw, 1939), rocks containing lower Pliocene fossils are exposed. Rocks about 4 miles northwest of Mojave contain fossils of middle Pliocene age (identifications by Lewis, Stock, and Tedford, as quoted by Hewett, 1955). A limestone from Castle Butte, east of Rosamond, yields lower Pliocene diatoms (determined by K. E. Lohman, quoted by Hewett, 1954a, p. 16). All the other fossil collections from areas south of the Garlock fault, within the Mojave Desert, are of Miocene or Quaternary age. North of the Garlock fault, in the southwestern Basin Ranges, dated lower Pliocene rocks are exposed in the Ricardo Formation of the El Paso Mountains (Dibblee, 1952, p. 25–30) and in Death Valley (Axelrod, 1940; Curry, 1941; Noble and Wright, 1954, p. 147–149), and very late Pliocene or Pleistocene rocks containing *Equus* (*Plesippus*) are exposed in the Coso Mountains (Schultz, 1937).

ALMOND MOUNTAIN VOLCANICS

The Almond Mountain Volcanics is a new formation named here. It includes both intrusive and extrusive volcanic rocks that are exposed in the southern half of the mapped area. The formation is named for Almond Mountain, located in the southern part of the map area. The type section is designated as the section exposed about a third of a mile northwest of the summit, but neither this nor any other one section is representative of the formation over a large area. The type section diagrammed in figure 11 is about 900 feet thick but includes only the lower half of the formation exposed in this vicinity; (see pl. 2, section *D–D'*); the rocks that form the upper half crop out east of Almond Mountain, but they are not as well exposed as those at the type section and cannot be stratigraphically tied to that section with the desired accuracy.

This formation includes rocks that were divided by Hulin (1925, p. 42–58) between the "Rosamond Formation" and the "Red Mountain Andesite." He reported that tuffs and vocanic breccias were represented in both formations, but did not indicate either that they were markedly concentrated along the top of his Rosamond Formation and the base of his Red Mountain Andesite, or that they were mostly separated from the lavas and sandstones by an unconformity. By comparing his geologic map with the one accompanying this report, though, it is evident that the rocks here assigned to the Almond Mountain Volcanics were divided between those two formations.

Rocks of the Almond Mountain Volcanics are intruded into, or rest with an angular unconformity on, the middle Pliocene Bedrock Spring Formation and

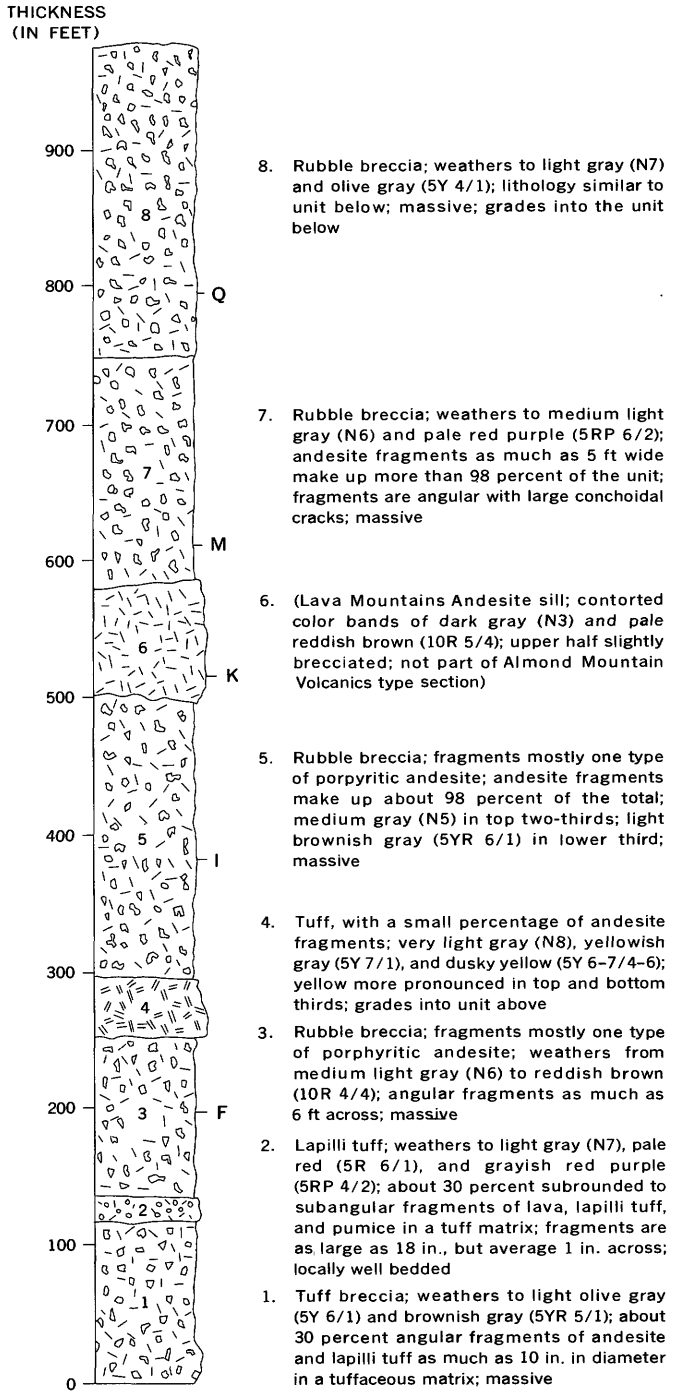

FIGURE 11.—Type section of the Almond Mountain Volcanics. The measured column extends 1,700 feet S. 70° E. from sec. E34–c. The letters show the relative positions of the 124–22 series of samples described in table 5. Unit 6, part of the Lava Mountains Andesite, is not part of the type section.

older rocks. The other upper Pliocene(?) volcanics shown on the geologic map are in most places demonstrably younger than the Almond Mountain Volcanics, but the exposures are inadequate to rule out some of them as contemporaneous or a little older. The Almond Mountain Volcanics are intruded or unconformably overlain by the Lava Mountains Andesite.

On the geologic map (pl. 1), rocks of the Almond Mountain Volcanics have been divided into nine lithologic map units, of which four make up the eastern facies of the formation and five the western facies. The rocks of the two facies are areally separated by the valley containing the Brown's Ranch fault zone except at the northeast end of the valley where they are interbedded. Though the rocks constituting the eastern and western facies are similar, they can be distinguished in the field by their lithology or lateral distribution. The distinction made in the field between facies is retained on the geologic map (pl. 1) and in this description because it clarifies the depositional pattern, namely, the simultaneous eruption of volcanic material from an eastern and a western center to form a continuous layer of debris over 75 to 100 square miles. Both eruptive centers apparently consisted of several irregularly shaped vents that brought lavas to the surface to form domes immediately above the vents, and a much larger area of fragmental volcanic debris around them. The rocks closest to the western eruptive center were subsequently altered.

Some interbedded lenses of arkosic sandstone are included in the Almond Mountain Volcanics. Though they might well be considered part of another formation because of their distinctly different lithologies and origin, they are included in this formation because they constitute too small a unit to be separated, and their stratigraphic position relative to the Bedrock Spring Formation is too different to allow their inclusion in it.

The eastern facies of the Almond Mountain Volcanics includes the type section and consists of a variety of rock types that have been divided on the geologic map among four lithologic map units. These units have varying stratigraphic relations within the formation; they are therefore considered as a group to be contemporaneous. One of these lithologic map units consists of unstratified volcanic rocks that are mostly intrusive, although the field relations show that they also grade laterally into the stratified members. The other lithologic map units are stratified. These layered rocks have been combined into three categories: (a) "volcanic breccia," which includes all flow breccias, rubble breccias, lapilli breccias, and tuff breccias; (b) "tuff," which includes all tuffs and lapilli tuffs, and (c) "sandstone," which includes all sandstones and a few conglomerates.

The western facies consists of five lithologic map units. Two of them constitute a hydrothermally altered volcanic complex; the other three are composed of stratified rocks. The rocks characterized by the more intense hydrothermal alteration are propylites.[1] In this report, the rocks that are less intensely altered are called "subpropylite." The subpropylite appears to overlie the propylite, but this reflects a boundary in the intensity of hydrothermal alteration rather than a stratigraphic or intrusive succession. Reconnaissance mapping suggests that this alteration zone extends another 2 or 3 miles southwest of the mapped area. The stratified rocks plunge into or overlie the altered volcanic complex in many places, but probably this too reflects the outer and upper limits of alteration rather than an order of deposition. Most of the rocks of the hydrothermally altered volcanic complex are intrusive necks or dikes; the bedded volcanic rocks are apparently extrusive equivalents.

The thickness of each of these lithologic map units varies markedly from place to place. The number of separable units in any given stratigraphic section also varies. Both their thickness and number depend chiefly on the distance between the stratigraphic section being considered and the center of the contemporaneous volcanic activity. The stratigraphic order of units is also variable, and even the lithology of the basal unit varies to include all the layered rock types represented in the formation. Because of this variability, individual stratigraphic sections have only local significance, and the sequence of lithologic map units in one area cannot generally be duplicated in another.

DESCRIPTIONS OF LITHOLOGIC MAP UNITS

ROCKS OF THE EASTERN FACIES

Volcanic intrusives

The lithologic map unit designated "volcanic intrusives" includes the porphyritic andesites of the eastern facies that are not bedded. Most of the outcrops of this unit are inferred to be shallow volcanic intrusives on the basis of crosscutting relations or steeply dipping flow structures, although some are probably volcanic domes or very thick flows.

The largest outcrops of this unit are on the west and south sides of Almond Mountain, and on the large hill 1½ miles northeast of it. The rocks form steep-sided hills whose lower slopes are almost entirely sheathed by talus. On weathered surfaces, the color varies from the dark brown of desert varnish to that of the fresh rock, which is light brownish gray.

The petrography of the massive volcanic intrusives is similar to that of the fragments in the stratified breccias. Most of the rocks contain plagioclase, biotite, oxyhornblende, clinopyroxene, and orthopyroxene; a few contain quartz. The biotite and oxyhornblende crystals are heavily altered, but the plagioclase and

[1] Propylite is a term that was first used by von Richthofen (1868) for rocks in the Comstock Lode that are now known to be hydrothermally altered andesites. The thoroughly altered rocks at the original locality are characteristically greenish and contain secondary epidote, chlorite, albite, calcite, sericite, and quartz (Coats, 1940, p. 11–12).

pyroxene crystals are almost fresh. The groundmass consists of 75 to 95 percent glass or cryptocrystalline material, the balance being skeletal crystals and opaque minerals. The maximum size of the plagioclase, biotite, and oxyhornblende crystals is about 3 mm; the orthopyroxene and clinopyroxene crystals are mostly less than 1 mm.

Volcanic breccia

Volcanic breccia forms the bulk of the Almond Mountain Volcanics in the area around and south of Almond Mountain. The best exposures are found at the type section and in sections F19 and E25. In outcrop, these rocks form resistant beds and ledges, the flow and rubble breccias being somewhat more resistant than those containing a large percentage of tuff or lapilli tuff. The colors of the breccia fragments are distinctive, and provide one means of distinguishing rocks of this formation from those of the overlying Lava Mountains Andesite; these distinctive colors vary from medium light gray (*N* 5–7), through light olive gray (5*Y* 6/1) and brownish gray (5*YR* 4–8/1), to pale red (10*R* 6–7/2) and pale red purple (5*RP* 6/2). Most of the mapped layers are 100 feet or more thick; one may exceed 1,000 feet in thickness. Within these layers, beds defined by textural changes are rare, but stratigraphic successions of distinctively colored breccias are common. Along the strike, rocks assigned to this map unit may be continuous for a mile or more, but the textural detail of any given volcanic breccia normally changes within a distance of a few hundred feet.

Most of the rocks of this unit are rubble breccias, and fragments form more than 90 percent of the total volume. Flow breccias, lapilli breccias, and tuff breccias are subordinates. The fragments are without exception volcanic rocks. All are blocky and angular; neither bombs nor fragments having bread-crust structures were observed. The matrix in the rubble breccias generally is lapilli tuff. The matrix of the flow breccias is lava, which in some places is identical with the fragments and in others is different in color though of about the same mineralogy.

Results of thin-section study emphasize the similarity between the fragments contained in widely separated outcrops of these rocks. All contain plagioclase phenocrysts, and three-quarters of the rocks also contain biotite, oxyhornblende, and orthopyroxene. Only about one-third contain quartz. The plagioclase is found as megaphenocrysts and microphenocrysts in about equal proportions; zone and twin development is variable, and a calcic rim is present on the megaphenocrysts in about half the rocks. Many of the biotite and oxyhornblende crystals show partial or complete deuteric alteration to opaque materials and pyroxene; plagioclase grains in the crystals may be either alteration products or inclusions. The orthopyroxenes are virtually unaltered. Clinopyroxene is found in about two-thirds of the rocks and shows partial alteration in well over half.

The results of modal, normative, chemical, and spectrochemical analyses of fragments from four units exposed at the type section are presented in table 5. These four (samples 124–22 F, I, M, and Q) represent a stratigraphic thickness of about 600 feet. Although their modal percentage of plagioclase ranges from 15 to 27 percent, and their groundmass percentage ranges from 67 to 78 percent, their chemical and normative compositions show very little difference. The SiO_2 percentage ranges from 64.8 to 66.9, and most other constituents are similarly constant. Their normative compositions are also similar, and the normative feldspar compositions are all between An_{34} and An_{39}.

Most of these rocks are slightly vesicular and have a pronounced lineation resulting from the alinement of the plagioclase microphenocrysts and the oxyhornblende crystals. The plagioclase megaphenocrysts are very commonly clustered together. The euhedral shape of some of these crystals shows that clustering occurred after they had grown to nearly normal shape and size, but more commonly it occurred at an earlier time so that there was a mutual interference of growth. Microphenocrysts of plagioclase rarely appear as attached pairs. In most rocks, the plagioclase, oxyhornblende, and biotite crystals range in size from about ½ to 3 mm. The orthopyroxene and clinopyroxene crystals are generally less than 1 mm long.

Tuff

The rocks constituting the tuff map unit of the eastern facies are mostly lapilli tuff; tuff is present but definitely subordinate. The best exposures of these rocks are found in the type section and in sections E24, F6, and F19. The rocks are well exposed and form cliffs where associated with soft sandstone or conglomerate, and are poorly exposed in areas where associated with rubble breccia, flow breccia, or flows of the overlying Lava Mountains Andesite. Most of the rocks weather to subdued shades of yellow, orange, red, or purple. Typically, they form mappable units that are several tens of feet thick, the units composed of lapilli tuff being thicker than those composed of tuff. Rocks containing an appreciable amount of sedimentary epiclastic material or pumice are locally well bedded and even graded; rocks composed entirely of other volcanic materials are generally massive. Along strike, individual beds are lenticular and rarely can be traced more than a mile.

The tuff and lapilli tuff included in this lithologic map unit consist chiefly of fine-grained glassy or cryptocrystalline material, although individual grains of euhedral biotite, feldspar, and hornblende crystals and small

TABLE 5.—*Modal, normative, chemical, and spectrochemical analyses of nine samples of the stratified lithologic members of the Almond Mountain Volcanics*

[A dash means that the element was not present in amounts greater than the limit of detection. Chemical analyses by P. L. D. Elmore, H. F. Phillips, and K. E. White; spectrochemical analyses for Li and Rb by Robert Mays, remaining spectrochemical and modal analyses by G. I. Smith]

	Western facies					*Eastern facies*			
	97-38L	*97-38K*	*97-38I*	*97-38F*	*128-33*	*124-22F*	*124-22I*	*124-22M*	*124-22Q*
Modes [Volume percents]									
Plagioclase megaphenocrysts	9.0	9.6	8.9	10.7	5.9	22.9	3.3	6.7	11.2
Plagioclase microphenocrysts	9.3	13.9	13.1	11.7	7.4	4.5	12.0	11.6	13.0
(Total plagioclase)	(18.3)	(23.5)	(22.0)	(22.4)	(13.3)	(27.4)	(15.3)	(18.3)	(24.2)
Biotite	1.2	1.0	.1	.7	0	2.2	.3	.3	.7
Hornblende	0	0	0	0	0	0	0	0	0
Oxyhornblende	.6	.8	.7	.6	Trace	0	.1	.4	1.0
Orthopyroxene	.9	.9	1.3	1.1	Trace	1.7	2.4	2.4	1.0
Clinopyroxene	.8	.6	.6	.4	.3	0	.6	.3	.7
Quartz	.1	.1	1.1	.6	.1	0	.1	0	Trace
Opaque minerals	4.1	8.1	3.3	3.6	10.2	1.2	1.6	1.3	3.1
Other minerals	1.0	4.7	.1	.4	.2	.1	.8	.1	.5
Groundmass	73.0	60.2	70.8	70.2	75.9	67.4	78.8	76.9	68.8
Chemical analyses [Weight percents]									
SiO_2	62.2	61.0	63.6	62.5	67.7	65.4	66.8	66.9	64.8
Al_2O_3	16.5	17.0	16.9	16.6	16.5	16.5	16.2	16.2	16.2
Fe_2O_3	2.4	2.3	1.5	1.8	3.3	1.2	1.1	1.0	1.9
FeO	1.6	1.9	2.6	2.4	.14	2.0	1.9	2.0	1.4
MgO	3.1	2.8	2.8	2.3	.57	1.2	1.2	1.8	1.2
CaO	4.6	5.0	4.4	5.0	4.0	3.9	3.8	3.5	5.0
Na_2O	3.8	3.6	3.9	3.8	4.3	4.2	3.9	3.8	3.6
K_2O	2.2	2.2	2.8	2.7	2.8	2.6	2.7	2.9	2.8
TiO_2	.65	.69	.68	.68	.54	.55	.50	.50	.50
P_2O_5	.24	.26	.25	.24	.19	.18	.16	.16	.17
MnO	.06	.06	.06	.06	.02	.05	.05	.04	.05
H_2O	3.1	3.2	1.1	1.8	.38	2.1	2.0	1.9	2.2
CO_2	.05	.05	.05	.05	<.05	.05	.05	.05	.11
Total	100	100	101	100	100	100	100	101	100
Norms [Weight percents]									
Q	17.7	17.4	15.7	18.9	23.2	20.1	23.0	22.6	21.7
C	0	.3	0	0	0	0	0	.4	1
or	12.8	12.8	16.7	16.1	16.7	15.6	16.1	17.2	16.7
ab	32.0	30.4	33.0	32.0	36.2	35.6	33.0	32.0	30.4
an	21.7	23.1	20.3	20.3	17.5	18.4	18.6	17.5	19.7
di	.9	0	1.3	3.6	1.7	.9	.2	0	2.6
hy	7.4	7.4	8.7	5.7	.6	4.3	4.6	6.6	2.7
mt	3.2	3.2	2.1	2.6	2.1	1.9	1.6	1.4	2.8
il	1.2	1.4	1.4	1.4	1.1	1.1	1.4	.9	.9
hm	.2	0	0	0	1.9	0	0	0	0
tn	0	0	0	0	0	0	0	0	0
ru	0	0	0	0	0	0	0	0	0
ap	.3	.7	.7	.3	.3	.3	.3	.3	.3
Symbol (C.I.P.W.)	II.4.3.4	II.4.3.4	II.4.3.4	II.4.3.4	I.4.3.4	I.4.3.4	I.4.3.4	I.4.3.4	I.4.3.4
Spectrochemical analyses [Parts per million]									
Cr	70	90	100	80	40	20	30	40	30
Co	30	40	60	50	30	20	20	40	40
Mn	370	460	400	380	210	320	340	300	340
Ni	50	60	60	50	20	10	10	10	10
Sc	5	10	5	5	2	5?	1	5?	10?
V	60	70	80	70	30	40	40	50	40
Fe	22,000	30,000	26,000	25,000	16,000	17,000	14,000	19,000	16,000
Cu	30	30	30	20	5?	10?	10	10?	10
Ga	20	20	10	10	10	10	10	10	10
Ti	2,200	2,700	2,700	2,000	1,800	2,200	1,800	2,100	2,200
B	30	30	40	30	10	40	30	50	50
Ba	2,300	2,200	1,800	1,400	1,900	1,400	1,200	1,700	2,100
Be									
Li	34	15	2	24	21	36	19	16	12
Pb	20	10	10	10	20	10	10	10	10
Rb	50	60	40	60	50	40	60	50	70
Sr	1,600	2,200	1,700	1,300	1,200	1,100	800	1,200	1,500?
Yb	1	1	1	1	1	1	1	1	1
Y	5	10	5	5?	5	5?	3	5	10?
Zr	100	150	120	80	110	100	80	100	120?

LOCATION OF SAMPLES

97-38L. Sec. E 6-j, from section trending S. 35 W. on face of cliff. Sample collected about 5 feet below top of section.
97-38K. Same section, collected about 20 feet below top of section.
97-38I. Same section, collected about 50 feet below top of section.
97-38F. Same section, collected about 100 feet below top of section.
128-33. Sec. E 10-d, sample from top of hill.
124-22Q. Type section of Almond Mountain Volcanics, ½ mile northwest of Almond Mountain; see fig. 11 for location of sample.
124-22M, 122-22I, 124-22F. Same section, see fig. 11.

rock fragments are locally common enough to be conspicuous. These components are generally angular and unsorted. In a few beds, up to a quarter of the material is sand-sized epiclastic material which normally shows some sorting and bedding. Most beds also contain a small percentage of angular to subrounded fragments, 1 to 3 inches in diameter, of purple, tan, or gray porphyritic andesite, or light-colored well-indurated lapilli tuff all embedded in the softer matrix of tuff or lapilli tuff.

A distinctive lapilli tuff bed is found northeast of Almond Mountain, especially in sections E23–h, E24–f, E25–k, and E35–f. One-third to two-thirds of it consists of light-gray or white pumice as well-rounded fragments up to an inch in diameter; the matrix is pale yellow-orange tuff or tuffaceous sandstone. Pumice is present but rare in other parts of the eastern facies of this formation; it is virtually absent in the western facies. As is evident from the position of this distinctive unit in the geologic sections (pl. 2), the bed lies a short distance above the top of the type section. More detailed mapping would fix the position of the bed relative to the type section, and it could probably then be used to relate the rest of the layered volcanic rocks east of Almond Mountain.

Sandstone

Sandstone in the eastern facies of the Almond Mountain Volcanics is well exposed in only one area, about 2½ miles northeast of Almond Mountain (in sec. E24–g). Here, it crops out in a canyon as a 50-foot bed of medium- to very coarse grained faintly bedded arkosic sandstone containing very few pebbles. It is well cemented by calcium carbonate. It weathers to yellowish gray (5*Y* 8/1), a color that is distinctly different from the pinkish-tan hues characteristic of the sandstone in the Bedrock Spring Formation. At this outcrop, the bed is overlain and underlain by lapilli tuff. East and south of here, it becomes relatively flat lying and its presence can only be inferred from the arkosic float.

ROCKS OF THE WESTERN FACIES

Propylite

The propylites of the Almond Mountain Volcanics were formed by the hydrothermal alteration of three different volcanic rock types: (a) brecciated porphyritic andesite, apparently intrusive in most places, which forms over 90 percent of the outcrop area, (b) thinly bedded lapilli tuff, and (c) porphyritic andesite dikes which are less brecciated than the first variety. The dikes cut both the lapilli tuff and brecciated porphyritic andesite. These rocks form steep-sided and hummocky hills, although the dike rocks are generally more resistant to erosion than the others.

The common characteristic of these rocks is the type of hydrothermal alteration, and the contacts shown on the map convey information about the upward or outward extent of this alteration, not about the original stratigraphic or intrusive succession of the altered volcanic rocks. Although the term "propylite" was originally applied to altered volcanic rocks with slightly different secondary mineral content (see Coats, 1940, p. 11–15), its application to these rocks is thought to be within the intended scope of the term.

The propylites of this area are megascopically characterized by distinctive colors, and though the contacts shown on the map are based primarily on these colors, they seem to represent very closely the actual limits of propylitization. These colors include olive gray (5*Y* 5/1), pale olive (10*Y* 6/2), and greenish gray (5*GY* 6–8/1). Unweathered samples collected from the dumps around exploratory shafts are very light blue green, green, or gray.

Small patches of unaltered rock show that prior to propylitization, the andesite consisted of plagioclase, green hornblende, and a very few biotite phenocrysts, all in a fine-grained or glassy groundmass. Plagioclase was present as both megaphenocrysts and microphenocrysts, and had an average composition of about An_{40}. In the megaphenocrysts, twinning was only moderately developed; oscillatory and mottled zoning were present, but calcic rims were rare. Plagioclase crystals were as long as 5 mm, but averaged 1 or 2 mm; biotite and hornblende crystals averaged 1 to 3 mm in length. Hydrothermal alteration has resulted in perhaps a third of the plagioclase being replaced with calcite (or some other carbonate), sericite, and a small amount of albite. In most specimens, the hornblende and biotite have been entirely altered to opaque minerals, chlorite, calcite, chalcedony, epidote, and serpentine(?). The groundmass is now a nonvesicular fine-grained mottled material with undulatory extinction; it appears to be mostly plagioclase, clay, and secondary quartz. Unweathered samples from the dumps of small mines also contain a small percentage of chlorite and pyrite. These two minerals are generally lacking in weathered rocks, apparently because surface weathering oxidizes the pyrite to iron oxides and sulfuric acid, and the acid attacks the chlorite to form an unidentified yellowish-brown mineral which gives the rocks of this unit their distinctive color. The groundmass of some specimens of this rock includes other silica minerals or zeolites, some of which are laumontite or its alteration product leonhardite.

The modal, normative, chemical, and spectrochemical compositions of one sample of propylite from one of the porphyritic andesite dikes are listed in table 6. These

rocks are generally less altered than other types from this unit, and therefore allow a more accurate estimate of the original modal composition of the rock. Prior to alteration, this rock probably contained about 16 percent plagioclase (approximately the present percentage of plagioclase plus calcite and other nonopaque minerals) and about 6 percent oxyhornblende, biotite, and opaque minerals (approximately the present percentage of chlorite and opaque minerals). The plagioclase percentage is a little lower than in most volcanic rocks from this area (see table 11); the percentage of dark minerals is close to normal. The chemical analysis confirms the small degree of alteration by indicating only 1.8 percent water and 0.64 percent CO_2. Comparison of this chemical analysis with those of other volcanic rocks in the Lava Mountains (fig. 26) shows that even though slightly altered, the present chemical composition of the rock resembles that of the others; the only significant differences are a notably higher percentage of CO_2, and slightly higher percentages of CaO, H_2O, and possibly Na_2O.

TABLE 6.—*Modal, normative, chemical, and spectrochemical analyses for one sample of propylite from the western facies of the Almond Mountain Volcanics*

[Sample 29–22 from outcrop along south side of canyon in sec. D24–f. A dash means the element was not present in detectable amounts. Chemical analyses by P. L. D. Elmore, H. F. Phillips, and K. E. White; spectrochemical analyses for Li and Rb by Robert Mays, remaining spectrochemical and modal analyses by G. I. Smith]

Modes [Volume percents]		Chemical analyses [Weight percents]	
Plagioclase megaphenocrysts	4.2	SiO_2	65.8
Plagioclase microphenocrysts	7.3	Al_2O_3	16.2
Total plagioclase	(11.5)	Fe_2O_3	1.4
Biotite	0	FeO	1.8
Hornblende	0	MgO	1.2
Oxyhornblende	0	CaO	3.9
Orthopyroxene	0	Na_2O	4.6
Clinopyroxene	0	K_2O	2.3
Quartz phenocrysts	.4	TiO_2	.51
Opaque minerals	3.2	P_2O_5	.16
Calcite	[1] 4.2	MnO	.05
Chlorite	2.3	H_2O	1.8
Other minerals	.2	CO_2	.64
Groundmass (mostly quartz)	78.1	Total	100

Norms [Weight percents]		Spectrochemical analyses [Parts per million]	
Q	20.5	Cr	50
C	0	Co	80
or	13.3	Mn	360
ab	38.8	Ni	10
an	17.0	Sc	5
di	2.0	V	40
hy	3.0	Fe	18,000
mt	2.1	Cu	10
il	.9	Ga	10
hm	0	Ti	2,600
tn	0	B	10
ru	0	Ba	1,900
ap	.3	Be	------
Symbol (C.I.P.W.)	I.4.3.4	Li	90
		Pb	10
		Rb	50
		Sr	1,400
		Yb	1
		Y	10
		Zr	110

[1] Calcite percentage is higher than in most samples of dike rocks from this unit. Modal average probably between 1 and 2 percent.

Subpropylite

The subpropylites of the Almond Mountain Volcanics were formed by hydrothermal alteration of the same varieties of volcanic rocks as propylite, namely, brecciated intrusive porphyritic andesite, thin-bedded lapilli tuff, and crosscutting andesite dikes. The outcrop terrain is also similar; only the color and secondary minerals are distinctive. The colors vary from medium gray (*N* 5), through purplish blue (10*PB* 6–7/2) and very pale purple (5*P* 7–8/1–2), to pale reddish purple (5*RP* 4–6/2). The secondary minerals are less abundant than in the propylite, and chlorite is not found. Inasmuch as the type of hydrothermal alteration in these rocks is obviously related and very similar to that in the propylite, but is less intense, the term "subpropylite" is adopted.

These rocks are characterized by white plagioclase phenocrysts and well-developed hexagonal flakes of biotite. The plagioclase is euhedral, sometimes forming crystals up to 8 mm long but more commonly 1 to 3 mm long. Most of the plagioclase is andesine. Zones range from weak to strong and the amount of twinning is variable. Many of the plagioclase crystals have been altered to calcite and sericite. Some of the biotite crystals, as large as 3 mm across, are unaltered, although most have been changed to iron oxide. Hornblende or oxyhornblende, which is much less abundant than biotite, is almost invariably altered to sericite, calcite, serpentine(?), epidote, or opaque materials. Clinopyroxenes and quartz occur locally but are generally not altered. The groundmass consists of impure glass, cryptocrystalline material, quartz, K-feldspar, and montmorillonite. In one outcrop, in section D25–m, stilbite(?) forms several percent of the rock. Like the propylites, these rocks generally contain no vesicles.

Chemical, normative, and modal analyses of one sample are presented in table 7. The modal analysis of this sample lists no original dark minerals, and the 5.7 percent of opaque minerals represents their altered residue. The plagioclase content of the original rock was a few percent higher than in the altered rock, but a large part of the 11.4 percent of calcite reported in this modal analysis is in the form of vesicle or vein fillings rather than a plagioclase replacement. The chemical analysis indicates 5.1 percent H_2O and 1 percent CO_2; calcite furnishes the CO_2, and montmorillonite probably furnishes much of the H_2O. Otherwise, this analysis resembles those of the other volcanic rocks of this area (fig. 26) except that the subpropylite is depleted in CaO and Na_2O, and possibly in total Fe as Fe_2O_3.

In gross aspect, the relations between the propylite and subpropylite are simple, but in detail they are complex. On most hillsides where both types are exposed, the subpropylite is above the propylite; in schematic cross section, the subpropylite would be projected to form an arch over the propylite. In detail, however, it is not uncommon to find irregularly shaped fragments

TABLE 7.—*Modal, chemical, and normative analyses of one sample of the subpropylite of the Almond Mountain Volcanics*

[Sample 29–36 from dump of city well in sec. D22–r. Chemical analyses by P. L. D. Elmore, S. D. Botts, I. H. Barlow, and Gillison Chloe; spectrochemical analyses for Li and Rb by Robert Mays; modal analyses by G. I. Smith]

Modes [Volume percents]		Norms [Weight percents]		Chemical analysis [Weight percents]	
Plagioclase megaphenocrysts	6.8	Q	26.4	SiO_2	63.1
Plagioclase microphenocrysts	14.5	C	3.5	Al_2O_3	15.8
Total plagioclase	(21.3)	or	15.6	Fe_2O_3	2.6
Biotite	0	ab	25.2	FeO	.54
Hornblende	0	an	12.0	MgO	2.8
Oxyhornblende	0	di	0	CaO	2.6
Orthopyroxene	0	hy	7.0	Na_2O	3.0
Clinopyroxene	0	mt	.5	K_2O	2.6
Quartz	.8	il	.9	TiO_2	.48
Calcite	11.4	hm	2.2	P_2O_5	.16
Opaque minerals	5.7	tn	0	MnO	.06
Other minerals	.6	ru	0	H_2O	[1] 5.1
Groundmass	60.2	ap	.3	CO_2	1.0
		Symbol (C.I.P.W.)	I.4.2.4	Li	.0012
				Rb	.006
				Total	100

[1] Analysis of similar material gives $H_2O+=2.5$ percent and $H_2O^-=2.4$ percent; analysis by Sarah Neil.

or "dikes" of one material in the other, but the contacts between the two rocks are rarely sharp. The color change is gradational over a zone of several millimeters or a few centimeters.

The original mineralogy of both types was similar. In most respects, the products of hydrothermal alteration are also similar—calcite, albite, or sericite replacing the plagioclase; and calcite, sericite, serpentine(?), zeolite, epidote, pyrite, or opaque minerals replacing the groundmass, biotite, and hornblende. The present differences between the two types lie chiefly in the alteration intensity and in the formation of chlorite in the propylite. These reflect differences in the degree of alteration but not in its types. Presumably, the alteration resulted from the postdepositional introduction of hot waters containing CO_2, H_2S, and perhaps other components. The more intense alteration, in the lower and central parts of the volcanic complex, produced chlorite in addition to the other alteration products. But the presence of these other products in the overlying rocks shows that the hydrothermal solutions also reached the upper and outer parts of the complex. A drop in the temperature of the solutions may have been chiefly responsible for the disappearance of the chlorite phase.

Volcanic breccia

The volcanic breccia of the western facies is mostly rubble breccia but includes some flow breccia, lapilli breccia, and tuff breccia. It resembles the volcanic breccia of the eastern facies, but is distinguished from it by slight differences in color, its virtual lack of pumice fragments, and by its areal distribution. Good exposures of rocks included in this unit of the western facies are in sections D11, D23, and E6. The volcanic breccia fragments are mostly either pale red (10*R* 6/2) or light olive gray (5*Y* 5/1); the matrix material is generally a lighter shade of the same hue. The units weather to form jagged surfaces on which the fragments stand out in relief from the less resistant matrix. Some of the volcanic breccia beds shown on the map (pl. 1) are massive, others consist of two to five distinct beds. Although the lithologies of these units vary greatly along strike, most can be traced several thousand feet or a few miles.

Most of the volcanic breccias of this map unit are extrusive; they rest conformably on each other or underlying units of the same formation, and show no cross-cutting relations. Along the northwest side of the Brown's Ranch fault zone, though, intrusive breccias included in this unit are also exposed. The lithologies of both intrusive and extrusive breccias in this area are similar; some are tuff breccias, others are flow breccias. A grayish-purple color is characteristic of both types. The composition of a sample of extrusive flow breccia differs in detail from other breccias of this facies (see table 5, sample 128–33), but the petrographic properties of these rocks are similar, and they all occupy the same position in the stratigraphic section.

The fragments in the volcanic breccias of this facies are mostly angular, although some units contain some rounded material. The average fragment size ranges from 1 to 6 inches; the maximum is most commonly between 1 and 2 feet, but in some rocks it is as much as 6 feet. There is a crude direct correlation between the percentage of large fragments in the rock and the size of these fragments. The small percentage of matrix in the rubble breccia is most commonly lapilli tuff. In the flow breccias, the matrix is lava of about the same composition as the fragments.

The fragments are gray or purplish porphyritic andesite in which minerals make up one-fourth to one-third of the rock and groundmass the rest. Plagioclase crystals are divisible into megaphenocrysts and microphenocrysts in about one-third of the samples; zones in most large crystals are medium to weak, and a calcic rim is found on about one-quarter; twin development is not pronounced. Biotite, present in about 90 percent of the rocks, shows nearly complete alteration in about half. Hornblende or oxyhornblende, present in all the rocks studied, is almost entirely altered in over half of them. Orthopyroxene, present in about two-thirds of the rocks, is nearly fresh; and clinopyroxene, present in three-quarters of the rocks, is most generally unaltered. Quartz is found in about 80 percent of the samples as rounded and embayed crystals, some showing alteration halos of fine clinopyroxene. The groundmass composition is variable, but on an average consists of one-half cryptocrystalline material, one-fourth small acicular crystals or crystallites, and one-fourth glass; it also con-

tains a light to medium dust of reddish or black opaque materials.

Many of the individual volcanic fragments have flow lineation defined by the acicular hornblende or oxyhornblende crystals, and by the microphenocrysts of plagioclase; some have elongated vesicles. The plagioclase crystals have an average length of ½ to 1 mm and are as much as 4 to 8 mm long; hornblende, oxyhornblende, and biotite have maximum dimensions of about 1 to 2 mm; orthopyroxene and clinopyroxene rarely are larger than 0.5 mm. Quartz is usually 1 or 2 mm in the maximum dimension.

Chemical, spectrochemical, normative, and modal compositions of five samples are given in table 5. Four samples (97–38 L, K, I, and F) were fragments that came from four distinct breccia beds within a single mapping unit in the upper part of the formation exposed three-quarters of a mile northeast of Dome Mountain; one sample (128–33) was a fragment from a resistant layer that crops out on the northwest side of the Brown's Ranch fault zone.

The modal compositions of the four samples from the same section are similar (except that one sample has an uncommonly high percentage of opaque minerals because the fragments in this bed were very heavily altered). They also have nearly identical percentages of oxides, but all are lower in silica and are more mafic than most of the volcanic rocks in the Lava Mountains area. The norms confirm this difference, and classify these four rocks by the C.I.P.W. system (Washington, 1917) as tonalose. Their normative plagioclase ranges from An_{39} to An_{44}. The remaining sample (128–33) has distinctly lower percentages of plagioclase and dark minerals, and a higher percentage of groundmass. It is also higher in silica and is more felsic than most volcanic rocks of the area. Its norm confirms this tendency, although it classifies the rock in the same group as most of the other volcanic rocks of the area (yellowstonose). The normative plagioclase is An_{33}.

Tuff

The tuff of the western facies includes tuff, lapilli tuff, and a few beds of tuff breccia too thin to separate on the map. The best exposures are found on the north sides of Klinker and Dome Mountains, especially in sections E5–p, D11–f, D11–m, and D12–d. The rocks exposed there resemble the tuffs included in the eastern facies, but tend to be a little better sorted, more persistent along the strike, perhaps more intensely colored, and are virtually free of pumice. Some of the tuffs in the western facies form cliffs whereas others form soft slopes. The weathered surfaces are usually uneven and some are cavernous. The rocks weather to light or bright shades of gray, yellowish gray, green, pinkish gray, and red. In general, the finer tuffs are lighter colored than the coarser ones. The layers range from 5 to 50 feet in thickness, and thicknesses of 10 to 20 feet are commonest. Within these layers, the rocks are generally massive, but there is some local stratification. Along the strike, the individual layers can be traced 2,000 or 3,000 feet and a few can be traced a mile.

Most of these rocks are lapilli tuff. The individual lapilli are composed of lava, indurated tuff, or rarely pumice. Ash-sized euhedral crystals of biotite are common; euhedral crystals of hornblende and plagioclase are less common. Many beds also contain a small percentage of epiclastic sand. A small percentage of larger angular to subrounded fragments of purple or gray porphyritic andesite or lapilli tuff is commonly found in these rocks. Most are a few inches across although some measure several feet.

In the vicinity of the Brown's Ranch fault zone, the rocks included in this lithologic map unit are poorly exposed. They weather as if very soft, but the crushing that occurred during movement on the fault may be largely responsible for this lack of resistance. Most of them are probably tuff, but local patches of lapilli tuff, tuff breccia, and lapilli breccia are included. The colors are conspicuously variegated, but tend toward shades of purple. Some hydrothermal alteration and bleaching is suggested in the vicinity of the large sheared zone (in secs. E17 and E20); this may be responsible in part for the variegated color.

Sandstone

Conglomerate, sandstone, and some tuffaceous sandstone, siltstone, and claystone assigned to this formation are exposed at several places in the vicinity of Dome and Klinker Mountains. The best exposures are located in sections D11–f, D12–k, and E6–j. In general, these rocks are not resistant to weathering and form soft slopes that are largely concealed by debris; beds that contain an appreciable percentage of tuff are somewhat more resistant. Most of the rocks weather to yellowish gray; the conglomeratic facies tend to be more brown, and the finer grained rocks more red or green. In many areas, layers of these rocks exceed 100 feet in thickness and in one area apparently exceed 1,000 feet. Within these thick sections, bedding is faint, and in many outcrops is marked only by stringers of pebbles or by beds of fine-grained material.

The sandstone is in most places a poorly sorted arkose with fragments that usually range in size from very coarse to medium sand, but in some areas are of fine-sand size. It also includes beds of siltstone and claystone, although they are not common. Some of the detritus appears to have been derived from the pink leucocratic

Atolia Quartz Monzonite, for many fragments are freshly broken pink feldspar or clear quartz. Some parts of this member contain an appreciable percentage of pyroclastic material. The pebbles in the sandstone and conglomerate are subrounded to subangular and rarely exceed 3 inches in diameter. Most of the volcanic pebbles are purplish or gray andesite, apparently derived from other members of the Almond Mountain Volcanics. A few banded rhyolitic rocks were found that probably were reworked from the Bedrock Spring Formation. Nonvolcanic pebbles include fragments of quartz, schist, and Atolia Quartz Monzonite.

Rocks of this map unit are distinguishable from the sandstone and conglomerate of the Bedrock Spring Formation by the higher percentage of volcanic rocks among the pebbles and cobbles. In these sandstones, the prevailing ratio of volcanic fragments to others is about 5 or 10 to 1; in those of the Bedrock Spring Formation, the reverse ratio is more general. The sandstone in the Almond Mountain Volcanics also tends to be yellower than that in the Bedrock Spring Formation, but this characteristic is not consistent enough to serve as a basis for distinguishing the rocks of the two formations.

VOLCANIC SOURCE AND DISTRIBUTION OF ROCK TYPES

The distribution of the bedded volcanic rock facies of the Almond Mountain Volcanics indicates that volcanic rocks erupted chiefly from two centers. Today, volcanic necks and dissected domes mark the positions of these centers; coarse volcanic breccias surround them and finer fragmental volcanic rocks predominate some distance away. The petrographic and chemical similarity between the intrusive rocks and the fragments in bedded volcanic rocks supports the conclusion that they represent the same volcanic episode.

These eruptive centers are recognized by the abundance in them of massive volcanic rocks that have steeply dipping planar flow structures, and the lack of internal or basal contacts.

The center for the western facies is approximated by the outcrops of propylite and subpropylite southwest of Dome Mountain; a small area of such rocks also crops out southwest of Klinker Mountain, but this is probably an outlier of the same center. The eruptive center for the eastern facies is in the vicinity of Almond Mountain.

The marked zonation of fragmental volcanic rocks around both eruptive centers is evident on the geologic map (pl. 1). In the western facies, volcanic breccias form most of the sections exposed within a mile of the center; the tuffs and sandstones form an appreciable percentage of this facies only outside of this zone. The sandstones are thickest near the north and east edges of areas containing this formation because they were derived by erosion of the Atolia Quartz Monzonite and Bedrock Spring Formation, which cropped out to the north and east. Comparison of stratigraphic sections in three areas illustrates these changes. In sections D23–d and D14–n, adjacent to the western eruptive center, the formation is about 550 feet thick and consists of 85 percent volcanic breccia and 15 percent tuff. In section D11–f, located about 1 mile from the edge of this center, the formation is 600 feet thick and consists of 60 percent volcanic breccia, 12 percent tuff, and 28 percent sandstone. In section E6–j, located 1½ miles north of the center, the formation is 500 feet thick and consists of 47 percent volcanic breccia, 3 percent tuff, and 50 percent sandstone.

The same distribution of the stratified rocks can be discerned around the eruptive center in the eastern part of the area. At the type section, located within the eruptive center, the formation is 900 feet thick and consists of 93 percent volcanic breccia and 7 percent tuff. In sections E24–h, –j, on the northeast edge of the center, the formation is 475 feet thick and consists of 55 percent volcanic breccia, 35 percent tuff, and 10 percent sandstone. In section E6–q, approximately 2½ miles northeast of the nearest part of the center, it is about 150 feet thick and consists of 20 percent volcanic breccia, and 80 percent well-indurated tuff and lapilli tuff.

ENVIRONMENT OF DEPOSITION

Prior to the first eruption of the Almond Mountain Volcanics, the Lava Mountains was an area of low hills. The Atolia Quartz Monzonite and Bedrock Spring Formation, which underlay these low hills, had been folded and probably faulted. Along the axis of the Dome Mountain anticline, the Bedrock Spring Formation was tilted at angles ranging from 20° to nearly vertical, and, as is evident from sections of the area (pl. 2, especially section *B–B′*), several thousand feet of the formation had been removed by erosion.

Simultaneous faulting may have created a northeast-trending topographic grain in these low hills. The composition of the basal layer of the Almond Mountain Volcanics varies on the two sides of several northeast-trending faults exposed on the northeast side of Dome Mountain; this lithologic variation suggests that topographic breaks existed along these lines by the time the first volcanic debris was deposited, and the most likely sources of such breaks are earlier vertical displacement along these faults.

Volcanic activity originated in the two eruptive centers almost contemporaneously as shown by interbedding of the eastern and western facies near the northeast end of the Brown's Ranch fault zone. A

southwest-trending valley apparently formed between these two volcanic centers, either by graben-forming fault activity along the Brown's Ranch fault zone, or simply as a result of the relatively greater growth of the volcanic hills on both sides. To the north of these centers, volcanic debris vied with the arkosic sediments from the north in locating the central axis of the east-west valley. When volcanic activity was most continuous or intense, the size of the volcanic pile increased rapidly and the valley axis was shifted to the north; when such activity was reduced, the arkosic alluvial fan north of the valley was built up, and the toe migrated southward over the volcanic pile. The average position of this valley is approximated by the township line separating T. 28 S. from T. 29 S. There is some evidence that the largest of these alluvial fans grew toward the southwest across the area now occupied by Dome Mountain, for the southernmost outcrops of sandstone in this formation lie in this area.

On all other sides of the eruptive centers, volcanic debris extended to the edge or outside of the mapped area. The lack of arkosic sediments in the outermost exposures of this debris shows that either the limits of the volcanic debris extended well beyond the area mapped, or that these outside areas did not slope toward the Lava Mountains.

AGE AND RELATION TO OTHER FORMATIONS

The Almond Mountain Volcanics lie with a marked angular unconformity on the Bedrock Spring Formation; typical examples of this relation can be seen in sections D2–f, E3–c, E3–k, and F7. The Almond Mountain Volcanics are unconformably overlain by the Lava Mountains Andesite, and typical examples of this relation can be seen in sections E7–l, D2–m, and D11–n. The regional characteristics of the unconformities at the base and top of this formation, however, are different. In the interval between the deposition of the Bedrock Spring Formation and the deposition of the Almond Mountain Volcanics, much of the deformation consisted of folding, so most of these contacts are angular unconformities with several thousand feet of the underlying formation removed by erosion; in the interval between the Almond Mountain Volcanics and the Lava Mountain Andesite, much of the deformation consisted of faulting without appreciable tilt of the fault blocks, so most of these contacts are disconformities.

No fossils were found in the Almond Mountain Volcanics. Inasmuch as it rests on the Bedrock Spring Formation, it is at least as young as middle Pilocene, and the intensity of tilting and amount of erosion associated with the unconformity suggests that an appreciable period of time had elapsed. The Almond Mountain Volcanics are overlain, in turn, by the Lava Mountains Andesite and several deformed and eroded Pleistocene rock units. As appreciable time was also required to form this succession of rock units, an age of late Pliocene seems probable for the Almond Mountain Volcanics.

LAVA MOUNTAINS ANDESITE

The Lava Mountains Andesite, a new formation named here, consists mostly of dark-gray porphyritic andesite. It is found as flows, large domes, and small moundlike intrusives throughout the southern two-thirds of the mapped area. Typically, it forms the caps of rolling or flat-topped hills, cropping out to form soft or boulder-strewn areas on the top and blocky cliffs along the edges.

The type locality is on the southeast side of Dome Mountain (in sec. E8–m; see sample 98–7 in table 8); the name is derived from the Lava Mountains of which it forms an important part. This formation is approximately equivalent to Hulin's (1925, p. 55–58) "Red Mountain Andesite." Although that formational name has been widely used in subsequent geologic studies of the Mojave Desert area, a new name is used here because the prefix "Red Mountain" was already in use for another group of rocks at the time of Hulin's publication.

The Lava Mountains Andesite rests unconformably on the Almond Mountain Volcanics and its predecessors. Four of the five rock units mapped as "other upper Pliocene(?) volcanics" could be either contemporaneous with or slightly older than the Lava Mountains Andesite; the fifth, the tuff breccia, is equivalent in age to the lower part of the andesite. Although no rocks other than a few patches of gravel rest on top of the Lava Mountains Andesite, five Quaternary rock units are inferred to be younger on the basis of indirect evidence.

Three lithologic map units of the Lava Mountains Andesite are distinguished on the geologic map. "Andesite flows," consisting of dark gray, red, or brown plagioclase andesite porphyry, constitute the most abundant and widespread rock type in the formation. "Flow breccia," consisting of angular fragments of the Lava Mountains Andesite in a matrix of the same material, occurs as bodies large enough to be distinguished on the map. A single layer of "flow conglomerate," containing rounded fragments of light-gray Lava Mountains Andesite in a matrix of red-brown andesite, is prominent on the west side of the range.

DESCRIPTIONS OF LITHOLOGIC MAP UNITS

ANDESITE FLOWS

Flows of Lava Mountains Andesite form most of the formation, although some outcrops included in this unit,

especially near Dome Mountain and Almond Mountain, are probably the upper parts of volcanic necks or domes. Small patches of volcanic breccia are also included in the unit, but they are of very limited extent. On the tops of the mesalike hills, these rocks crop out as a field of boulders resting on fine-grained chocolate-brown regolith. Around the edges of these areas, especially in sections B31, D1, E1, and E34, sections of the andesite flows are well exposed except where sheathed in their own talus. Near the basal contacts of these flows, the rock commonly weathers to flaggy slabs an inch or two thick that are parallel to the contact at the base and gradually change toward vertical upward from it. Above this flaggy zone, perhaps 20 or 30 feet thick, the rock either is irregularly blocky or forms columnar joints a foot or two across.

Most of the flows are uniformly dark reddish brown or very dark gray in outcrop. On freshly broken surfaces, the groundmass very commonly exhibits the same two colors, and this characteristic is one of the most reliable means of distinguishing these volcanic rocks from others in the area. Generally, medium gray (*N* 4–5) is predominant, and pale red (10*R* 4–6/2–4) forms streaks about 1 mm wide and 10 mm long. In many outcrops, however, the colors are the same, but their relative abundance is reversed. In most samples from this unit, the plagioclase crystals are very faintly yellow or orange; this seems to be a characteristic independent of the groundmass color but restricted to the formation.

The rocks of this map unit locally are as thick as 600 feet, although only 200 to 400 feet of section is generally present. Only along the west edge of the area, west of Klinker Mountain, are thicknesses less than 200 feet characteristic. In most places, the formation appears to consist of a single flow; in a few places, though, it consists of several superposed flows separated by a thin zone of volcanic breccia. Some of the outcrops thickest in appearance—for example, the hills southeast of Almond Mountain and the hill east and south of Bedrock Spring—are massive, have steeply dipping nearly concentric flow structure, and apparently cut nearby layered rocks; therefore, they are believed to be volcanic necks or domes.

About 45 samples of the andesite flows were carefully selected to give a proportionate sampling of the entire unit, and thin-section studies of them furnish a semiquantitative estimate of its petrographic characteristics. In 95 percent of the samples, plagioclase is present both as megaphenocrysts and microphenocrysts; their combined volume percentages range from about 10 to 30. The average composition of the feldspar in both size groups is close to An_{40}; it commonly ranges from An_{30} to An_{55}, although some crystals have zones with An percentages as low as 20 or as high as 60. Most of the megaphenocrysts have well-developed zones, and twinning in them is conspicuous. In over half the samples, a majority of megaphenocrysts have calcic rims, but in no samples do all megaphenocrysts have calcic rims. The last major resorption of the plagioclase megaphenocrysts occurred after the crystals had clustered to form a glomeroporphyritic texture. In every instance noted, the resorbed area, and the subsequent calcic rim, were formed only on the outward faces of the crystal group (as shown in fig. 22*A*). Small inclusions of yellowish glass(?) throughout the megaphenocrysts give the crystals a yellowish color in hand specimens. Biotite is present in 80 percent of the samples, and strongly altered in more than half. Oxyhornblende, present in 90 percent, shows a similar degree of alteration. Clinopyroxene and orthopyroxene are each present in about 75 percent of the rocks, and are nearly unaltered in two-thirds of them. Quartz, though present in 70 percent of the samples, is sparse in all but a few of those rocks.

Generally, the groundmass consists of about 30 percent microscopic crystals and crystallites, 45 percent cryptocrystalline material, and 25 percent glass, although the percentages vary greatly. In part, the unidentified crystalline material consists of small percentages of submicroscopic cristobalite and clay that can be detected by X-ray; K-feldspar is not detected. The concentration of opaque materials is variable, ranging from a few small fragments in some rocks to virtually the entire groundmass in others. The reddish-brown rocks contain the highest percentage of opaque minerals. The nature of these opaque materials varies; some are small euhedral crystals that appear black, whereas others are featherlike, hairlike, or fibrous objects that appear black in plane light and red in conoscopic light.

Texturally, these rocks are characterized by the porphyritic plagioclase, biotite, hornblende, and pyroxene. Plagioclase crystals may be as long as 5 or 6 mm; biotite and oxyhornblende crystals are mostly less than 3 mm long, and pyroxene crystals are mostly less than 1 mm long. The average lengths are about one-third of these maximums. Quartz is generally present as crystals 1 to 3 mm across. Many rocks also have small but numerous vesicles, some forming a quarter to a third of the volume. A few of these have linings of opal, chalcedony, tridymite, or a yellowish or greenish fibrous anisotropic material.

Deuteric alteration has affected virtually all these rocks, although it is extreme in some and light in others. A well-exposed flow in section E9–h provides good evidence that such alteration takes place very late in the cooling history of a rock. The upper part of this flow

consists of red-brown lava, and this grades downward over a distance of a few inches into an unaltered gray microperlite (fig. 22*E*), which apparently was chilled so quickly after reaching the surface that normal alteration was prevented. Comparison of these rocks shows that during the normal period of cooling, deuteric alteration changed all light-colored clear hornblende ($c\wedge Z=14°$) to oxyhornblende ($c\wedge Z=10°$), all light-colored biotite ($\gamma'=1.69$) to darker colored biotite ($\gamma'=1.72$), all clear orthopyroxene crystals to discolored or opaque crystals, and most opaque minerals and much of the groundmass to reddish opaque minerals. The plagioclase crystals were not affected.

Original textures are also well preserved in this unaltered flow, and they provide evidence that there are few xenocryst minerals included in these rocks. The crystal faces are not altered, rounded, or resorbed, and the phenocrysts in this rock clearly are not fragments broken from a larger crystal and have not grown from a nucleus consisting of a broken crystal.

Modal, normative, chemical, and spectrochemical analyses of nine samples are given in table 8. These samples include the full range of rock types found in the Lava Mountains Andesite flows, and modal analyses of them indicate the amount of mineral variation normally found in these rocks. Plagioclase megaphenocrysts constitute 4 to 12 percent of these rocks and microphenocrysts 7 to 20 percent; mafic minerals make up 1 to 3 percent of most of them, and quartz generally makes up less than 1 percent. The chemical analyses show even more uniformity. The SiO_2 percentages mostly lie between 63 and 66, the Al_2O_3 percentages between 16 and 17, the $CaO+Na_2O$ percentages between 6.2 and 7.0, and the CaO percentages between 3.9 and 5.0. Elements detected by spectrochemical analysis are also present in similar amounts in these rocks. The normative compositions reflect the uniformity evident in the chemical analyses; by Washington's terminology (1917) (which draws fairly fine distinctions between analyzed rocks) seven are yellowstonose and two are tonalose. Normative orthoclase makes up between 18 and 24 percent of the total feldspar, and the normative plagioclase has compositions ranging from An_{33} to An_{39}. The chemical and normative compositions show that if these rocks were crystallized to a more advanced degree, they would be classified as dacite or rhyodacite; and if crystallized completely, they would be granodiorite or quartz diorite. The analyzed rocks of this formation are compared with other volcanic rocks of the Lava Mountains area in a later section.

FLOW BRECCIA

Flow breccias as much as 150 feet thick form a distinctive unit of the Lava Mountains Andesite in two areas, one on the southwest side of Dome Mountain and the other on the south end of Klinker Mountain. They crop out as jagged resistant rocks ranging in color on the weathered surfaces from grayish red to brownish gray. On fresh surfaces, they are lighter colored.

The fragments are not sorted and range in size from sand size up to a foot across; exceptionally, 2-foot fragments are found. Generally, the smaller fragments are angular to subangular, and the larger ones are subangular to subrounded. In most exposures they form half to three-fourths of the total rock, the lava matrix forming the balance. These fragments are mostly blocks of Lava Mountains Andesite. The matrix lava appears to be identical with that constituting the andesite flows of this formation.

FLOW CONGLOMERATE

Flow conglomerate forms a distinctive bed of the Lava Mountains Andesite that crops out on the crest and on the west side of Klinker Mountain. The origin of the rounded fragments is not known. In most places, the bed is several tens of feet thick. The rock consists of very well rounded fragments, several inches across, of medium-gray andesite embedded in a matrix of pale-brown andesite. The outcrops shown on the map are apparently all part of the same flow, suggesting that the western part of the Lava Mountains represents an area that was part of one slope at the time of extrusion. Presumably this slope was toward the west, although the variation in flow thickness is inadequate to confirm this direction.

VOLCANIC SOURCE AND DISTRIBUTION OF ROCK TYPES

The Lava Mountains Andesite covers most of the higher hills in the southern two-thirds of the mapped area. The andesite flows are most abundant in the vicinity of Klinker Mountain, Dome Mountain, and Almond Mountain, and in the large area 3 to 5 miles northeast of Almond Mountain. The flow conglomerates and flow breccias are restricted to the southwestern part of the mapped area.

The relatively constant thickness of the Lava Mountains Andesite flows suggests that a number of sources existed. If it is assumed that the underlying surface was flat, and that a slope at the flow surface greater than about 200 feet per mile was necessary to maintain flow (this is about 2° and approximately the flattest slope formed by basalt flows in Hawaii; see Wentworth, 1954, p. 430), it follows that a flow of Lava Mountains Andesite that has a maximum thickness of 600 feet, and a minimum thickness of 200 feet, is all within 2 miles of its source. Although the preexisting surface was generally not flat, the viscosity of the andesite was undoubtedly greater than that of basalt, and this would

TABLE 8.—*Modal, chemical, normative, and spectrochemical analyses of nine samples of the Lava Mountains Andesite flows*

[A dash means the element was not present in detectable amounts. Chemical analyses by P. L. D. Elmore, H. F. Phillips, and K. E. White; spectrochemical analyses for Li and Rb by Robert Mays, remaining spectrochemical and modal analyses by G. I. Smith]

	27-21	*27-23*	*98-7*	*97-38O*	*124-23J*	*124-23F*	*124-23B*	*124-22K*	*181-28*
Modes [Volume percents]									
Plagioclase megaphenocrysts	13.8	8.5	10.9	10.6	12.4	12.5	10.5	4.3	7.9
Plagioclase microphenocrysts	10.7	20.2	10.0	12.2	9.4	6.8	6.8	11.6	8.3
(Total plagioclase)	(24.5)	(28.7)	(20.9)	(22.8)	(21.8)	(19.3)	(17.3)	(15.9)	(16.2)
Biotite	.3	.1	.5	.3	.1	.3	0	.5	0
Hornblende	0	.2	0	0	0	0	0	0	0
Oxyhornblende	.4	0	2.1	.1	3.1	7.6	.7	.2	Trace
Orthopyroxene	1.4	.2	.2	.1	.1	.9	.1	2.5	.7
Clinopyroxene	.8	2.0	.3	.2	0	.1	0	.1	.9
Quartz	.5	.1	.1	.2	0	.3	.1	0	3.2
Opaque minerals	5.4	2.5	6.7	6.0	9.5	2.2	11.4	1.4	8.2
Other minerals	.5	.6	.7	2.9	.1	.2	0	.5	.7
Groundmass	66.2	65.6	68.5	67.3	65.3	69.2	70.5	78.9	69.9
Chemical analyses [Weight percents]									
SiO_2	64.5	63.3	63.8	65.0	64.2	64.1	64.9	66.1	60.6
Al_2O_3	16.4	16.4	16.7	16.7	16.8	16.7	16.9	16.2	16.2
Fe_2O_3	2.1	1.4	3.8	3.8	3.7	1.8	4.1	2.3	2.8
FeO	1.9	2.8	.14	.34	.44	2.1	.02	.88	2.4
MgO	2.3	2.4	2.3	.75	2.3	2.1	2.0	1.6	3.5
CaO	4.4	5.0	4.7	4.2	4.4	4.1	4.3	3.9	5.8
Na_2O	4.2	4.2	4.1	4.4	4.5	4.0	4.5	4.0	3.8
K_2O	2.3	2.3	2.1	2.6	2.5	2.7	2.5	2.7	2.4
TiO_2	.66	.68	.58	.68	.66	.64	.66	.50	.76
P_2O_5	.23	.28	.29	.24	.28	.26	.30	.18	.28
MnO	.06	.06	.06	.02	.06	.06	.06	.04	.07
H_2O	1.0	1.2	1.2	1.8	.17	1.4	.20	1.4	1.2
CO_2	<.05	<.05	<.05	<.05	<.05	<.05	<.05	.21	.74
Total	100	100	100	101	100	100	100	100	101
Norms [Weight percents]									
Q	18.4	15.9	19.0	21.0	17.6	18.5	17.7	21.7	14.0
C	0	0	0	0	0	0.3	0	0	0
or	13.3	13.3	12.2	15.6	15.0	16.1	15.0	16.1	13.3
ab	35.6	35.6	34.6	37.2	37.2	34.1	38.2	34.1	32.0
an	19.2	19.2	21.1	18.1	18.6	18.6	18.4	18.1	20.3
di	2.2	4.5	.4	1.3	.9	0	0	1.1	5.4
hy	5.3	6.6	5.6	1.3	5.1	6.5	5.0	3.5	6.9
mt	3.0	2.1	0	0	0	2.6	0	1.6	4.2
il	1.4	1.4	.3	.8	.9	1.2	0	.9	1.5
hm	0	0	3.8	3.8	3.7	0	4.2	1.1	0
tn	0	0	1.2	.8	.6	0	1.0	0	0
ru	0	0	0	0	0	0	.3	0	0
ap	.3	.7	.7	.3	.7	.7	.7	.7	.7
Symbol (C.I.P.W.)	I.4.3.4	II.4.3.4	I.4.3.4	I.4.3.4	I.4.3.4	I.4.3.4	I.4.3.4	I.4.3.4	II.4.3.4
Spectrochemical analyses [Parts per million]									
Cr	80	80	70	60	40	40	40	40	70?
Co	60	80	30	20	80	60	40	50	60
Mn	390	420	390	170	420	420	380	280	470
Ni	50	60	60?	50	30	20	30	10	50
Sc	5?	5	10?	5	5	5	5	5	5?
V	60	70	60	70	70	60	60	40	90?
Fe	22,000	22,000	28,000	24,000	28,000	22,000	25,000	16,000	31,000
Cu	20	20	20	30	20	10	20	10	30
Ga	10	10	10	20	20	10	20	10	10
Ti	2,600	2,400	2,100	2,800	2,500	2,100	2,600	2,100	2,400
B	40	40	20	20	30	30	20	40	20
Ba	1,700	1,600	2,000	1,800	2,000	1,400	2,000	2,000	1,900
Be									
Li	19	2	40	6	27	16	21	27	36
Pb	10	10	10	10	20	10	10	10	10
Rb	30	30	30	40	50	60	30	80	40
Sr	1,400	2,000?	1,600	1,400	1,500	1,200	1,800	1,000	1,600
Yb	<1	<1	<1	<1	<1	<1	1	<1	1
Y	5	5	10	5	10	5?	10	10	5?
Zr	120	110?	100	110	110	80	120	110	90

LOCATION OF SAMPLES

27-21. Sec. D 2-r, sample from top of ridge.
27-23. Sec. D 3-d, sample from southwest side of hill.
98-7. Sec. E 8-n, sample from about 50 feet above marker contact shown on pl. 1.
97-38O. Sec. E 6-j, sample from about 100 feet above base of formation.
124-23J. Sec. E 34-k, on southwest side of Almond Mountain, sample collected about 375 feet above base of formation.
124-23F. Same section, sample collected about 210 feet above base of formation.
124-23B. Same section, sample collected about 50 feet above base of formation.
124-22K. Sill intruded into Almond Mountain Volcanics type section; see fig. 11 for position.
181-28. Sec. E 1-n, sample from about 40 feet above base of flow.

tend to offset the error introduced by assuming a flat surface.

The specific locations of the many sources of andesite flows can only be inferred. Steeply dipping flow structures have been mapped in many areas, but their attitudes are too inconsistent to be reliable criteria. Fortunately, this formation is young enough to have some of the original topographic features remaining on the flow surfaces. Among these are numerous small mounds and small to large domes, quite similar to those described by Williams (1932, see especially figs. 20c and 37) and Coats (1936). Many of these also have steeply dipping flow structures, and it is inferred that most of these mounds and domes indicate areas that were centers of upwelling lava. The best examples of such features are the mounds and domes of Lava Mountains Andesite that lie to the east and southeast of Almond Mountain (fig. 12). Fifteen or twenty smaller and less clear-cut examples are present elsewhere in the mapped area, and they are spread over an area almost as large as the present areal extent of the Lava Mountains Andesite.

ENVIRONMENT OF DEPOSITION

Flows of Lava Mountains Andesite crop out in the highest part of the range and also near the level of the

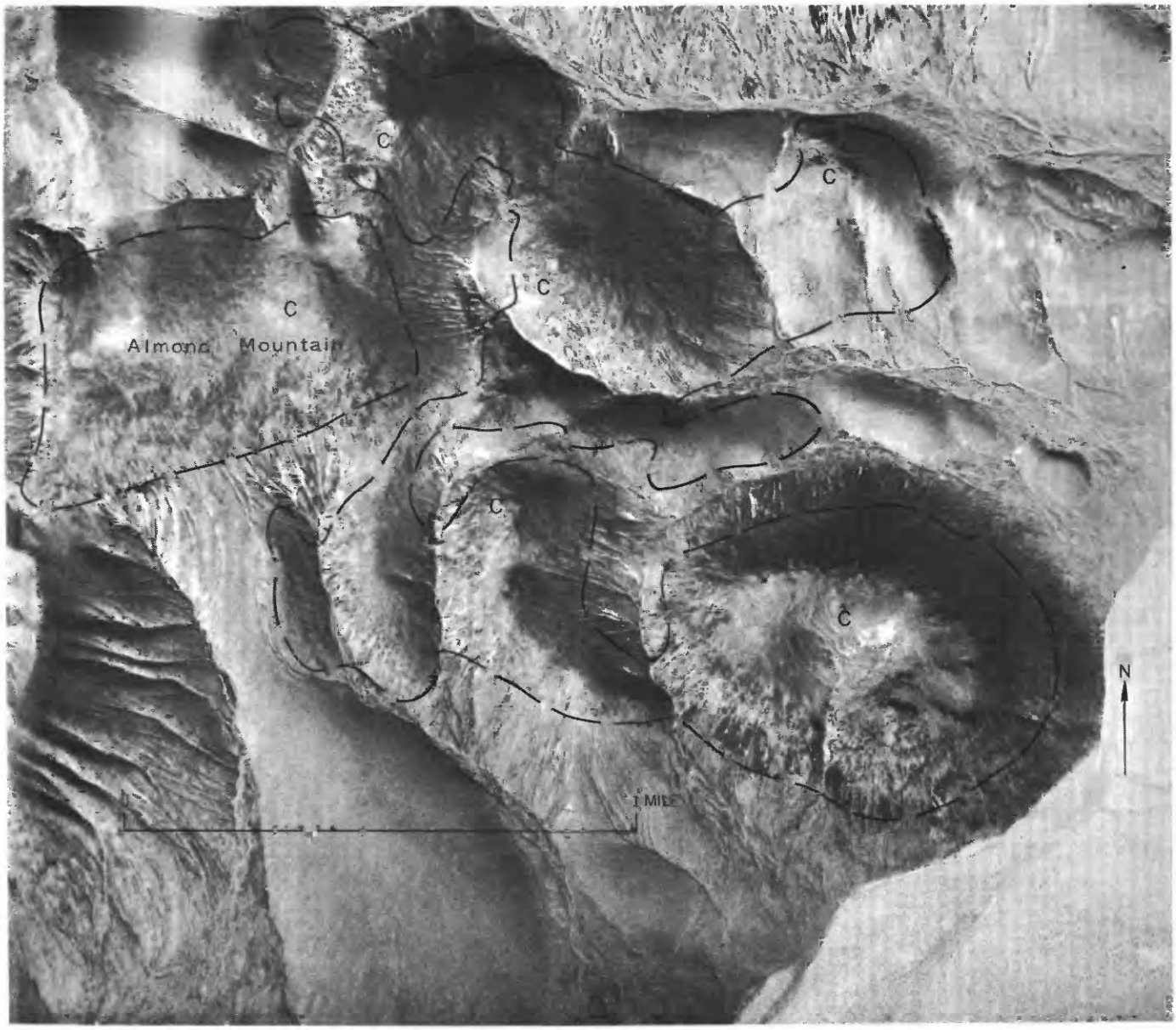

FIGURE 12.—Vertical aerial photograph of area east of Almond Mountain. Outcrop areas of Lava Mountains Andesite enclosed by dashed lines. Some of the topographic mounds and domes believed to indicate areas that were centers of upwelling Lava Mountains Andesite are indicated by C. U.S. Navy aerial photograph PTK–5–^{030}.

alluvium in the southern part of the area. This represents nearly 2,000 feet of relief. There has not been enough faulting and tilting since deposition to account for this amount of relief, so it is reasonable to conclude that in the southern part of the area, the surface on which the flows were originally deposited provided most of this relief.

The contacts shown on the geologic map (pl. 1) and sections (pl. 2), though, show that relative to the present topography, the depositional surface was gently rolling and nearly undissected. Most of the slopes indicated for this preexisting surface are less than 5°, although a few dip as steeply as 15°. For example, the large flows in sections D3, D14, E8, E9, and F7 rest on surfaces that are nearly horizontal; the flow conglomerate rests on a west-dipping slope of about 5°; and the lava flow in section D1–c, noted by Hulin (1925, p. 56), rests on a surface that dips north about 15°.

AGE AND RELATION TO OTHER FORMATIONS

The Lava Mountains Andesite is probably of very late Pliocene age although it may in part be Pleistocene. In many places it is clearly unconformable on both the Bedrock Spring Formation of middle Pliocene age and the Almond Mountain Volcanics interpreted to be of late Pliocene age. Most of the rocks grouped with the other upper Pliocene(?) volcanics are either contemporeaneous with or older than the Lava Mountains Andesite. The relation of this andesite to all the younger units can also be established. The older gravels contain fragments of Lava Mountains Andesite; the Quaternary andesite appears to cut the Lava Mountains Andesite (sec. D1–e) and is contemporaneous with these older gravels. The Christmas Canyon Formation, dated as Pleistocene(?) on the basis of a single fossil, contains fragments of the Lava Mountains Andesite in fairly high proportions; hence both it and the basalt that cuts it are also younger.

Within this part of the Mojave Desert, many volcanic sections have been correlated with these volcanic flows under the name of Red Mountain Andesite, as they were called by Hulin (1925, p. 55). Although many of these correlated flows have a similar lithology and occupy a comparable position with respect to the stratigraphic sequence of the area, there is little reason to think that they are correlative in the sense of being once connected or contemporaneous. The evidence in the Lava Mountains area indicates that the flows of the Lava Mountains Andesite were very local and did not extend more than a few miles from their source in any direction. There are, to be sure, numerous sources within the Lava Mountains area, but they form a very distinct cluster which is isolated from the other parts of the Mojave Desert by large andesite-free outcrops of older rocks.

Nevertheless, many parts of the Mojave Desert do have the same general succession of Cenozoic rocks, namely (a) sandstones and conglomerates, (b) pyroclastic breccias and tuffs, (c) capping flows of dark-colored andesite, and (d) very young looking basaltic rock. This repetition of the sequence from place to place suggests that some widespread fundamental process controlled Cenozoic deposition.

OTHER UPPER PLIOCENE(?) VOLCANICS

Five other volcanic rock units have been mapped separately. All are of relatively small areal extent, but have sufficiently diverse lithologies to be mapped and treated separately. Because of their lithology and stratigraphic position, none can be logically included in the more extensive upper Pliocene volcanic formations, although most or all may be genetically related.

TUFF BRECCIA

Along the west edge of the mapped area, upper Pliocene(?) tuff breccias crop out to form steep debris-covered slopes. The best exposures within the mapped area are found in sections D3–q, D9–j, and D15–b, although the most extensive outcrops of these rocks are a few miles to the west. Generally they are a little better exposed than the underlying Bedrock Spring Formation, and not as well exposed as the overlying flows of Lava Mountains Andesite. On hillsides, the rocks are light reddish purple or light brownish gray; where well exposed on canyon walls they are somewhat browner.

The tuff breccia ranges from an impure lapilli tuff in which rock fragments less than 1 inch across constitute 20 to 50 percent, to a rubble breccia in which fragments up to 4 feet across constitute about 90 percent of the unit. Rocks with an average composition contain about 60 percent rock fragments in a matrix of tuff. The fragments are predominantly purplish porphyritic andesite from the Almond Mountain Volcanics, but up to 30 percent of them are derived from early flows of the Lava Mountains Andesite. Also included is a small percentage of metamorphic fragments, mostly knotty schist. The mapped relations in sections D10–h and D15–a suggest that these breccias lie unconformably on the Almond Mountain Volcanics, but the exposures are not adequate to make this certain. These breccias clearly lie on the Bedrock Spring Formation with a slight unconformity in at least one area (D15–g). The tuff breccias are clearly overlain by late flows and flow conglomerates of the Lava Mountains Andesite, but are apparently contemporaneous with the early flows, for they contain rock types not abundant in the area prior to that formation. Probably they were deposited

as mud flows that resulted indirectly from the volcanic activity in early Lava Mountains Andesite time.

INTRUSIVES

Five distinguishable varieties of upper Pliocene(?) porphyritic or aphanitic intrusive rocks crop out in the central and western part of the mapped area. Each variety forms several individual intrusives that are limited to a discrete area as much as a square mile in size, but the areas characterized by each variety do not overlap. The upper Pliocene(?) intrusives in four of these areas form dikes; in the fifth they form small plugs and necks.

In sections D1–k and D1–q, dike rocks form resistant ridges that project above the eroded surface of the Bedrock Spring Formation. The groundmass is a distinctive grayish orange pink (*5YR* 8/2). The phenocrysts of plagioclase are the same color as the groundmass, whereas those of biotite form relatively unaltered dark-brown euhedral books. Light-brown areas, as much as 20 mm long, may represent altered acicular hornblende.

In sections D1–h, E5–e, E6–c, and E6–e, dike rocks also form resistant ridges, but pronounced swirling color patterns and filled vesicles allow them to be easily distinguished from those in the previously described area. The fresh surface is mostly grayish orange pink or very light orange; darker colors form the swirling, contorted patterns. Vesicles are very abundant, commonly lenticular and alined, and commonly coated with a lighter orange fine-grained material. Phenocrysts of plagioclase, biotite, and hornblende(?) rest in the groundmass of microcrystals of plagioclase(?) and an unidentified anisotropic material. The plagioclase present as megaphenocrysts up to 4 mm long as well as microphenocrysts, is weakly zoned and twinned; the composition ranges up to An_{55}. The biotite is almost entirely altered to opaque material, plagioclase, and discolored calcite. The hornblende(?) is entirely altered to opaque minerals.

In section A35, dike rocks intrude Atolia Quartz Monzonite. All these rocks weather to shades of red, red brown, and purple. They are so strongly brecciated and altered, however, that none of the included minerals can be accurately identified in thin section.

In section A23, dikes crop out that have weathered to soft, crumbly, dark-grayish rock containing small white phenocrysts of plagioclase as the only visible mineral. These rocks are also very strongly brecciated because of their nearness to the Garlock fault. The color and recognizable plagioclase distinguish them from the dikes in section A23.

In sections D13, D14, and E18, several small volcanic plugs and necks form steep-sided round hills. Most weather to dark grayish red. In detail, planar fractures, color banding, and lineation are sometimes visible; they generally dip at high angles, but have no regional pattern. In hand specimen, these rocks appear somewhat coarser grained than the other volcanic rocks of the area, and also contain a higher percentage of quartz. They range in composition from andesite to dacite and are composed of plagioclase, biotite, oxyhornblende, orthopyroxene, clinopyroxene, and quartz, in a groundmass predominantly of microcrystals of plagioclase and cryptocrystalline material. The plagioclase shows zones that are commonly well developed and often have a calcic rim; twins are not common and the composition ranges from andesine to sodic labradorite. Most of the biotite is partially altered to opaque materials. Usually, the oxyhornblende is strongly or entirely altered. Orthopyroxene and clinopyroxene, present as small euhedral crystals, are not altered. Quartz, which ranges from fairly common to abundant, is present as rounded and embayed crystals, some of which show a reaction rim of clinopyroxene. Most of the samples show a faint alinement of the plagioclase microphenocrysts and contain a small number of vesicles. Maximum crystal sizes are: plagioclase, 4 mm; quartz, 2 mm; biotite, 2 mm; oxyhornblende, 1.5 mm; orthopyroxene and clinopyroxene, about 0.75 mm. The average sizes are about two-thirds of these lengths.

The four series of dikes described in this unit are known to be intrusive only into the Bedrock Spring Formation and the Atolia Quartz Monzonite. The small plugs and volcanic necks are probably intrusive into the Almond Mountain Volcanics, although they could represent topographic highs that existed prior to the time the Almond Mountain Volcanics were being deposited. The relation between these intrusives and the Lava Mountains Andesite is not known. The rocks are considered late Pliocene(?) in age, but the possibility cannot be precluded that they may be in part late middle Pliocene or Pleistocene.

FELSITE

Felsite of late Pliocene(?) age crops out in two areas in the central part of the map. In one of these areas, it forms a northeast-trending steep hill about 1 mile east of Dome Mountain; in the other, which lies about 3 miles northeast of the first, it forms two large hills and a small dike that lie along the axis of the Dome Mountain anticline. These outcrops are thought to be mostly volcanic plugs, although in a few places a small remnant of the associated flow remains.

This rock is characterized by a strong tendency to spall off as flaggy slabs as illustrated in figure 13; these planar fractures are parallel to the thin bands of darker colors and to the alined minerals, and probably to the

original direction of flow. Normal to this planar fracture, it breaks with a smooth conchoidal fracture. The fracture planes dip at high angles either toward the center of the volcanic plug (as in secs. E5 and E8) or away from it (as in sec. B27). The weathered surfaces of these felsites are mostly light brown; the fresh surfaces are somewhat lighter and slightly more gray or orange.

FIGURE 13.—Typical outcrop of the upper Pliocene(?) felsite. Hill in background consists entirely of Quaternary andesite.

The felsite consists of a few plagioclase and biotite megaphenocrysts in a groundmass of very fine grained microphenocrysts, crystallites, and cryptocrystalline material. The plagioclase megaphenocrysts are euhedral, have very sharp edges, and are faintly zoned and twinned. The composition is variable, ranging from about An_{25} to An_{45}; the average is perhaps An_{35}. The plagioclase microphenocrysts have a similar average composition, although some have a composition as high as An_{55}. Biotite, partially or totally altered to opaque materials, is found as very thin books about 0.02 mm thick. Some oxyhornblende(?) occurs in trace amounts. The groundmass consists predominantly of microscopic crystals, crystallites, and cryptocrystalline material which X-ray diffraction shows to be predominantly cristobalite and sanidine; glass makes up less than 20 percent of the material. The groundmass contains a light to medium dust either of equant black opaque or of irregular red translucent fragments.

The texture of these rocks is notable for the almost perfect alinement of the plagioclase microphenocrysts, crystallites, and biotite crystals. Some specimens show vesicles, but most have none. Plagioclase and biotite crystals are as much as 3 mm long, but the plagioclase microphenocrysts average about 0.02 mm.

The results of modal, chemical, spectrochemical, and normative analyses of one specimen are shown in table 9. The modal analysis indicates that about 90 percent of this rock is groundmass and 10 percent identifiable minerals; this proportion is probably close to the average for this unit. A chemical analysis confirms the felsic composition suggested by the rock's color and texture, and shows it to be the most silicic volcanic rock analyzed. Its normative composition shows that on more complete crystallization this rock would be a very light colored rhyodacite, dacite, or quartz latite composed almost entirely of plagioclase (An_{27}), K-feldspar (30 percent of total feldspar), and quartz.

TABLE 9.—*Modal, normative, chemical, and spectrochemical analyses for one sample of the upper Pliocene(?) felsite*

[Sample 97-39, from top of ridge in north half of sec. E 5-r. A dash means the element was not present in detectable amounts. Chemical analyses by P. L. D. Elmore, H. F. Phillips, and K. E. White; spectrochemical analyses for Li and Rb by Robert Mays, remaining spectrochemical and modal analyses by G. I. Smith]

Modes

[Volume percents]

Plagioclase megaphenocrysts	1.2
Plagioclase microphenocrysts	6.3
(Total plagioclase)	(7.5)
Biotite	.3
Hornblende	0
Oxyhornblende	0
Orthopyroxene	0
Clinopyroxene	0
Quartz	0
Opaque minerals	1.1
Other minerals	1.2
Groundmass	89.9

Norms

[Weight percents]

Q	30.1
C	.8
or	19.5
ab	34.1
an	12.5
di	0
hy	0
mt	0
il	.5
hm	1.4
tn	0
ru	0
ap	.3
Symbol (C.I.P.W.)	I.4.2.4

Chemical analyes

[Weight percents]

SiO_2	71.5
Al_2O_3	15.6
Fe_2O_3	1.5
FeO	.01
MgO	.02
CaO	2.5
Na_2O	4.0
K_2O	3.3
TiO_2	.24
P_2O_5	.10
MnO	.02
H_2O	1.5
CO_2	<.05
Total	100

Spectrochemical analyes

[Parts per million]

Cr	12
Co	24
Mn	110?
Ni	1.7
Sc	<1
V	6
Fe	6,900
Cu	1.8
Ga	9.3
Ti	830
B	22
Ba	2,600
Be	<1?
Li	12
Pb	22
Rb	80
Sr	1,200
Yb	—
Y	10
Zr	100

In two outcrops, in sections E5–j and E8–a, felsite either intrudes or rests on top of the Bedrock Spring Formation. In sections E5 and E8, it either intruded the Almond Mountain Volcanics or formed a hill in the area in which they were subsequently deposited. Its relation to other Tertiary formations is unknown. The only sediments containing fragments of felsite are the Quaternary gravels. It is thus probably late Pliocene in age, although it could be of early Pleistocene age.

TUFF

Well-indurated tuff and lapilli tuff are exposed in the northeastern part of the mapped area. The best ex-

posures are in section B23–l and B26–f. Most of the rocks are extremely resistant to weathering and form jagged cliffs and steep-sided hills. The colors vary from shades of green to light red, gray, or brown. In some exposures, especially those along the west side of the outcrop area, the rocks are well bedded, but in most they are massive.

Between 75 and 95 percent of the rocks making up this unit is tuff or lapilli tuff; the balance is coarser volcanic fragments. Some of the well-bedded rocks also contain epiclastic material. The tuff underlies upper Pliocene(?) volcanic breccia. It probably overlies the Bedrock Spring Formation, although the field relations are obscure. The age relative to the Almond Mountain Volcanics and the Lava Mountains Andesite is not known.

VOLCANIC BRECCIA

Coarse volcanic breccia of late Pliocene(?) age is exposed in the northeastern part of the mapped area where it forms caps on the well-indurated tuff described above. The best exposures of this rock type are in sections B22–l, B24–q, and B25–h. The rocks are resistant to weathering and form jagged surfaces in outcrop. Pale reds and browns are the characteristic colors.

In the western half of the outcrop area, the rocks are flow breccias; most of the angular lava fragments are a fraction of an inch to a few inches across, but some are measurable in feet. The matrix of these breccias is apparently lava, although it may be welded tuff. The rocks in the eastern half are more homogeneous and contain light-gray phenocrysts of plagioclase, up to 5 mm long, and some visible biotite and amphibole(?); the matrix is a medium-gray fine-grained tuff or pumice which is highly vesicular on a microscopic scale.

These rocks clearly lie unconformably on the middle Pliocene Bedrock Spring Formation. They also overlie the upper Pliocene(?) tuff. Their relation to the Christmas Canyon Formation of Pleistocene(?) age can only be inferred. There is a faint line around these volcanic breccia hills which is interpreted as marking the position of the upper surface of the Christmas Canyon Formation when it buried the lower part of these breccia hills. The rocks above this line are very well exposed, and below it they are partly covered with debris. If the evidence is valid, the age indicated for the volcanic breccias lies between middle Pliocene and Pleistocene(?). An age of late Pliocene(?) seems likely.

CHRISTMAS CANYON FORMATION

The Christmas Canyon Formation, a new formation named here, is present only in the northeastern part of the mapped area. The type section, illustrated in figures 14 and 15, is located in section C8–e; the formation is named for Christmas Canyon, about 1 mile east of the type section.

The formation consists of two distinct facies, although they are not distinguished on the geologic map. South of the Garlock fault, a sandstone facies is restricted to a strip about half a mile wide and parallel to the fault; the type section is located in this facies. A boulder conglomerate facies, characterized by a small percentage of vesicular andesitic, basaltic, and rhyolitic boulders 1 to 2 feet across, is found both on top of and south of the sandstone facies. North of the Garlock fault, both facies are exposed.

FIGURE 14.—Typical exposure of the sandstone facies of the Christmas Canyon Formation. All but the top 20 feet of the 140-foot thick type section was measured on the slope below the arrow; the top 20 feet was measured on the northern (left) part of this ridge. The rocks in the immediate foreground are typical lag gravels formed on the surface of the boulder conglomerate facies of the formation. View looking northeast.

The Christmas Canyon Formation ranges in thickness from about 50 to 500 feet, although in most places it is between 75 and 150 feet thick. Where the formation rests on the Bedrock Spring Formation, the basal beds generally contain enough material derived from the underlying unit to make the contact indistinct. In the area of metamorphic outcrops, near Christmas Canyon and the type section, a basal bed of coarse breccia is characteristic. In many areas, the top of this formation probably approximates the final surface of deposition. Only the top few feet of finer material has been removed, and the surface now is an uneven desert pavement or lag gravel, consisting of pebbles, cobbles, and boulders of rhyolitic, andesitic, and basaltic rocks.

DESCRIPTION OF ROCK TYPES

The rocks of the sandstone facies are for the most part weakly indurated and form badland topography or low rounded hills. The outcrops are light yellowish gray,

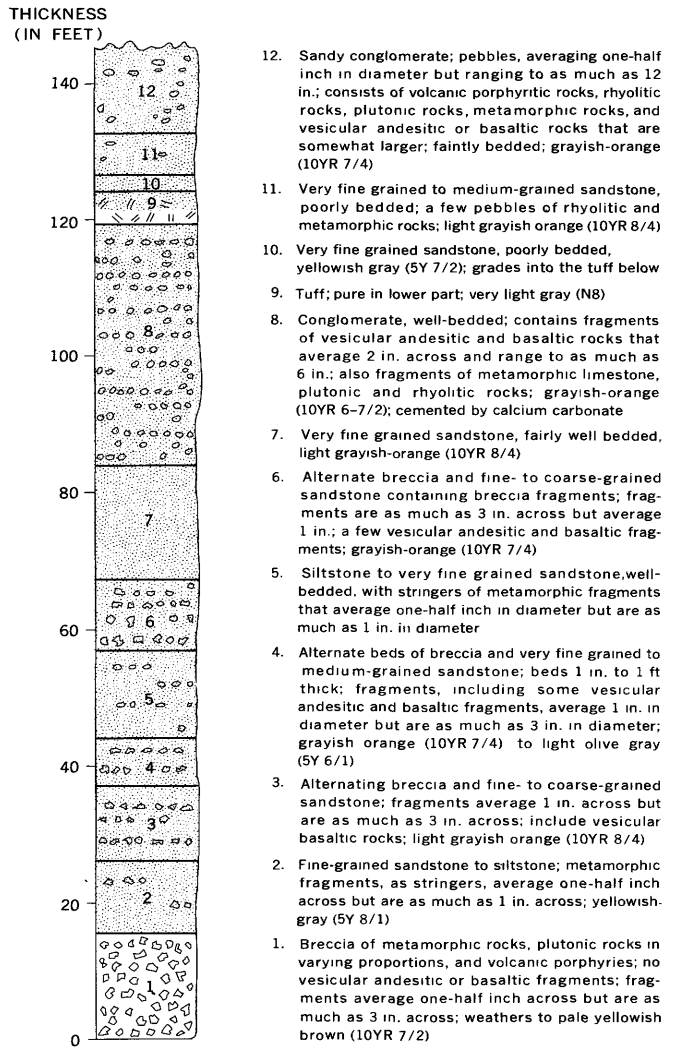

12. Sandy conglomerate; pebbles, averaging one-half inch in diameter but ranging to as much as 12 in.; consists of volcanic porphyritic rocks, rhyolitic rocks, plutonic rocks, metamorphic rocks, and vesicular andesitic or basaltic rocks that are somewhat larger; faintly bedded; grayish-orange (10YR 7/4)
11. Very fine grained to medium-grained sandstone, poorly bedded; a few pebbles of rhyolitic and metamorphic rocks; light grayish orange (10YR 8/4)
10. Very fine grained sandstone, poorly bedded, yellowish gray (5Y 7/2); grades into the tuff below
9. Tuff; pure in lower part; very light gray (N8)
8. Conglomerate, well-bedded; contains fragments of vesicular andesitic and basaltic rocks that average 2 in. across and range to as much as 6 in.; also fragments of metamorphic limestone, plutonic and rhyolitic rocks; grayish-orange (10YR 6-7/2); cemented by calcium carbonate
7. Very fine grained sandstone, fairly well bedded, light grayish-orange (10YR 8/4)
6. Alternate breccia and fine- to coarse-grained sandstone containing breccia fragments; fragments are as much as 3 in. across but average 1 in.; a few vesicular andesitic and basaltic fragments; grayish-orange (10YR 7/4)
5. Siltstone to very fine grained sandstone, well-bedded, with stringers of metamorphic fragments that average one-half inch in diameter but are as much as 1 in. in diameter
4. Alternate beds of breccia and very fine grained to medium-grained sandstone; beds 1 in. to 1 ft thick; fragments, including some vesicular andesitic and basaltic fragments, average 1 in. in diameter but are as much as 3 in. in diameter; grayish orange (10YR 7/4) to light olive gray (5Y 6/1)
3. Alternating breccia and fine- to coarse-grained sandstone; fragments average 1 in. across but are as much as 3 in. across; include vesicular basaltic rocks; light grayish orange (10YR 8/4)
2. Fine-grained sandstone to siltstone; metamorphic fragments, as stringers, average one-half inch across but are as much as 1 in. across; yellowish-gray (5Y 8/1)
1. Breccia of metamorphic rocks, plutonic rocks in varying proportions, and volcanic porphyries; no vesicular andesitic or basaltic fragments; fragments average one-half inch across but are as much as 3 in. across; weathers to pale yellowish brown (10YR 7/2)

FIGURE 15.—Type section of the Christmas Canyon Formation in sec. C8–e. The exact location of the measured section is shown in fig. 14.

except for included beds of volcanic ash or calcareous material, which are nearly white. The bedding is characteristically distinct, and individual beds, ranging in thickness from less than an inch to a few feet, may be traced for several hundred feet. Minor angular discordances between beds are common but local, and perhaps resulted from contemporaneous movement on the Garlock fault. The sandstones and siltstones of this formation are poorly sorted and consist of angular arkosic fragments. Many of the beds, especially the finer grained materials, contain calcium carbonate, which forms a white efflorescence. Locally, as in the type section, tuffaceous beds are found. Conglomeratic sandstones and conglomerates that are interbedded with the finer material contain rounded to subangular pebbles of the following rock types: porphyritic andesitic rocks, metamorphic rocks of the types exposed nearby, rhyolitic rocks showing contorted color banding, plutonic rocks including the pink leucocratic phase of the Atolia Quartz Monzonite, and small vesicular andesitic or basaltic rock pebbles.

The boulder conglomerate facies forms steep-sided hills that are covered with slumped debris. Most of the outcrops are tan to dark brown. Bedding is rarely seen. In most places, this facies consists of pebbles, cobbles, and boulders in a matrix of very coarse angular sandstone. The pebbles and cobbles include diorite, quartz monzonite, marble, slate, phyllite, quartz, quartzite, and porphyritic andesitic and rhyolitic fragments; the boulders are almost all banded rhyolitic rocks and vesicular andesitic and basaltic rocks, commonly measuring about 1 foot across. The thickness of this facies rarely exceeds 200 feet, and in most exposures it is about 75 feet thick.

DISTRIBUTION OF ROCK TYPES

South of the Garlock fault, the sandstone facies of the Christmas Canyon Formation is limited to the half-mile-wide strip along the south edge of the fault; the conglomerate facies forms the top few feet of the formation where composed mostly of sandstone, and all of it south of the area containing the sandstone facies. The lateral facies change occurs along the line indicated on plate 1 as a concealed fault. Both facies are exposed north of the Garlock fault in sections C4–j and C4–k, and apparently extend north and east of the mapped area to form outcrops along the north side of the Garlock fault for about 15 miles (fig. 17).

The sandstone facies of the Christmas Canyon Formation probably forms much of the fill in Searles Valley. Some of the deeper parts of the fill under Searles Lake are equivalent in age, though the basin fill down to 875 feet consists of salines and silt and is quite dissimilar (Smith and Pratt, 1957, p. 25–51).

AGE AND RELATION TO OTHER FORMATIONS

The conglomerate facies of the Christmas Canyon Formation is unconformable on the Bedrock Spring Formation; the sandstone facies is not in depositional contact with it. The Christmas Canyon Formation is also younger than the Almond Mountain Volcanics, Lava Mountains Andesite, and the fresh-looking Pleistocene(?) basalts of the Black Hills several miles to the southeast (figs. 2 and 3) which are so abundantly represented as boulders in the conglomerate facies. It is also inferred to be younger than the other upper Pliocene(?) volcanic breccias. The older gravels and the Quaternary andesite may be in part equivalent in age to the Christmas Canyon Formation, for the sur-

faces on which all three units were deposited were similar and possibly continuous.

One fossil, a hoof bone, was found in the Christmas Canyon Formation by Richard Tedford and Robert Shultz, Jr., about a thousand feet north of the type section. According to G. E. Lewis (written commun., 1956): "The size of the hoof bone permits reference either to a large species of *Pliohippus* (Pliocene) or a small *Equus* (Quaternary)." On the basis of this fossil, whose identity is admittedly inconclusive, plus the presence of the Pleistocene(?) lava boulders in the formation, an age of Pleistocene(?) is assigned.

SEDIMENT SOURCE AND ENVIRONMENT OF DEPOSITION

Sources for the predominant rock types in the Christmas Canyon Formation are the Black Hills (where vesicular andesitic or basaltic flows and quartz monzonite are exposed (fig. 2)), the hills west of Grass Valley (where banded rhyolite, quartz monzonite, and diorite are exposed), and the western part of the Lava Mountains (where leucocratic quartz monzonite, arkosic sandstone, and andesitic volcanic rocks are exposed). The andesitic fragments could have been either derived from the volcanic hills northeast of the Black Hills or reworked from the Bedrock Spring Formation. The metamorphic rock fragments were from outcrops in the vicinity of Christmas Canyon. Tuff beds in the sandstone indicate intermittent volcanic activity.

The lithologies of the conglomeratic and sandstone facies of this formation closely resemble those of present day alluvial fans and intermittent or playa lakes, and they probably were formed in such environments. That the sandstone facies was formed in a lake is further indicated by the high calcium carbonate content of some beds, and the numerous calcium carbonate tubes which probably represent the calcified roots of water plants. Along the south side of the Slate Range (figs. 2 and 17), shale, siltstone, and sandstone thought to be an eastward extension of this formation contain sodium sodium chloride, sodium sulfate, calcium sulfate, and trace amounts of nitrates (Noble, 1931, p. 10–13), and those rocks probably also represent a desert-lake environment.

Part of the south edge of this lake was apparently localized by a fault or fault-line scarp parallel to and about half a mile south of the Garlock fault. It is shown as concealed on plate 1. This fault is inferred entirely from indirect evidence. (1) Interfingering relations between the sandstone and conglomerate facies are exposed at several places along this line, the lateral transition occurring over a zone a few feet wide; and (2) the shapes of the northernmost metamorphic rock outcrops suggest north-facing triangular facets of a partly dissected and buried fault scarp.

QUATERNARY BASALT

Several northeast-trending basaltic dikes and very small flows are found in the northeastern part of the area (secs. B13 and C18). These weather to resistant ridges and spines, generally in shades of dark red or dark gray. Most of these rocks are massive vesicular basalt; some, especially the northern dikes, are basaltic volcanic breccias. At the westernmost end of the outcrop area, a very small basaltic flow breccia rests with a horizontal contact on the top surface of the conglomerate facies of the Christmas Canyon Formation.

The rock consists of phenocrysts of plagioclase, pyroxene, and olivine(?) which is now entirely altered to iron oxides, in a matrix of vesicular glassy or partly crystalline material. Most vesicles within an inch of the surface of the breccia fragments contain calcium carbonate; vesicles more than an inch in from weathered surfaces contain none.

These basalt dikes are younger than the Christmas Canyon Formation and thus the basaltic flows in the Black Hills (southeast of the Lava Mountains). Hulin (1925, p. 59) correlated a few small patches of basalt exposed in the Summit Range (fig. 2) with the Black Mountain Basalt, named by Baker (1912, p. 126–128) after flows that crop out on the north side of the El Paso Mountains, about 10 miles to the west. Correlating the basalt dikes described in this report with Baker's Black Mountain Basalt, however, does not seem warranted.

QUATERNARY ANDESITE

Andesite sills, dikes, plugs, and flows crop out in an east-west belt through the middle of the mapped area. This belt is approximately along the line between T. 28 S. and T. 29 S., and also along the inferred axis of the valley formed in Almond Mountain Volcanics time (see p. 32). The best exposures of these rocks are in sections B32, D1, D2, and E5.

The rocks weather to olive gray (5*Y* 3–5/1–2) or dark greenish gray (5*GY* 3–5/1), colors that are easily distinguished from those characterizing the other volcanic formations of the area. Some, especially the intrusive rocks, are nonresistant to weathering and form zones of dark-colored decomposed volcanic material, but most are more resistant and form cliffs or steep-sided hills. Locally (as in sec. D1–p), columnar joints a foot or two in diameter have formed; both intrusive and extrusive rocks have these features. In the remaining flows (as in sec. E5), the rocks are unjointed and form smooth dip slopes (shown in the background of fig. 13); where dissected, the rocks forming these slopes are characterized by alternating light and dark layers which lie parallel to the contacts.

In section E5-h, the toe of one of these flows is well exposed in the canyon bottom (fig. 16), indicating that the present topography was to some extent established, and that the original areal extent and thickness of these flows is now virtually the same as it was originally.

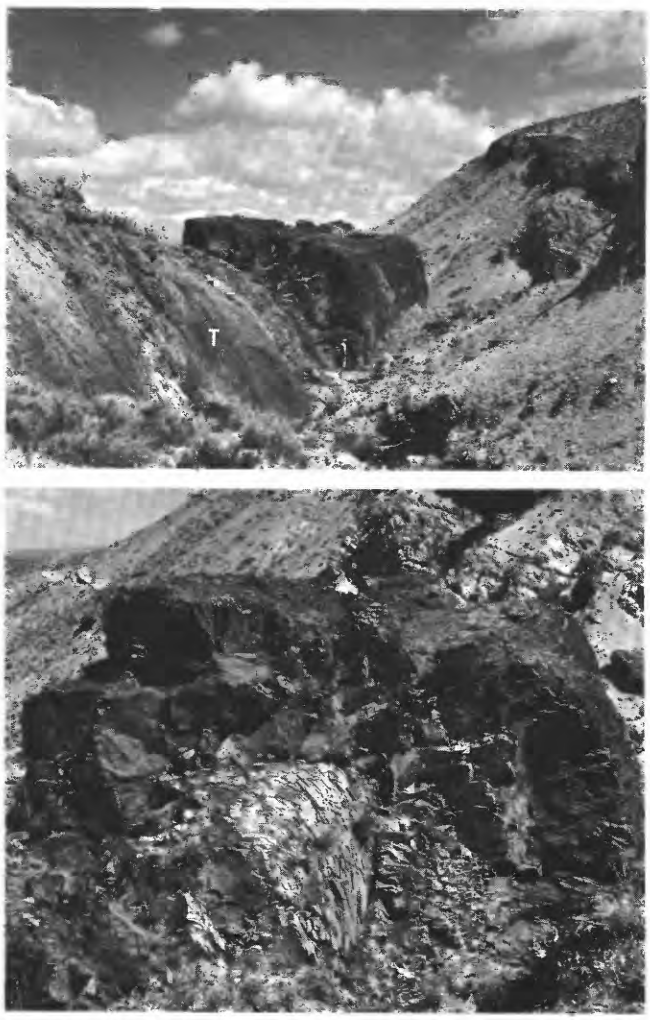

FIGURE 16.—Upper photograph shows the toe (T) of a Quaternary andesite flow exposed in sec. E5–h. The flow came from left. The lower photograph is a detailed view of the cross section exposed in the central part of the upper photograph. Note the "roll-over" structures. Views toward the east. Both photographs by R. F. Yerkes.

The most distinctive megascopic feature of the rocks of this unit is the greenish-yellow coating present on the walls of the elongated vesicles. These coatings, which were present in the vesicles of every specimen of this rock examined, appear as streaks less than 1 mm across. They apparently consist of serpentine, stained chalcedony, opal, tridymite, and zeolite.

The rocks of this unit are all porphyritic andesite. They consist of phenocrysts of plagioclase, biotite, oxyhornblende, orthopyroxene, clinopyroxene, and sometimes quartz, in a groundmass of microcrystals and cryptocrystalline material. The plagioclase crystals, always found as two size groups, are most commonly strongly zoned and generally also have a calcic rim; twins show weak to strong development. Most of the biotite is partially altered to opaque materials. The amphibole—green hornblende in the intrusive rocks of the northwestern part of the area, and oxyhornblende in the intrusive plugs and associated flows of the central part of the area—is heavily altered to opaque materials. Clinopyroxene and orthopyroxene are fresh in most rocks, but in some have been partially or totally altered to serpentine(?). Quartz is present in a little over half of the rocks examined. The groundmass consists of about 20 percent glass, the rest being about half microcrystals and half cryptocrystalline material; the groundmass of many samples also has numerous disseminated fibers of a light green to colorless mineral (which may be serpentine), and most have a medium-light "dust" of opaque minerals. Some of the rocks show a faint lineation in the groundmass. In most of these rocks, the phenocrysts reach the following maximum sizes: plagioclase, 6 mm; biotite, 3 mm; hornblende or oxyhornblende, 3 mm; quartz, 1 mm; and clinopyroxene and orthopyroxene, 1 mm. The average sizes are generally one-half to one-third of these figures.

Modal, chemical, normative, and spectrochemical analyses for two of these rocks are shown in table 10.

TABLE 10.—*Modal, normative, chemical, and spectrochemical analyses for two samples of the Quaternary andesite*

[A dash means that the element was not present in detectable amounts. Chemical analyses by P. L. D. Elmore, H. F. Phillips, and K. E. White; spectrochemical analyses for Li and Rb by Robert Mays; remaining spectrochemical and modal analyses by G. I. Smith]

Modes
[Volume percents]

	28–17	*128–34*
Plagioclase megaphenocrysts	9.7	10.7
Plagioclase microphenocrysts	9.7	11.1
(Total plagioclase)	(19.4)	(21.8)
Biotite	.9	.4
Hornblende	1.8	0
Oxyhornblende	0	.1
Orthopyroxene	.1	.3
Clinopyroxene	.2	.3
Quartz	.2	.5
Opaque minerals	1.7	4.4
Other minerals	6.0	4.6
Groundmass	69.7	67.6

Norms
[Weight percents]

	28–17	*128–34*
Q	19.7	18.5
C	------	------
or	15.6	15.6
ab	35.6	35.6
an	18.6	17.8
di	2.6	2.8
hy	1.3	2.5
mt	.5	0
il	1.2	.9
hm	2.9	4.0
tn	0	.4
ru	0	0
ap	.3	.3
Symbol (C.I.P.W.)	I. 4. 3. 4	I. 4. 3. 4

Chemical analyses
[Weight percents]

SiO_2	64.4	63.9
Al_2O_3	16.6	16.3
Fe_2O_3	3.2	3.6
FeO	.78	.44
MgO	1.0	1.5
CaO	4.4	4.4
Na_2O	4.2	4.2
K_2O	2.6	2.6
TiO_2	.62	.64
P_2O_5	.20	.22
MnO	.04	.04
H_2O	2.2	2.3
CO_2	<.05	.22
Total	100	100

Spectrochemical analyses
[Parts per million]

Cr	45	45
Co	24	20
Mn	330	340
Ni	40	40
Sc	6.6	9.6?
V	50	36
Fe	20,000	17,000
Cu	18	6?
Ga	12	12?
Ti	2,100	2,100
B	Trace?	13
Ba	2,300	2,200
Be	------	<1
Li	40	36
Pb	12	10
Rb	40	40
Sr	1,400	1,800
Yb	<1	<1
Y	8.0	8.4
Zr	130	94

LOCATION OF SAMPLES

28–17. Sec. D 12–c, from upper contact of sill exposed in bottom of canyon.
128–34. Sec. E 3–b, from base of small flow surrounding volcanic neck.

The two sampled outcrops are about 4½ miles apart. One sample (28–17) is from an exposure of this rock where it is intrusive, and the other (128–34) is from an exposure where it is extrusive. Yet modal, chemical, normative, and spectrochemical analyses of both samples are nearly identical. Normative orthoclase forms 22 and 23 percent of the total feldspar in these two rocks, and their normative plagioclase compositions are An_{34} and An_{33}. Both are classified by the C.I.P.W. system (Washington, 1917) as yellowstonose. The greatest difference between samples is in the mafic mineral content reported in the modal analysis. This intrusive rock contains nearly 2 percent of both hornblende and opaque minerals, and no oxyhornblende; whereas the extrusive rock contains no hornblende, a little oxyhornblende, and a little over 4 percent opaque minerals. The hornblende has clearly changed to oxyhornblende and opaque alteration products during extrusion, and evidence of this change is believed to be a reliable criterion in this area for identifying other volcanic rocks as extrusive (although not all extrusive rocks have undergone this change).

Most of the rocks mapped as Quaternary andesite intrude or overlie the Bedrock Spring Formation. One exposure determines the age more closely: in section B32–q, Quaternary andesite rests on the upper part of a surface that was elsewhere covered by older gravels of early Quaternary age (fig. 21). The andesite is almost certainly of the same age or very slightly older.

OLDER GRAVELS

The deposits shown on the map as older gravels are mostly pediment gravels and older alluvium. The pediment gravels occur as relatively flat caps of uniform thickness on top of the truncated beds of the Bedrock Spring Formation in the central and north-central part of the area (fig. 21). They weather to grayish orange or tan colors; because of the contribution from volcanics, these gravels have a distinctively more brownish hue than the underlying sedimentary rocks. In general, they show little resistance to erosion. Bedding, where found, can be traced for only a short distance. The pebbles, cobbles, and boulders in these pediment gravels were derived, in every instance noted, from the rocks that now crop out uphill from them, indicating that no great shift has occurred in the directions of debris transport since they were deposited. The fragments range from subangular to well rounded and are found in all sizes up to 2 feet across. The matrix is very coarse sand, apparently derived in part from the Bedrock Spring Formation and in part from the volcanic outcrops.

Older alluvium, a term used here to designate the alluvial deposits that are now being dissected, is found along the sides of most of the canyons and washes. The included pebbles and cobbles are generally volcanic and plutonic rocks in the ratio of two or three to one; the matrix is arkosic sand. In most areas, this older alluvium is undeformed, although in some places along the Garlock fault zone it is slightly tilted.

The older gravels near the northwest corner of the mapped area (in secs. A21 and A22) are erosional remnants of a thick alluvial-type deposit of probable Quaternary age. The debris is distinct from the other gravels included in this map unit, and contains basaltic and banded rhyolitic boulders derived from nearby outcrops of pre-middle Pliocene(?) volcanic rocks.

The small outcrop of sediments on the top of the round hill in the southeast corner of the map (in sec. E36) is probably a local deposit that formed in a closed depression in the top of the hill before it was breached. The sediments are 20 or 30 feet thick, weather to a soft, nonresistant material, and contain notable amounts of caliche and an opaline substance.

Most of the older gravels can be distinguished from the conglomeratic facies of the Christmas Canyon Formation by the presence in the latter of vesicular andesite or basalt and banded rhyolite, derived from exposures southeast of the mapped area; the older gravels contain only locally derived volcanic rocks.

ALLUVIUM

Alluvium is now being deposited in all the canyons of the Lava Mountains and in large areas north and southeast. The composition is that of an arkosic gravel. The pebbles and cobbles of volcanic rocks are derived locally from the Pliocene and Quaternary volcanic formations and the pebbles of plutonic rocks, as well as the arkosic matrix, are mostly reworked from the Bedrock Spring Formation.

TUFA AND TRAVERTINE

Along the highest of the Pleistocene shorelines of Searles Lake (Gale, 1914, p. 265–268), deposits of tufa rest on alluvium and older rocks. Within the area shown on plate 1, most of these measure only a few feet in each dimension, and form porous tabular deposits. One of these occurs in section B12–e where the Christmas Canyon Formation has been uplifted along the Garlock fault. This tufa, deposited when Searles Lake stood near its maximum level, rests on the most recent north-sloping scarp of the fault (fig. 18). The last high stand of this lake is estimated to have been at least 50,000 years ago (Smith, 1960a), and the displacement of the Garlock fault that formed this scarp is thus dated as having occurred prior to that time.

Along the west edge of the Lava Mountains—in sections D–3m, D3–n, D10–k, D22–d, and D27–g—are five

outcrops of fine-grained porous travertine. The travertine weathers to shades ranging from light olive gray to grayish orange pink, though on fresh surfaces it is somewhat lighter. On weathered surfaces, structures of contorted bands and layering stand out in relief. These outcrops are at similar elevations, and all lie along the foot of hills that form the west edge of the Lava Mountains. They are probably spring deposits formed when the regional water table in this area was higher and springs flowed from the base of these hills.

Two small lenticular outcrops of travertine occur in the Brown's Ranch fault zone in section E17–k. Both are yellowish gray and contain pebbles of the surrounding volcanic rock types. The thicker one, which measures about 150 by 50 feet, is elongated parallel to the direction of faulting and shows faint vertical lineation of the calcareous structures. The thinner travertine outcrop, which measures about 200 feet along the strike and is 35 feet thick, has horizontal lineation. Both were probably deposited by springs associated with the fault zone. One is overlain by the Almond Mountain Volcanics, the other by the Lava Mountains Andesite, suggesting that they were deposited prior to those formations; it is more probable, however, that they were formed by a spring issuing from the base of those formations at a later time.

STRUCTURE

Within the Lava Mountains area, three sets of faults converge. The Garlock fault and its associated faults trend N. 75° E. along the north side of the area. The Blackwater fault, trending N. 45° W., is a conspicuous feature in the southeastern part of the area. The Brown's Ranch fault zone, which has an average trend of about N. 55° E., dominates the tectonic character of the central and southwestern parts of the area. The Garlock fault is a left-lateral fault; the Blackwater fault is a right-lateral fault; the Brown's Ranch fault zone has probably sustained both lateral and dip-slip movement. A small thrust fault crops out on the south side of the Garlock fault. The Dome Mountain anticline, the major fold within the area, trends nearly parallel to the Garlock fault.

The relative ages of intersecting faults can be established in several places, and all three fault sets give evidence of intermittent activity extending into the Quaternary. Inferred order of first activity on these fault sets is: (a) Garlock fault, (b) Brown's Ranch fault zone, and (c) Blackwater fault. The thrust fault is post-middle Pliocene but cannot be assigned a place in this sequence. The date of last significant activity on these faults is less certain; many of the later displacements are small and probably reflect stresses that were relieved chiefly along other faults, but were also expressed along any lines of crustal weakness created earlier. These small, chiefly passive displacements cannot readily be distinguished from the larger ones in every instance, but the available evidence indicates that the probable sequence of the last significant displacements is: (a) Blackwater fault, (b) Brown's Ranch fault zone, and (c) Garlock fault.

In the regional tectonic environment, described by Hewett (1954b, pl. 1; 1955, p. 378–386), the Garlock fault is the most important of the three fault sets; it extends over a total distance of about 160 miles and separates distinct geologic provinces. The Blackwater fault represents a very common but less continuous set that is distributed throughout the western Mojave Desert; the fault extends over a distance of about 30 miles and throughout part of its length separates areas with distinct fault patterns (although this is not a characteristic of the other northwest-trending faults of the Mojave Desert; see Hewett, 1954b, p. 17). The Brown's Ranch fault zone represents a much less common set of faults that is found in the Mojave Desert region chiefly in the northeastern third and in the vicinity of Garlock fault; in the Lava Mountains, the fault zone extends over a total distance of about 10 miles.

The most important conclusion reached by a study of the structural pattern of the Lava Mountains is that, in this area, the activity along these three fault sets has been in part contemporaneous. This does not mean that displacements occurred along two or more faults at the same moment, but the small amounts of geologic time that did elapse between displacements rule out the probability that differently oriented fundamental stress patterns are responsible for the individual fault sets. Each is apparently the result of a stress pattern that has been repeated several times as a phase of a continuing tectonic process.

FAULTS

GARLOCK FAULT

The Garlock fault, first recognized and named by Hess (1910, p. 25), is one of the master tectonic features of this part of California, and it is a dominant element in the structural history of the Lava Mountains. At its western extremity, about 85 miles southwest of the Lava Mountains, the fault trends approximately N. 60° E.; along the north side of the Lava Mountains it trends N. 75° E.; at the south end of Panamint Valley, approximately 15 miles to the east, the fault trends east; from that point eastward the trend gradually changes to S. 85° E. until it loses its identity 75 miles to the east near the Avawatz Mountains.

Throughout most of its 160-mile extent, the Garlock fault is expressed as a complex of anastomosing faults and crushed zones. Noble (1926, p. 423–425), Simpson (1934, p. 403), Wiese (1950, p. 39–41), Dibblee (1952, p. 38–39), Hulin (1925, p. 62–64), Muehlberger (1954a, b), and Noble and Wright (1954, p. 157–159) have described segments of the fault. In most places it has created a zone of crushed rock several hundred feet or more in width, and commonly consists of two or more major shears up to a mile apart. On the north side of the Lava Mountains, however, it is a relatively simple fracture that is expressed as one or two adjacent breaks and an associated crushed or deformed zone. Although the Atolia Quartz Monzonite that crops out in the northwestern part of the Lava Mountains is extensively fractured throughout, the zone of intense crushing and staining attributable to the fault itself is only a few hundred feet wide. Bedrock Spring(?) Formation crops out below the thrust fault adjacent to the Garlock fault; the beds are gently folded, but even though only 200 feet away from the Garlock fault trace, they are nearly unfaulted. Where the Garlock fault cuts the Christmas Canyon Formation, some parallel faults have been formed, and the bedding is extremely contorted for a few hundred feet on either side, but deformation that is directly attributable to the Garlock fault forms a zone that rarely exceeds a thousand feet in width.

In the Lava Mountains area, as in many other areas, the Garlock fault has alluvium on one or both sides of its trace. In these areas it is not easily identified from the ground, but on aerial photographs (fig. 18) the locations of its last displacements are almost invariably quite evident. The better exposures of the Garlock faults are found in sections A23, A29, B12, C4, and C7. In all other places, its location is inferred solely or largely from aerial photographs.

DISPLACEMENT

Along the north side of the Lava Mountains, field evidence indicates both left-lateral and vertical displacements on the Garlock fault during Quaternary time. A high scarp and uplifted Quaternary(?) pediment in the northwestern part of the Lava Mountains indicate several hundred feet of vertical displacement in early or middle Quaternary time. Horizontal displacements may also have occurred during the uplift of the scarp, but they would not be detected from the types of field evidence that are available. Late Quaternary displacements, though, have a demonstrable horizontal component. Stream courses that cross the fault trace in the alluvium at the foot of this scarp are offset left-laterally as much as 200 feet. Scarps formed by vertical displacements on the faults during this period rarely exceed 50 feet.

The sense of pre-Quaternary displacement along this segment of the fault cannot be demonstrated directly, but indirect evidence from the Lava Mountains also indicates both left-lateral and vertical components. A left-lateral displacement that is measurable in miles is probably indicated by a 6,500-foot left-lateral separation on a late Pliocene(?) fault parallel to the Garlock fault (see p. 47). Middle and late Pliocene vertical displacements that formed a positive area along the south side of the fault are indicated by the debris in the Bedrock Spring Formation and the sandstone beds of the Almond Mountain Volcanics which came from this positive area.

Evidence from other parts of the Garlock fault also indicates that its displacements have been dominantly left lateral. At the type exposure of the Garlock fault, near the west edge of the area shown on figure 2, about 500 feet of Quaternary left-lateral displacement is suggested by the offset tip of a terrace gravel remnant (Dibblee, 1952, p. 39 and pl. 1). Near the east end of the fault, stream channels are offset left laterally as much as 2,000 feet and Cenozoic rocks are displaced 1½ miles (Muehlberger, 1954a, b).

Estimates of total or post-Mesozoic lateral displacements are similarly varied. An average total displacement of as much as 25 miles has been estimated on the basis of published studies and regional considerations (Nolan, 1943, p. 186). A fault nearly parallel to the west end of the Garlock fault has caused 2 to 3 miles of post-Jurassic left-lateral displacement (Wiese, 1950, p. 41), suggesting that the total displacement of the master fault is at least this much and probably more. Along the central segment of the fault, just west of the Lava Mountains, a left-lateral total displacement of about 5 miles is inferred on the basis of a shifted contact between Mesozoic and older rocks (Hulin, 1925, p. 62–64). Near the east end of the fault, total horizontal displacements of at least 1 or 2 miles are inferred from the general character of the fault zone (Muehlberger, 1954b), and rocks that crop out nearby in the Owlshead Mountains, north of the fault, are tentatively correlated with rocks that form a block within the fault zone 8 to 12 miles to the east (Noble and Wright, 1954, p. 159), suggesting a greater relative displacement of the blocks north and south of the zone. A total displacement of about 40 miles on the east half of the fault is indicated by the correlation of a displaced Mesozoic(?) dike swarm (Smith, 1960b; 1962).

AGE

The Garlock fault has probably been active intermittently from late Mesozoic or early Tertiary time to the present. Hewett (1954a, p. 15) notes that pre-Miocene Cenozoic rocks are not present in the Mojave

Desert south of the Garlock fault, but are present in several places just north of it. From this he infers that the "Mojave block" was undergoing erosion during Eocene and Oligocene time, and that early Tertiary activity along the Garlock fault was responsible for the distinction between the two areas. Independent evidence of early Tertiary activity is furnished by a thrust fault on the north side of the Garlock fault, about 50 miles southwest of the Lava Mountains, which Smith (p. 56)[2] dated as pre-lower Miocene; this thrust moved normal to the Garlock fault and is interpreted to reflect contemporaneous activity along that fault. Within the Lava Mountains area, middle Pliocene activity on the Garlock fault is probably indicated by the fragments in the Bedrock Spring Formation that were eroded from the northwestern outcrops of Atolia Quartz Monzonite, which probably had been elevated by the Garlock fault. Other indirect evidence of middle Pliocene activity is furnished by the position of the belt of finer facies in the Bedrock Spring Formation and the general shape of the inferred sedimentary basin (see p. 20 and fig. 9), both of which are elongated parallel to the Garlock fault.

The last major displacement on this part of the Garlock fault was more than 50,000 years ago, as indicated by a tufa deposit on the fault scarp (p. 44; Smith, 1960a). This conclusion seems to be corroborated by aerial photographs, which show that the wave-cut shoreline in the vicinity of Christmas Canyon apparently has not been offset by the fault (figs. 17 and 18), although the angle between the shoreline and the fault is so small that only a large displacement would be detected.

FAULTS PARALLEL TO THE GARLOCK FAULT

Within the mapped area, only two major faults parallel the Garlock fault. One of these is a concealed fault-line scarp about a mile west of Christmas Canyon (in secs. C7 and C8) which is inferred from an abrupt change of facies in the Christmas Canyon Formation along this line, and an apparent linear break in the bedrock topography (pl. 2, sec. *A–A′*). It seems to have been active only in pre-Christmas Canyon time.

A larger fault is exposed along the south side of the Atolia Quartz Monzonite outcrop in the northwestern part of the mapped area. This fault, which separates Atolia Quartz Monzonite from younger rocks throughout much of its length, is nearly vertical in its eastern half and dips 60° to 70° S. in its western half. It continues westward from the Lava Mountains area and probably joints the concealed Cantil Valley fault inferred from a gravity survey in the valley north of the Rand Mountains (Mabey, 1960, pl. 10, p. 60). In the Lava Mountains, the horizontal separation by this fault of the nearly vertical(?) contact between the volcanic rocks older than the Bedrock Spring Formation and the Atolia Quartz Monzonite is about 6,500 feet, with the south side moved relatively east; hence a large lateral component of slip is probable. A sizable vertical component of displacement is also probable, because the Bedrock Spring Formation is only about 100 feet thick north of the fault and is probably more than a thousand feet thick on the south. The undisturbed flow overlying the fault trace at its west end indicates that displacement along this fault occurred in pre-Lava Mountains Andesite time.

BROWN'S RANCH FAULT ZONE

The northeast-trending faults in the central part of the map are here called the Brown's Ranch fault zone after the abandoned buildings in section G5, known locally as Brown's Ranch. The faults that are specifically included in this zone are shown on the geologic map. They are not readily separable by any objective criteria from the many parallel faults outside of the zone, but are thought to be the ones that have sustained the most displacement. The Brown's Ranch fault zone trends approximately N. 45°–65° E. At its northeast and southwest ends, the trend is more northward. The best exposures of this fault zone are in sec. E17–r, where about 500 feet of grayish-orange fault breccia is found. Here, the breccia consists of angular siliceous fragments embedded in a siliceous matrix. Southwest of these exposures, however, the zone cuts through soft material mapped as tuffaceous rocks of the Almond Mountain Volcanics. In this area there are also some flat-lying layers of siliceous fault breccia, which probably are the result of secondary silicification along certain horizons after brecciation.

DISPLACEMENT

Many of the faults of the Brown's Ranch fault zone cut beds that are nearly flat, in some places displacing them vertically by more than 100 feet. At the northeast end of the fault zone, most of the faults have the downthrown block on the southeast side; all the faults in this area dip northwest or are vertical. The valley containing the southwest end of the fault zone is a graben; the faults consistently have the downthrown block on the side of the valley and also dip toward it.

Most of these faults are relatively straight. Some also have opposite types of separation at their two ends. It is common to find such linearity and changeable separation along strike-slip faults, and for this reason, some slip with this component is inferred. The sense of the horizontal component of slip is not evident. The

[2] Smith, G. I., 1951, The geology of the Cache Creek region, Kern County, California: Pasadena, California Inst. Technology, M.S. thesis, 72 p.

FIGURE 17.—Oblique aerial photograph showing the Garlock fault (G) and the Searles Lake shorelines (S) exposed near the northeast corner of the mapped area (the boundaries of which are shown by a dashed line). Christmas Canyon (C) is in the right foreground. The Slate Range (SR) and the probable eastern extension of the light-colored Christmas Canyon Formation (CC?) are in the central background. View looking east. Photograph by R. C. Frampton and J. S. Shelton.

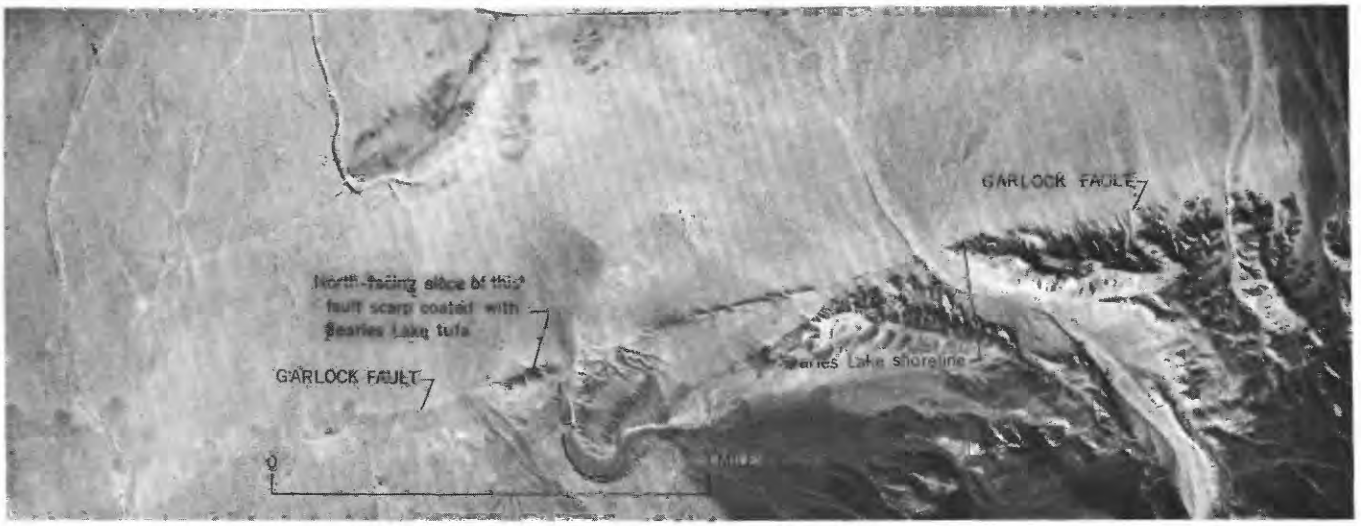

FIGURE 18.—Vertical aerial photograph showing part of Garlock fault trace. Scarp coated by tufa at least 50,000 years old, and shorelines that are apparently not offset by the fault, are indicated. Note that the fault is represented in most places by a single fracture so that no other scarps along this segment could be considered more recent. North is toward top of photograph. U.S. Navy aerial photograph PTK–5–025.

only evidence in the fault zone is furnished by slickensides on a small fault surface in section E20–c which plunge 60° E. and indicate a slip having both normal and left-lateral components. Indirect evidence from the parallel strike-slip faults northwest of the zone is conflicting: two indicate right-lateral slip and one indictates left-lateral slip (p. 49–50).

AGE

The faults of the Brown's Ranch zone have been active from the middle Pliocene into the Quaternary, but the inconsistent effect of these faults on alluvium suggests that they have been nearly quiescent in late Quaternary time. They have consistently displaced beds of both the Bedrock Spring Formation and the Almond Mountain Volcanics. Perhaps half of them also displace beds of the Lava Mountains Andesite. Two can be traced across alluvium. Thus, most of the direct field evidence records displacements that occurred after the deposition of the Almond Mountain Volcanics, but before or during deposition of the Lava Mountains Andesite. Indirect evidence, however, suggests that some activity occurred during deposition of both the middle Pliocene Bedrock Spring Formation and the Almond Mountain Volcanics. This inference is based on the distribution and facies of the two formations. The Bedrock Spring Formation seems to have been deposited in a basin that was generally parallel to the Garlock fault but was elongated southward along the Brown's Ranch fault zone. The concentration of the tuff facies of the Almond Mountain Volcanics along the present fault zone trough suggests that at that time the faults of this zone partly controlled the topography.

FAULTS PARALLEL TO THE BROWN'S RANCH FAULT ZONE

Most of the faults in the western half of the mapped area have about the same trend as the Brown's Ranch fault zone. These parallel faults are the most abundant in the Lava Mountains area. Typically, their trend ranges from N. 40° E. to N. 55° E.; their strikes change gradually from one end to the other. Most can be traced for a mile or more. Dips are variable; some are to the northwest, others are to the southeast, and many are vertical; no one direction or amount of dip appears predominant.

Although an appreciable displacement has occurred along many of these faults, most of them consist either of a single fault surface or of a few feet of brecciated material. In most places, the beds on the two sides of the fault are neither contorted nor extensively fractured.

DISPLACEMENT

This group includes both normal and reverse faults. Most of them displace gently dipping beds, and the main direction of movement presumably was dip slip; vertical separations range from several tens of feet to 1,000 feet near Dome Mountain. Three faults also have a large strike-slip component, two of them right-lateral and the other left-lateral.

The fault having left-lateral slip is about a mile northwest of Bedrock Spring (sec. A36-a). It causes a 2,000-foot horizontal offset where it crosses a high-angle fault that separates Atolia Quartz Monzonite from the Bedrock Spring Formation. The offset fault is nearly vertical, and thus the horizontal separation

is almost a direct measure of the strike-slip component.

One of the examples that illustrates probable right-lateral slip involves two faults that extend northeastward from a point 1½ miles east of Dome Mountain (in sec. E9–d). The shorter of these faults displaces a distinctive marker bed (in sec. E4–p) about 700 feet, and the longer fault displaces another distinctive bed of volcanic breccia about 600 feet (from sec. E3–e to E3–c). The offset of both beds is right lateral even though the dips of the two offset beds are directly opposed. The displacement by both faults is probably of the same type, so vertical displacements are unlikely and right-lateral displacement is indicated.

The second example of a right-lateral fault is 1 mile northeast of Dome Mountain (in sec. E5–e) where the axis of the Dome Mountain anticline is offset. If the axial plane of the anticline is vertical, then about 800 feet of right-lateral slip is demonstrated. The south end of this same fault, however, has about 1,000 feet of normal dip separation (pl. 2, section *D–D'*), showing that its overall displacement is either oblique or variable.

AGE

The earliest demonstrable activity along faults parallel to the Brown's Ranch fault zone is late Pliocene. All recognized faults belonging to this system displace rocks of the Atolia Quartz Monzonite, Bedrock Spring Formation, and Almond Mountain Volcanics, but not all of them displace rocks of the Lava Mountains Andesite. However, activity on faults of this system is inferred to have occurred prior to and during the deposition of the Almond Mountain Volcanics; the distribution of the rock types forming the lower part of this formation can be generalized into blocks that parallel these faults, and this pattern may be attributed to slightly earlier faulting that caused a northeast-trending topographic grain in the older rocks, which, in turn controlled the initial sedimentation patterns. Still earlier activity, middle Pliocene, has been inferred for the faults within the Brown's Ranch fault zone; it is reasonable to suspect that these parallel faults were contemporaneous with those of the main fault zone, but no positive evidence is available.

The latest displacement on these faults was probably early Quaternary. The older gravels are not displaced along any of these faults. In one place, 1½ miles northeast of Dome Mountain (in sec. E5–h), Quaternary andesite covers a fault which truncates a small fault parallel to the Brown's Ranch fault zone.

BLACKWATER FAULT

The Blackwater fault, named by Hewett (1954b, pl. 1), is a long, gently curving fault that enters the area from the southeast as shown in figure 2. Within the segment shown on that map, the trend shifts from N. 20° W. at the south edge to about N. 45° W. in the Lava Mountains. In detail, the fault consists of a branching row of fractures, few more than 2 or 3 miles long. Where it adjoins quartz monzonite, it has created a crushed zone several hundred feet wide. Where it cuts through the Bedrock Spring Formation, the associated deformation is less intense, but affects a zone of similar width.

The Blackwater fault has a low but distinct scarp along most of its trace in the Lava Mountains area. However, the northwesternmost mile of its extent shown on plate 1 is inferred solely from a linear zone of contorted beds. Still farther to the northwest, no evidence of this fault has been found; it probably has been truncated by the inferred fault from the Brown's Ranch fault zone, as shown on plate 1, but it may simply die out.

DISPLACEMENT

Southeast of the Lava Mountains, the displacements along the Blackwater fault are both right lateral and dip slip, with the position of the upthrown block alternating from side to side. Within the Lava Mountains the upthrown block is on the southwest side of the fault. Appreciable vertical displacement along this fault is precluded in this area by the very small offset of nearly horizontal basal contacts of the Bedrock Spring Formation and Almond Mountain Volcanics. Right-lateral slip is suggested by drag on the northeast-trending faults in E1 and F6, and on resistant beds in the Bedrock Spring Formation and Almond Mountain Volcanics which are bent nearly into alinement with the fault.

Further evidence of strike-slip displacement is found about 10 miles southeast of the mapped area. Here, in an area shown as granitic rocks in figure 2, a series of east-trending steeply dipping aplitic and rhyolitic dikes are truncated by a fault parallel to the Blackwater fault that is assumed to have the same sense of displacement. These dikes are found only on the southwest side of this parallel fault, thus suggesting that the truncated ends have been horizontally displaced beyond the outcrop area. Other evidence of right-lateral displacement on this fault has been noted by Dibblee (1961, p. 198).

AGE

The earliest displacement of the Blackwater fault that can be demonstrated is very late Cenozoic, probably early Quaternary. The fault consistently cuts rocks of the Atolia Quartz Monzonite, Bedrock Spring Formation, and Almond Mountain Volcanics. Al-

though the fault cuts some of the basaltic lava caps in the Black Hills (fig. 2), it does not cut them all; these caps are probably early Quaternary in age, but are older than the Pleistocene(?) Christmas Canyon Formation. Slightly earlier activity—late Pliocene or even middle Pliocene—is implied by evidence from parallel faults (described below), but the relation between the Blackwater fault and these parallel faults is not established. There is no reflection of the trend of the Blackwater fault in the outline of the inferred middle Pliocene basin of sedimentation (fig. 9), but this does not disprove its existence because in most places it does not exert much control on the topography.

The most recent measurable displacement is only a little younger than the earliest. The fault does not displace a small patch of older gravels along its trace (in sec. F8), and does not form any prominent scarps in alluvium (although it can be traced across these areas on aerial photographs).

FAULTS PARALLEL TO THE BLACKWATER FAULT

Several faults that parallel the Blackwater fault are mapped west of it. The most important of these are in the central part of the mapped area (in secs. E2 and E3). Although their trends are variable, they average about N. 50° W. These faults offset distinctive marker contacts in the Bedrock Spring Formation which dip at angles ranging from 20° to vertical. The steeply dipping marker contacts are now separated from each other more than those with shallow dips, demonstrating that all these faults are predominantly strike slip. The sense is right lateral. One of these distinctive marker contacts, at the top of a bed shown separately on the map as volcanic breccia, has been displaced southeast about 3,500 feet (from sec. E3–a to E2–f), then displaced to the northeast a short distance (to sec. E2–b) by a fault of the Brown's Ranch fault zone. The mapped relations show that this right-lateral faulting took place after much of the folding of the middle Pliocene Bedrock Spring Formation, but before deposition of the late Pliocene Almond Mountain Volcanics.

One small fault, in section B31–q, half a mile southeast of Bedrock Spring, is parallel to the Blackwater fault and apparently was active during Bedrock Spring time. This is indicated by a layer of epiclastic Bedrock Spring material, about 25 feet thick, that separates tuff and volcanic breccia on the northeast side of the fault, but is absent on the southwest. Apparently this fault formed a small scrap, and epiclastic deposition was limited for a short period of time to the northeast side.

In summary, activity is recorded on the faults of this group both during the deposition of the Bedrock Spring Formation and after the folding of the Bedrock Spring Formation, but not since the deposition of the Almond Mountain Volcanics.

THRUST FAULT

A small thrust fault is well exposed along the south side of the Garlock fault (in secs. A23 and A24). Here, Atolia Quartz Monzonite overlies red sandstone and siltstone tentatively correlated with the middle Pliocene Bedrock Spring Formation. The dip of the fault ranges from 55° S., through flat, to about 10° N. The direction of thrusting is not known.

This is the only exposed thrust fault within the mapped area. Hulin (1925, p. 64) also mapped this thrust and postulated that it was connected with a fault along the north side of the Rand Mountains, but nothing in the present study supports that interpretation. The thrust is truncated on the west by the Garlock fault. To the east, it disappears under alluvium. Although there is a possibility that the eastern extension of this fault swings southward under the alluvium and connects with the curving vertical fault that ends about a mile to the southeast, the disparity in the dips of the two faults indicates this is unlikely.

FOLDS

The main fold within the Lava Mountains is here called the Dome Mountain anticline, after Dome Mountain, which lies about 1 mile south of the fold near its west end. The trace of the axial plane is nearly parallel to the Garlock fault throughout most of its length. The plunge is variable. Pre-Bedrock Spring rocks are exposed at several places along the axis.

Relations shown on the map (pl. 1) and sections (pl. 2) indicate that folding began along this line after the deposition of the Bedrock Spring Formation. Most beds of this formation were then tilted 20° to 40° and some almost vertical; several thousand feet of formation was removed by erosion from the crest of the axial plane. These rocks were then eroded to a valley that was centered on the anticline axis prior to the deposition of the Almond Mountain Volcanics.

Folding continued during or after the deposition of the Almond Mountain Volcanics. In the vicinity of the axial plane, the volcanic debris of this formation was transported north, indicating initial dips in this direction; on the south flank of the anticline, near Dome Mountain, these layers now dip 20° S., thus demonstrating at least this much renewed tilting along the south flank of the anticline.

Folding along the western part of the anticline may affect slightly the beds of Lava Mountain Andesite, Quaternary andesite, and older gravels, but their present attitudes could all be accounted for by initial dips.

In the eastern part of the mapped area, the Pleistocene(?) Christmas Canyon Formation has been warped along the Dome Mountain anticline into a broad arch. Detritus contained in the Christmas Canyon Formation came from the southeast, and initial dips were undoubtedly a few degrees northwest; beds on the southeast flank of the axis now dip 5° to 10° toward the southeast (pl. 2, section *A–A'*) to form a surface that also drains in this direction and blocks the earlier drainage. Folding along the easternmost part of this axis may have been restricted to post-Bedrock Spring time; dips in the underlying rocks of this formation do not indicate an anticline although exposures are so rare in this area that a broad anticline might have been missed.

Several other broad folds can be distinguished, but they have been omitted from the map because the trace of their axial planes cannot be plotted accurately. Some of these folds parallel the Garlock fault; the best defined of these are the arched pediment surface in the northwestern Lava Mountains (p. 54), and the syncline in the Christmas Canyon Formation near the north end of Christmas Canyon. Others are broad folds that plunge from the sides of the Dome Mountain anticline and represent only minor undulations in its flanks. Still others are unrelated to any major tectonic feature.

ORIGIN OF STRUCTURAL PATTERN

The Garlock and Blackwater faults are probably related to the same tectonic stresses that produced the San Andreas fault. Displacements on all three faults have been in part contemporaneous, and each appears to have reacted with, or determined the extent of, the adjoining fault: the Garlock fault is terminated at its west end by the San Andreas fault (fig. 19); the San Andreas fault is bent near its junction with the Garlock fault as if dragged by this left-lateral fault; the Garlock fault is bent along the segment adjoining faults like the Blackwater fault as if dragged by these right-lateral faults; and the Blackwater fault and all similar faults in the Mojave Desert are restricted to the south side of the Garlock fault. Furthermore, the fault pattern at the junction of the Garlock and Blackwater faults is an

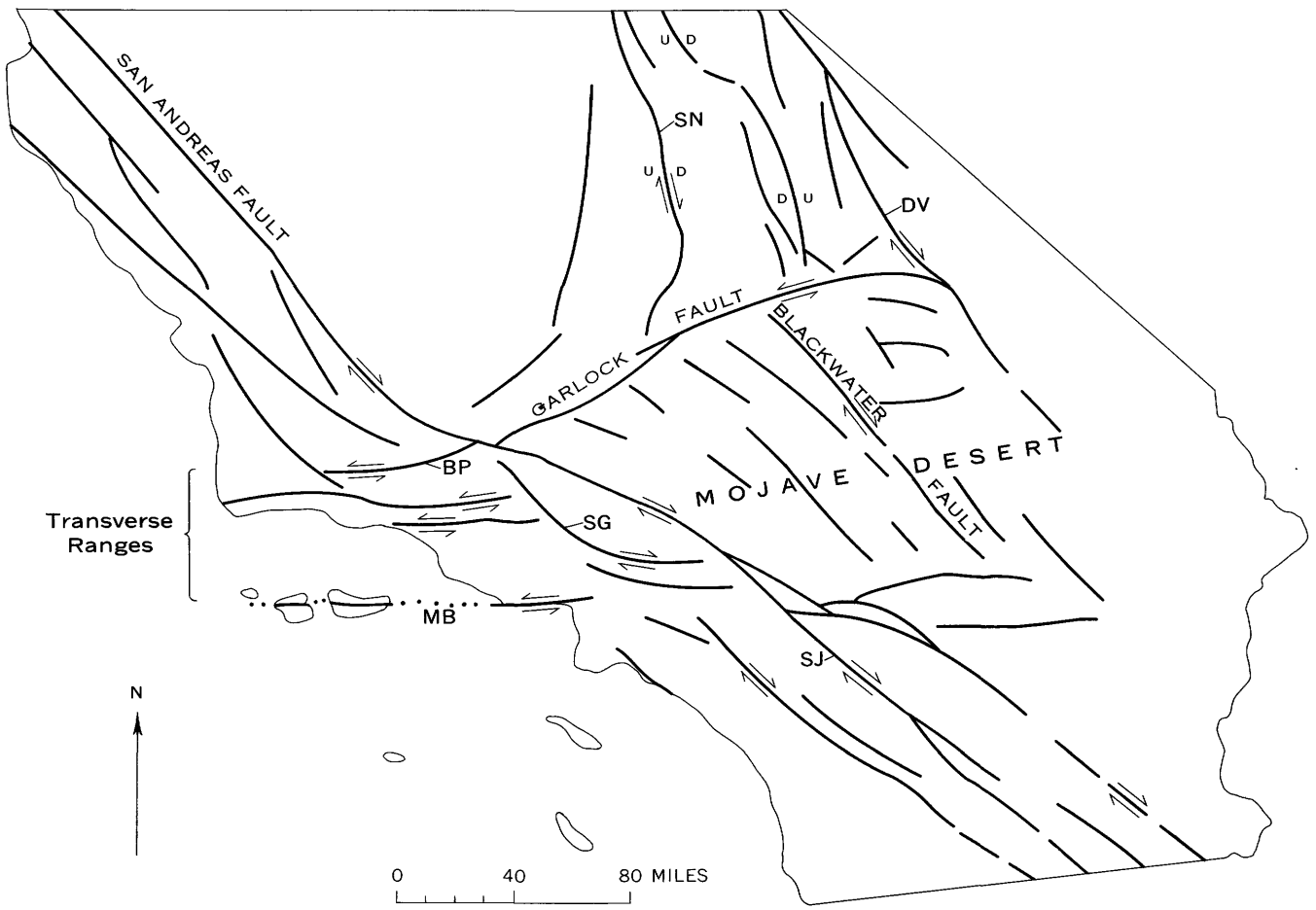

FIGURE 19.—Map of southern California showing location and sense of slip of major late Cenozoic faults. Abbreviations as follows: (SN) Sierra Nevada fault; (DV) Death Valley fault; (BP) Big Pine fault; (MB) Malibu Beach fault; (SG) San Gabriel fault; (SJ) San Jacinto fault. Data adapted chiefly from Hill and Dibblee (1953, pl. 1), Hill (1954, fig. 1), Allen (1957, fig. 1), and Grose (1959, fig. 3).

approximate mirror image of that at the junction of the San Andreas and Garlock faults. Hence, satisfactory explanations of the San Andreas-Garlock fault system should not only provide for those faults and their junction relations, but also for faults like the Blackwater fault.

Hill and Dibblee (1953, p. 454–458) suggested that the Garlock and San Andreas faults are simple complementary fractures created by north-south horizontal stresses, though, as noted by Cloos (1955, p. 254), the areal pattern of these faults seems to preclude this possibility. At their junction, as can be seen in figure 19, the blocks bounded by acute angles have been moved away from the apex, and according to theoretical and experimental data (for example, see Anderson, 1951, p. 7–21; Cloos, 1955; Griggs and Handin, 1960), blocks having this displacement during compression of homogeneous material are invariably bounded by obtuse angles. This anomalous relation between fault-block angles and displacements exists, though, throughout the Mojave Desert and Transverse Range provinces wherever left- and right-lateral faults approach each other. Figure 19 shows the most important of these junctions, but the same relation is found at less important junctions as well, and may thus be considered a tectonic characteristic of the two provinces.

The proper relation between junction angle and displacement was created by Cloos (1955, p. 253–255) in a two-stage scale model experiment. He first formed complementary fractures in the experimental material by north-south horizontal compression, then rotated the fractured material until the angles and displacements of the fractures resembled those of the Garlock and San Andreas faults. This produced the correct junction angle, but failed to produce a large displacement along both the Garlock and San Andreas faults. Furthermore, his illustrated result (Cloos, 1955, pl. 8, fig. 1) does not show bends in the fractures analogous to the San Andreas and Garlock faults, or fractures comparable with the fault set represented by the Blackwater fault.

Moody and Hill (1956, p. 1219) suggested that the Garlock fault was a second order [3] response to displacements on the San Andreas fault. Though the junction angles, relative displacements, and age relations predicted by their theory approximate those of the San Andreas and Garlock faults (and also those of the Blackwater fault if proposed as a third order fault), their explanation has at least one serious shortcoming. This is that the bend in the San Andreas fault seems very clearly to express left-lateral crustal drag in response to displacement along the Garlock fault, and the theoretical basis for their conclusion precludes the possibility of the second order Garlock fault deflecting the trace of the first order San Andreas fault that created it. Similarly, the curvature of the Garlock fault cannot be attributed to drag created by right-lateral displacement of faults like the third order Blackwater fault.

The major characteristics of the fault pattern being discussed are interpreted here as indications that the area has been alternately subjected to two horizontal stress patterns that are oriented differently, one pattern oriented as if the major stress at the surface was from the north and south so that it formed the San Andreas and Blackwater faults, and a second pattern oriented as if the major stress at the surface was from the southwest and northeast so that it formed the Garlock and Transverse Range faults. Stresses with these apparent orientations account satisfactorily for the observed fault pattern and displacements. Alternation of these stress patterns accounts for both the history of contemporaneous fault displacements, and the bends in the San Andreas and Garlock faults which are interpreted as crustal drag related to subsequent activity along the opposing set of faults. This interpretation requires the Blackwater fault to be very young because it parallels the northern part of the San Andreas fault rather than its deflected trace to the south; consequently, it must have been formed after most of the deflection was completed. The segments of the Garlock and Blackwater faults in the Lava Mountains indicate this age relation, so this interpretation is supported by the evidence presented locally.

A possible source for such alternating fracture patterns was indicated by Anderson (1951), and applied by Allen (1957) to a complex of strike-slip and thrust faults exposed along one segment of the San Andreas fault. They point out that if nearly equal major and intermediate stresses are acting on a region, small irregularities in the intensity of one can temporarily reverse their relative intensities, and that this reversal can create a different fault pattern at the surface. Ideally, the stresses indicated by these two fault patterns would be complimentary, yet as noted previously, the stress orientations indicated by the observed fault pattern shown in figure 19 are not complementary. In all likelihood, though, the stresses creating the major faults being discussed are applied at great depth, and the resulting deformation transmitted upward through rocks with different mechanical properties. Further-

[3] Second order faults, as used by Moody and Hill (1956), are crustal fractures similar to those predicted on theoretical grounds by McKinstry (1953, p. 405–413) and Anderson (1951, p. 160–173) that form in response to stresses set up in blocks undergoing displacement along first order faults. Third order faults result from stresses set up by displacements along second order faults, etc.

more, the basement rocks of the area probably have marked lines of weakness so that they will break in some directions more easily than others. Both factors will cause some deviation from the ideal complementary fault pattern, and the tectonic interpretation given here depends on such factors to produce the pattern that is observed.

The faults within and parallel to the Brown's Ranch fault zone differ from the strike-slip faults described above. Not only are the faults of this zone predominantly dip-slip, but their extent is short, their sense of displacement is variable, and their fault zone uncommonly wide. The near parallelism of these faults probably means that they originated as fractures caused by one set of stresses, but have since sustained other kinds of displacements that obscure their original similarities. These initial stresses are inferred to have been either expressions of vertical forces related to the incipient Pliocene volcanic activity, or stresses that normally would have produced faults parallel to the Garlock fault but were deflected by a subsurface grain in the concealed rocks.

The Dome Mountain anticline is probably a shallow compressional feature related to the Garlock fault which it parallels throughout most of its length. It is probably not related to the Blackwater fault, as the anticlinal axis crosses the projection of that fault without any change in average strike or character.

The thrust fault along the Garlock fault is probably also a result of local stresses but the direction of thrusting is not known.

GEOMORPHOLOGY

PEDIMENTS

Remnants of one or more pediments are found in the northern half of the Lava Mountains area. For description, these remnants have been combined into three groups on the basis of the composition of the capping material. This grouping may separate surfaces that originally were parts of the same pediment; it is unlikely, however, that any of the three groups include remnants of different pediments.

The largest of these pediment remnants is exposed in the northwestern part of the mapped area and is illustrated in figure 20. Except where dissected, it consists of a gently sloping surface covered with a thin layer of weathered granitic debris. Its north and east edges, however, are deeply dissected and the pediment destroyed where adjacent areas have been faulted downward or lowered by erosion. The pediment surface was originally all graded west-southwestward to the level of the valley west of the Lava Mountains to which it is connected by a narrow alluvial strip (in sec. A32).

FIGURE 20.—Profile view of the dissected pediment (P) cut on Atolia Quartz Monzonite in the northwest corner of the mapped area. The trace of the thrust fault along the north side of the quartz monzonite area is indicated by the dashed and dotted line. The Garlock fault (G) is exposed along the near edge of the outcrops but is obscure when viewed from this direction. View looking south.

The surface is now slightly warped and the eastern half forms an arch that plunges east-northeastward.

In the north-central part of the mapped area, several pediment relicts dip 2° to 5° north or northeast (fig. 21). Near the east edge of their areal extent, however, in sections B26, B27, and B35, they dip north, and are about on the same grade as, and may have been continuous with, the pediment described in the next paragraph on which the Christmas Canyon Formation was deposited. The capping material of the north-central group of relicts consists of older gravels which are, in every instance noted, composed of rocks that are on the uphill projection of the surface, indicating that no appreciable deformation has occurred since their formation. The underlying rocks are mostly those of the Bedrock Spring Formation, and beds dipping as much as 60° are truncated by the erosional surface.

In the northeastern quarter of the mapped area are remnants of a buried pediment. It was formed just

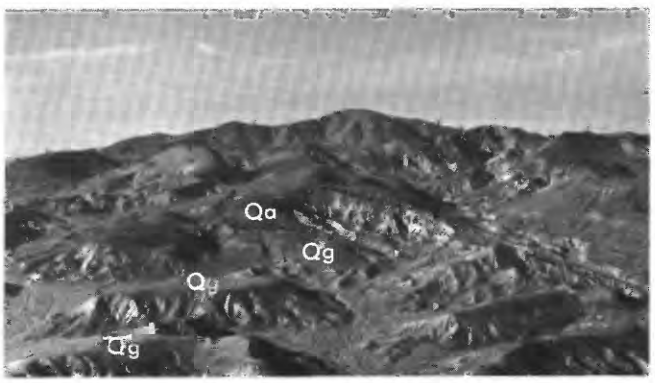

FIGURE 21.—Remnants of gravel-covered pediment surface cut on Bedrock Spring Formation dominate the left-foreground (Qg); Quaternary andesite flows deposited on the same surface are well exposed in the central part of the photograph (Qa). Dashed lines are the contacts between these flows and the Quaternary gravels or the underlying Bedrock Spring Formation. Dome Mountain is the highest point on the skyline. View looking southwest.

prior to deposition of the Christmas Canyon Formation, which remains as a capping up to 200 feet thick. Most of this pediment was cut on the Bedrock Spring Formation, but the northeasternmost part was cut on metamorphic rocks and Atolia Quartz Monzonite. The part of this surface that was underlain by the Bedrock Spring Formation was nearly flat in Christmas Canyon time, whereas the remainder had slight relief. Since its burial by the Christmas Canyon Formation, the east end of this pediment has been warped into a broad arch.

Though all three pediments were constructed at about the same time, each has subsequently recorded different tectonic activity: the pediment cut on Atolia Quartz Monzonite has been slightly warped into a broad arch parallel to the Garlock fault; the pediment cut on Bedrock Spring Formation in the north-central part of the area has remained undeformed; the pediment cut on pre-Quaternary rocks in the northeast quarter of the map has been partly warped into a broad arch by the Dome Mountain anticline.

AGE

All three pediments in the area are probably of early or middle Pleistocene age. The pediment cut on Atolia Quartz Monzonite is an extension of a surface that is veneered by older gravels (in sec. A33); these deposits rest on a surface that was almost undissected, indicating that the age of the pediment surface is only slightly older than the sediments that cover it. The pediment in the north-central part of the mapped area was also only slightly dissected at the time the Quaternary andesite and older gravels were deposited on it, and the pediment in the northeastern part of the map is only slightly older than the Pleistocene(?) Christmas Canyon Formation which rests on it. As noted previously, remnants of these two surfaces nearly grade into each other, and this evidence indicates a similar age for both surfaces. All three surfaces are thus dated as slightly older than the lower or middle Quaternary formations which rest on them, and appreciably younger than the deformed and truncated middle and upper Pliocene rocks on which they are cut. The pediment in the northeastern part of the area is also slightly warped where it crosses the axis of the Dome Mountain anticline, whereas the pediment surface in the north-central part of the area is not; this difference is probably due to an uneven intensity of folding along this axis in Quaternary time.

SHORELINES

Along the northeast edge of the area, an excellent shoreline was cut during the highest stand of Searles Lake at an elevation of about 2,250 feet, about 630 feet above the present lake surface (fig. 17). Throughout much of its length, the shoreline takes the form of benches 10 or 20 feet wide with wave-cut cliffs 5 or 10 feet high. Lacustrine tufa was deposited in this part of the lake at several levels between 2,200 and 2,250 feet. As noted previously (p. 44), these deposits are probably more than 50,000 years old, but are more recent than the last major displacement on the Garlock fault in this area.

A very faint shoreline(?) is visible at two places on the north shore of Cuddeback Lake (in E32 and G4) at an elevation of 2,660 feet, approximately 110 feet above the present playa level. This shoreline(?) is defined by the upper limit on the slope of a slight concentration of fine sand. Although there is no evidence of wave erosion or of lake-shore tufa, the occurrence of similar deposits at the same elevation on the two hills would be a highly unlikely coincidence unless they were formed by a lake. A better defined shoreline, indicated by beach sands and sandbars, lies about 10 feet above the present playa surface.

ECONOMIC GEOLOGY

METALS

In the Lava Mountains, gold mining has been attempted only in Christmas Canyon. Two adits, the longer about 300 feet, extend into Atolia Quartz Monzonite, and two shafts connect them with the surface. The mine has been inactive since about 1930. Some of the prospect pits in the Lava Mountains were probably made in the search for gold, for the claim notices associated with them were dated in the early 1900's—5 to 10 years after gold was discovered at Randsburg.

Most of the mines and prospect pits in the region east of City Well resulted from the search for silver—an outgrowth of the discovery in 1919 of the California Rand (Kelley) silver mine. One of these, the North Rand mine, in section D27-h, was described by Hulin (1925, p. 141). It consists of a 400-foot shaft inclined to the south at about 60°; it is apparently all in the propylite of the Almond Mountain Volcanics. This mine reportedly (Joe Foisie, Johannesburg, oral commun., 1955) had ore near the surface but none at depth. Material on the dump consists of altered tuff and sandstone containing small crystals of pyrite disseminated throughout the rock and concentrated along some of the fractures. Another mine, just south of the mapped area, about half a mile southwest of the North Rand mine, is reported to have a shaft about 500 feet deep which was too hot to be continued deeper (Joe Foisie, oral commun., 1955).

In section D24–q, a shaft estimated to be more than 100 feet deep is at the contact between the propylite and subpropylite rocks of the Almond Mountain Volcanics. Samples from the dump are fine-grained grayish yellow-green volcanic rocks that contain disseminated pyrite.

A flurry of mercury prospecting occurred at approximately the same time as the search for silver. There was no production from this area. The Steam Well, in section D25, was drilled as a mercury prospect.

RADIOACTIVE DEPOSITS

On the north side of the mapped area, along the Garlock fault, is a large prospect for radioactive minerals called the Alpha Beta Gamma mine. It is reported to have a radioactive count of 3× background (Walker and others, 1956, p. 13). No development work was underway when visited in 1960.

WATER

The water supply for the towns of Randsburg and Johannesburg comes from the wells in the southwest corner of the mapped area. Two of these wells, as reported by Thompson (1929, p. 221), were 380 and 400 feet deep with water levels at 375 and 390 feet, respectively. The water, which is of good quality, must be pumped about 6 miles with a net vertical lift of about 150 feet; the sale price in 1956 was about one cent per gallon.

Bedrock Spring, in the northeastern part of the area, consists of an adit about 10 feet long that projects into volcanic rock and has a few inches of brackish water standing on the floor. It was reportedly (Joe Foisie, oral commun., 1955) dug for water about 1900 by the members of the Spangler family. No springs or other evidence of near-surface water were found elsewhere in the mapped area.

Within the area shown on the map, there are no highly favorable areas for ground-water accumulation. The areas that drain west and south—potential water sources for Randsburg and Johannesburg—are not large. The area that drains northward is more favorable because the collection area is larger and the Garlock fault might serve as a ground-water barrier to bring water nearer the surface, although there is no evidence of near-surface water along the fault. Water found in the northward-draining area might be brackish or saline from contact with the saline parts of the Christmas Canyon and Bedrock Spring Formations, and from disseminated salines deposited in the alluvium during the higher stands of Searles Lake.

In section D25, a well was drilled about 1920 as a prospect for mercury. This 415.6-foot well, known locally as Steam Well, brings to the surface water vapor at a temperature of 96°C (W. R. Moyle, Jr., written commun., 1961). It lies along a fault parallel to the Brown's Ranch fault zone.

ZEOLITE AND ALUNITE

Immediately surrounding the Steam Well is an area of light-tan, yellow, or white rock that consists of an intimate mixture of alunite—$KAl_3(SO_4)_2(OH)_6$—and opal. The area of outcrop of this material is about 500×1,200 feet; if it extends 100 feet downward, about 3 million tons of this material are available. A small area of subpropylite about 1,000 feet southwest of the Steam Well contains a large percent of the zeolite clinoptilolite; the extent of this material was not determined.

GRAVEL

Gravel has been quarried from the alluvium in Christmas Canyon since about 1948 for use as road metal on nearby blacktop roads. Apparently this is the only gravel in the area that has been commercially exploited. Most of the material in the Bedrock Spring Formation is too fine for such uses, although some beds in the coarser facies of the Christmas Canyon Formation are suitable.

FAVORABLE AREAS FOR FUTURE PROSPECTING

The Lava Mountains area has been prospected many times. It seems unlikely that large deposits of any of the materials sought (gold, silver, tungsten, mercury, uranium, and thorium) have been overlooked in outcrop. Several exploratory shafts and adits in the southwestern part of the area have also sampled the concealed rocks. Although the chances of success are small, the most likely area for future discoveries seems to be within or near the elongated zone of propylitization. The presence of propylite, zeolite, and alunite is reminiscent of several other mining districts (for example, the Comstock Lode), though a genetic connection between these minerals and ore has never been firmly established. The surface trace of the contact between the propylite and subpropylite has been extensively prospected in the past, and additional exploration of this zone at depth, combined with detailed geochemical sampling, might detect ore that has been overlooked. Some of the areas of subpropylite that lie outside of the main zone have equal promise, and they appear to have been prospected less carefully in the past. Similarly, the zone of bleached tuffs along the northwest side of the Brown's Ranch fault zone has probably undergone secondary hydrothermal alteration of some type, and these tuff areas, too, have probably

been explored less intensively than the main area of hydrothermal alteration.

VOLCANIC PETROLOGY

SUMMARY

Modal, chemical, normative, and spectrochemical analyses of 25 volcanic rocks have been presented in this report. Observations on thin sections representing about 200 other samples of volcanic rocks show that the analyzed rocks are representative of the units they came from. The analyzed rocks include samples from the oldest and youngest, from the most mafic and most felsic, and from the most altered and least altered of the widespread volcanic rocks in the area. They also include samples from mapping units considered the same though separated by several miles, and from mapping units considered different though superposed. But in spite of the number of ways these analyzed rocks can be regarded as different, their mineral and chemical compositions are strikingly similar.

The volcanic rocks are virtually all porphyritic andesite. Most contain plagioclase, oxyhornblende, and biotite phenocrysts, and many contain minor quartz. Under a microscope, plagioclase microphenocrysts, orthopyroxene, and clinopyroxene also are visible. The groundmass is slightly crystalline to glassy.

The chemical compositions and the normative values further indicate that there is little difference. The range of SiO_2 percentages in the analyzed suite is about 12 percent, and all but three samples fall within a range of 6 percent. The ranges of other major and minor components are similarly small. The alkali-lime index is about 58, indicating the suite to be calc-alkalic. Seventeen of the analyzed rocks have C.I.P.W. normative compositions of yellowstonose (I.4.3.4.), six are tonalose (II.4.3.4.), and two are lassenose (I.4.2.4.). Even within this small range of rock compositions, though, most major and minor elements show percentage variations that are clearly interrelated.

All late Cenozoic volcanic rocks in the Lava Mountains area are part of one suite. This is indicated primarily by the compositional similarity of the rocks, and is strongly supported by field evidence which shows that these deposits were all formed within a relatively short period of geologic time, and were areally restricted to one small part of the Mojave Desert area.

The evidence that these rocks are part of the same suite means that they are also genetically related, and that the differences and similarities in the nature of successively erupted rocks reflect processes that generated the magma and transported it to the surface. Petrographic and petrochemical evidence suggests that the magma was generated as follows: Sometime prior to the deposition of the middle Pliocene Bedrock Spring Formation, differentiation of mafic magma produced a magma of more felsic composition. By the time of the first eruption of this new magma, though, differentiation had virtually ceased, and diffusion and mixing were causing it to become progressively more homogeneous. The small amount of compositional variation in the erupted rocks is chiefly a result of this early differentiation. Between middle and late Pliocene time, a magma of similar composition was added to the magma chamber; this resulted in some resorption of the crystals already formed, but did not cause any detectable shift in the chemical composition of subsequently erupted rocks.

The process that transported the magma to the surface is indicated by three lithologic variables correlative with age: (a) Most of the earlier volcanic rocks are products of explosive volcanism, whereas the later volcanic rocks resulted from effusive activity; (b) the fragmental volcanic rocks become more homogeneous in successive deposits; and (c) interbedded epiclastic rocks form thinner units in progressively younger volcanic formations, showing that less time elapsed between successive eruptions. These progressive changes are interpreted to mean that between middle Pliocene and early Quaternary times, additional conduits were formed by faulting, the rocks surrounding the conduits became heated, and eruptive pressures within the magma chamber increased. These processes combined to allow the molten rock to reach the surface more and more frequently even though solidified and brecciated in the process, and ultimately they permitted it to reach the surface still fluid.

PETROGRAPHY

ORIGIN AND SIGNIFICANCE OF VOLCANIC LITHOLOGIES

Most of the layers of tuff, lapilli tuff, and tuff breccia in the Lava Mountains area were probably deposited as mud flows (lahars) shortly after their components were erupted, although some may represent volcanic debris that was deposited in place. The layers are well indurated and massive, and contain appreciable percentages of both fine- and coarse-grained volcanic debris that is unsorted and angular. This debris was probably formed by at least three mechanisms: (a) Explosive eruption of volcanic material which formed a mantle of talus or airborne debris on the terrain; (b) autobrecciation in the volcanic neck of nearly solid lava (Curtis, 1954, p. 467–471) that was subsequently remobilized and extruded; and (c) extreme brecciation

of lava flows as they reached the late stages of solidification.

The individual layers of tuff, lapilli tuff, tuff breccia, and rubble breccia were probably deposited within a very short period of time. The few bedding planes that do occur within the layers of tuff and lapilli tuff suggest only a short delay in deposition, for the material that forms the lower contact appears to have been unconsolidated when deposition was renewed. Most of the coarser breccias are texturally massive. In a few of these layers, though, contacts defined by abrupt changes in rock colors suggest that their deposition may have been interrupted although these contacts do not show signs of an intervening period of erosion.

The large fragments in the rubble breccias apparently formed when lava that solidified in volcanic necks was subsequently brecciated and extruded. The complete absence of volcanic bombs, bread-crust structures, and glassy edges among the component fragments means that the fragments did not solidify individually. Most rubble breccia layers do not contain pockets of very fine material or massive lava as if formed by late-stage brecciation of large lava masses or flows (Curtis, 1954, p. 462–464). Furthermore, they form layers too tabular to be considered talus formed on the flanks of a volcanic vent, yet contain so little fine material that they cannot be considered mud flows. Their properties are best explained if the lavas are considered to have been first solidified in the volcanic necks, subesquently brecciated, and then forced out as rubble. Brecciation may have resulted from autobrecciation (Curtis, 1954, p. 467), or from crushing as a result of great pressure from below. Material brecciated in this way, and subsequently transported to the surface, would consist of angular fragments intimately mixed with hot gases, hot water, or lava. This mixture might well have a mobility that would allow it to flow far down the adjacent slopes to form tabular bodies. Matrix-free rubble breccia would result when the lubricating material was water and gas; flow breccia would result when it was lava.

The massive volcanic flows in the Lava Mountains area were mostly of small extent. They formed by the extravasation of fairly viscous lava from many vents and probably did not extend more than 2 miles from their source (see p. 34). The flow breccia and flow conglomerate layers were formed by the same processes as were the flows, but contained angular or well-rounded fragments that were mixed with the lava prior to or just after its extrusion.

The volcanic rocks found in the Lava Mountains area are distributed throughout the stratigraphic section so as to demonstrate a progressive change from explosive to effusive volcanic activity. The volcanics in the middle Pliocene Bedrock Spring Formation are estimated to be about half tuff and lapilli tuff, and half volcanic breccia. The volcanic rocks in the lower half of the Almond Mountain Volcanics are sandy tuff, tuff, lapilli tuff, and tuff breccia, which generally grade upward into massive rubble breccia and flow breccia without any sign of a long break in the depositional history. The overlying very late Pliocene Lava Mountains Andesite consists of andesite flows and intrusives plus a few flow breccias. The Quaternary andesite consists entirely of effusive flows, plugs, and sills.

An increase in the homogeneity of the extrusive fragmental volcanic rocks also follows this chronological order. Where the fragments in the pyroclastic breccias of the Bedrock Spring Formation are coarse enough to be identified as to rock type, they are found to include a large variety. In the lower part of the Almond Mountain Volcanics, a comparable variety of volcanic rock types is noted, but in the upper part, the breccias are nearly monolithologic. The Lava Mountains Andesite consists mostly of flows, but the fragments in the small percentage of flow breccias are generally all the same and commonly of about the same composition as the matrix lava. The extruded Quaternary andesites are all flows. The positions of the other late Pliocene(?) volcanic rocks in the chronological sequence are not clear, so it is not known whether or not they conform to this pattern.

The frequency of volcanic eruptions probably also increased with time, grading from an intermittent activity in Bedrock Spring time to a point when such activity accounts for all the deposits formed in Lava Mountains Andesite and Quaternary andesite times. Thick beds of nonvolcanic epiclastic material separating beds of volcanic rocks presumably indicate long periods of quiescence between eruptions, whereas little or no epiclastic material, even around the outer edges of the area containing volcanic rocks, indicate very short periods of quiescence. In the Bedrock Spring Formation, zones of epiclastic rocks separating the volcanic units are hundreds and even thousands of feet thick. In the overlying Almond Mountain Volcanics, zones of epiclastic rocks are generally a few hundred feet thick, and most of them are in the lower half of the section. The overlying Lava Mountains Andesite and Quaternary andesite contain no interbedded epiclastic rocks.

VOLCANIC ROCK TEXTURES

The volcanic rocks of all formations contain both megascopic and microscopic phenocrysts. All contain megaphenocrysts of plagioclase and most include biotite, oxyhornblende (or hornblende), and opaque min-

erals; some quartz is visible in most rocks. The microphenocrysts are generally plagioclase, pyroxene, and opaque minerals. The groundmass consists of small needlelike crystals of plagioclase(?), cryptocrystalline material, glass, and a dust of opaque minerals. The plagioclase megaphenocrysts commonly are as large as 6 mm in the long dimension, biotite and oxyhornblende (or hornblende) 3 mm, quartz 2 mm, and pyroxene crystals 0.5 mm. The average sizes are usually a quarter to a half of these lengths. Plagioclase microphenocrysts have average lengths between 0.1 and 0.2 mm.

In many rocks some minerals are alined. Plagioclase microphenocrysts and hornblende phenocrysts are commonly parallel; plagioclase megaphenocrysts, pyroxene, and biotite are rarely so.

Many of the rocks contain vesicles, most commonly between 0.1 mm and 0.5 mm in diameter, which rarely exceed 5 percent of the rock. A few of these vesicles show a tendency to be elongated, but most are nearly spherical.

DESCRIPTIONS AND PROPERTIES OF ROCK CONSTITUENTS

PLAGIOCLASE

Composition.—Although some estimates of plagioclase compositions were made by means of refractive indices, most were made by measuring extinction angles in sections approximately normal to (010) and (001). These measurements provide an estimate only of the minimum anorthite percentage in the part of the crystal that was measured. The An percentages indicated throughout this paper were estimated from such data applied to the curves constructed by Tertsch (1942, p. 209) for high-temperature (disordered) plagioclase crystals oriented normal to (010) and (001). Plotting these angles on similar curves for the low-temperature (ordered) feldspars would increase the indicated anorthite by 8 to 12 percent. Even though the method used may not give the actual chemical composition of the phenocrysts very accurately, it gives at least a roughly quantitative measure of the range of plagioclase composition in individual crystals, and also permits a semiquantitative comparison of the compositions of similarly oriented crystals.

Most of the plagioclase phenocrysts in these rocks are apparently high-temperature (relatively disordered) crystals. F. C. Calkins carefully studied a dozen representative thin sections, and summarizes the results of his study of magaphenocrysts as follows:

> The only simple way that I know of to get evidence regarding thermal state solely from thin sections on the flat stage is to measure concurrent angles in Carlsbad-albite twins cut nearly normal to *a*. * * * Carlsbad twins are not very numerous in these thin sections, and some of the phenocrysts that look like Carlsbad twins may be only coalescing crystals. I have found a moderate number that I believe to be Carlsbad twins, but only a few of these are cut nearly normal to *a*.
>
> One of these is in section 29–6. This I feel sure is a Carlsbad twin, though in part distorted. The albite lamellae are fairly sharp, and distinct basal cleavage is visible in one of the two Carlsbad individuals, showing that the crystal is cut, in that individual, very nearly normal to *a*. Most of the inner part has the concurrent angles 30° and 12°. In a low-temperature plagioclase this combination gives, on my diagram for Carlsbad twins in low-temperature plagioclase, the composition An_{35}, and a value for lambda of 45°. The latter figure is in conflict with the evidence afforded by the thin section, but on Tertsch's (1942) diagram for high-temperature plagioclase these extinction angles give, approximately, An_{45} and lambda 65°, and this value for lambda is just about what it should be in a crystal cut normal to *a*. I regard this as evidence that that particular phenocryst was formed at high temperature, as is inherently probable. I got similar evidence from three crystals in two other slides. From this evidence, as far as it goes, I think it likely that the plagioclase in these slides is mostly, and perhaps all, high temperature.

The results of my extinction angle measurements on about a thousand megaphenocrysts show that about 5 percent of the crystals have apparent compositions in at least one zone that are as high as An_{55}, so that their true compositions are probably a little higher. Refractive index measurements indicate compositions below An_{25} for about 5 percent of the measured grains. A compositional spread of at least An_{30} is thus likely. The observed range in apparent 2V confirms this spread.

For each volcanic unit, the average of several hundred extinction angle measurements is within 4° of the others. This probably means that the average anorthite percentages are separated by less than 5 percent. These indicated average compositions are close to An_{40}. According to Tertsch's high temperature plagioclase curves (1942, fig. 3), the errors introduced by measuring sections close to but not normal to (010) and (001) are fairly small, and it is improbable that the true An percentage is more than 10 percent higher.

The plagioclase megaphenocrysts and microphenocrysts in most of the volcanic rocks of this area thus have an average composition of calcic andesine. Individual megaphenocrysts in specimens from this volcanic suite may differ by more than 30 percent anorthite content, and those in a single thin section by more than 20 percent, but the average anorthite content of all the plagioclase in any two units probably does not differ by more than about 5 percent. It is nearly impossible, however, to determine the overall composition of even a single phenocryst accurately in a thin section, because most of the phenocrysts are corroded, strongly zoned, and mottled. This uncertainty would exist even if there were an undeviating correlation between composition and extinction angles, and we were certain of the ther-

735–720 O—64——5

mal state of the plagioclases in these rocks, neither of which is true. The compositions given throughout this paper must therefore be regarded as estimates.

The composition of the microphenocrysts is even more difficult to determine because they are not commonly twinned. The few determinations made, some of which are supported by measurements of the refractive index, suggest that microphenocrysts with an average composition have 2 to 5 percent more anorthite.

Zones.—The plagioclase megaphenocrysts are conspicuously zoned in almost all thin sections of these volcanic rocks. The most common type of zoning is oscillatory normal, although normal and reverse zones are found.

Strong mottling is present in the inner parts of many megaphenocrysts. This mottling is evident in thin sections observed with crossed nicols, but is not visible in plane-polarized light. Its origin is not known, but it evidently reflects inhomogeneities in the crystal compositions. Though common in megaphenocrysts, it is not found in their calcic rims or in microphenocrysts.

Many of the megaphenocrysts have calcic rims (fig. 22*A*). This feature seems unusual, but it has been observed by Larsen and others (1938a, p. 233 and fig. 17) in volcanic rocks of similar composition from Colorado. In the rocks collected from the Lava Mountains, these rims occupy the outer 5 to 15 percent of the crystal radius. They are always clear, whereas the inner parts of the crystals are commonly corroded and resorbed. The rim usually shows a small amount of smooth normal zoning. Extinction angles indicate that the rim contains 5 to 10 percent more anorthite than the feldspar just inside it, and that it has approximately the same composition as the inner core. This inference is confirmed by the high refractive indices of the rims. Calkins (written commun., 1962) says of them, "As you have already noted, many of the phenocrysts have rims in which the extinction angle is larger than that of the plagioclase adjoining them on the inner side. I find by means of inclined illumination that these rims all have distinctly higher indices of refraction than the plagioclase inside them, which indicates that they are actually more calcic, not merely of different thermal history."

The megaphenocrysts in a given thin section usually differ considerably in character of zoning, and there may be many zones in one phenocryst and few in another one nearby. In most of the slides, one- to two-thirds of the plagioclase megaphenocrysts have calcic rims, but even among this selected sample, the inner crystals have no zonal characteristics in common.

Most of the microphenocrysts show a very faint smooth normal zoning in which the An content has a range of less than 5 percent.

Twinning.—Albite twins are visible in all these plagioclase crystals (fig. 22*A*, *D*.). Most of the twin lamellae are not notably even or uniformly developed. In some crystals, the zones interrupt these twin lamellae, and in others they do not. Most of the twins that appear to follow the Carlsbad law have an undulating twin plane. Other twin types are noted; of these, pericline twins are the most common.

Many twins that appear to follow the Carlsbad law could not be verified, so the extinction angles of Carlsbad twins in conjunction with albite twins were not used routinely as a means of estimating plagioclase composition. This uncertainty stems from the relations observed among the small plagioclase crystals, where once-independent crystals have in a few instances become attached on their side faces; if this happened during the early growth stages of the megaphenocrysts, and those crystals had continued to enlarge while attached in that position, the results would resemble a Carlsbad twin, but its components would of course lack the precise angular relation necessary to make the extinction-angle curves valid.

Size and habit.—The plagioclase crystals in most of the volcanic rocks from this area are divided into two groups, and the crystals of each group contribute about equally to the total volume percent of plagioclase in these rocks. One group includes the larger crystals, which are referred to throughout this report as megaphenocrysts; besides being larger, they characteristically also have strongly developed zones, round corners, and length-to-breadth ratios between 1 : 1 and 3 : 1. The other group includes the smaller crystals, which are referred to as microphenocrysts; these crystals characteristically have weakly developed zones, square corners, and length-to-breadth ratios between 4 : 1 and 10 : 1. The properties of these two groups are illustrated by figure 22*D*. For convenience, individual crystals have been assigned to groups on the basis of whether their lengths are greater or less than 0.3 mm, but in almost all instances this criterion separates crystals with the other distinctions as well.

Megaphenocrysts tend to form crystal clumps in which some of the member crystals are nearly perfect in shape and others have only partially developed faces. A typical cluster of such crystals is seen in figure 22*A*. If a calcic rim is present, it invariably envelopes the entire group rather than any one of the member crystals, indicating that the clumping occurred prior to the last crystallization of megaphenocryst feldspar. Microphenocrysts are generally separate.

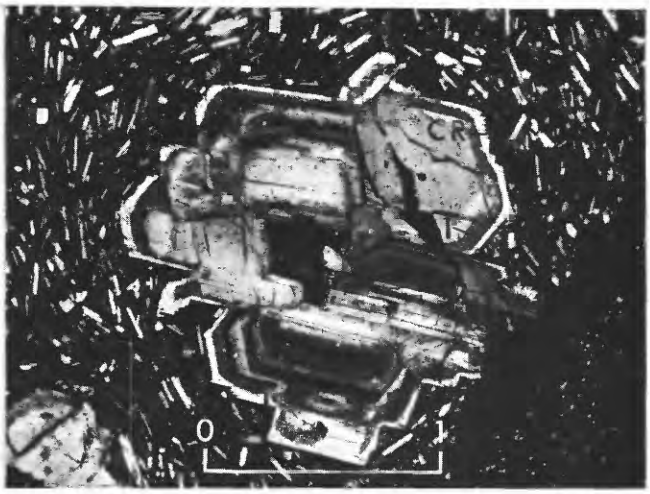

A

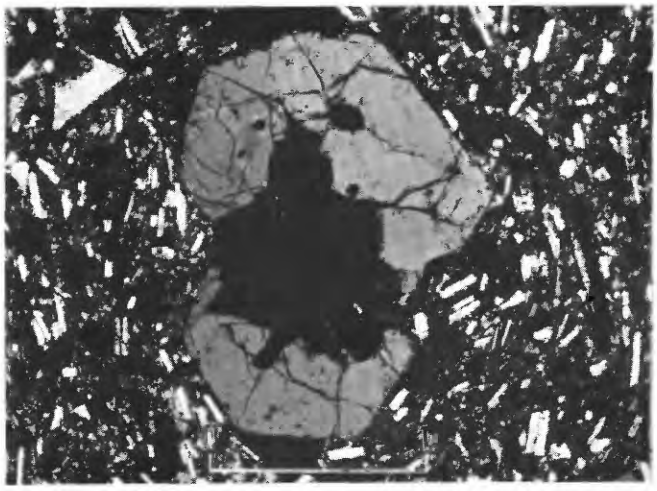

B

C

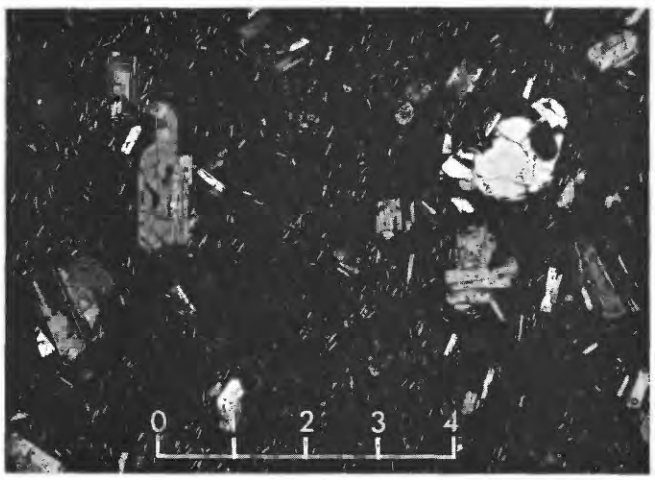

D

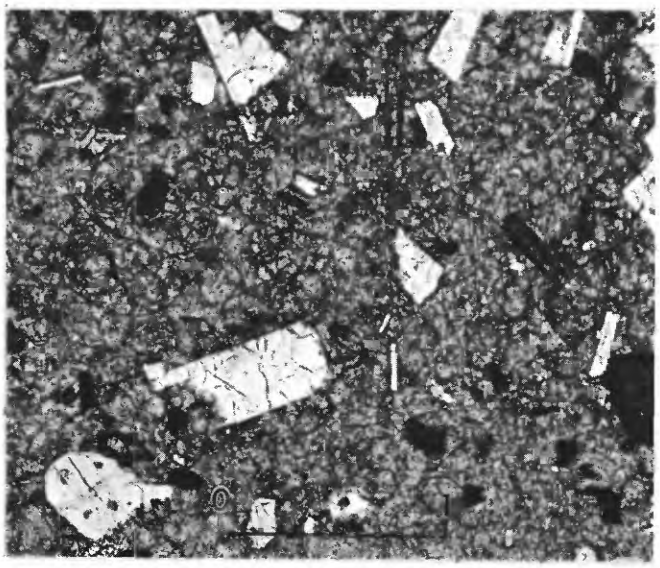

E

FIGURE 22.—Photomicrographs showing selected mineral relations. Four of the five are samples from the Lava Mountains Andesite; one (*C*) is from the Almond Mountain Volcanics. The scale at the base of each photograph is in millimeters. *A*, a cluster of zoned plagioclase crystals (in sample 97–38–o) showing a calcic rim (CR) and an underlying zone of inclusions (I), both surrounding the entire group of crystals. Note also the variation in the zoning pattern of the component crystals. Crossed nicols. *B*, quartz crystals in a glassy to semicrystalline groundmass (in sample 27–14). The nearly straight edges are believed to indicate that these were euhedral crystals that grew in the melt. Crossed nicols. *C*, biotite and plagioclase crystals (in sample 124–22J). The biotite has been altered to opaque minerals along the edge not protected by plagioclase. This indicates that the alteration occurred after the two minerals had become attached. Plane-polarized light. *D*, typical thin section of Lava Mountains Andesite. Note the two sizes of plagioclase crystals (megaphenocrysts and microphenocrysts) and the differences in their dimensions. Large irregular crystal in upper right is partly resorbed quartz. Crossed nicols. *E*, microperlitic fractures in a glassy sample of a Lava Mountains Andesite flow (sample 128–5). Note that the crystals are sharp edged and unaltered. Plane-polarized light.

Inclusions.—Almost all crystals of plagioclase, especially the megaphenocrysts, have formless or runic inclusions of clear or yellowish glass. Small acicular or prismatic apatite crystals, generally less than 0.1 mm long, are also common. Inclusions of opaque minerals (probably magnetite), oxyhornblende, pyroxene, biotite, chalcedony(?), zircon(?), and rutile(?), are less commonly found.

Alteration.—In most of the rocks studied, the feldspar is not heavily altered. Evidence of slight alteration and partial resorption is commonly found within a crystal. Alteration that affected the outermost rims of crystals is rare. Only in the propylite and subpropylite have the feldspar been extensively replaced. In these, the feldspar crystals have been replaced chiefly by calcite, usually in the form of stringers laced through the crystal; but secondary albite, sericite, and fibrous anisotropic minerals are also noted.

BIOTITE

Composition.—The pleochroic formula and the refractive index of flat-lying cleavage flakes of relatively unaltered biotite crystals suggest that most of them have compositions that appoach annite, the high Fe, low Mg member of the group. The pleochroism is strong, and the refractive index (γ') ranges from 1.67 to 1.73.

Color and pleochroism.—Pleochroism is normally strong, the most common formula being as follows:

X=grayish orange (10*YR* 7–8/4–6).
Y=pale brown (5*YR* 4/2).
Z=grayish brown (5*YR* 3/2).

In thin section, the biotite in these rocks is commonly darker along cleavage planes or fractures. The darker parts of the biotite flakes have a higher refractive index than the lighter parts showing that the color and index are related effects.

Size and habit.—In most rocks, biotite forms hexagonal packets of thin plates, measuring 1 to 2 mm in width. Some rocks, such as the late Pliocene(?) felsite, contain biotite only as very thin wafers or shreds.

Inclusions.—Inclusions of opaque material are common (fig. 22*C*). Many of these appear to be magnetite. Plagioclase, twinned and zoned, is also found, and some of the plagioclase inclusions themselves contain included magnetite. A few biotite crystals also contain oxyhornblende and pyroxene (clinopyroxene?), but it is possible that they are alteration products rather than original inclusions.

Alteration.—Deuteric activity has partially to completely altered the biotite crystals in the majority of rocks. The first phases of alteration have darkened the crystals and formed equant opaque minerals (magnetite?) around the outer rim of the crystal or embedded in its edges. More intensive alteration commonly obliterated the euhedral outline of the opaque minerals. This alteration was a process that took place after most of the lava was solid; where biotite and plagioclase are in contact, there has been no alteration of the protected biotite edges, indicating that the crystals were fixed in this position prior to deuteric action (fig. 22*C*).

Many mineralogical source books do not acknowledge the existence of altered biotite with a cleavage-flake (γ') index of more than 1.70, although both field and laboratory studies have reported examples of it. For example, field studies by Larsen and others (1937, p. 901) report that biotite crystals from rocks such as latitic andesite have γ indexes ranging from 1.70 to 1.73.

Laboratory studies by Kozu and Yoshiki (1929, p. 181–182) proved that high-index biotites could be formed by heating normal crystals (γ=1.655) to temperatures of 1,000°C and apparently at 1 atmosphere pressure. In their experiments, the biotite began to change index appreciably at about 400°C and continued at a fairly uniform rate to the highest temperature measured. They found that at 900°C, γ=1.700, and at 1,000°C, γ=1.703. They also found that naturally occurring high-index biotite showed no marked change in properties within this range of heating.

Annite has been synthesized by Eugster (1956, 1957), Ostrovskiĭ (1956), and Eugster and Wones (1962) at vapor pressures between 500 and 4,000 bars, and temperatures between at least 400°C and 840°C. The position of its stability field is slightly sensitive to changes in water pressure and total pressure, but is highly sensitive to changes in temperature and oxygen partial pressures. Iron oxides, the common alteration products in the volcanic rocks of the Lava Mountains, are produced by a decrease in temperature, or increases in the partial pressures of oxygen which depend partly on the quantity of water in the system and the extent to which it is dissociated. With falling temperatures, the oxygen supplied by dissociation of water would normally decrease, and additional oxygen must be supplied. In lavas, this may be accomplished by the relative increase in the amount of water available for dissociation when the groundmass solidifies, or by the introduction of oxygen from air. The shallow intrusive volcanic rocks in the Lava Mountains were probably not formed in a zone reached by atmospheric oxygen; the biotite in some of those rocks is altered, although generally less altered than in extrusive rocks, and this suggests the oxygen is derived from both sources.

The darkening of biotite probably also took place at the time of alteration. In hornblende, the change to oxyhornblende accompanies the oxidation of Fe^{+2} and loss of OH; as the optical changes during alteration of

hornblende and biotite are similar, the chemical changes are probably also similar. Although it seems paradoxical that OH ions should be lost during a period of increasing water percentages and decreasing temperatures, this is interpreted to be a secondary result of oxidation; as Fe^{+2} is oxidized, some of it is removed from the biotite crystal lattices to form dispersed ion oxides, and the OH chemically bonded to this Fe^{+2} is probably lost at the same time.

AMPHIBOLE

Composition.—Hornblende, which for emphasis in this report is sometimes called green hornblende, is found chiefly in the dikes and sills of Quaternary andesite. The mineral is found only locally in extrusive rocks (such as the perlitic layer of Lava Mountains Andesite described on p. 34 and illustrated in fig. 22*B*). Most of the hornblende crystals have extinction angles of about 15°, and the refractive indices are near $\alpha=1.68$ and $\gamma=1.70$.

In the volcanic rocks of the Lava Mountains, oxyhornblende is the most abundant amphibole. These oxyhornblende crystals have extinction angles between 5° and 10°, deep coloration, and refractive indices higher than those of hornblende. Although there seems to be no quantitative correlation between specific optical-property variations and specific composition changes, compared to hornblende, oxyhornblende is generally depleted in (OH) and enriched in Fe^{+3} (at the expense of Fe^{+2}).

The distinction between oxyhornblende and hornblende is somewhat arbitrary as there seems to be little agreement among mineralogical source books about where the line should be drawn. With regard to oxyhornblende, Winchell and Winchell (1951, p. 437) cite theoretical compositions of four "end members," none of which contains any Mg; the extinction angle ($Z \wedge c$) ranges from 0° to 15°, and γ is as high as 1.80. Rogers and Kerr (1942, p. 287) state that the extinction angle range is 0° to 12° and that γ is as high as 1.76. Larsen and Berman (1934, p. 221) use the equivalent term "basaltic hornblende" for "those members containing appreciable Ti with less Mg+Fe than hastingsite and less (OH) than the normal amphiboles." The optical properties of minerals so defined vary; extinction angles range from 0° to 21° and γ is as high as 1.718. The minerals included by their definition contain more Mg than Fe.

In the Lava Mountains rocks, the most conspicuous change in the pleochroic formula occurs between crystals having extinction angles just above and just below 10°. Because color is one of the more obvious differences between the two amphiboles, but is difficult to measure quantitatively, the associated extinction angle of 10° has been used here as the dividing line between the two.

Color and pleochroism.—The hornblende found in these rocks is generally green or straw colored in thin section. The pleochroism is marked but not intense. The oxyhornblende is more deeply colored and intensely pleochroic; its average pleochroic formula is as follows:

X=light moderate yellow (5*Y* 8/6).
Y=dark yellowish orange (10 *YR* 6/6).
Z=moderate brown (5*YR* 4/6).

All intermediate variations are found.

Size and habit.—Both hornblende and oxyhornblende are found as elongated prismatic crystals, which in cross section have a lozenge shape. They are rarely more than 3 mm long and most are between 0.5 mm and 1.5 mm long.

Inclusions.—Inclusions are common, the most frequent being euhedral opaque minerals, probably magnetite. Biotite, apatite, clinopyroxene (containing magnetite?), and plagioclase (possibly of secondary origin) are also common.

Alteration.—The most common deuteric alteration products are opaque materials. Others are plagioclase, epidote(?), and fine-grained pyroxene(?). In one rock the green hornblende was partly altered to chlorite (penninite?) and calcite.

It seems clear, as a result of investigations by several mineralogists, that in the vicinity of 750°C, common hornblende changes to oxyhornblende at atmospheric conditions (Belovsky, 1891, p. 291; Weinschenk, 1912, p. 292; Graham, 1926, p. 122–123; Kozu and Yoshiki, 1927; and Kozu, Yoshiki, and Kani, 1927). In the studies by Kozu and his associates, common hornblende was subjected to ever-increasing heat in an atmosphere of air. Between 700° and 800°C, the extinction angle diminished from 12° to 0.3° and γ increased from 1.687 to 1.720. Above and below these temperatures the changes were slight. At about 750°C, a marked increased in the rate of weight loss (calibrated as percent of weight loss per degree centigrade) was also noticed. Oxyhornblende, also subjected to similar treatment, showed little change in optical properties when heated, although the rate of weight loss changed slightly at 750°C.

Synthetic hornblende with the optical properties of oxyhornblende has not been made, but probably the experimental data for biotite noted above are qualitatively applicable; in both minerals, the optical changes produced by deuteric alteration are similar, and apparently the OH^{-1} ions bonded to the Fe^{+2} ions are released when the Fe^{+2} is oxidized.

Field evidence in the Lava Mountains shows that hornblende crystals commonly existed in volcanic magmas up to the time of their extrusion, but that shortly thereafter they were changed to oxyhornblende. For example, this is shown by the flow of Lava Mountains Andesite in section E9–a, which consists partly of hornblende-bearing perlite and partly of oxyhornblende-bearing red-brown andesite (see p. 34) ; the hornblende-bearing perlite apparently represents a chilled basal layer and thus approximates the mineralogical composition of the lava immediately after its extrusion. Judging from the experimental data cited above, the temperature of this flow must have still been above 750°C at the time of extrusion (or was raised above this temperature by oxidation shortly afterward) inasmuch as most of the hornblende crystals in the flow were changed eventually to oxyhornblende, but the other conditions necessary to promote alteration were fulfilled only in the very late stages of solidification.

ORTHOPYROXENE

The orthopyroxene in these rocks is hypersthene. In all the rocks examined, the orthopyroxene is optically negative and the optic angle is medium to large. In most rocks, the crystals are slightly pleochroic, the formula being:

X=very pale orange (10*YR* 8/2).
Y=Z=clear, to very slightly bluish tint.

Most of the crystals are stubby prisms that have well-developed prism faces and very faintly developed terminations. Many contain inclusions of euhedral opaque minerals, probably magnetite.

Some crystals are stained orange or light brown around the edges, and such colors commonly form a band around the inner edge of the opaque alteration products. Where deuterically altered, the mineral has changed to a fine-grained opaque material or a fibrous greenish material, probably bastite. Experimental data that outline conditions under which pyroxenes alter to iron oxides are not available, but presumably an increase in the partial pressure of oxygen is one change that would promote this reaction. As temperatures drop below 500°C, pure enstatite alters to serpentine (bastite) at pressures below 2,000 bars and in an excess of water vapor (Bowen and Tuttle, 1949, p. 453, fig. 2).

CLINOPYROXENE

The volcanic rocks in the Lava Mountains generally contain only a few tenths of a percent clinopyroxene. In some rocks, the optic angle and extinction angle suggest that the clinopyroxene is pigeonite, whereas in others, augite or diopside are indicated.

Clinopyroxenes are found in three habits. The most common habit is the same as that of the orthopyroxenes, namely, small stubby prisms. The second, which is much less common, is clusters of small, well-terminated crystals that converge inward from the walls of a cavity. The third is a band of small anhedral crystals forming a reaction rim around partially altered crystals of quartz.

Some crystals contain inclusions of euhedral magnetite(?) crystals. Where deuterically altered, clinopyroxene generally is changed to fine-grained opaque minerals or to bastite.

QUARTZ

A fraction of a percent of quartz is found in most volcanic rocks in this area. Its most common form is that of irregularly embayed fragments. In many thin sections these fragments have a uniform reaction rim of fine-grained clinopyroxene, whereas in others they are free of such rims. The development of this reaction rim is generally consistent within a single sample, but it may be thick, thin, or absent in successive samples from the same mapping unit. In a small percentage of specimens, nearly euhedral crystals of quartz are preserved (fig. 22*B*), indicating that this mineral formed during early stages of crystallization; in most specimens, though, quartz crystals are largely resorbed, showing that quartz did not remain stable during later stages.

Many quartz crystals contain round or oval-shaped inclusions of yellowish or clear glass, and very small needles or prisms of apatite.

OPAQUE MATERIAL

Four types of opaque material are present: (1) Euhedral equant crystals that appear as squares or polygons in thin section, probably magnetite, although ilmenite may be present in appreciable percentages; (2) irregular dustlike fragments that appear black in conoscopic light; (3) clumps of equidimensional fine-grained material that most commonly are semiopaque and appear a deep red in conoscopic light; and (4) fibrous and hairlike fragments that are deep red or brown in conoscopic light. Most of these are presumed to be iron oxides.

OTHER MINERALS

Minerals that were noted but not specifically described above include the following: chlorite, calcite, zeolite, apatite, opal, chalcedony, cristobalite, K-feldspar, sericite, alunite, epidote, and bastite. Minerals that are tentatively identified are: tridymite, chlorophaeite, serpentine, and olivine.

GROUNDMASS

Most rocks in this area have a hemicrystalline groundmass that consists predominantly of microcrystals, crystallites, cryptocrystalline material, and glass. The glass is most often clear, slightly yellowish, or greenish.

The crystallites and microcrystals appear to be plagioclase, although no definitive optical properties could be measured. Opaque materials generally form a light to heavy "dust."

In figure 23, the refractive indices of the glassy portions are plotted against the silica percentages of

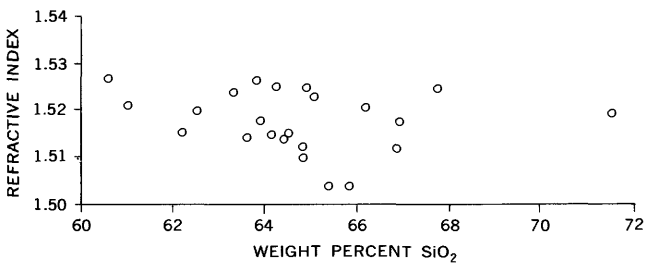

FIGURE 23.—Diagram showing the relation between the SiO_2 content of the whole rock and the refractive index of the glassy part of the groundmass. The analyzed samples of volcanic rocks older than the Bedrock Spring Formation, subpropylite, and the propylite contained no glass.

the whole rock. All the indices are between 1.50 and 1.53. According to George (1924, p. 365), this would indicate a silica range of 57 to 72 percent. This range of inferred silica percentages happens to be about right, but there is little correlation between the refractive index of the glass and the silica percentage of any one rock.

An appreciable percentage of silica minerals and K-feldspar are commonly found as submicroscopic minerals in volcanic rocks from other areas. X-ray diffraction of the analyzed volcanic rocks from the Lava Mountains area, though, shows that with one exception, cristobalite and clays are the only detected minerals not also present as larger crystals reported in the modal analyses. The exception is the analyzed sample of upper Pliocene(?) felsite which also contains large percentages of submicroscopic K-feldspar; that rock thus might be classified as a dellenite (or quartz latite). Probably most of the cryptocrystalline material in rocks is cristobalite, although some of it may consist of highly imperfect molecule-like arrangements of other rock-forming components that appear slightly anisotropic in polarized light but do not cause distinctive X-ray diffraction patterns.

MODAL COMPOSITION OF THE SUITE

Average modal compositions of the analyzed volcanic rocks in the three major volcanic formations are listed in table 11. The modal composition of one sample of volcanic rock from the Bedrock Spring Formation is added for comparison. In rocks from all four formations the groundmass is the most abundant material and forms from 60 to 90 percent of the total volume, averaging about 70 percent. Plagioclase is invariably present; the total volume in individual volcanic rocks varies from 10 to 30 percent, but in all four volcanic rock-bearing formations, the average percentage is very close to 20. Of this percentage, megaphenocrysts generally constitute one-third to two-thirds of the total. Biotite locally constitutes over 2 percent of the rock but more generally about 0.5 percent. Oxyhornblende or hornblende make up as much as 10 percent of fresh rocks, but the average is less than 1 percent; it is typically about twice as abundant as biotite, but either mineral may be absent. Orthopyroxene and clinopyroxene form less than 2.5 percent of every rock and may be locally absent. Quartz exceptionally forms over 3 percent but the average is less than 1 percent. Opaque materials are invariably present and constitute between 1 and 11 percent of the mode total; these figures, however, are probably too high because of the tendency for fine-grained opaque minerals embedded within the thin section to be projected onto the top surface, the surface on which the point count is theoretically being made. Other minerals make up as much as 6 percent of the rock but average only a few percent.

MODAL CHANGES WITH AGE

The purpose in comparing the modal compositions of successively deposited volcanic rocks is to find if any changes are sequential. Figure 24*A* shows in stratigraphic order the modal composition of individual specimens collected from the type section of the Almond Mountain Volcanics and the overlying cap of Lava Mountains Andesite. Figure 24*B* shows a comparable set of modal analyses of rocks from the same formations collected about 1 mile north of Dome Mountain. These stratigraphic sections are presumably typical, and data from them illustrate the amount of modal variation (a) between successive volcanic strata of the Almond Mountain Volcanics, (b) between the eastern and western facies of the Almond Mountain Volcanics, and (c) within a single flow of Lava Mountains Andesite.

The percentages of amphibole, biotite, and pyroxene in the modal analyses are determined not only by the percentages in the original lava, but also by the intensity of deuteric alteration. Hornblende, oxyhornblende, and biotite in these rocks are more readily altered than orthopyroxene and clinopyroxene; but in some rocks, the modal percentages of all are greatly reduced and the percentages of opaque minerals correspondingly increased. Of the upper three samples plotted in figure 24*A* two are relatively unaltered, and

TABLE 11.—*Averaged modal compositions of volcanic rocks from the Almond Mountain Volcanics, Lava Mountains Andesite, and Quaternary andesite. Modal composition of one sample of volcanic rock from the Bedrock Spring Formation added for comparison*

[All values are volume percent. $\bar{x}$, average or mean $\left(\frac{\Sigma X}{N}\right)$; s, standard deviation $\left(\left[\frac{\Sigma(X-\bar{x})^2}{N-1}\right]^{1/2}\right)$; $s_{\bar{x}}$, standard error $\left(\frac{s}{(N)^{1/2}}\right)$; where X=percentage of mineral in individual sample and N=number of samples analyzed]

Mineral	Bedrock Spring Formation (1 sample)	Almond Mountain Volcanics (9 samples)			Lava Mountains Andesite (9 samples)			Quaternary andesite (2 samples)		
		$\bar{x}$	s	$s_{\bar{x}}$	$\bar{x}$	s	$s_{\bar{x}}$	$\bar{x}$	s	$s_{\bar{x}}$
Plagioclase megaphenocrysts	15. 1	9. 8	5. 5	1. 8	10. 2	2. 9	1. 0	10. 2	0. 71	0. 50
Plagioclase microphenocrysts	5. 1	10. 7	3. 1	1. 0	10. 7	4. 1	1. 4	10. 4	. 99	. 70
(Total plagioclase)	(20. 2)	(20. 5)	4. 5	1. 5	(20. 9)	4. 2	1. 4	(20. 6)	1. 7	1. 2
Biotite	. 5	. 7	. 69	. 23	. 2	. 20	. 07	. 6	. 36	. 25
Hornblende	6. 3	0			Trace			. 9	1. 3	. 90
Oxyhornblende	0	. 5	. 36	. 12	1. 6	2. 5	. 8	. 1	. 10	. 07
Orthopyroxene	1. 2	1. 3	. 77	. 26	. 7	. 82	. 27	. 2	. 14	. 10
Clinopyroxene	0	. 5	. 24	. 08	. 5	. 66	. 22	. 2	. 10	. 07
Quartz	0	. 2	. 37	. 12	. 5	1. 0	. 3	. 4	. 22	. 16
Opaque minerals	1. 5	4. 1	3. 1	1. 0	5. 9	3. 4	1. 2	3. 0	1. 9	1. 4
Other minerals	. 1	. 9	1. 5	. 5	. 7	. 87	. 29	5. 3	. 99	. 70
Groundmass	70. 2	71. 3	5. 7	1. 9	69. 0	4. 1	1. 4	68. 6	1. 5	1. 0

one is highly altered. The contrasts between their mafic mineral percentages probably represent the maximum variation in these rocks that can be attributed to alteration.

Figure 24*A* suggests an upward decrease in the percentages of microphenocryst feldspar, orthopyroxene, clinopyroxene, and groundmass, and an upward increase in the percentages of megaphenocryst feldspar, oxyhornblende, and opaque minerals. All but two of these trends must be regarded as chance or a product of local conditions, however, because the stratigraphic section plotted in figure 24*B* does not repeat them. The upward increase of the opaque minerals is repeated in both sections, but this must only reflect alteration differences because it is not correlative with increasing iron or titanium percentages in the same rocks. The upward decrease in orthopyroxene percentages, however, is repeated in both sections. This trend is probably real because it shows better than normal consistency and is partly supported by the averaged data described below.

The averaged modal compositions listed in table 11 show the volcanic rocks in successive formations to be quite similar. The relatively large sizes of the standard deviations and standard errors are chiefly results of the small number of samples analyzed, but they also indicate that appreciable modal variation does occur within these rock units, and that the small differences between these averages might not be confirmed by additional analyses. Figure 25 compares graphically the average values of each component in the three major volcanic formations, and shows their 50-, 75-, and 90-percent confidence limits—the limits that will, with these probabilities, enclose the true average if the components of these formations have statistically normal distributions. The statistical data for the Almond Mountain Volcanics and Lava Mountains Andesite are based on nine samples from each; those for the Quaternary andesite are based on only two, so they have uncertain significance when compared with those from the other two rock units. However, they permit approximate limits to be set on the probabilities that the three successive formations actually have the averaged modal relations indicated, and on the range over which these averages might migrate with additional sampling.

The average percentages of plagioclase megaphenocrysts, plagioclase microphenocrysts, and total plagioclase are almost identical in the three volcanic formations. The slight differences between them are not significant. The confidence limits plotted in figure 25 indicate a 75-percent chance that more extensive sampling would not separate the megaphenocryst or microphenocryst averages by as much as 4 percent, or the total plagioclase averages by as much as 5 percent, but the relation between such averages is not indicated.

Some of the differences between average percentages of biotite, hornblende and oxyhornblende, clinopyroxene, quartz, opaque mineral, nonopaque mineral, and groundmass are much greater, and testing the differences between them (Arkin and Colton, 1950, p. 127) indicates chances ranging from 50 to 99 percent of their being confirmed by additional sampling. However, some of the indicated differences reverse their trends with time, and others are appreciable only between two of the three formations. None are indicative of progressive changes in the magma. The confidence limits show the ranges over which these averages might migrate with complete sampling.

The orthopyroxene averages differ from the others because they show a trend. The chances of the indicated

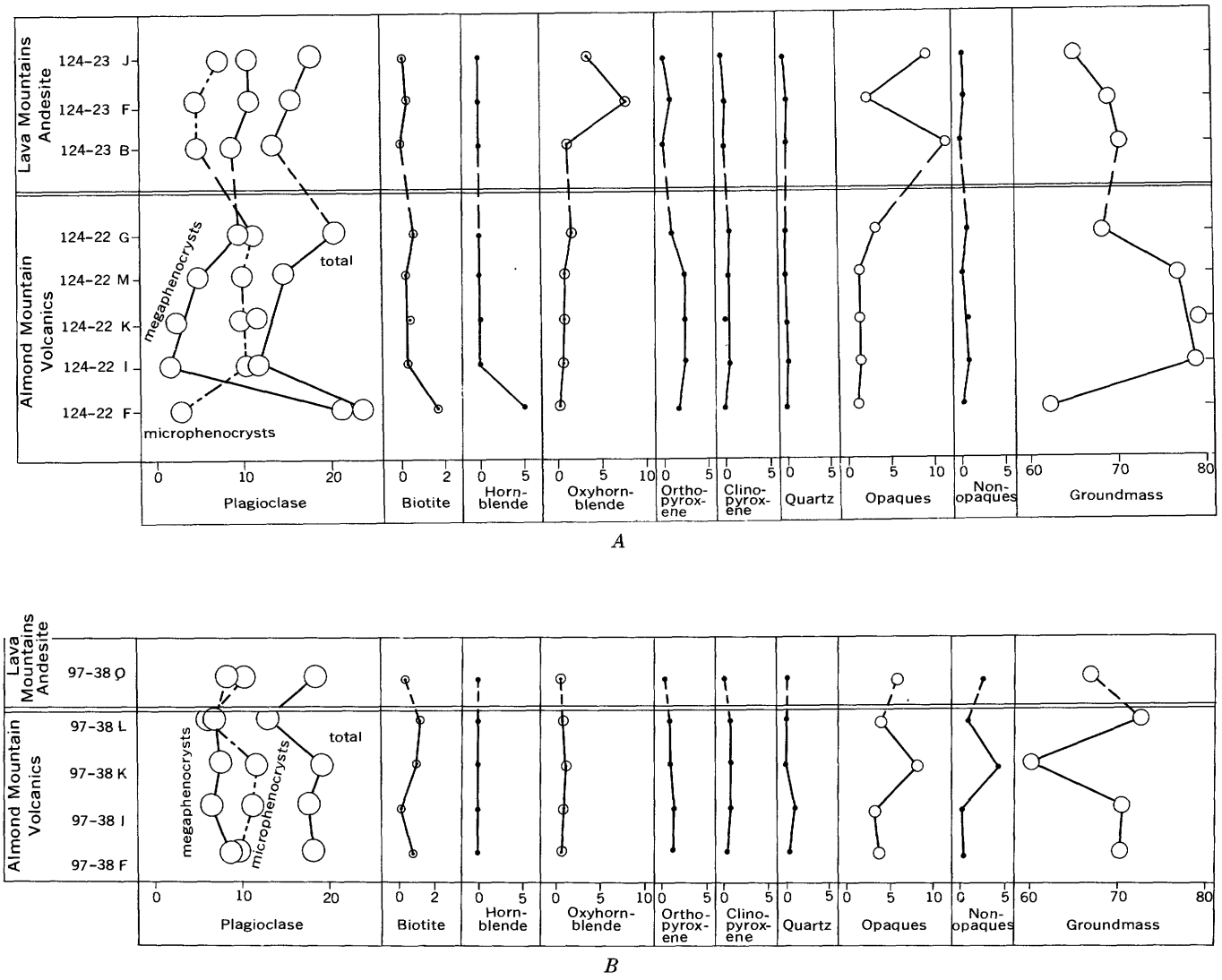

FIGURE 24.—Diagrams showing the variation in modes of rocks from the Almond Mountain Volcanics and Lava Mountains Andesite. The locations of samples are described in table 21. The radii of the circles represent the average analytical errors calculated in table 18. Data are from tables 5 and 8; values are in volume percent. *A*, samples are from the type section of the Almond Mountain Volcanics and from the west side of Almond Mountain. The stratigraphic positions of the lower five samples are shown in fig. 11. Sample 124–22k is from a Lava Mountains Andesite sill in the Almond Mountain Volcanics. *B*, samples are from 1 mile north of Dome Mountain.

shifts being confirmed by additional sampling are 75 percent for the lower pair of formations, and 55 percent for the upper pair. This modal trend may indicate contemporaneous settling of these crystals in the magma, but may also result from the greater alteration of mafic minerals in younger rocks. The percentages of mineral involved are too small, however, to be detected by comparison of chemical analyses.

PETROCHEMISTRY

CHEMICAL COMPOSITION OF THE SUITE

MAJOR ELEMENT AND NORMATIVE COMPOSITIONS

The analyzed volcanic rocks in this suite contain between 60 and 72 percent SiO_2. All but three of them contain between 62 and 68 percent SiO_2. The narrow range of rock compositions is striking. Similarly restricted are the average Al_2O_3 percentages, which lie mostly between 15 and 16 percent. The comparatively wide scatter of Fe_2O_3 and FeO percentages reflects deuteric alteration; a more useful estimate of the similarity between formations is furnished by the percentages of total Fe as Fe_2O_3, which are mostly close to 4 percent. Individual MgO values range from 0.5 to 3.5 percent, but most are near the middle of this range. The CaO percentages mostly lie between 3.5 and 6 percent, the Na_2O percentages between 3 and 5 percent, and the K_2O percentages between 2 and 3 percent. In all but one rock, the percentages of CaO and Na_2O both exceed the percentage of K_2O; in about half of these, the per-

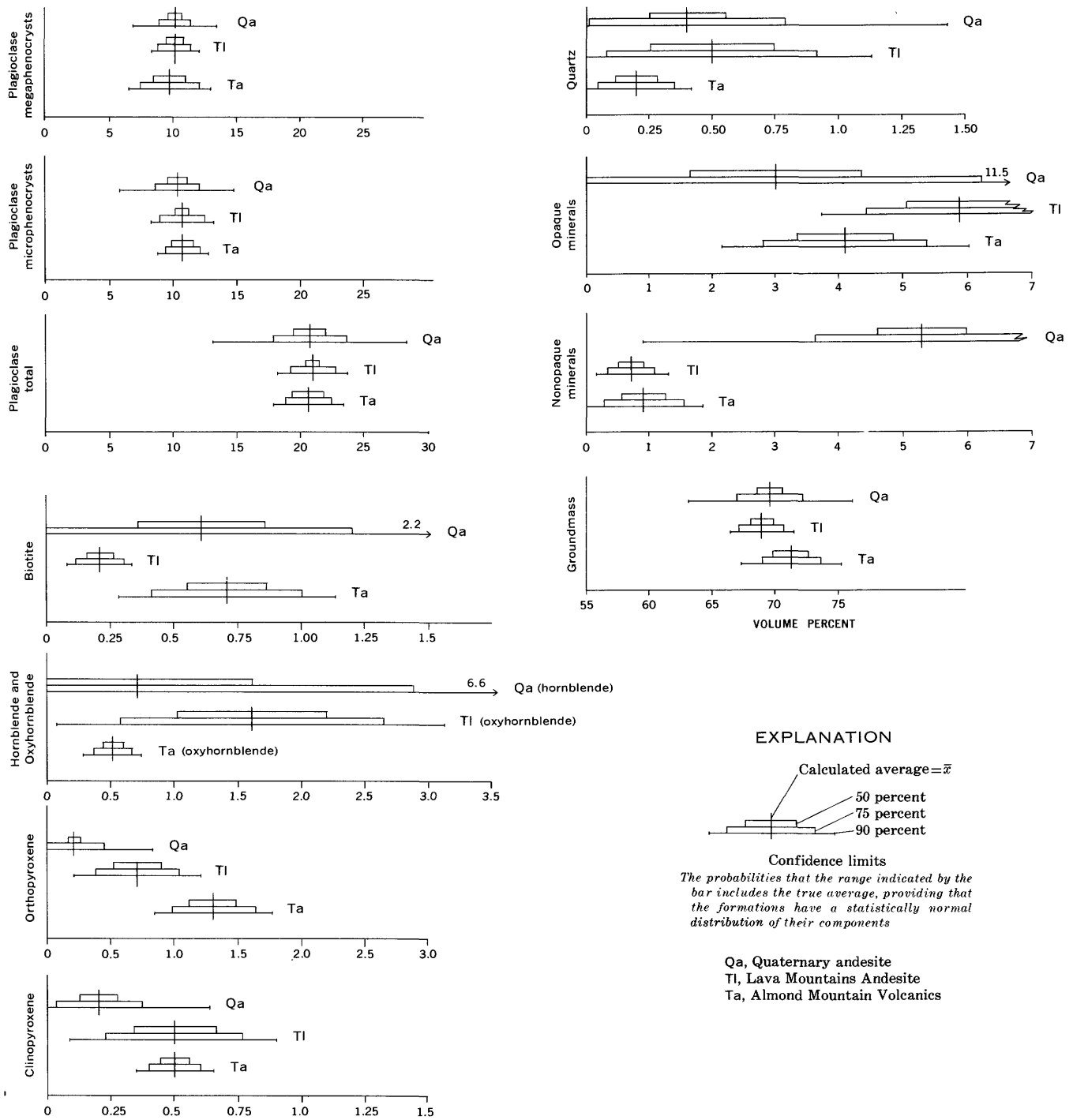

FIGURE 25.—Diagram comparing calculated average percentages of components in the Almond Mountain Volcanics, Lava Mountains Andesite, and Quaternary andesite. Data from table 11. Limits calculated by the t-distribution method (Bennett and Franklin, 1954, p. 153–157).

centage of CaO exceeds that of Na_2O. The variation in TiO_2 and P_2O_5 percentages is about 0.5; the variation in MnO is about 0.05. The percentages of CO_2 and total H_2O vary greatly because they depend chiefly on the degree of alteration.

In figure 26, the percentages of SiO_2 in these volcanic rocks are plotted against the percentages of oxides of other major components. The points representing percentages of Al_2O_3, total Fe as Fe_2O_3, Na_2O, K_2O, TiO_2, P_2O_5, and MnO show the least scatter along a line; the points representing percentages of MgO and CaO show more. The points representing H_2O and CO_2 percentages show no trends because they are dependent on alteration. Although even the most systematic of these

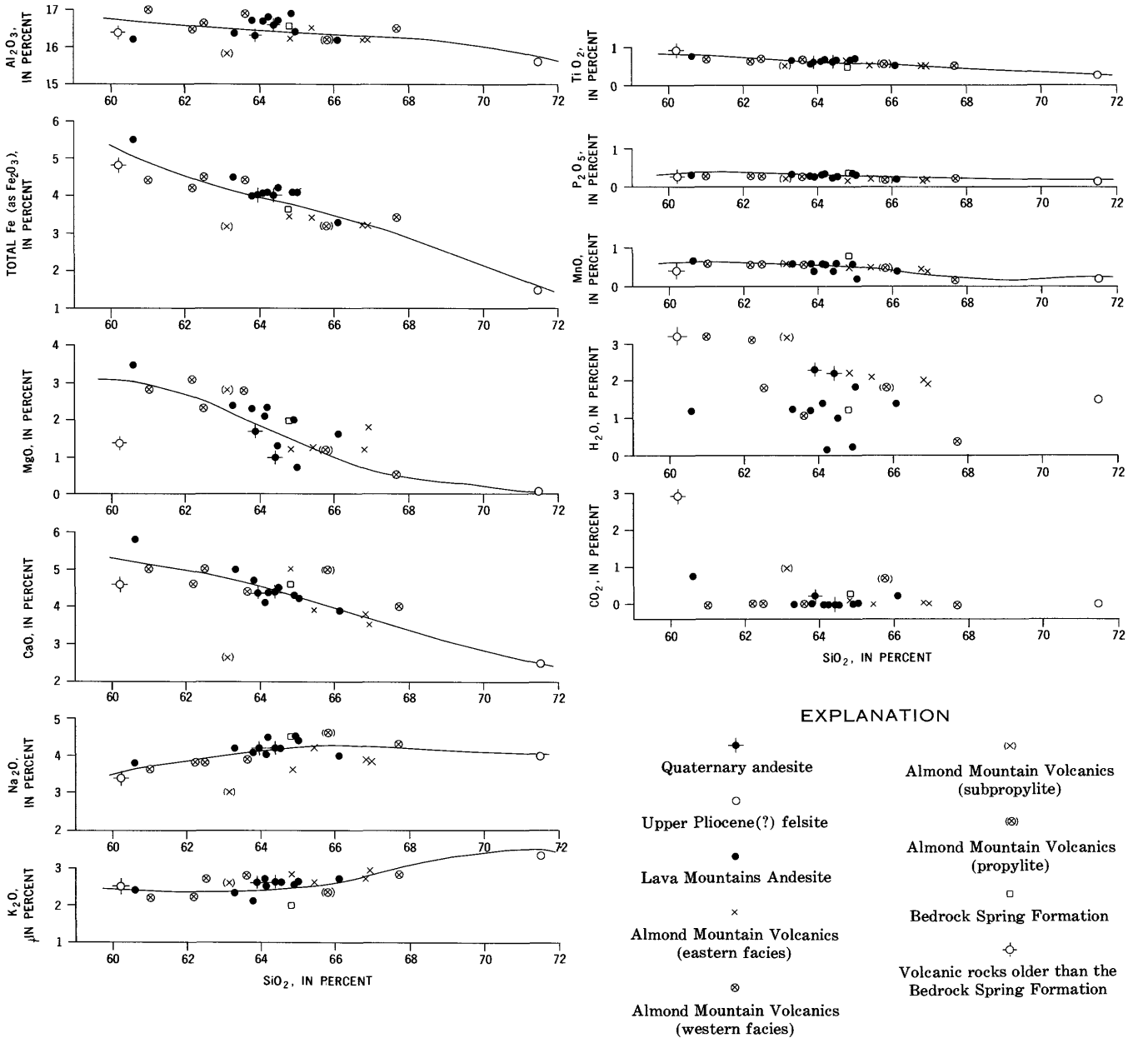

FIGURE 26.—Variation diagram showing the relations between the oxides of the major elements and silica. Data from tables 3–10.

do not fall along a smooth line, they define statistical trends as well as most suites of analyzed rocks. This further corroborates the evidence that the volcanic rocks of this area are all members of a single suite.

Excluding the point representing the upper Pliocene(?) felsite, the data for all rock-forming oxides except one define curves that slope in one direction or the other. The exception is the curve for K_2O. This is a significant exception, and its implications are discussed in the section on "Volcanic petrogenesis."

Figure 27 shows the interrelations between percentages of Na_2O+K_2O, CaO, MgO, and $FeO+Fe_2O_3$ in selected volcanic rocks of the area. All percentages, except the upper Pliocene(?) felsite (*pf*) lie in a distinct group. A faint elongation is detectable in all three diagrams, and this probably reflects differentiation. The distribution of the points, however, is not correlative with the age of the rocks they represent, and the differentiation trends were apparently created before eruptions began.

By extrapolation, the alkali-lime index (Peacock, 1931, p. 57)—that percentage of Si_2O at which $Na_2O+K_2O=CaO$—is about 58. According to Peacock's classification, these rocks would be calc-alkalic. Table 12 lists the alkali-lime index values for 14 other volcanic areas in western North America selected to

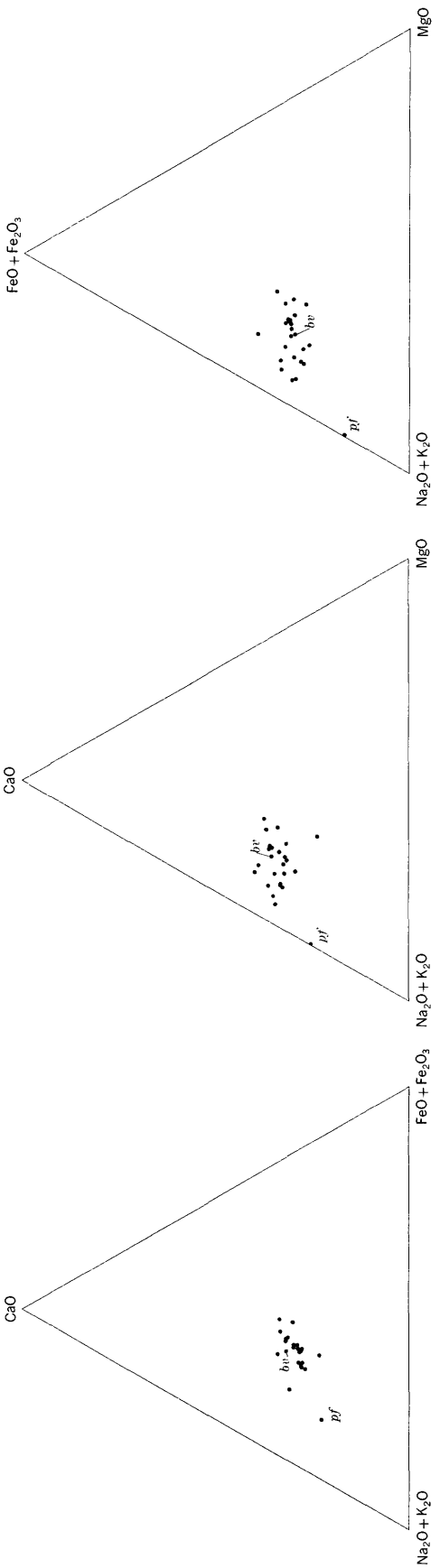

FIGURE 27.—Variation diagrams showing selected interrelations between Na_2O+K_2O, CaO, $FeO+Fe_2O_3$, and MgO in volcanic rocks form the Lava Mountains area. Propylitized rocks are omitted. Point *pf* represents upper Pliocene(?) felsite; point *bv* represents volcanic rock from the Bedrock Spring Formation. Data from tables 4, 5, 7–10.

represent the range of volcanic suites of this area. Compared to most of these, the Lava Mountains suite is relatively deficient in calcium.

The C.I.P.W. norms of the analyzed rocks are listed with the chemical analyses in the section on "Stratigraphy." Seventeen of the rocks are yellowstonose with a symbol I.4.3.4.; six (four from the western facies of the Almond Mountain Volcanics, and two from the Lava Mountains Andesite) are tonalose with a symbol II.4.3.4.; two (the Pliocene(?) felsite, and the subpropylite from the Almond Mountain Volcanics) are lassenose with a symbol I.4.2.4.

TABLE 12.—*List of alkali index values (Peacock, 1931) of 14 volcanic areas in western North America*

Area	*Alkali index*	*Source of data*
Lava Mountains, Calif	58	This report, p. 69.
Newberry volcano, Oreg	58	Williams (1935, p. 297).
Steen's Mountain, Oreg	58	Fuller (1931); index computed by Williams (1935, p. 297).
Markleeville, Calif	59. 8	Curtis.[1]
Neovolcanic zone of Mexico	60	Williams (1950, p. 265).
Medicine Lake Highland, Calif.	60. 5	Anderson (1941, p. 401).
Parícutin region, Mexico	61. 5	Wilcox (1954, p. 315).
Parícutin volcano, Mexico	62	Do.
Crater Lake, Oreg	62	Williams (1942, p. 153).
Clear Lake area, Calif	62	Anderson (1936, p. 661).
Mount St. Helens, Wash	62. 3	Verhoogen (1937, p. 292).
Mount Shasta, Calif	63. 7	Quoted by Williams (1942, p. 153).
Mount Lassen, Calif	63. 9	Do.
Glendora area, Calif	65	Shelton (1955, p. 71).
Los Angeles basin, Calif	65. 2	Eaton (1957, p. 311. See footnote on page 74).

[1] Curtis, G. H., 1951, Geology of the Topaz Lake quadrangle and eastern half of the Ebbetts Pass quadrangle: Berkeley, California Univ., Ph. D. thesis.

In figure 28, the normative compositions of selected volcanic rocks are plotted on the four sides of the tetrahedron representing the phase system Q-or-ab-an at 5,000 bars water vapor pressure. All compositions but that of the upper Pliocene(?) felsite (*pf*) fall in a cluster. This cluster is nearly equidimensional, indicating that these phases have not participated significantly in differentiation.

The lack of variety in the rocks of the Lava Mountains suite is emphasized by the small number of C.I.P.W. normative rock names needed to describe them. The difference between yellowstonose and tonalose is solely in the class number (I and II), which depends on the ratio of normative quartz plus feldspars to dark minerals; the higher the Roman numeral, the higher the percentage of normative dark minerals. The similarities between these rocks (excepting lassenose) are more impressive: the same order, rang, and subrang result from very similar ratios of normative quartz to feldspar, alkalies to lime, and potash to soda. The lassenose is anomalous because of the higher ratio of alkalies to lime than in the rest of the rocks.

Washington's normative tables (1917) can be used as a guide to other areas containing fine-grained rocks with similar normative (and thus chemical) compositions, and as an approximate measure of rock abundances—at least in the areas that attracted the attention of volcanic petrologists up to the time of his compilation. Of the three types found in the Lava Mountains, tonalose is the most common volcanic rock listed in Washington's tables, lassenose is next, and yellowstonose the least common. In the Lava Mountains suite, yellowstonose forms the greatest percentage rather than the smallest implying that the Lava Mountains rocks are deficient in normative dark minerals compared with most areas.

When Washington's lists (1917) of yellowstonose, tonalose, and lassenose localities are tabulated, it is found that the fine-grained examples of these three rock types are concentrated in Cenozoic orogenic regions, namely the west edge of North and Central America, the western Pacific region, the West Indies, and the area surrounding the Mediterranean Sea. The yellowstonose samples were chiefly derived from Central America, northern California, the Yellowstone National Park area, and the East Indies, Philippines, and Japan areas; the tonalose samples from northern California, southern Oregon, and the West Indies and Mediterranean areas; and the lassenose samples predominantly from northern California, southern Oregon, Arizona, New Mexico, and some from the Mediterranean area.

The Lava Mountains rocks are thus representative of common although not prevalent volcanic rock types in orogenic regions. Perhaps the major distinction of the suite in the Lava Mountains is the limited range of compositions; most areas contain several types of volcanic rocks, even though only brief periods of time are represented. The Lava Mountains are composed chiefly of one.

MINOR ELEMENT COMPOSITION

A total of 36 elements were sought in the spectrochemical analyses. Three of these, Fe, Mn, and Ti, were also included in the major element analyses. Those elements detected in virtually all the analyzed rocks are: B, Ba, Co, Cr, Cu, Fe, Ga, Li, Mn, Ni, Pb, Rb, Sc, Sr, Ti, V, Y, Yb, and Zr. Those elements that were sought but not detected in any rocks are: Ag, As, Bi, Cs, In, La, Pt, Sb, Sn, U, and Zn. Elements that were questionably detected in some rocks are: Ga (in 128–34, 97–38K, and 97–38I), Mo (in 41–34, 124–22K, 97–38I, and 181–29), and Nb (in most samples). The lower limits of detection for the elements not found are listed in the following table.

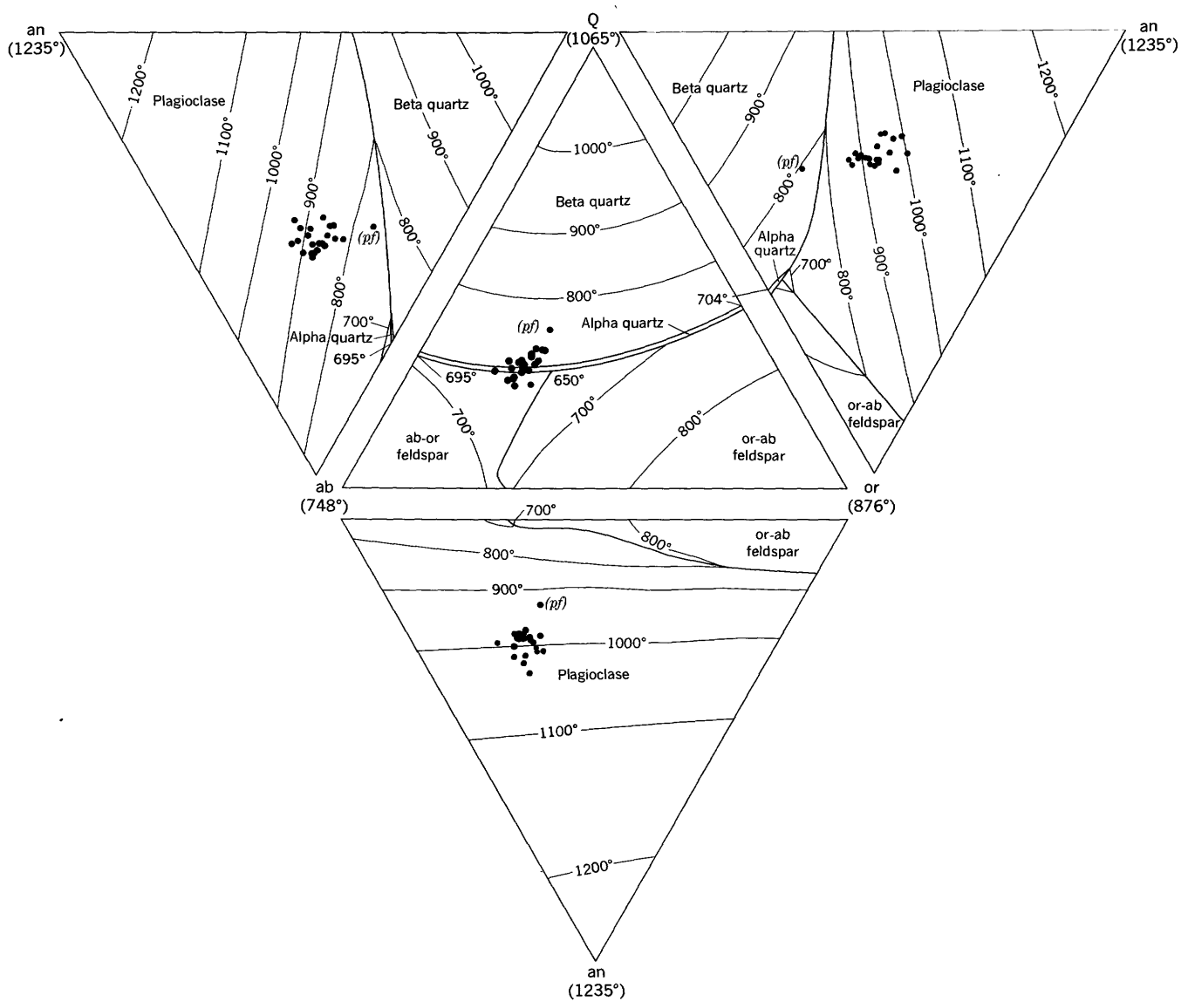

FIGURE 28.—Phase diagram of the system Q-or-ab-an at 5,000 bars of water vapor pressure showing normative composition of selected volcanic rocks. Point *pf* represents composition of the upper Pliocene(?) felsite. Diagram adapted from compilation by Bateman and others (1963, p. 34). Normative compositions of selected volcanic rocks from the Lava Mountains area are shown; propylitized rocks are omitted. Data from tables 4, 5, 8–10.

Lower limits of detection of elements sought but not consistently found in the volcanic and plutonic rocks

Element	Approximate lower limit of sensitivity (ppm)	Element	Approximate lower limit of sensitivity (ppm)	Element	Approximate lower limit of sensitivity (ppm)
Ag	0.5	Ga	1	Pt	50
As	200	Ge	20	Sb	200
Be	.8	In	10	Sn	5
Bi	10	La	100	U	500
Cd	20	Mo	2	Th	200
Cs	50	Nb	20	Zn	100

In figure 29, the minor element contents are plotted against the SiO_2 content of the host rock. Sloping relations are indicated by the points representing Ga, Mn, Sc, Sr, Ti, V, and Y. Three elements—Cr, Ni, and Cu—show a steplike curve, the break coming between 64 and 65 percent SiO_2. No slope is defined by the points representing B, Ba, Co, Cs, Li, Pb, Rb, Yb, and Zr. The lack of sloping relations between SiO_2 and Ba, Cs, Pb, and Rb results from the same factors that cause the lack of slope in the K_2O–SiO_2 diagram, and they are discussed in the section on "Volcanic petrogenesis." The lack of slope on the curves for B, Co, Li, and Zr remains unexplained.

Spectrochemical analyses of five volcanic suites from the western United States have been published by Nockolds and Allen (1953, tables 2, 3, 4, 7; 1954, table 16). A similar set of data has been assembled by

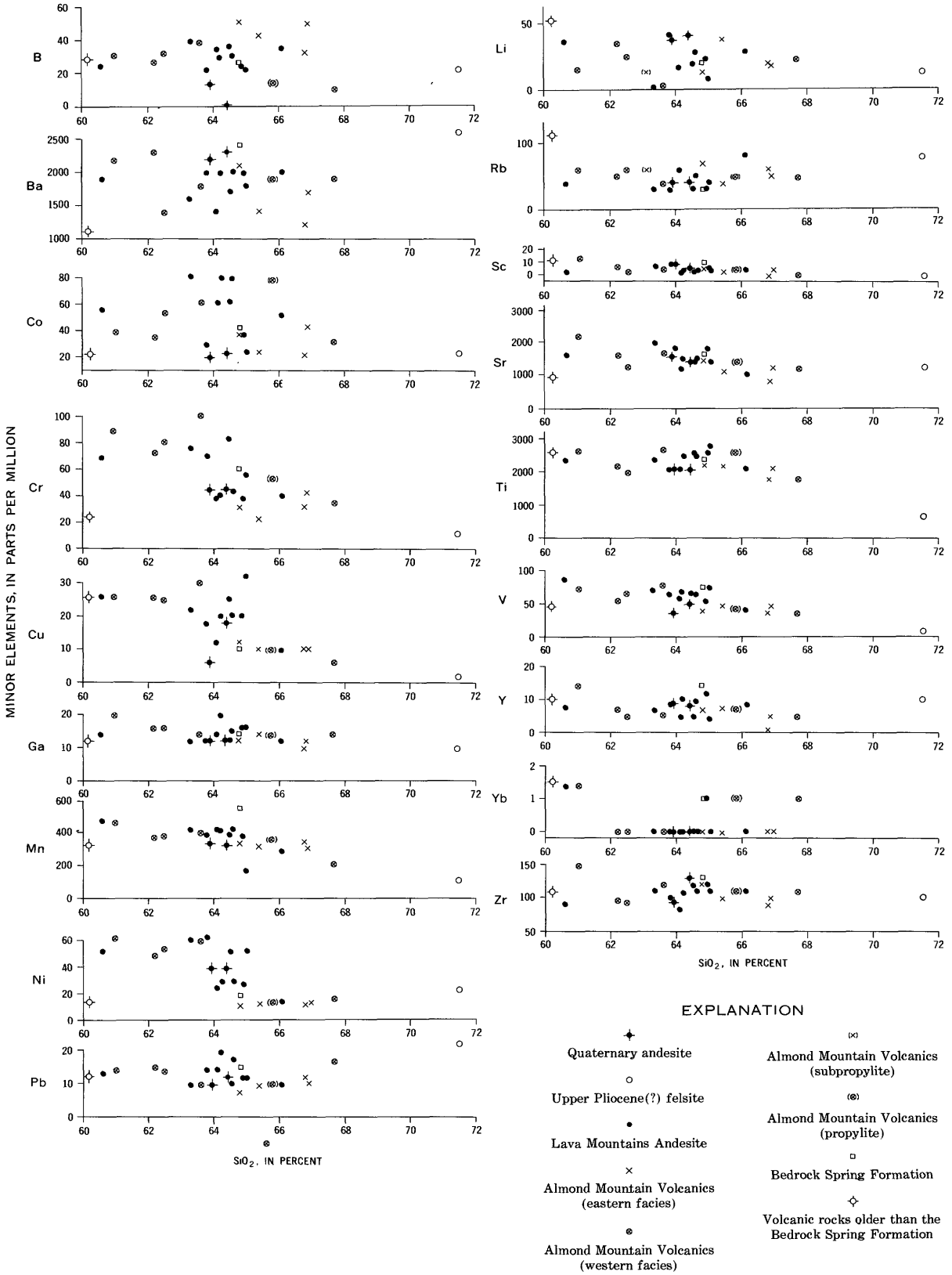

FIGURE 29.—Variation diagram showing the relations between the minor elements and silica. Data from tables 3–6, 8–10.

Eaton [4] for rocks of the Los Angeles basin. All six suites show general similarities with the suite from the Lava Mountains, although distinct differences occur in the quantities of Ga and Pb in the rocks from the Los Angeles basin area. The remaining five suites were not analyzed in the same laboratory as were the Los Angeles and Lava Mountains rocks, and the quantitative differences between the two groups of results are not large enough to be necessarily significant.

RELATIONS BETWEEN CHEMICAL AND MODAL COMPOSITIONS

The volcanic rocks of the Lava Mountains show two significant correlations between the chemical and modal compositions; the SiO_2 content is directly proportional to the percentage of groundmass, and it is inversely proportional to the percentage of total plagioclase. Both relations undoubtedly reflect in part the higher viscosity and slower crystallization rate correlative with the SiO_2 percentage of a melt. The correlation between SiO_2 and plagioclase partly reflects compositional changes in the magma, however, as shown by a similar variation pattern between SiO_2 and normative plagioclase (fig. 30). Of course all other elements that vary systematically with SiO_2 can also be shown to be related to these two modal percentages, so the significance of these correlations is unknown. There is no detected correlation between the percentage of minerals containing mafic constitutents and the percentages of Fe, Mg, Mn, Co, V, Ni, or Cr. A correlation probably existed prior to deuteric alteration, but the mafic mineralogy has been changed so greatly that all such relations have been obscured.

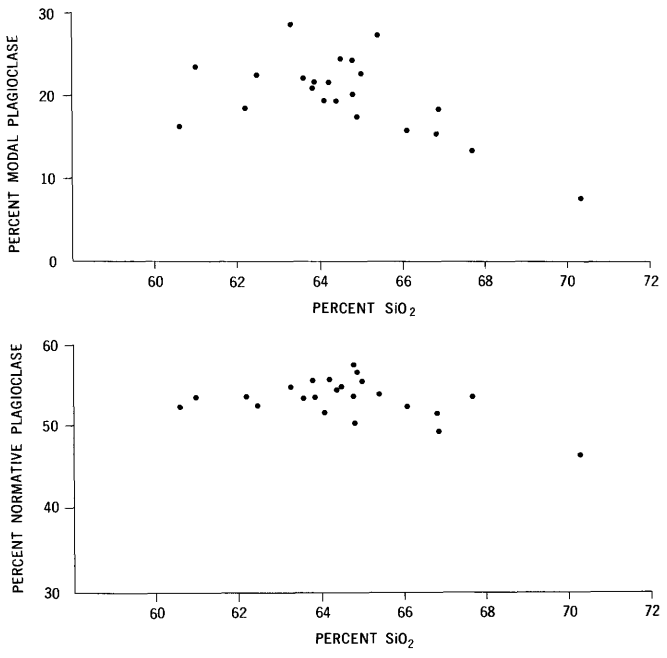

FIGURE 30.—Diagrams showing variation between SiO_2 and modal and normative plagioclase in selected volcanic rocks. Propylitized rocks omitted. Data from tables 4, 5, 8–10.

[4] Eaton, G., 1957, Miocene volcanic activity in the Los Angeles basin and vicinity: Pasadena, California Inst. Technology, Ph.D. thesis, table 11.

CHEMICAL CHANGES WITH AGE

The chemical data indicate few progressive changes in the composition of the melt. Figure 31 shows the percentages of major element oxides in successive layers of volcanic rocks that form the eastern and western facies of the Almond Mountain Volcanics, and in the Lava Mountains Andesite flows that immediately overlie them. The upper three samples in figure 31*A* are from a single flow of Lava Mountains Andesite, and the diagram shows the chemical variation that exists between samples differing chiefly in the degree of deuteric alteration. Each of the remaining samples represents a different flow or breccia layer.

The data in figure 31 show that any progressive change in the chemical composition of the magma was smaller than the sporadic and local changes, and that any such change is not reliably indicated by comparison of individual analyses that represent only one part of the volcanic province.

The upper part of figure 31 shows faint trends toward lower percentages of SiO_2 and H_2O in younger rocks, and toward higher percentages of Al_2O_3, total Fe as Fe_2O_3, MgO, CaO, Na_2O, TiO_2, P_2O_5, and MnO in younger rocks. The lower part of the figure shows trends toward lower percentages of total Fe as Fe_2O_3, MgO, CaO, and MnO, and toward higher percentages of SiO_2, Na_2O, and TiO_2 in younger rocks. The small trends in Na_2O and TiO_2 percentages are the same in both sections, but the percentage differences between successive samples, however, commonly exceed the total range of the inferred trend, and the indicated trends are thus not very reliable. Any trends indicated by these data can be recognized only by a study of averages representing larger numbers of samples collected from more widespread areas.

Table 13 lists the average percentages of major element oxides in the three most widespread volcanic formations. For comparison, the single analysis of volcanic rock in the Bedrock Spring Formation, and the average of two representative rocks from the Atolia Quartz Monzonite are added. The standard deviations and standard errors are listed; they measure the scatter of the data that produced these averages, and the probable proximity of these calculated averages to the true ones. Chemical data on rocks of the Almond Mountain Volcanics and Lava Mountains Andesite are based on nine analyses of each formation, so the statisti-

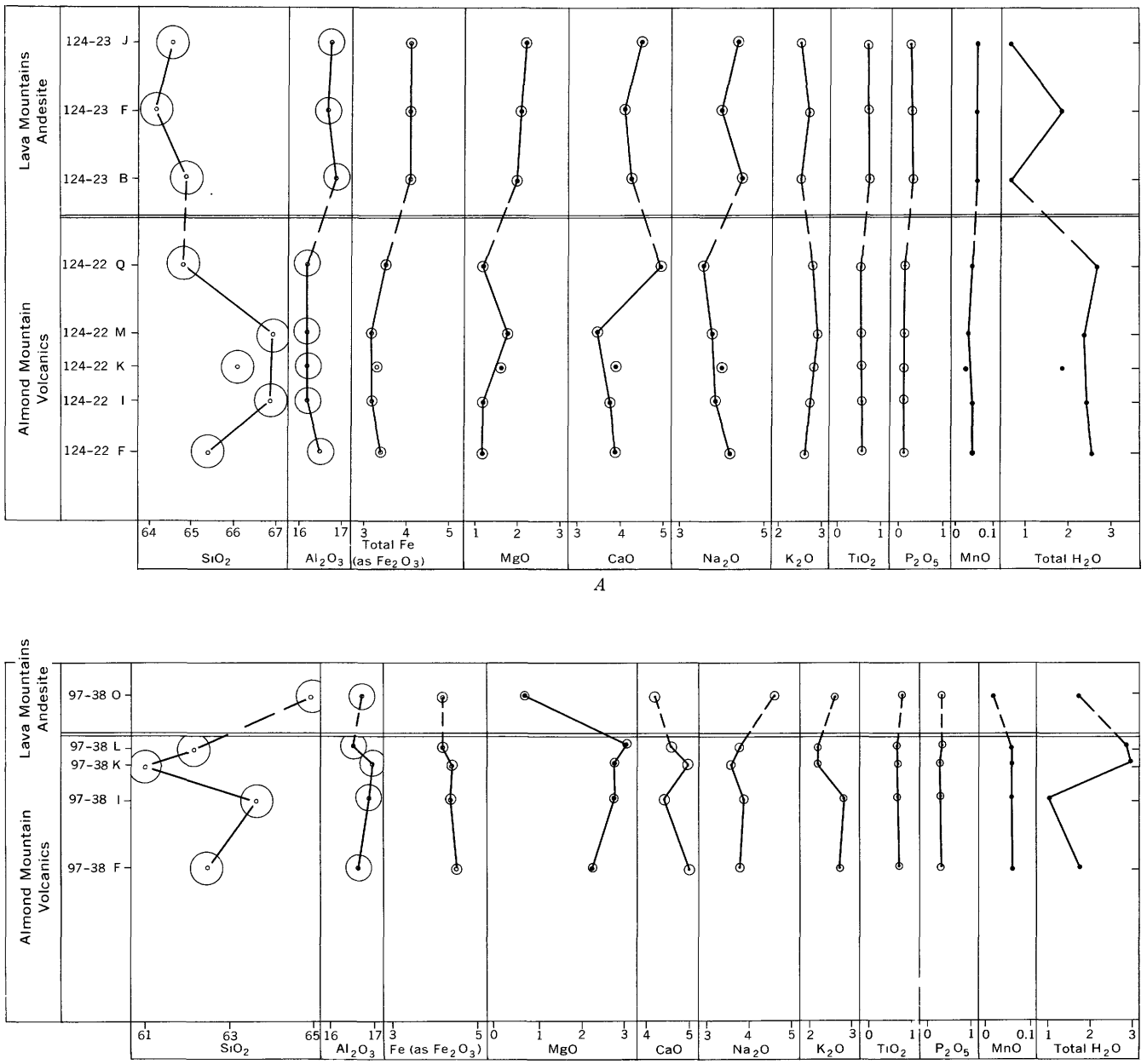

FIGURE 31.—Diagrams showing the variation in the percentage of major element oxides in superposed rocks of the Almond Mountain Volcanics and Lava Mountains Andesite. The location of samples is described in table 21. The radii of the circles represent the average absolute deviation as listed by Shapiro and Brannock (1952, p. 16). Data from tables 5 and 8; all values in weight percent. *A*, samples are from the type section of the Almond Mountain Volcanics and from the west side of Almond Mountain. The stratigraphic positions of the lower five samples are shown in figure 11. Sample 124–22K is from a Lava Mountains Andesite sill in the Almond Mountain Volcanics. *B*, samples are from 1 mile north of Dome Mountain.

cal parameters are moderately accurate measures of the same parameters that would be calculated from a much larger number of samples. However, data on the Quaternary andesite are based on only two samples, and their statistical parameters are only approximations.

The similarity between most of the average values supports the conclusion that any magmatic trend correlative with the time at which the rocks were extruded is small. The average Fe_2O_3 percentage increases and the FeO percentage decreases, but this only reflects the extent of deuteric alteration of rocks of similar chemical composition, as shown by the nearly constant percentages of Fe as total Fe_2O_3. Table 14 expresses the same information in the form of norms. The secondary Fe_2O_3–FeO relation described above, here causes the progressive increase in hm and the decrease in mt with age.

TABLE 13.—*Averaged major oxide compositions, by chemical analysis, of volcanic rocks from the Almond Mountain Volcanics, Lava Mountains Andesite, and Quaternary andesite. The major oxide composition of one sample from the Bedrock Spring Formation and the average of two representative samples (26–2 and 41–34) of Atolia Quartz Monzonite are added for comparison*

[Data from tables 2, 4, 5, 8, and 10. All values are in weight percent. $\bar{x}$, average or mean $\left(\frac{\Sigma X}{N}\right)$; s, standard deviation $\left(\left[\frac{\Sigma(X-\bar{x})^2}{N-1}\right]^{1/2}\right)$; $s_{\bar{x}}$, standard error $\left(\frac{s}{(N)^{1/2}}\right)$; where X=percentage of oxide in individual sample and N=number of samples analyzed]

Oxide	Bedrock Spring Formation (1 analysis)	Almond Mountain Volcanics (9 analyses)			Lava Mountains Andesite (9 analyses)			Quaternary andesite (2 analyses)			Representative samples of Atolia Quartz Monzonite (2 analyses)
	$\bar{x}$	$\bar{x}$	s	$s_{\bar{x}}$	$\bar{x}$	s	$s_{\bar{x}}$	$\bar{x}$	s	$s_{\bar{x}}$	x
SiO_2	64.8	64.8	2.36	0.79	64.0	1.52	0.51	64.2	0.36	0.25	67.6
Al_2O_3	16.6	16.5	.29	.10	16.6	.26	.09	16.4	.22	.16	15.8
Fe_2O_3	1.4	1.8	.75	.25	2.9	1.01	.34	3.4	.28	.20	1.7
FeO	2.2	1.8	.71	.24	1.2	1.13	.38	.6	.28	.20	1.2
(Total Fe as Fe_2O_3)	(3.6)	(3.8)	(.56)	(.19)	(4.2)	(.57)	(.19)	(4.1)	[1](.07)	[1](.02)	(3.0)
MgO	2.0	1.9	.90	.30	2.1	.72	.24	1.2	.36	.25	.58
CaO	4.6	4.4	.58	.19	4.5	.57	.19	4.4	[1].07	[1].02	2.4
Na_2O	4.5	3.9	.24	.08	4.2	.24	.08	4.2	[1].07	[1].02	3.9
K_2O	2.0	2.6	.26	.09	2.5	.20	.07	2.6	[1].07	[1].02	3.9
TiO_2	.58	.59	.084	.028	.65	.072	.024	.63	.014	.010	.48
P_2O_5	.20	.21	.042	.014	.26	.037	.012	.21	.014	.010	.16
MnO	.08	.05	.013	.004	.05	.016	.005	.04	[1].007	[1].002	.07
H_2O	1.2	2.0	.88	.29	1.1	.55	.18	2.2	.10	.07	1.1
CO_2	.27	.05			.05?			.1	.10	.07	1.0

[1] Calculation assumes maximum possible difference between analyses before rounding last significant figure.

TABLE 14.—*Averaged normative compositions of volcanic rocks from the Bedrock Spring Formation, Almond Mountain Volcanics, Lava Mountains Andesite, and Quaternary andesite. The average of two representative samples (26–2 and 41–34) of Atolia Quartz Monzonite are added for comparison*

[All values are weight percents]

Norm (C.I.P.W.)	Bedrock Spring Formation (1 sample)	Almond Mountain Volcanics (9 samples)	Lava Mountains Andesite (9 samples)	Quaternary andesite (2 samples)	Representative samples of Atolia Quartz Monzonite (2 samples)
Q	18.2	20.0	18.2	19.1	24.5
C	0	.1	<.1	0	1.4
or	11.6	15.6	14.4	15.6	23.0
ab	38.2	32.7	35.4	35.6	33.0
an	19.2	19.7	19.1	18.2	9.9
di	2.9	1.2	1.8	2.7	0
hy	5.1	5.3	5.1	1.9	2.1
mt	2.1	2.3	1.5	.2	1.7
il	1.2	1.2	.9	1.0	1.0
hm	0	.2	1.8	3.4	.6
tn	0	0	.4	.2	0
ru	0	0	<.1	0	0
ap	.3	.4	.3	.3	.3

The time that elapsed between deposition of the three major volcanic formations was probably appreciable, and any significant changes that took place continuously in deep magma chambers should be represented by significant sequential changes in the composition of the extruded rocks. Figure 32 graphically compares the averaged data listed in table 13 for these formations, and shows the 50-, 75-, and 90-percent confidence limits of these averages. For three components, the averaged percentages in successive units are very similar; the SiO_2 values differ by only 0.5 percent, the Al_2O_3 values by 0.2 percent, and the CaO values by 0.1 percent. Testing these slight differences (Arkin and Colton, 1950, p. 127) shows that there is less than a 50-percent chance that this relation between averages would be confirmed by additional analyses. The confidence limits do show, however, that there is a greater than 75-percent chance that the true average values for SiO_2 in these formations would not be separated by more than 2 percent, the true values for Al_2O_3 by more than 0.8 percent, and the true values for CaO by more than 0.6 percent. Petrogenetic mechanisms requiring a larger spread in the average percentages of these three components are unlikely and can be disregarded.

For the remaining components, one or both of the averaged values differs appreciably from the unit above or below it. The trends toward lower percentages of Na_2O and TiO_2 in the Lava Mountains Andesite than in the Almond Mountain Volcanics, as indicated by figure 31, are supported by these averaged data, but they do not continue upward into the Quaternary andesite. Other compositional differences between successive formations are also indicated by figure 32, and for some, chances of confirmation by additional sampling are as great as 95 percent. The trends indicated by them are not continued by the third formation in the sequence, though, and for this reason the differences are not attributed to sequential changes in the deep-seated magma. They are regarded instead as the result of either random differences in these magmas or changes that took place in the process of transporting the magma to the surface.

Figure 33 shows in stratigraphic order the minor-element content of rocks in the stratigraphic sequences

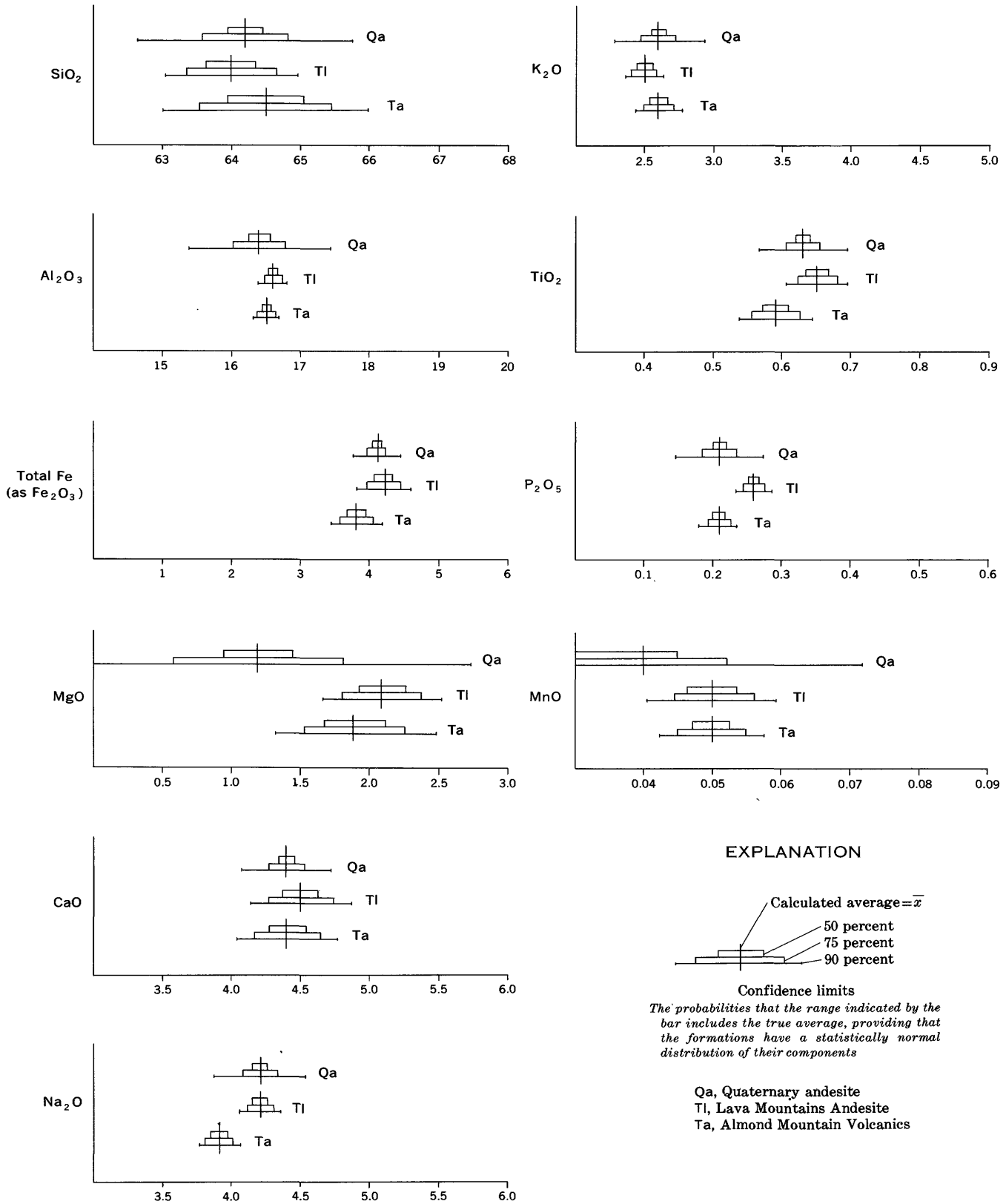

FIGURE 32.—Diagram comparing calculated averages and confidence limits of major components of the Almond Mountain Volcanics, Lava Mountains Andesite, and Quaternary andesite. Data, expressed in weight percent, from table 13. Confidence limits calculated by the t-distribution method (Bennett and Franklin, 1954, p. 153–157). For the total Fe as Fe_2O_3, CaO, Na_2O, K_2O, and MnO in the Quaternary andesite, which have standard deviations and errors of zero in table 13, the confidence limits shown assume the maximum possible spread between the percentages prior to being rounded off.

TABLE 15.—*Averaged minor element compositions of volcanic rocks from the Almond Mountain Volcanics, Lava Mountains Andesite, and Quaternary andesite. Minor element composition of one sample from the Bedrock Spring Formation added for comparison*

[Data from tables 4, 5, 8, and 10. All values are parts per million. $\bar{x}$, average or mean $\left(\frac{\Sigma X}{N}\right)$; s, standard deviation $\left[\frac{\Sigma(X-\bar{x})^2}{N-1}\right]^{1/2}$; $s_{\bar{x}}$, standard error $\frac{s}{(N)^{1/2}}$; where X= parts per million of element in individual sample, N = number or rock samples analyzed]

Minor element	Bedrock Spring Formation (1 sample)	Almond Mountain Volcanics (9 samples)			Lava Mountains Andesite (9 samples)			Quaternary Andesite (2 samples)		
	$\bar{x}$	$\bar{x}$	s	$s_{\bar{x}}$	$\bar{x}$	s	$s_{\bar{x}}$	$\bar{x}$	s	$s_{\bar{x}}$
B	30	34	12.4	4.1	29	9.3	3.1	7	9.2	6.5
Ba	2,400	1,780	386	129	1,820	217	72	2,250	71	50
Be								<1		
Co	40	37	13.2	4.4	53	20.6	6.9	22	2.8	2.0
Cr	60?	56	29.6	9.9	57	17.9	6.0	45	[1].7	[1].5
Cu	10	17	10.3	3.4	20	7.1	2.4	12	8.5	6.0
Ga	10	12	4.2	1.4	13	5.0	1.7	12	[1].7	[1].5
Li	19	20	10.6	3.5	22	12.5	4.2	38	8.0	5.6
Ni	20	31	23.2	7.7	40	18.0	6.0	40	[1].7	[1].5
Pb	20	12	4.2	1.4	11	3.4	1.1	11	1.4	1.0
Rb	30	53	10.0	3.3	43	17.3	5.6	40	[1].7	[1].5
Sc	10	5	3.1	1.0	6	1.7	.6	8	2.2	1.6
Sr	1,600	1,400	403	134	1,500	300	100	1,600	283	200
V	70	53	17.3	5.8	64	13.3	4.4	43	9.9	7.0
Y	10	6	2.3	.8	7	2.6	.9	8.2	.3	.2
Yb	1	1	[1].05	[1].02	<1			<1		
Zr	130	107	21.9	7.3	105	13.3	4.4	112	25.5	18.0

[1] Calculation assumes maximum possible difference between analyses before rounding last significant figure.

illustrated in figure 31. The section plotted in the upper part of the illustration indicates a statistical upward decrease in the quantity of B, and an upward increase in the quantities of Co, Cr, Ga, Ni, Pb, Sc, Sr, V, and possibly in Ba, Cu, and Y. The section plotted in figure 33*B* shows a decrease in B, Co, and Cr, and an increase in Ba and Cu. The changes in B, Ba, and Cu are similar in both sections. As in figure 31, though, the differences between successive samples commonly exceed the total range of the inferred trend. The differences indicated must thus be compared with averages representing larger numbers of samples from more widespread areas.

Table 15 lists the averaged minor-element contents (in parts per million) of the three most widespread volcanic formations. The standard deviations and standard errors are also listed. For comparison, the single analysis of volcanic rock from the Bedrock Spring Formation is also added. As for the major elements, the differences between successive formations are mostly small.

Figure 34 compares graphically the averaged data listed in table 15, and shows the 50-, 75-, and 90-percent confidence limits of these averages. The small differences between the averages for Ga, Ni, Pb, Sr, Y, and Zr have less than a 50-percent chance of being confirmed by additional analyses, so are not significant. The differences between average quantities of B, Ba, Co, Cr, Cu, Li, Sc, and V in the Lava Mountains Andesite and overlying Quaternary andesite have chances ranging for 50 to 98 percent of being confirmed; the differences between average quantities of B, Co, Rb, and V in the Almond Mountain Volcanics and overlying Lava Mountains Andesite have similar chances of being confirmed. The significant differences between Co and V averages indicate a trend that reverses with time, so are not indicative of sequential changes in the magma chamber. The consistently indicated decreases of B in rocks of the three successive formations have 50- and 75-percent chances of being confirmed by more analyses, and this supports the decrease suggested by the data plotted in figure 33. As B is normally concentrated in rocks formed late in the crystallization sequence, this decrease in progressively younger rocks is anomalous. It may reflect loss of B in a volatile compound contained in the gases lost during the explosive eruptions that characterized the early stages of the volcanic sequence.

VOLCANIC PETROGENESIS

The geologic characteristic of the volcanic rocks in the Lava Mountains help outline the processes that formed them. Their lithologic and stratigraphic characteristics, described in the section on "Stratigraphy," reflect processes that contributed to the escape and travel of the magma from its chamber to the surface. Their petrographic, modal, and chemical characteristics, described in the sections on "Petrography" and "Petrochemistry," reflect differentiation and crystal-

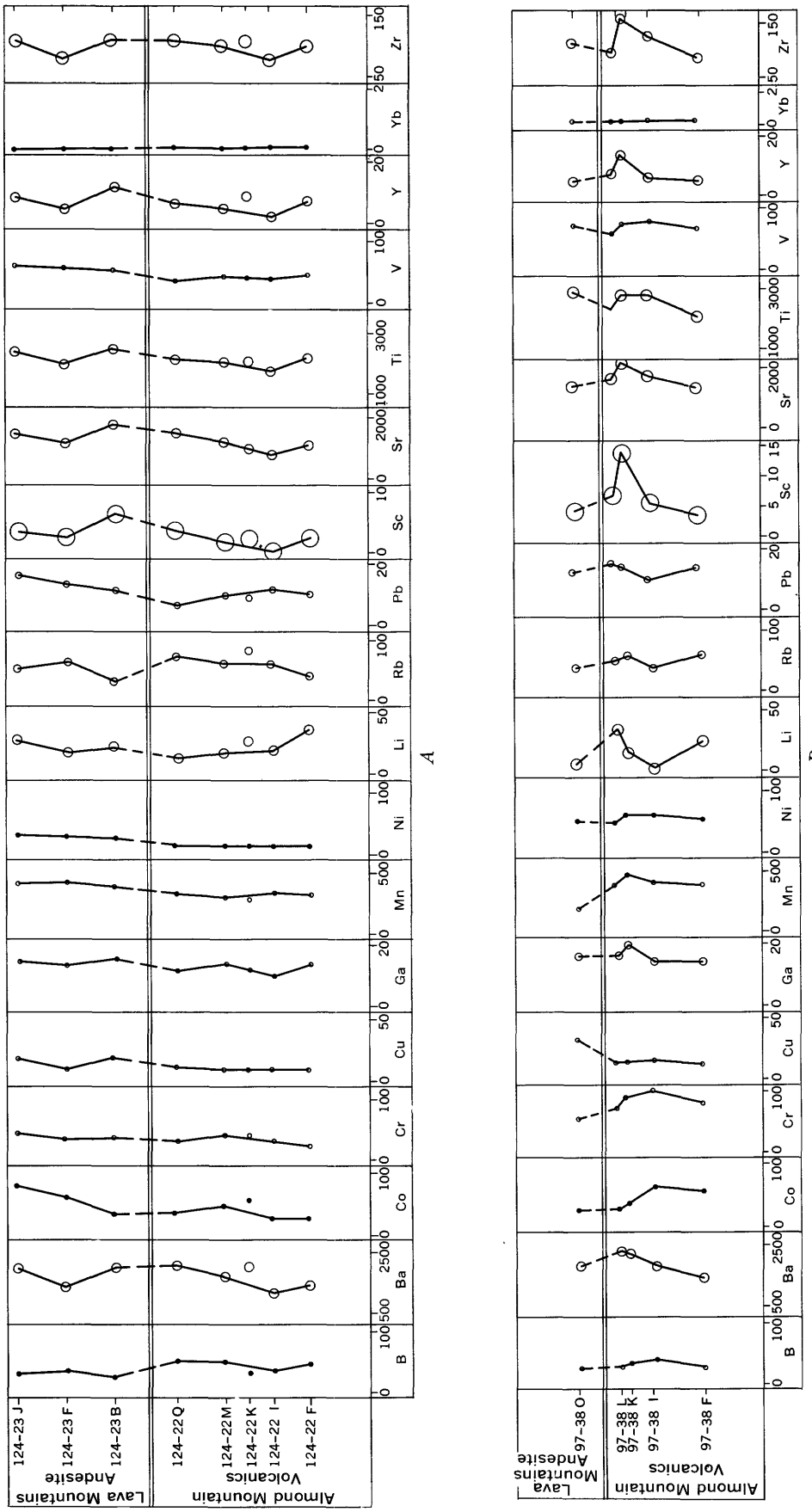

FIGURE 33.—Diagram showing variation in the amounts of minor elements in superposed rocks from the Almond Mountain Volcanics and Lava Mountains Andesite. The location of samples is described in table 21. The radii of the circles represent the average analytical errors calculated in table 18. Data from tables 5 and 8; all values in parts per million. *A*, samples are from the type section of the Almond Mountain Volcanics and from the west side of Almond Mountain. The stratigraphic position of the lower five samples is shown in fig. 11. Sample 124–22K is from a Lava Mountains Andesite sill in the Almond Mountain Volcanics. *B*, samples from 1 mile north of Dome Mountain.

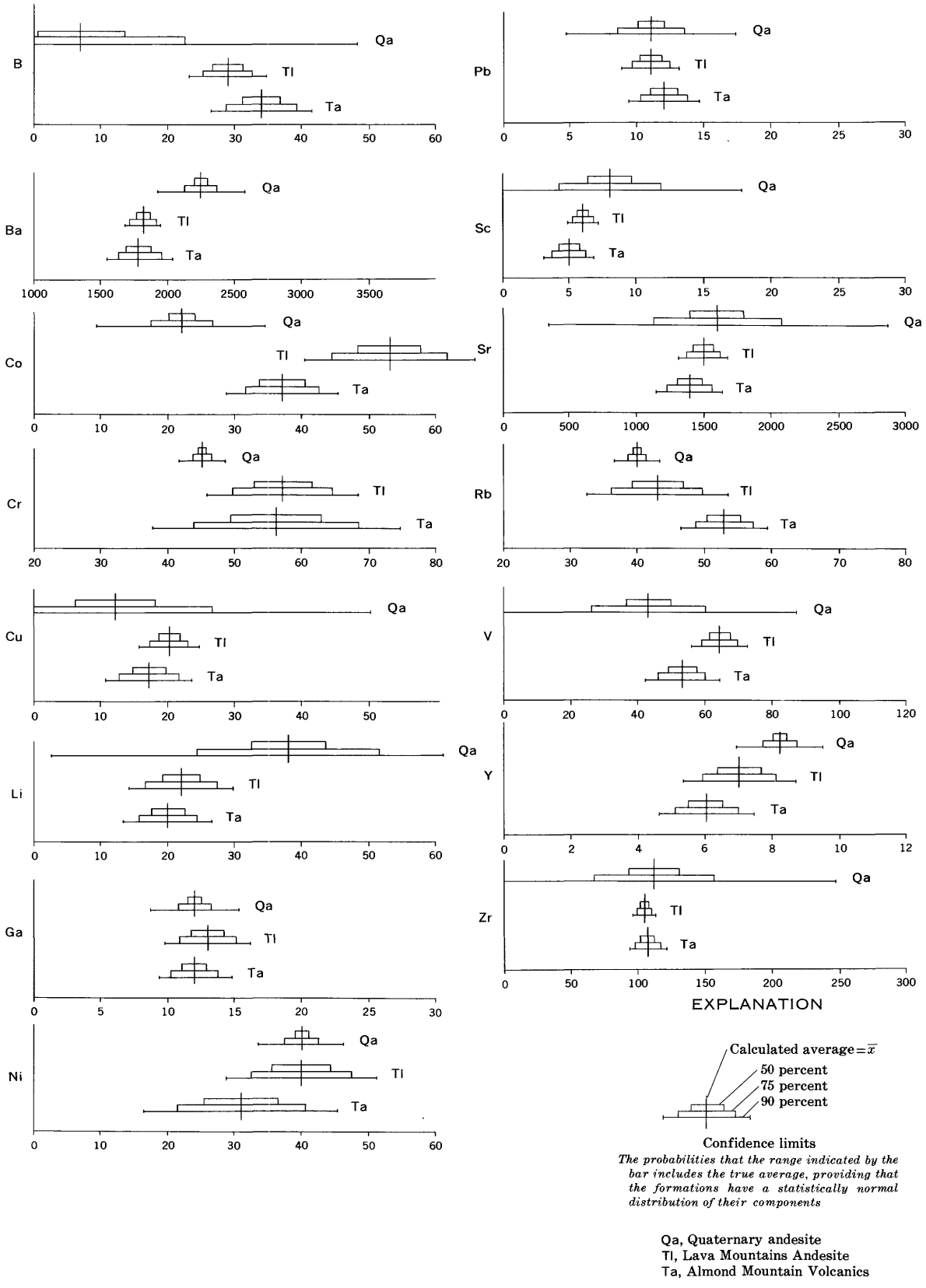

FIGURE 34.—Diagram comparing calculated averages and their confidence limits of minor elements in the Almond Mountain Volcanics, Lava Mountains Andesite, and Quaternary andesite. Data, expressed in parts per million, from table 15. Confidence limits calculated by the t-distribution method (Bennett and Franklin, 1954, p. 153–157).

lization processes that took place previously in the magma chamber.

MECHANICS OF ERUPTION

Some of the mechanisms that contributed to the escape and travel of magma from its chamber to the surface are inferred from lithologic and stratigraphic evidence. This evidence indicates the following general progression in time. Most of the early volcanic activity was characterized by sporadic eruptions of fine- to medium-grained fragmental material composed of a large number of volcanic rock types. Following this there were frequent eruptions of medium- to coarse-grained fragmental material composed entirely of one volcanic rock type. The final period of activity consisted of frequent eruptions of effusive material.

The change from sporadic to frequent eruptions is interpreted as the result of two unrelated processes. The first process was the continual faulting that took place during late Cenozoic time; this contributed to an increased frequency of eruption because each new fault added a line of crustal weakness available for magma to follow to the surface. The second process was the steady increase in the percentage of undissolved water in the magma crystallizing at depth, and this produced a marked increase in the eruptive pressures exerted on lines of weakness in the walls of the magma chamber.

The change from fine to coarse fragmental rocks took place during the deposition of the Almond Mountain Volcanics. This change is attributed to a progressive decrease in the depth at which magmas began to solidify and brecciate. Field evidence indicates that most of the lavas in the Almond Mountain Volcanics traveled to the surface by the same two conduits. As lavas and hydrothermal solutions transferred heat from depth to the walls of these conduits, the depth at which the rising lavas first solidified was presumably reduced. When these solidified lavas were brecciated and forced upward, further brecciation took place, and those materials that traveled a long distance in this conduit before reaching the surface were more extensively broken than those that were solidified and brecciated near the surface. The autobrecciation mechanism described by Curtis (1954, p. 469–471) may also have contributed to this progressive increase in fragment size. This mechanism depends on the vapor pressures confined in the rock at the time of subsurface solidification to create fracturing; as confined vapor pressures in rocks solidified at depth are presumably greater than near the surface, and as these pressures govern the violence of autobrecciation, material brecciated at depth is probably more comminuted than material brecciated nearer the surface.

The change from heterogeneous to homogeneous fragmental volcanic rocks is interpreted as a second result of this decrease in depth of solidification. Rocks brecciated at great depths traveled a long distance in the conduit before eruption, and fragments of other rocks lining the conduit were undoubtedly incorporated; material brecciated at shallow depths had a shorter distance to travel, and contamination was probably less. Material brecciated very near the surface might have traveled through a conduit lined with nothing but rocks formed from the same lava.

The change from fragmental to effusive material was probably the late stage result of two processes described above. One was the growing water vapor pressure in the magma chamber; this increased the force driving the magma upward, and thus increased the rate of flow of lava through the conduits. A second was the increased rock temperatures along faults that became conduits. In the early stages, these processes combined to reduce the depth of first solidification, and eventually they enabled magma rising in a conduit to reach the surface before solidifying.

These processes combined to create the following sequence. In Bedrock Spring Formation time, when relatively few faults had formed, and when eruptive pressures were low, few volcanic rocks reached the surface. The few that did solidified first at depth, but were subsequently brecciated and forced to the surface. The erupted products consisted of heterogeneous rock types and contained a high percentage of fine-grained material. Subsequently, faulting formed more conduits, hydrothermal activity continued to heat their walls, and eruptive pressures increased in the magma chamber. By Almond Mountain Volcanics time, enough lava passages had formed to permit frequent eruption of volcanic rocks, but the products were still fragmented because they solidified before reaching the surface. By Lava Mountains Andesite and Quaternary andesite times, almost all lavas that reached the surface were fluid.

PROCESSES OF CRYSTALLIZATION

The textures of these lavas indicate three stages of crystallization. The first stage produced the large phenocrysts of feldspar, quartz, biotite, and hornblende, and probably the small euhedral crystals of orthopyroxene, clinopyroxene, and opaque minerals. The second stage produced both the calcic rims on the large plagioclase crystals, and the small plagioclase crystals. The third stage produced the microcrystalline and glassy material of the groundmass. Deuteric activity subsequently altered the resulting mineralogy to that of the final rock.

The minerals formed during the first stage of crystallization indicate approximate limits for the temperature and water vapor pressure in the magma. Figure 35 shows diagrammatically the changes in the felsic composition of the liquid phase as this and subsequent crystallization stages progressed. This diagram is a two-dimensional representation of a tetrahedron, in which three of the faces have been "folded" downward into the plane of the Q-or-ab face which is in the plane of the diagram. Each face shows the stability relations between three of the four solid components (Q, or, ab, and an) in an environment in which all liquid phases are saturated with a fifth component, water vapor at 5,000 bars pressure. Also shown are isotherms for the system represented on each face.

Changes in the felsic composition of the liquid during crystallization are projected onto these faces. It must be noted, however, that changes in the composi-

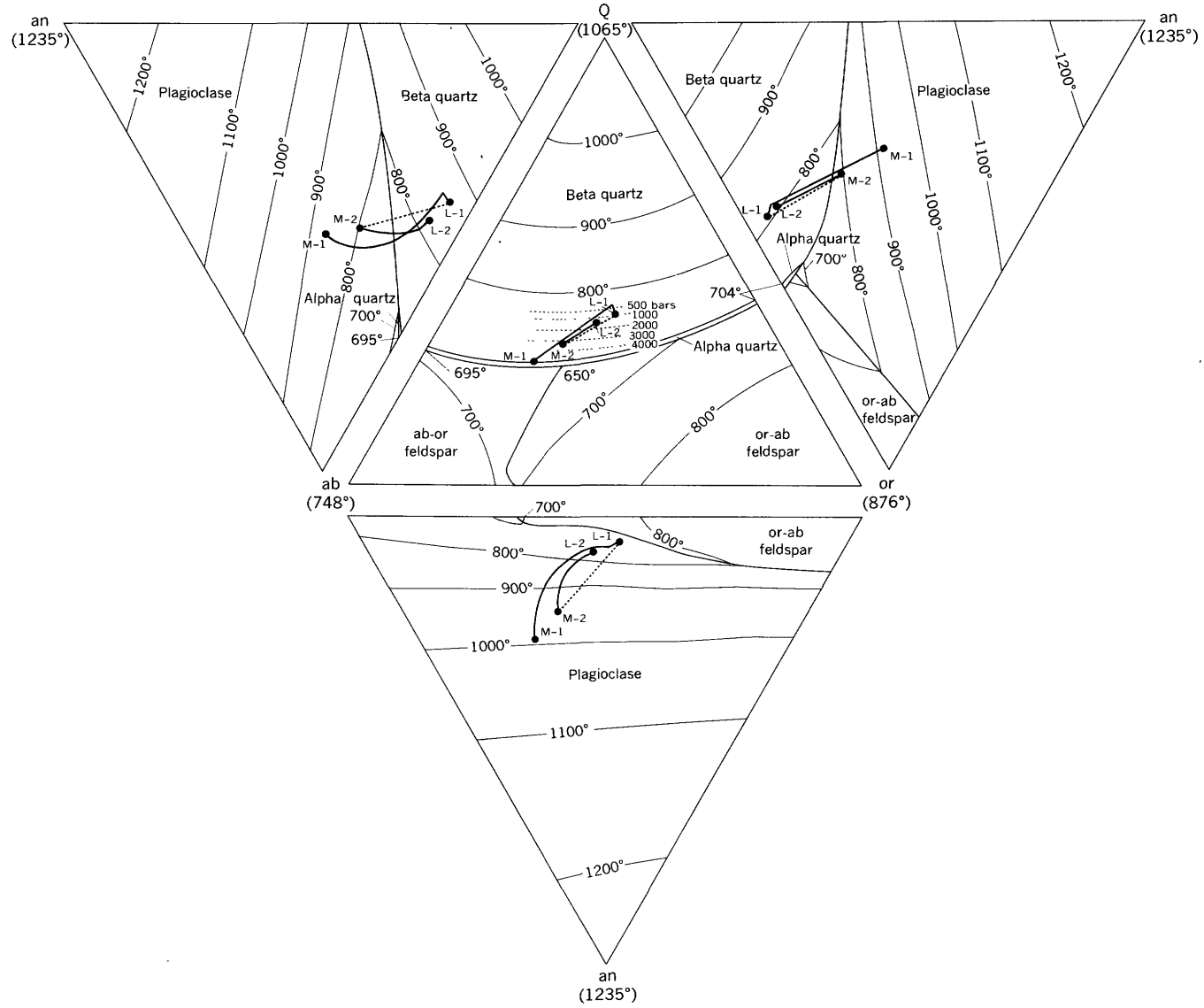

FIGURE 35.—Phase diagrams of the subsystems represented on the faces of the tetrahedron portraying the five-component system Q-or-ab-an-H_2O at 5,000 bars water vapor pressure. Also shown on the Q-or-ab-H_2O diagram are positions of the alpha quartz-alkali feldspar boundary at 4,000, 3,000, 2,000, 1,000, and 500 bars pressure. Phase data and isotherms (in degrees centigrade) compiled by Bateman and others (1963, p. 34) from published and unpublished sources. The progressive changes in the relative amounts of felsic components in this magma at four stages in its crystallization are projected onto the four-component diagrams. Symbols are as follows: M–1, approximate composition of original magma from which volcanic rocks in Bedrock Spring Formation were formed; L–1, approximate composition of liquid remaining after first generation of crystals formed; M–2, approximate composition of liquid in new magma from which volcanic rocks in the Almond Mountain Volcanics and younger units were formed; L–2, approximate composition of liquid remaining after second generation of crystals formed. The compositional change resulting from the addition of more liquid to the partly crystallized magma is shown by a dotted line between L–1 and M–2; compositional changes resulting from crystallization are shown by solid lines.

tion of this five-component liquid phase should be portrayed on a diagram having three dimensions. In this two-dimensional representation, the lines representing these changes will cross the phase boundaries and isotherms plotted on each tetrahedron face in a manner that would be impossible if only those three solid components were being considered. The reason all five components in the liquids must be considered even though only three of the solid phases are crystallized is that this crystallization brings about shifts in the relative amounts of all components remaining in the liquid.

In figure 35, the points and connecting lines representing the changes in the felsic composition of the liquid are somewhat diagrammatic. Point M–1 is the projection of the average composition of the felsic components in the volcanic rocks of the Lava Mountains (exclusive of the propylitized rocks and the late Pliocene(?) felsite). The position of point L–1 is dictated chiefly by the compositions of the crystallized feldspar and its equilibrium liquid which are, respectively, about An_{45} and An_{10}. Although these compositional estimates are based on phase data from two- and three-component melts, they probably are applicable to more complex systems; the relation between the liquidus and solidus of the ab-an system is changed very little by the addition of water vapor, and it is reasonable to assume that the addition of small percentages of other components will have a similarly small effect (compare Bowen, 1928, fig. 9, with Yoder and others, 1957, fig. 36). Point M–2, the new composition of the magma after adding more liquid with the composition of M–1, is of course on a line between L–1 and M–1, but its actual position along this line is hypothetical. Point L–2 is calculated by assuming that the average composition of the second generation of feldspar is about An_{50} and that these crystals formed in contact with a liquid having a composition of An_{15}.

Point M–1 in figure 35 approximates the relative quantities of the felsic components in the magma after differentiation from a mafic magma but before the first eruption. At 5,000 bars vapor pressure, and probably all other pressures below 5,000 bars, point M–1 lies in the plagioclase field of the five-component system. The line connecting point M–1 to point L–1 represents the changing composition of the magmatic liquid as the plagioclase megaphenocrysts and quartz of the first generation of crystals formed; the long segment of the line is a projection of these changes as feldspar crystallized alone, and the short segment is a projection of them as quartz and plagioclase precipitated together. The projected composition of the end point L–1 is far below the plagioclase-quartz boundary in both the Q-ab-an-H_2O and Q-or-an-H_2O systems at 5,000 bars of water vapor pressure. It was actually on this boundary in the magma, however, as shown by the relict crystals of euhedral quartz in the rocks. This discrepancy may be partly attributed to the assumptions used in constructing the diagram and to the effect of mafic ions in the melt, but it is attributed primarily to the existence of a lower vapor pressure in the magma at the time of crystallization. The Q-or-ab-H_2O diagram shows how the position of the alpha quartz-alkali feldspar boundary shifts with the changes in vapor pressure, and the Q-ab-an-H_2O and Q-or-an-H_2O diagrams show how the plagioclase-quartz boundary approaches the projection of point L–1 with this shift. Thus, the lower the vapor pressure, the closer this phase boundary is to point L–1, and the larger the difference between the volume percentages of plagioclase and quartz precipitated as the liquid phase changes composition from point M–1 to L–1.

Modal analyses of the volcanic rocks from the Lava Mountains show that at the end of the first stage of crystallization, the volume percentage of plagioclase was probably 10 to 20 times that of quartz, and in figure 35, the two segments of the line between M–1 and L–1 have been plotted so as to have about this proportion. The point at which the two segments join is projected onto the Q-ab-or-H_2O system about at the position of the alkali feldspar-quartz boundary at 500 bars, and this is theoretically the point at which the composition of the melt first reached the quartz-plagioclase boundary. Within the limits of accuracy afforded by these projections of experimental data, this relation shows that the water vapor pressure was probably 500 bars or a little more at the time of crystallization. If the vapor pressure had been much below 500 bars, the second phase formed would have been feldspar instead of quartz. Load pressures of 500 bars are found at depths a little below 1 mile.

Figure 35 shows isotherms of the four subsystems at 5,000 bars water vapor pressure. Phase data for the dry systems show that temperatures at comparable points are mostly 300°C to 400°C higher (Bowen, 1928, fig. 9; Schairer, 1950, p. 514), but at 500 bars vapor pressure, these temperatures might be raised only 200°C to 300°C. Projecting such isotherms into the three-dimensional diagram would show point L–1, on the quartz-plagioclase boundary, to lie at some temperature between 950°C and 1,150° C. The other components that were in the magma but are not represented in figure 35 would have reduced the crystallization temperatures indicated by this approximation, perhaps by several hundred degrees.

The temperatures in the magma prior to crystallization, represented by point M–1, would have been several hundred degrees higher.

The stability fields of the mafic minerals formed at this time are not represented in figure 35, but apparently they all exist within the proposed range of pressure and temperature. Not enough is known of the clinopyroxene in these rocks to compare them with the experimental evidence, and applicable phase data for hornblende and oxyhornblende are not available. Phase data for biotite and orthopyroxene are applicable, however, and they do not conflict with the above conclusion.

The phenocrysts of biotite in these rocks probably approach the composition of annite, the Fe^{+2} end member of the biotite series. Phase diagrams for pure annite (Eugster, 1957, fig. 14; Eugster and Wones, 1962, figs. 4, 6, 8) show that it may form at vapor pressures near 500 bars at temperatures ranging from at least 400°C to about 750°C. The biotite in the volcanic rocks described here probably contains some Mg and other mafic cations, and the data compiled by Heinrich (1946) suggest that the stability fields of biotites containing Mg extend to higher temperatures.

The small phenocrysts of orthopyroxene in these volcanic rocks have compositions intermediate between enstatite and hypersthene. Pure enstatite forms at water vapor pressures and temperatures above about 350 bars and 700°C (Bowen and Tuttle, 1949, p. 442). Phase data for the dry system show that crystals composed of equal percentages of enstatite and hypersthene are stable at temperatures as much as 50°C below the limit for pure enstatite (Bowen and Schairer, 1935, fig. 8). Other components in solution will further lower the minimum temperature of this stability field, so the intermediate orthopyroxene in these rocks is a likely phase within all parts of the pressure and temperature range inferred for this step in crystallization.

The second stage of crystallization formed the plagioclase microphenocrysts and the calcic rims on the megaphenocrysts. Possibly some of the small crystals of orthopyroxene, clinopyroxene, and opaque minerals also formed at this time, but the evidence is inconclusive. The volcanic rocks in the Bedrock Spring Formation do not have a distinct second generation of microphenocrysts, and calcic rims are absent. As all subsequent volcanic rocks do have these petrographic characteristics, it is evident that they resulted from events that occurred after the deposition of the Bedrock Spring Formation but before that of the Almond Mountain Volcanics.

Certain petrographic relations in the volcanic rocks younger than the Bedrock Spring Formation suggest that also within this same interval of time, but prior to this stage of crystallization, some new magma of similar bulk composition but relatively uncrystallized was added to the magma chamber. The volume of new magma added was enough to first raise the An content of the liquid 5 to 10 percent, and to then allow plagioclase to form calcic rims and microphenocrysts constituting 10 to 15 percent of the rock without reaching the stability field of quartz or alkali feldspar. The composition of the liquid portion of this new mixture is indicated diagrammatically by point M–2 in figure 35. A similar composition for this new magma is indicated by comparison of the chemical composition of rocks erupted before and after the mixing. Figures 26 and 29 show that relative to the sample of rock from the Bedrock Spring Formation (formed before magma mixing), later rocks have both similar percentages of SiO_2 and similar ratios of SiO_2 to most major and minor elements. In the younger rocks formed from mixed magmas, the percentages of MgO, Na_2O, MnO, Ba, Sc, V, Y, Yb, and Zr may be slightly lower, and the percentages of K_2O and Cu may be slightly higher, but the differences are not great.

The petrographic relations attributed to this magma mixing are: (a) the calcic rims on the resorbed megaphenocrysts, (b) the composition of the microphenocrysts (which is probably a little more calcic than the average composition of the megaphenocrysts formed earlier), and (c) the resorbed euhedral quartz crystals. The magma already in the chamber was partially crystallized, so introducing a second magma of similar bulk composition but mostly liquid raised the temperature in the magma chamber and made the composition of the liquid portion more calcic relative to L–1. As a result, quartz and the last-formed plagioclase were no longer stable phases; the crystals of quartz developed reaction rims of clinopyroxene, and the plagioclase megaphenocrysts were partially resorbed. Subsequent cooling of this mixture then produced calcic rims on the partially resorbed megaphenocrysts, plus the small euhedral crystals of similar composition that are now distinguished as microphenocrysts. New crystals of quartz were not formed.

Comparing major and minor element analyses of formations deposited after new magma was added to the chamber shows that diffusion and convection were tending to homogenize the magma within the chamber. Rock samples for these analyses were collected from separated areas, and they probably represent magma samples derived from different parts of the chamber. Differences between them presumably indicate compositional variations at depth. A small part of this variation may have resulted from differences between the

original and introduced magmas, but most was inherited from the differentiation process that created the magmas originally. Variations within groups of samples can be expressed as coefficients of variation—the smaller the coefficient, the less variation there is between samples included in the group. The coefficients of variation calculated from analyses of the Almond Mountain Volcanics, Lava Mountains Andesite, and Quaternary andesite are listed in table 16.

A notable reduction in the variation within these three successive formations is indicated. The coefficients for SiO_2, Al_2O_3, Fe_2O_3, total Fe, MgO, CaO, Na_2O, K_2O, TiO_2, and P_2O_5 become progressively smaller in younger samples. The coefficient for MnO shows a reversal, but it has a distinctly small value for the youngest unit. The variations in CO_2 and H_2O percentages are unsystematic because they chiefly reflect alteration differences. The coefficients of variation

TABLE 16.—*Variations in major-element and minor-element compositions of volcanic rocks in the Almond Mountain Volcanics, Lava Mountains Andesite, and Quaternary andesite*

[Coefficient of variation = $\frac{\text{standard deviation} \times 100}{\text{arithmetic mean}}$. Based on data in tables 13 and 15]

Coefficient of variation in major element composition

	SiO_2	Al_2O_3	Total Fe as Fe_2O_3	MgO	CaO	Na_2O	K_2O	TiO_2	P_2O_5	MnO	H_2O	CO_2
Quaternary andesite	0. 6	1. 3	1. 7	30	1. 6	1. 7	2. 7	2. 2	6. 7	1. 8	4. 5	100
Lava Mountains Andesite	2. 4	1. 6	14	34	13	5. 7	8	11	14	32	50	------
Almond Mountain Volcanics	3. 6	1. 8	15	47	13	6. 2	10	14	20	26	44	------

Coefficient of variation in minor element composition

	B	Ba	Co	Cr	Cu	Ga	Li	Ni	Pb	Rb	Sc	Sr	V	Y	Yb	Zr
Quaternary andesite	132	3. 1	13	1. 6	71	5. 8	21	1. 8	13	1. 8	28	18	23	3. 4	------	23
Lava Mountains Andesite	32	12	39	31	35	39	57	45	30	40	29	20	21	38	<50	13
Almond Mountain Volcanics	36	22	36	53	61	35	53	75	35	19	61	29	33	38	------	20

for about half of the minor elements also become progressively smaller in younger samples, although they are inconsistent for the others. Some of these inconsistencies exist because analyses of minor elements are not as reproducible as those of major elements.

The approximate composition of the liquid portion of the magma at the close of this second stage of crystallization is represented by point L–2 in figure 35. Calcic rims and microphenocrysts of plagioclase, which constitute 10 to 15 percent of the rock, were formed during the crystallization represented by the line between points M–2 and L–2. Quartz was not formed, so point L–2 is in the plagioclase field. With only one crystal phase formed, it is not possible to place close limits on vapor pressure and temperature conditions. However, the absence of quartz and alkali feldspar means that when this stage of crystallization ended, the temperature was probably above that of point L–1.

The chemical composition of the upper Pliocene(?) felsite, shown as point *pf* in figure 28, is fairly close to the crystallization path between M–2 and L–2. The felsite may represent a pocket of magmatic liquid that was almost entirely separated from its crystals during crystallization and subsequently was erupted.

The third stage of crystallization took place as the lava approached the surface or was extruded. The rate of cooling was accelerated, and the remaining solution solidified to form the cryptocrystalline and glassy groundmass. The chemical composition of this groundmass is approximated by point L–2 in figure 35. The mineral content of the groundmass, as indicated by X-ray diffraction, consists in most rocks of the same minerals that form larger identifiable crystals, plus cristobalite.

The cristobalite in these rocks is metastable. Its presence may mean that water vapor pressures were lower than those that prevailed during the first stage of crystallization, but it does not place useful limits on the temperatures. From a pure SiO_2 melt, stable cristobalite forms above 1,470°C; below that temperature, tridymite or quartz is the stable phase (Fenner, 1913). Experimental and thermodynamic evidence suggests that if tridymite is not formed, only quartz should form from a pure melt below about 1,000°C (Mosesman and Pitzer, 1941, table 8, fig. 3; Tuttle and England, 1955, fig. 1). The presence of other ions in solution, however, tends to lower the temperature range of this metastable phase boundary. For example, the addition of MgO and 1,000 to 2,000 bars of water vapor pressure to the SiO_2 system permits formation of metastable cristobalite at temperatures as low as 400°C (Bowen and Tuttle, 1949, p. 444). Curiously, high water-vapor pressures and large percentages of alkalis reportedly tend to discourage the crystallization of cristobalite in simple melts (Tuttle and England, 1955, fig. 1; Flörke, 1955), but petrographic evidence reported from many areas

shows that the other ions present in complex melts such as lavas reverse or overcome this tendency.

The third stage of crystallization presumably began at about the temperature at which the second stage of crystallization ceased. The presence of unaltered biotite and green hornblende in some of these rocks shows that it was below 850°C, as solidification temperatures much above would have altered the biotite to K-bearing minerals (Eugster, 1957, fig. 14).

After the rocks solidified, most of them were partially altered by deuteric activity. Although there may have been some reheating of the extruded rocks as oxidation occurred, alteration generally resulted from the large increase in the percentage of water. In most extrusive rocks, biotite and hornblende crystals are partly dehydrated and replaced by fine-grained iron oxides; in those rocks more strongly altered, the orthopyroxene and clinopyroxene crystals are partially changed to fine-grained iron oxides and bastite. In many shallow intrusive rocks, the hornblende and biotite crystals are relatively fresh, though the pyroxene crystals are generally as altered as those in extrusive rocks. Volcanic rocks from both environments generally contain plagioclase crystals that were not affected by deuretic alteration.

SOURCE OF MAGMA

The sources of magmas that reach the earth's surface as volcanic melts have long been a favorite topic of speculation (for example, see Bowen, 1928; Kennedy, 1933, p. 256; Kennedy and Anderson, 1938; Larsen and others, 1938b, p. 429; Tilley, 1950, p. 59; Wilcox, 1954, p. 326–347; Powers, 1955, p. 95–101; Larsen and Cross, 1956, p. 269–297). Most of the proposed hypotheses derive a relatively homogeneous magma by one of the following mechanisms:

1. Tapping a source of primary basaltic magma.
2. Tapping a source of primary basaltic magma that has undergone contamination by other rocks or magmas, generally more felsic.
3. Partially remelting solidified basaltic or peridotitic rocks.
4. Totally remelting solidified basaltic or peridotitic rocks.
5. Partially remelting crustal granitic rocks.
6. Totally remelting crustal granitic rocks.

Starting from this magma, most hypotheses then either introduce diversity into the material by some combination of crystal settling, wall-rock assimilation, and magma mixing, or retain homogeneity by diffusion and convection.

The volcanic rocks in the Lava Mountains area have a very small range of chemical compositions even though they represent samples removed from the magma chamber over a span of several million years. Apparently, they formed from a magma that was generated before Bedrock Spring time, and that maintained a constant average composition thereafter.

The interrelations between components illustrated in figures 26, 27, and 29 indicate differentiation as the cause of the small compositional spread that is present, but the increase in homogeneity of progressively younger rocks illustrated in table 16 shows that this differentiation was not taking place during the span of time these rocks were being erupted. It is more likely that this compositional spread was entirely created by differentiation prior to the first eruption, and that it is still detectable only because the processes of homogenization had not yet obliterated it by the time the first of the magmas came to the surface.

The original magma was probably produced by differentiation of a more mafic magma such as basalt, with the mafic differentiate retained in the magma chamber. This mechanism is preferred because in these partially crystallized volcanic rocks, only elements that participate in the minerals that have actually formed show convincing interrelations. Plagioclase and mafic minerals have crystallized in these rocks, and the percentages of all major elements (and most minor elements) concentrated in them vary systematically with SiO_2 so that variation diagrams such as shown in figures 26 and 29 indicate trends that slope in one direction or the other. K-feldspars, however, have not crystallized in these rocks, and the percentages of elements concentrated in them (K, Pb, Rb, Sr, and possibly Cs) do not vary in a manner related to the percentage of SiO_2 or other components; in figures 26 and 29, these elements indicate trends that are horizontal. Sloping trends in variation diagrams are normally attributed to sorting of elements that takes place as the crystals are formed, and in a wholly crystallized rock, if some elements display these characteristics, presumably all should. It thus seems unlikely that the material composing the volcanic rocks in the Lava Mountains has ever been crystallized to a greater degree.

This eliminates the likelihood that the original magma was formed by partial or total remelting of a fully crystallized rock that contains K-feldspar, or by mixing of a mafic magma with appreciable quantities of such rock. The relatively felsic composition of these rocks eliminates the possibility of producing this magma by partial or total remelting of peridotite. By elimination, differentiation of a mafic magma such as basalt becomes the most probable source, although evidence is not available as to whether this basalt was primary or remelted.

REFERENCES CITED

Allen, C. R., 1957, San Andreas fault zone in San Gorgonio Pass, southern California: Geol. Soc. America Bull., v. 68, no. 3, p. 315–349.

Anderson, C. A., 1936, Volcanic history of the Clear Lake area, California: Geol. Soc. America Bull., v. 47, no. 5, p. 629–664.

——— 1941, Volcanoes of the Medicine Lake highland, California: California Univ., Dept. Geol. Sci. Bull., v. 25, no. 7, p. 347–422.

Anderson, E. M., 1951, The dynamics of faulting and dyke formation with application to Britain: 2d ed., Edinburgh and London, Oliver and Boyd, 206 p.

Arkin, Herbert, and Colton, R. R., 1950, Outline of statistical methods: 4th ed., New York, Barnes & Noble, 271 p.

Axelrod, D. I., 1940, A record of *Lyonothamnus* in Death Valley, California: Jour. Geology, v. 48, no. 5, p. 526–531.

Baker, C. L., 1912, Physiography and structure of the western El Paso Range and the southern Sierra Nevada: California Univ. Dept. Geology Bull., v. 7, no. 6, p. 117–142.

Bateman, P. C., Clark, L. D., Huber, N. K., Moore, J. G., and Rinehart, C. D., 1963, The Sierra Nevada batholith—a synthesis of recent work across the central part: U.S. Geol. Survey Prof. Paper 414–D, p. D1–D46.

Belowsky, Max, 1891, Ueber die Aenderungen, welche die optischen Verhältnisse der gemeinen Hornblende biem Glühen erfahren: Neues Jahrb, Min., Bd. 1, p. 291–292.

Bennett, C. A., and Franklin, N. L., 1954, Statistical analysis in chemistry and the chemical industry: New York, John Wiley & Sons, 724 p.

Bowen, N. L., 1928, The evolution of the igneous rocks: Princeton, N.J., Princeton Univ. Press, 334 p., 82 figs.

Bowen, N. L., and Schairer, J. F., 1935, The system MgO–FeO–SiO_2: Am. Jour. Sci., 5th ser., v. 29, no. 170, p. 151–217.

Bowen, N. L., and Tuttle, O. F., 1949, The system MgO–SiO_2–H_2O: Geol. Soc. America Bull., v. 60, no. 3, p. 439–460.

Chayes, Felix, 1949, A simple point counter for thin section anlaysis: Am. Mineralogist, v. 34, nos. 1–2, p. 1–11.

Cloos, Ernst, 1955, Experimental analysis of fracture patterns: Geol. Soc. America Bull., v. 66, p. 241–256.

Coats, R. R., 1936, Intrusive domes of the Washoe district, Nevada: California Univ., Dept. Geol. Sci. Bull., v. 24, no. 4, p. 71–84.

——— 1940, Propylitization and related types of alteration on the Comstock Lode: Econ. Geology, v. 35, no. 1, p. 1–16.

Curry, H. D., 1941, Mammalian and avian ichnites in Death Valley [abs.]: Geol. Soc. America Bull., v. 52, no. 12, pt. 2, p. 1979.

Curtis, G. H., 1954, Mode of origin of pyroclastic debris in the Mehrten formation of the Sierra Nevada: California Univ., Dept. Geol. Sci. Bull., v. 29, no. 9, p. 453–502.

Dibblee, T. W., Jr., 1952, Geology of the Saltdale quadrangle, Kern County, California: California Div. Mines Bull. 160, p. 7–43.

——— 1958, Tertiary stratigraphic units of western Mojave Desert, California: Am. Assoc. Petroleum Geologists Bull., v. 42, no. 1, p. 135–144.

——— 1961, Evidence of strike-slip movement on northwest-trending faults in Mojave Desert, California: Art. 82 *in* U.S. Geol. Survey Prof. Paper 424–B, p. B197–B199.

——— 1964, Geology of the Opal Mountain and Fremont Peak quadrangles, California: California Div. Mines Bull. (In press.)

Eugster, H. P., 1956, Stability of hydrous iron silicates, *in* Geophysical Laboratory [report]: Carnegie Inst. Washington Yearbook 55, 1955–56, p. 158–161.

——— 1957, Stability of annite, *in* Geophysical Laboratory [report]: Carnegie Inst. Washington Yearbook 56,' 1956–57, p. 161–164.

Eugster, H. P., and Wones, D. R., 1962, Stability relations of the ferruginous biotite, annite: Jour. Petrology, v. 3, no. 1, p. 82–125.

Fairbairn, H. W., and others, 1951, A cooperative investigation of precision and accuracy in chemical, spectrochemical, and modal analysis of silicate rocks: U.S. Geol. Survey Bull. 980, 54 p.

Fenner, C. N., 1913, The stability relations of the silica minerals: Am. Jour. Sci., 4th ser., v. 36, p. 331–384.

Flörke, O. W., 1955, Structural anomalies in tridymite and cristobalite. Berichte der Deutschen Keramischen Gesellschafte, v. 32, no. 12, p. 369–381, reviewed *by* Eitel, W., 1957, Ceramic Bull., v. 36, no. 4, p. 142–148.

Fuller, R. E., 1931, The geomorphology and volcanic sequence of Steens Mountain in southeastern Oregon: Washington Univ. Geology Pub., v. 3, no. 1, p. 1–130.

Gale, H. S., 1914, Salines in Owens, Searles, and Panamint basins, southeastern California: U.S. Geol. Survey Bull. 580–L, p. 251–323.

George, W. O., 1924, The relation of the physical properties of natural glasses to their chemical composition: Jour. Geology, v. 32, no. 5, p. 353–372.

Goddard, E. N., chm., and others, 1948, Rock-color chart: Washington, Natl. Research Council, 6 p.; repr. by Geol. Soc. America, 1951.

Graham, W. A. P., 1926, Notes on hornblende; variations in the chemical composition of hornblende from different types of igneous rocks: Am. Mineralogist, v. 11, no. 5, p. 118–123.

Griggs, David, and Handin, John, 1960, Observations on fracture and a hypothesis of earthquakes, *in* Griggs, D., and Handin, J., eds., Rock deformation: Geol. Soc. America Mem. 79, p. 347–364.

Grose, L. T., 1959, Structure and petrology of the northeast part of the Soda Mountains, San Bernardino County, California: Geol. Soc. America Bull., v. 70, no. 12, pt. 1, p. 1509–1547.

Heinrich, E. W., 1946, Studies in the mica group; the biotite phlogopite series: Am. Jour. Sci., v. 244, no. 12, p. 836–848.

Henshaw, P. C., 1939, A Tertiary mammalian fauna from the Avawatz Mountains, San Bernardino County, California: Carnegie Inst. Washington Pub. 514, p. 1–30.

Hess, F. L., 1910, Gold mining in the Randsburg quadrangle, California: U.S. Geol. Survey Bull. 430–A, p. 23–47.

Hewett, D. F., 1954a, General geology of the Mojave Desert region, California, [pt.] 1 *in* chap. 2 *of* Jahns, R. H., ed., Geology of southern California: California Div. Mines Bull. 170, p. 5–20.

——— 1954b, A fault map of the Mojave Desert region [California], [pt.] 2 *in* chap. 4 *of* Jahns, R. H., ed., Geology of southern California: California Div. Mines Bull. 170, p. 15–18, pl. 1.

——— 1955, Structural features of the Mojave Desert region [Calif.], *in* Poldervaart, Arie, ed., Crust of the earth—a symposium: Geol. Soc. America Spec. Paper 62, p. 377–390.

Hill, M. L., 1954, Tectonics of faulting in southern California, [pt.] 1 *in* chap. 4 *of* Jahns, R. H., ed., Geology of southern California: California Div. Mines Bull. 170, p. 5–13.

Hill, M. L., 1959, Dual classification of faults: Am. Assoc. Petroleum Geologists Bull., v. 43, no. 1, p. 217–221.

Hill, M. L., and Dibblee, T. W., Jr., 1953, San Andreas, Garlock, and Big Pine faults, California—a study of the character, history, and tectonic significance of their displacements: Geol. Soc. America Bull., v. 64, no. 4, p. 443–458.

Hulin, C. D., 1925, Geology and ore deposits of the Randsburg quadrangle, California: California Mining Bur. Bull. 95, 152 p., 8 figs. 31 pls.

Jaffe, H. W., Gottfried, David, Waring, C. L., and Worthing, H. W., 1959, Lead-alpha age determinations of accessory minerals of igneous rocks (1953–1957): U.S. Geol. Survey Bull. 1097-B, p. 65–148.

Jenkins, O. P., 1938, Geologic map of California: California Div. Mines, 6 sheets, scale 1: 500,000.

Jennings, C. W., Burnett, J. L., and Troxel, B. W., 1962, Geologic map of California, Olaf P. Jenkins edition, Trona sheet: California Div. Mines and Geology.

Kennedy, W. Q., 1933, Trends of differentiation in basaltic magmas: Am. Jour. Sci., 5th ser., v. 25, no. 147, p. 239–256.

Kennedy, W. Q., and Anderson, E. M., 1938, Crustal layers and the orgin of magmas: Bull. volcanol., ser. 2, v. 3, p. 23–82.

Kozu, S., and Yoshiki, B., 1927, The dissociation-temperature of brown hornblende and its rapid expansion at this temperature: Sendai, Japan, Tohuku Univ. Sci. Repts., 3d ser., v. 3, no. 2, p. 107–117.

——— 1929, Thermo-optic studies of anomite-basaltic hornblende-quartz-andesite in association with biotite-common hornblende-quartz-andesite, which together form the volcano Sambé in Japan: Sendai, Japan, Tohuku Univ. Sci. Repts., 3d ser., v. 3, no. 3, p. 177–193.

Kozu, S., Yoshiki, B., and Kani, K., 1927, Notes on the study of the transformation of common hornblende into basaltic hornblende at 750°C: Sendai, Japan, Tohuku Univ. Sci. Repts., 3d ser., v. 3, no. 2, p. 143–159.

Larsen, E. S., Jr., and Berman, Harry, 1934, The microscopic determination of nonopaque minerals: 2d ed., U.S. Geol. Survey Bull. 848, 266 p.

Larsen, E. S., Jr., and Cross, Whitman, 1956, Geology and petrology of the San Juan region, southwestern Colorado: U.S. Geol. Survey Prof. Paper 258, 303 p., 4 pls., 58 figs.

Larsen, E. S., Jr., Irving, John, Gonyer, F. A., and Larsen, E. S., 3d, 1937, Petrologic results of a study of the minerals from the Tertiary volcanic rocks of the San Juan region, Colorado, pt. II: Am. Mineralogist, v. 22, no. 8, p. 889–904, 6 figs.

——— 1938a, Petrologic results of a study of the minerals from the Teritary volcanic rocks of the San Juan region, Colorado, pt. III: Am. Mineralogist, v. 23, no. 4, p. 227–257, 13 figs.

——— 1938b, Petrologic results of a study of the minerals from the Tertiary volcanic rocks of the San Juan region, Colorado, pt. IV: Am. Mineralogist, v. 23, no. 7, p. 417–429.

Mabey, D. R., 1960, Gravity survey of the western Mojave Desert, Calif.: U.S. Geol. Survey Prof. Paper 316-D, p. 51–73.

McKinstry, H. E., 1953, Shears of the second order: Am. Jour. Sci., v. 251, no. 6, p. 401–414.

Moody, J. D., and Hill, M. J., 1956, Wrench-fault tectonics: Geol. Soc. America Bull., v. 67, no. 9, p. 1207–1246.

Mosesman, M. A., and Pitzer, K. S., 1941, Thermodynamic properties of the crystalline forms of silica: Am. Chem. Soc. Jour., v. 63, p. 2348–2356.

Muehlberger, W. R., 1954a, Structure of a portion of the easternmost Garlock fault zone, San Bernardino County, California [abs.]: Geol. Soc. America Bull., v. 65, no. 12, pt. 2, p. 1288.

——— 1954b, Geology of the Quail Mountains, San Bernardino County, Map Sheet no. 16 *of* Jahns, R. H., ed., Geology of southern California: California Div. Mines Bull. 170.

Noble, L. F., 1926, The San Andreas rift and some other active faults in the desert region of southeastern California, *in* Seismology, Report of the advisory committee: Carnegie Inst. Washington Yearbook 25, 1925–1926, p. 415–428.

——— 1931, Nitrate deposits in southeastern California, with notes on deposits in southeastern Arizona and southwestern New Mexico: U.S. Geol. Survey Bull. 820, 108 p.

Noble, L. F., and Wright, L. A., 1954, Geology of the central and southern Death Valley region, California, [pt.] 11 *in* chap. 2 *of* Jahns, R. H., ed., Geology of southern California: California Div. Mines Bull. 170, p. 143–160.

Nockolds, S. R., 1954, Average chemical compositions of some igneous rocks: Geol. Soc. America Bull., v. 65, p. 1007–1032.

Nockolds, S. R., and Allen, R., 1953, The geochemistry of some igneous rock series [pt. 1]: Geochim. et Cosmochim. Acta, v. 4, no. 3, p. 105–142.

——— 1954, The geochemistry of some igneous rock series, Pt. 2: Geochim. et Cosmochim. Acta, v. 5, no. 6, p. 245–285.

Nolan, T. B., 1943, The Basin and Range province in Utah, Nevada, and California: U.S. Geol. Survey Prof. Paper 197-D, p. 141–196, pls. 40–41.

Ostrovskiĭ, I. A., 1956, Experiments in the systems biotite-water, fayalite-water; aspects of the role of hydrogen in granite magma: Akad. Nauk SSSR Doklady, v. 108, p. 1164–1166; *as summarized in* Chem. Abstracts, v. 51, p. 1783.

Peacock, M. A., 1931, Classification of igneous rock series: Jour. Geology, v. 39, no. 1, p. 54–67.

Peterson, D. W., 1961, Descriptive modal classification of igneous rocks: GeoTimes, v. 5, no. 6, p. 31–36.

Powers, H. A., 1955, Composition and origin of basaltic magma of the Hawaiian Islands: Geochim. et Cosmochim. Acta, v. 7, nos. 1–2, p. 77–107.

Richthofen, Ferdinand von, 1868, Principles of the natural system of volcanic rocks: California Acad. Sci. Mem., v. 1, pt. 2, 98 p.

Rittman, A., 1952, Nomenclature of volcanic rocks proposed for the use in the catalogue of volcanoes, and key tables for the determination of volcanic rocks: Bull. volcanol., ser. 2, v. 12, p. 75–102.

Rogers, A. F., and Kerr, P. F., 1942, Optical mineralogy: 2d ed., New York, McGraw-Hill Book Co., 390 p.

Rogers, J. J. W., 1958, Textural and spectrochemical studies of the White Tank quartz monzonite, California: Geol. Soc. America Bull., v. 69, no. 4, p. 449–464.

Schairer, J. F., 1950, The alkali-feldspar join in the system $NaAlSiO_4$–$KAlSiO_4$–SiO_2: Jour. Geology, v. 58, no. 5, p. 512–517.

Schultz, J. R., 1937, A late Cenozoic vertebrate fauna from the Coso Mountains, Inyo County, Calif.: Carnegie Inst. Washington Pub. 487, p. 75–109, 8 pls.

Shapiro, Leonard, and Brannock, W. W., 1952, Rapid analysis of silicate rocks: U.S. Geol. Survey Circular 165, 17 p.

——— 1956, Rapid analysis of silicate rocks: U.S. Geol. Survey Bull. 1036-C, p. 19–56.

Shelton, J. S., 1955, Glendora volcanic rocks, Los Angeles basin, California: Geol. Soc. America Bull., v. 66, no. 1, p. 45–90.

Simpson, E. C., 1934, Geology and mineral deposits of the Elizabeth Lake quadrangle, California: California Jour. Mines and Geology, v. 30, no. 4, p. 371–415.

Smith, G. I., 1960a, Time of the last displacement on the middle part of the Garlock fault, California: Art. 128 *in* U.S. Geol. Survey Prof. Paper 400–B, p. B280.

——— 1960b, Estimate of total displacement on the Garlock fault, southeastern California [abs.]: Geol. Soc. America Bull., v. 71, no. 12, pt. 2, p. 1979.

——— 1962, Large lateral displacement on Garlock fault, California, as measured from offset dike swarm: Am. Assoc. Petroleum Geologists Bull., v. 46, no. 1, p. 85–104.

Smith, G. I., and Pratt, W. P., 1957, Core logs from Owens, China, Searles, and Panamint basins, California: U.S. Geol. Survey Bull., 1045–A, p. 1–62.

Taylor, D. W., 1954, Nonmarine mollusks from Barstow formation of southern California: U.S. Geol. Survey Prof. Paper 254–C, p. 67–80.

Tertsch, Hermann, 1942, Zur Hochtemperaturoptik basischer Plagioclase: Miner. und Petrog. Mitt., v. 54, nos. 4–6, p. 193–217.

Thompson, D. G., 1929, The Mohave Desert region, California, a geographic, geologic, and hydrographic reconnaissance: U.S. Geol. Survey Water-Supply Paper 578, 759 p., 34 pls.

Tilley, C. E., 1950, Some aspects of magmatic evolution [presidential address]: Geol. Soc. London Quart. Jour., v. 106, pt. 1, no. 421, p. 37–61.

Travis, R. B., 1955, Classification of rocks: Colorado School Mines Quart., v. 50, no. 1, 98 p.

Tuttle, O. F., and England, J. L., 1955, Preliminary report on the system SiO_2–H_2O: Geol. Soc. America Bull., v. 66, no. 1, p. 149–152.

Verhoogen, Jean, 1937, Mount St. Helens, a recent Cascade volcano: California Univ., Dept. Geol. Sci. Bull., v. 24, no. 9, p. 263–302.

Walker, G. W., Lovering, T. G., and Stephens, H. G., 1956, Radioactive deposits in California: California Div. Mines Spec. Rept. 49, 38 p.

Washington, H. S., 1917, Chemical analyses of igneous rocks published from 1884 to 1913, inclusive, with a critical discussion of the character and use of analyses: U.S. Geol. Survey Prof. Paper 99, 1201 p.

Weinschenk, E. H. O. K., 1912, Petrographic methods: New York, McGraw-Hill Book Co., 396 p.

Wentworth, C. K., 1922, A scale of grade and class terms for clastic sediments: Jour. Geology, v. 30, no. 5, p. 377–392.

——— 1954, The physical behavior of basaltic lava flows: Jour. Geology, v. 62, no. 5, p. 425–438.

Wiese, J. H., 1950, Geology and mineral resources of the Neenach quadrangle, California: California Div. Mines Bull. 153, 53 p.

Wilcox, R. E., 1954, Petrology of Parícutin volcano, Mexico: U.S. Geol. Survey Bull. 965–C, p. 281–354.

Williams, Howel, 1932, The history and character of volcanic domes: California Univ., Dept. Geol. Sci. Bull., v. 21, no. 5, p. 51–146.

——— 1935, Newberry volcano of central Oregon: Geol. Soc. America Bull., v. 46, no. 2, p. 253–304.

——— 1942, The geology of Crater Lake National Park, Oregon, with a reconnaissance of the Cascade Range southward to Mount Shasta: Carnegie Inst. Washington Pub. 540, 162 p.

——— 1950, Volcanoes of the Parícutin region, Mexico: U.S. Geol. Survey Bull. 965–B, p. 165–279.

Winchell, A. N., and Winchell, Horace, 1951, Description of minerals, pt. 2 *of* Elements of optical mineralogy—an introduction to microscopic petrography: New York, John Wiley & Sons, 551 p.

Yoder, H. S., Stewart, D. B., and Smith, J. R., 1957, Ternary feldspars, *in* Geophysical Laboratory [report]: Carnegie Inst. Washington Yearbook 56, 1956–57, p. 206–214.

SUPPLEMENTARY DATA

735-720 O—64——7

TABLE 17.—*Reproducibility of modal analyses*

[Arithmetic mean and mean deviation: M, average or mean value $\left(=\frac{\Sigma X}{N}\right)$; D, mean deviation $\left[=\frac{\Sigma(M-X)}{N}\right]$, where X= the percentage of mineral observed in individual sample, and N=the number of observations]

	Replicate counts (unrounded)								Arithmetic mean and mean deviation						
	124-23B			124-23F		124-23J			124-23B		124-23F		124-23J		Average
	1st	2d	3d	1st	2d	1st	2d	3d	*M*	*D*	*M*	*D*	*M*	*D*	*D*
Plagioclase megaphenocrysts	10.43	7.51	10.48	11.52	12.46	8.99	11.34	12.39	9.47	1.31	11.99	0.47	10.91	1.28	1.02
(Total plagioclase)	(17.50)	(17.15)	(17.25)	(22.00)	(19.22)	(17.57)	(22.00)	(21.81)	(17.30)	(.13)	(20.61)	(1.39)	(20.46)	(1.93)	(1.15)
Plagioclase microphenocrysts	7.07	9.64	6.77	10.48	6.76	8.58	10.65	9.42	7.83	1.21	8.62	1.86	9.55	.73	1.26
Biotite	-------	-------	-------	-------	.33	-------	-------	.07	-------	-------	.16	.16	.02	.03	.10
Hornblende	-------	-------	-------	-------	-------	-------	-------	-------	-------	-------	-------	-------	-------	-------	-------
Oxyhornblende	1.93	.96	.70	8.16	7.63	2.88	1.82	3.10	1.20	.49	7.90	.27	2.60	.52	.43
Orthopyroxene	-------	-------	.06	1.20	.94	.07	.21	.07	.02	.03	1.07	.13	.12	.06	.07
Clinopyroxene	-------	-------	-------	-------	.07	-------	-------	-------	-------	-------	.04	.04	-------	-------	.04
Quartz	-------	-------	.06	-------	.28	-------	-------	-------	.02	.03	.14	.14	-------	-------	.08
Opaques	10.13	11.18	11.44	1.44	2.21	10.71	9.46	9.49	10.92	.52	1.82	.39	9.89	.55	.49
Nonopaques	-------	.12	-------	.16	.20	-------	.42	.13	.04	.05	.18	.02	.18	.16	.08
Groundmass	70.42	70.57	70.47	67.04	69.11	68.77	66.08	65.32	70.49	.03	68.08	1.03	66.72	1.37	.81
Total	99.98	99.98	99.98	100.00	99.99	100.00	99.99	99.99	-------	-------	-------	-------	-------	-------	-------

TABLE 18.—*Mean value, mean deviation, and percent error of values reported by replicate spectrochemical analyses of five rocks*

[Sample 28-17 was analyzed 6 times; the other samples were analyzed 4 times. M, average or mean value $\left(=\frac{\Sigma X}{N}\right)$; D, mean deviation $\left[=\frac{\Sigma(M-X)}{N}\right]$, where X=value in parts per million reported by an individual analysis, and N=number of analyses; percent error is the quotient of D/M]

Sample	B	Ba	Be	Co	Cr	Cu	Ga	Mn	Ni	Pb	Sc	Sr	Ti	V	Y	Yb	Zr	Fe (percent)
124-22Q																		
M	50	2100	-------	37	32	12	12	340	11	7.2	6.9?	1500?	2200	38	7.0	<1	120?	1.6
D	5.5	270	-------	6	7.2	1.2	.8	28	1.2	1.3	-------	-------	180	3.8	-------	0	-------	.2
Percent	11	13	-------	16	23	10	6.5	8.2	11	18	-------	-------	8.2	10	-------	0	-------	12
97-38I																		
M	39	1800	-------	61	100	30	14	400	60	10	5.8	1700	2700	79	5.8	<1	120	2.6
D	3.8	250	-------	4.7	8.5	1	.8	5	5	2.0	1.8	200	320	12	1.3	0?	16	.4
Percent	9.8	14	-------	7.7	12	3	5.7	1.2	8.3	20	31	12	2	15	22	0?	13	15
28-17																		
M	+?	2300	-------	24	45	18	12	330	40	12	6.6	1400	2100	50	8.0	<1	130	2.0
D	5.8?	330	<1	1.7	7.2	4.2	3.2	50	5	1.9	2.5	330	300	9.7	1.8	<1	31	.27
Percent	?	14	?	8.1	16	23	27	15	12	16	38	24	14	19	22	?	24	13
41-39																		
M	28	1100	-------	22	24	26	12	320	14	12	5.5	990	2600	48	10?	1.5	110	3.0
D	1.5	370	-------	1.5	3.5	3.2	.75	22	.5	4.5	4.8	210	150	2.9	6.2	.25	17	.1
Percent	5.4	34	-------	6.8	15	12	6.2	6.9	3.6	38	82	21	5.8	5.9	62	17	15	3.3
124-22K																		
M	35	2000	-------	52	40	9.4	12	280	13	9.5	4.5	1000	2100	40	8.3	<1	110	1.6
D	7.8	230	-------	2.9	2.7	.62	.75	12	.25	2.0	2.8	256	250	1.5	3.1	.25	22	.1
Percent	22	11	-------	5.6	6.8	6.6	6.2	4.3	1.9	21	62	26	12	3.8	37	?	20	6.2
Avg. *D*	4.9	290	-------	3.0	5.8	2.0	1.3	23	2.4	2.3	2.9	250	240	6.0	3.1	.25	22	.22
Avg. percent	12	17	-------	8.8	15	11	10	7.1	7.4	23	53	21	10	11	36	?	20	10

TABLE 19.—*Table showing experimental spectrochemical values (unrounded) for standard samples G–1 and W–1*

[Readings were made on the same plates and using the same curves as were the data for the Lava Mountains rocks. For descriptions of these standard samples, see Fairbairn and others (1951)]

	G–1					W–1						
	Plate 534		Plate 535		Average	Plate 534			Plate 535			Average
B	?	?				?	?	?	5	6	3	5
Ba	1700	1700	1700	1700	1700	320	320	300	420	340	420	360
Be	3	2										
Co	1	<1				66	72	48	64	54	56	60
Cr	15	10	12	13	12	160	180	110	110	96	120	130
Cu	20	19	26	14	20	170	160	160	160	160	150	160
Ga	19	16	21	18	18	5.4	5.6	4.0	7.0	4.6	4.0	5.1
Mn	140	160	210	200	180	1200	1400	1200	1700	1600	1600	1400
Nb	65	17	<4	<4	?							
Ni						120	140	100	130	100	110	120
Pb	50	54	62	56	56							
Sc	3	4	3	4	4	80	68	62	74	46	72	67
Sr	540	700	630	630	620	680	720	780	740	660	860	740
Ti	1300	1300	1500	1500	1400	400	3800	4200	5000	4200	4700	4300
V	22	19	22	20	21	150	130	130	260	200	260	190
Y	35?	14	8	12	11	36	28	24	28	18	36	28
Yb			1	<1	<1	3.6	5.0	3.2	2.4	1.9	2.3	3.1
Zr	240	190	210	240	220	190	190	120	170	140	150	160
Percent Fe	1.4	1.3	.60	.78	1.0	8.0	10	7.0	4.9	3.4	3.6	6.7

TABLE 20.—*Identifications of the Lava Mountains vertebrate fauna by locality*

[Asterisks (*) indicate critical fossils for dating. See pl. 1 for positions of the localities. All identifications by G. E. Lewis]

LM–1—
?*Pliohippus* cf. *P. leardi.*
?*Megatylopus* sp.
?*Pliauchenia* sp.
Fragment of canid jaw.
Mastodon tooth enamel fragments.

LM–2—
?*Pliohippus* cf. *P. leardi.*
Camelid, undet.
Testudo mohavense.

LM–3—
?*Megatylopus* sp.
Merycodus sp.

LM–4—
?*Pliohippus* cf. *P. leardi.*
?*Megatylopus* sp.
?*Pliauchenia* sp.

LM–5—
?*Pliohippus* cf. *P. leardi.*
?*Megatylopus* sp.

LM–6—
**Pliohippus* cf. *P. leardi.*
?*Pliauchenia* sp.
Merycodus sp.

LM–7—
Mammal, ungulate, undet.
Testudo mohavense.

LM–8—
**?Pliauchenia.*
Undetermined fragments.

LM–9—
?*Pliohippus* cf. *P. leardi.*
?*Megatylopus* sp.
Artiodactyls, undet.

LM–10—
Pliohippus sp.
?*Megatylopus* sp.

LM–11—
?*Pliauchenia* sp.

LM–13—
**Pliohippus* cf. *P. leardi.*
**?Pliauchenia* sp.
?*Merycodus* sp.
Testudo mohavense.

TABLE 20.—*Identifications of the Lava Mountains vertebrate fauna by locality*—Continued

LM–14—
Rhinoceros, undet.
Small camel, undet.
?*Merycodus* sp.
Testudo mohavense.

LM–15—
Cf. *Hypolagus* sp.
Neotomodon sp.
**Pliohippus* sp.
?*Pliauchenia* sp.

LM–16—
Cf. *Hypolagus* sp.
Neotomodon sp.
Leptocyon vafer
Merycodus sp.
?*Megatylopus* sp.
?*Pliauchenia* sp.

LM–17—
?*Pliohippus* sp.
?*Pliauchenia* sp.
Small camel, undet.

LM–18—
?*Pliauchenia* sp.

LM–19—
Cf. *Pliohippus* sp. or *Equus* (s.l.) sp.

LM–20—
**Pliohippus* cf. *P. leardi.*
**?Pliauchenia* sp.
Small camel, undet.
?*Merycodus* sp.
Carnivore metapodial fragment, undet.

LM–21—
Cf. *Aphelops* sp.
**Pliohippus* cf. *P. leardi.*
**?Megatylopus* sp.
Cervid metapodial fragment, undet.
Carnivore metapodial fragment, undet.

LM–22—
Mammal vertebrae, undet.

LM–23—
Cf. *Merycodus* sp.

LM–24—
Mammalian pelvis fragments, undet.

TABLE 21.—*Locations of rock samples described in this report*

Rock Sample	*Formation; location of sample*
26–2	Atolia Quartz Monzonite. From sec. A 34–b, along road.
27–14	Lava Mountains Andesite. From top of small ridge in sec. D 11–g.
27–21	Lava Mountains Andesite. From top of ridge in sec. D 2–r.
27–23	Lava Mountains Andesite. From southwest side of hill in sec. D 3–d.
28–17	Quaternary andesite. From upper contact of sill exposed in the bottom of the canyon in sec. D 12–c.
29–6	Upper Pliocene(?) volcanic plug. Sample from northwest side of small plug in sec. D 14–j.
29–22	Propylite member of Almond Mountain Volcanics. From outcrop along south side of canyon in sec. D 24–f.
29–36	Subpropylite member of Almond Mountain Volcanics. From dump of City Well in sec. D 22–r.
41–34	Atolia Quartz Monzonite. From outcrop a few feet north of small prospect along road, in sec. A 35–d.
41–35	Atolia Quartz Monzonite. From brecciated outcrop on southeast side of canyon in sec. A 35–r.
41–39	Pre-Bedrock Spring Formation volcanic rock. Sample is greenish brecciated rock from top of small ridge in south half of sec. A 35–q.
97–31	Lava Mountains Andesite. Sample from near base of flow in sec. E 8–g.
97–38 F	Breccia member of Almond Mountain Volcanics From section exposed in E 6–j; section measured on line trending S. 35° W., sample collected about 100 feet below top of section.
I	Same member and locality, sample collected about 50 feet below top of section.
K	Same member and locality, sample collected about 20 feet below top of section.
L	Same member and locality, sample collected about 5 feet below top of section.
97–38 O	Lava Mountains Andesite, same locality as samples above. Sample collected about 100 feet above basal contact of formation.
97–39	Upper Pilocene(?) felsite. From top of ridge in north half of sec. E 5–r.
98–7	Lava Mountains Andesite. From about 50 feet above marker contact in sec. E 8–n.
124–22 F	Breccia member of Almond Mountain Volcanics. From type section of formation; see fig. 11 for stratigraphic position of sample.
I	Do.
K	Lava Mountains Andesite. A sill interbedded in the type section of the Almond Mountains Andesite; see fig. 11 for location of sample.
M	Breccia member of the Almond Mountain Volcanics. From type section of formation, see fig. 11 for stratigraphic position of sample.
Q	Do.
124–23 B	Lava Mountains Andesite. Sample locality on southwest edge of Almond Mountain, in sec. E 34–K, sample collected about 50 feet above base of formation.
F	Same formation and locality, sample collected about 210 feet above base of formation.
J	Same formation and locality, sample collected about 375 feet above base of formation.
128–32	Breccia member of the Bedrock Spring Formation. Sample locality along south side of wash in sec. E 2–e.
128–33	Breccia member of Almond Mountain Volcanics. Sample from top of hill in sec. E 10–d.
128–34	Quaternary andesite. Sample from sec. E 3–b, at base of small flow surrounding the volcanic neck.
181–28	Lava Mountains Andesite. Sample from about 40 feet above base of flow in sec. E 1–n.
181–29	Atolia Quartz Monzonite. Sample from outcrop along east side of wash in sec. F 18–a.
184–6	Lava Mountains Andesite. Sample from about 100 feet south of wash in sec. E 25–n.

INDEX

[Italic page numbers indicate major references]

The U.S. Geological Survey Library has cataloged this publication as follows:

Smith, George Irving, 1927–

Geology and volcanic petrology of the Lava Mountains, San Bernardino County, California. Washington, U.S. Govt. Print. Off., 1964.

v, 96 p. illus., maps (1 col.) diagrs. (1 col.) tables. 30 cm. (U.S. Geological Survey. Professional Paper 457)

Part of illustrative matter fold. in pocket.

Prepared partly in cooperation with the State of California, Dept. of Natural Resources, Division of Mines and Geology.

Bibliography: p. 87–89.

(Continued on next card)

Smith, George Irving, 1927– Geology and volcanic petrology of the Lava Mountains, San Bernardino County, California. 1964. (Card 2)

1. Geology—California—San Bernardino Co. 2. Petrology—California—San Bernardino Co. I. California. Division of Mines and Geology. II. Title: Lava Mountains, San Bernardino County, California. (Series)